Universitat Autònoma de Barcelona

CHARACTERISATION AND ADDING VALUE TO AGRO-FORESTRY BIOMASS PRODUCTS OBTAINED FROM THERMOCHEMICAL PROCESSES

ANNA ARTIGUES AGRAMUNT

DOCTORAL THESIS

Under the supervision of:

Dr. Esteve Fábregas Martínez

Dra. Neus Puy Marimón

DOCTORAL DEGREE IN ENVIRONMENTAL SCIENCES.

Institut de Ciència i Tecnologia Ambientals

Departament de Química – Grup Sensors i Biosensors

Facultat de Ciències

2015

Acknowledgments

The present dissertation has been carried out tjanks to the PIF fellowship provided by Universitat Autònoma de Barcelona and the financial suport of Ministry of Science and Innovation (MEC), Madrid. Project “Desarollo de (bio)materiales basados en nanoestructuras. Optimización y caracterización para su aplicación en (bio)sensors y energías renovables. CTQ2009-13873 (Subprograma BQU).

Agraïments

En primer lloc, vull agrair als meus directors, Neus Puy i Esteve Fábregas el seu suport acadèmic, científic i personal al llarg de tota la tesi. He après molt amb vosaltres! També vull donar les gràcies al Jordi Bartrolí per enredar-me (en el bon sentit) a començar aquest doctorat. Jo no tenia cap intenció de embarrancar-me en aquesta història: JO?! DOCTORAT?!? QUE VA!! Gràcies en gran part a tu, estic on estic! Santi Alier moltes gràcies per el teu suport, sense ENERG-bas aquesta tesi no seria el que és ara.

També vull donar les gràcies a tots aquells que heu fet aquesta tesi possible:

- A tots els membres del Departament de Química Analítica, als del meu grup d'investigació i al PAS del Departament. Especialment a la Mireia Baeza pels consells i suports científic tant ara dins de GSB com durant el màster i al Santi Maspoch per ajudar-me en la part estadística. Moltes gràcies a aquells membres de GTS que heu fet sentir-me part del vostre grup. Cristina, Montse i Oriol milions de gràcies per tot el suport que m'heu donat.

- A la Caterina Maulini, al Xavier Font, a la Teresa Vicent i la Glòria Caminal del Departament d'Enginyeria Química per deixar-me part dels seus equips i instal·lacions per realitzar part d'aquest treball.

- A tot l'equip del SAQ, especialment al Josep Maria, l'Alba, la MariaJ i a l'Ignasi. Aquesta tesi no hagués estat possible sense la vostra ajuda i consells. Sempre és un plaer passar-se uns dies per SAQ a fer experimental.

- Al Juan Baeza, a l'Albert Guisasola i a la Mar Vargas per introduir-me en el món de la investigació. I a tots aquells ETSEROS que vau compartir amb mi aqueslla època. Molts dels quals encara formeu part de la meva vida, cosa que em fa molt feliç.

I evidentment no hi ha qui aguanti una tesi sense tenir a la seva gent al costat i per sort en tinc molta. Vull donar-vos les gràcies per tot el suport que m'heu donat.

Agraïments

- Sole, Susy i Tamara sou un dels regals que m'ha donat aquesta tesi. Cockteleros (un altre "regalazo"), Fran, Jose, Júlia i Elena gràcies pels soparet i els mojitos fets amb molt d'amor per acabar un dia intens al lab! Raquel, Sandra, Ale, Olga, Anna Herrera moltes gràcies pels bons moments i rises al lab.

- ETSEROS, Alfred, Marty, Calleja, Elena, Gerard, Leti i Ponte, gràcies pel suport i els bons moments al "Fran". Especialment vull donar les gràcies a l'Alfred i la Martina perquè sé que puc comptar amb vosaltres pel que necessiti i passi el que passi.

- Ambientòlegs, aquesta aventura va començar amb vosaltres. No tingueu cap dubte que si ara sóc ambientòloga i espero que en breu Doctora en Ciències Ambientals és en gran part gràcies a vosaltres.

- Nenes, sóc molt afortunada de tenir-vos al meu costat. Moltes gràcies per ser-hi sempre, sempre i sempre! Sé que puc comptar amb vosaltres per qualsevol cosa, 24h al dia, 365 dies l'any. Això no té preu!

- Lluís, gràcies per aguantar tots el "ho sento però m'haig de posar a escriure" tenint en compte el poquet que ens veiem i per suportar la història d'aquests últims mesos que explicada per telèfon encara es porta pitjor. Saps que els canvis d'etapa em fan pànic però sé que si el faig amb tu tot serà molt més fàcil. T'estimu!

- Gràcies a la meva família. Mama, papa, Sister per està sempre allà, tant amb les coses professionals, personals, en els bons moments i en els no tant. No seria qui sóc si no us tingués al meu costat. A la Iaia pel seu suport, tot i no entendre res de res del que faig. I a la padrina la seva confiança incondicional amb mi i amb el que faig. Us estimo moltíssim.

- També vull donar les gràcies a la Mari Angeles, al Lluís i a l'Ignasi. No us podeu imaginar que bé em va anar passar l'agost amb vosaltres, tant per l'escriptura com personalment. Manu, prometo que quan finalitzi tot aquest procés, quan baixi a Castelló faré vida social i no em passaré el dia tancada amb el Buddy escrivint.

GRÀCIES A TOTS

Table of contents

Table of contents……..…i
Table of figures ……v
Table of tables……ix
List of acronyms, abbreviations and notations……xiii
Summary……xiv

PART I: INTRODUCTION AND METHODOLOGY

1. Introduction 3
1.1. Demand of fuels 3
1.2. Overview of biomass as energy resource 4
1.2.1. Biofuels 6
1.2.2. Biomass conversion processes 9
1.3. Torrefaction 14
1.3.1. Torrefaction products 16
1.3.2. Technology development of torrefaction process 23
1.4. Fast pyrolysis 26
1.4.1. Fast pyrolysis products 27
1.4.2. Bio-oil upgrading processes 36
1.4.3. Fast pyrolysis development technology 43
1.5. Biorefinery 44
2. Motivations and objectives 47
2.1. Motivation 47
2.2. Objectives 49
3. Experimental Section 51
3.1. Analytical methods 51
3.1.1. Thermogravimetric analysis 51
3.1.2. Calorific value 52
3.1.3. Elemental analysis 52
3.1.4. Immediate analysis. 53
3.1.5. Inductively coupled plasma mass spectrometry (ICP-MS) 53

3.1.6. Gas chromatography - Mass Spectrometry (GC-MS) 54
3.1.7. pH 59
3.1.8. Total Acid Number (TAN) 60
3.1.9. Differential Acid Number (DAN) 62
3.1.10. Water content 64
3.1.11. Flame Atomic Absorption Spectroscopy (FAAS) 65
3.2. Experimental design of part II: adding value of agricultural waste biomass as torrefied pellet woody crop. 66
3.2.1. Implementation zone and its biomass potential 67
3.2.2. Semi-industrial pilot plant 69
3.2.3. Adding value to Agricultural Waste Biomass (AWB) as torrefied pellets by Energies Tèrmiques Bàsiques SL plant. 70
3.2.4. Economic assessment 71
3.3. Experimental design of Part III: Bio-oi characterisation and upgrading. 76
3.3.1. BTG-BTL bio-oil 76
3.3.2. Bio-oil catalytic upgrading process 77
3.3.3. Hydrogenation processes: preliminary assessment 79
3.3.4. *In situ* generation of nascent hydrogen via zinc oxidation. 81
References of Part I 87

PART II: ADDING VALUE OF AGRICULTURAL WASTE BIOMASS AS TORREDIED PELLETS

4. Adding value of agricultural waste biomass as torrefied pellets 103
4.1. Introduction of chapter 4: adding value of agricultural waste biomass as torrefied pellets 103
4.2. Feedstock characterisation 105
4.3. Optimum operational conditions to treat agricultural waste biomass in the torrefaction plant. 108
4.4. Characterisation of torrefaction products and their applications 111
4.4.1. Torrefied biomass 111
4.4.2. Torrefied biomass pelletisation 112
4.4.3. Liquid of torrefaction 112
4.5. Logistic costs of biomass supply to the plant 122

4.6. Economic analysis for torrefaction plant implementation 125

4.6.1. Economic analysis of the torrefaction plant implementation in a moderate torrefaction pellets production scenario. 125

4.6.2. Economic analysis of the torrefaction plant implementation in an intensive torrefaction pellets production scenario 131

4.6.3. Sensitivity analysis of including torrefaction liquid as torrefaction by-product..... 135

4.7. Conclusions of Chapter 4: Adding value to agricultural waste biomass as torrefied pellets..... 136

References of Part II 139

PART III: BIO-OIL CHARACTERISATION AND UPGRADING

5. Introduction of Part III: bio-oil characterisation and upgrading 143

6. Bio-oil characterisation 147

6.1. Bio-oil characterisation results 148

6.1.1. Bio-oil acidity and water content 148

6.1.2. Bio-oil chemical composition. 149

6.2. Quantitative assessment of bio-oil chemical composition..... 154

6.2.1. Selection of the quantified bio-oil compounds. 155

6.2.2. GC-MS method precision study for bio-oil chemical characterisation…
…156

6.2.3. Bio-oil chemical composition quantitative analysis…….161

6.3. Conclusions of Chapter 6: Bio-oil characterisation..... 174

7. Reduced energy cost bio-oil catalytic upgrading process..... 177

7.1. Introduction of Chapter 7: reduced energy cost bio-oil catalytic upgrading process 177

7.2. Effect of bentonite and HZSM-5 on bio-oil properties 178

7.3. Chemical changes in upgraded bio-oil using HZSM-5..... 183

7.4. HZSM-5 time life study 194

7.5. Conclusions of Chapter 7: reduced energy cost bio-oil catalytic upgrading process 197

8. Reduced cost bio-oil hydrogenation processes 199

Table of content

8.1. Introduction of Chapter 8: reduced cost bio-oil hydrogenation processes ……199

8.2. Hydrogenation processes: preliminary assessment 202

8.3. *In situ* generation of nascent hydrogen via Zn oxidation 208

8.3.1. Zn^{2+} generation..... 208

8.3.2. pH changes 213

8.3.3. DAN test..... 216

8.3.4. Nascent hydrogen production under optimum tested condition.. 218

8.3.5. Influence of bio-oil acidity on nascent hydrogen generation 219

8.3.6. Phase separation influence on ion zinc distribution 220

8.3.7. Influence of nascent hydrogen generated on bio-oil properties... 221

8.4. Conclusions of Chapter 8: reduced cost bio-oil hydrogenation processes ……231

References of Part III 233

PART IV: CONCLUSIONS AND FUTURE PERSPECTIVES

9. Conclusions..... 241

10. Future perspectives..... 247

PART V: ANNEX

Publications and conferences..... 251

Table of Figures

Figure 1.1. Lignocellulosic biomass main components. 5

Figure 1.2. Biomass chemical structure and some possible extractable chemical products. 5

Figure 1.3. Main conversion processes from biomass to secondary energy carriers 10

Figure 1.4. Decomposition curves of three main compounds of lignocellulosic biomass: hemicellulose; cellulose and lignin. 12

Figure 1.5. Product yields obtained from pyrolysis of pine wood as a function of the reactor temperature: liquid fraction, solid fraction and gas fraction. 12

Figure 1.6. Development stages of pyrolysis and torrefaction products regarding to their potential use. 14

Figure 1.7. Scheme of the basic torrefaction process 15

Figure 1.8. Colour changes during the torrefaction process. 15

Figure 1.9. A schematic of property variation of biomass undergoing torrefaction 17

Figure 1.10. Scheme of the basic TOP process. 21

Figure 1.11. Scheme of the basic fast pyrolysis process 26

Figure 1.12. Scheme of bio-oil potential applications. 34

Figure 1.13. Examples of reactions associated with catalytic bio-oil upgrading.. 38

Figure 1.14. Fast pyrolysis biorefinery scheme. 46

Figure 3.1. Gas Chromatograph TRACE GC ULTRA coupled to a DSQ II Mass Spectrometer and a TRIPLUS AS autosample from ThermoFisher Scientific. 54

Figure 3.2. pHmeter picture and Solvotrode electrode. 60

Figure 3.3. Crison micro TT 2050 potentiometer for Total Acid Number titration. 60

Figure 3.4. TAN titration curve. 62

Figure 3.5. 716 DMS titrino and 665 Dosimat for Karl Fischer titration. 64

Figure 3.6. Perkin–Elmer flame atomic absorption spectrophotometer. 66

Figure 3.7. Pilot project implementation area. 68

Figure 3.8. Uses of land of Ribera d'Ebre region: Agricultural land; forestry land; industrial and urban land pastureland and others. 69

Figure 3.9. Picture of Energies Tèrmiques Bàsiques biomass conversion plant.. 70

Figure 3.10. BTG-BTL bio-oil 77

Figure 3.11. Picture of experimental set-up for assessment of the catalytic upgrading process. 78

Figure.3.12. Scheme of: overall upgrading experiment (a) and catalyst replacement experiment (b). 79

Figure 3.13. Molecular hydrogen experimental set-up scheme. 80

Figure 3.14. Picture of the electrolytic nascent hydrogen production experimental set-up. 81

Figure 3.15. Picture of the shakers used and the pieces of Zn: orbital shaker with horizontal circular movements (a); Vertical rotation shaker (b); Zn pieces of 2.5 x 8 mm (c); Zn pieces of 2.5 x 80 mm. 84

Figure 4.1. Pictures of potential valuable raw biomasses: cherry pruning waste (a); almond pruning waste (b); olive pruning waste (c). 106

Figure 4.2. Thermogravimetric analysis of biomass coming from Ascó: almod wood; cherry wood; olive wood. 108

Figure 4.3. Comparison between raw and grinded biomass: almond pruning waste (a); olive pruning waste (b). 109

Figure 4.4. Picture of almond pruning waste (a); pellet of raw almond pruning waste (b); torrefied pellets of almond pruning waste at 280 ºC (c); and torrefied pellet of olive pruning waste at 250 ºC (d). 114

Figure 4.5. Picture of liquid fraction produced: at 280 ºC from almond pruning waste (a) and at 250 ºC from olive pruning waste (b). 116

Figure 4.6. Total Ion Chromatogram of torrefaction liquids from almond pruning waste (a) and olive pruning waste (b). ..... **Error! Bookmark not defined.**118

Figure 4.7. Logistic costs for each considered scenario: chipping cost, transport cost, storage cost and feeding plant cost 123

Figure 4.8. Estimation of the maximum biomass cost (€/t) of: biomass 50% of moisture in moderate scenario with pellet selling price of 206 €/t (a); biomass 30% of moisture in moderate scenario with pellet selling price of 206 €/t (b); biomass 50% of moisture in moderate scenario with pellet selling price of 233 €/t (c); biomass 30% of moisture in moderate scenario with pellet selling price of 233 €/t. 129

Figure 4.9. Estimation of the maximum biomass cost (€/t) of: biomass 50% of moisture in moderate scenario with pellet selling price of 206 €/t (a); biomass 30% of moisture in moderate scenario with pellet selling price of 206 €/t (b); biomass 50% of moisture in moderate scenario with pellet selling price of 233 €/t (c); biomass 30% of moisture in moderate scenario with pellet selling price of 233 €/t. 133

Figure 6.1. Total Ion Chromatogram (TIC) from a bio-oil sample showing the retention time and the main identified compounds. 150

Figure 6.2. Percentage of the summation of all compounds areas from the same chemical family related to the total area: Sugar; acid and esters; phenols and alcohols, ketones, aldehydes, furans and others. 154

Figure 6.3. Calibration curves using the peak area of (a) 2-propanol, 2-butanone, 2,5-dimethoxytetrahydrofuran; b) acetic acid, levoglucosan; (c) 2-methoxy-4-propyl-phenol, furfural, 2-hydroxy-3-methyl-2-cyclopenten-1-one, vanilline and 2(5H)furanone 165

Figure 6.4. Strength of linearity between days for each external calibration method: without internal standard (a); toluene as internal standard (b); 1,1,3,3-tetramethoxypropane as internal standard (c); 1-octanol as internal standard (d).... 172

Figure 7.1. Area ratio of acid and esters through the upgrading process at 60 ºC for 5, 10, 15 wt % of HZSM-5: 0 h, 2h, 4h, 6 h..... 191

Figure 7.2. Area ratio of alcohols through the upgrading process at 60 ºC for 5, 10, 15 wt % of HZSM-5. : 0 h, 2h, 4h , 6 h 192

Figure 7.3. Area ratio of aldehydes through the upgrading process at 60 ºC for 5, 10, 15 wt % of HZSM-5: 0 h, 2h, 4h, 6 h 193

Figure 7.4. Area ratio of ketones through the upgrading process at 60 ºC for 5, 10, 15 wt % of HZSM-5: 0 h, 2h, 4h, 6 h 193

Figure 7.5. pH changes for 2 h of reaction time using 10 wt % of HZSM-5..... 195

Figure 7.6. Bio-oil titration curve using NaOH (6M) solution 197

Figure 8.1. Influence of temperature on nasce0nt hydrogen production expressed as mmol Zn^{2+} per g bio-oil. Comparison of experiments carried out at 20 ºC and 37 ºC using orbital stirring and zinc size of 2.5x 8 mm under different initial weights of Zn: 1,5 wt % (a), 3 wt % (b), 4,5 wt % (c). 209

Figure 8.2. Influence of agitation on nascent hydrogen production expressed as mmol Zn^{2+} per g bio-oil. Comparison of non-stirring and orbital stirring at 20 ºC using zinc metal pieces of 2.5x 8 mm under different initial weights of initial zinc metal: 1.5 wt % (a), 3 wt % (b) and 4.5 wt %. And comparison between orbital stirring and rotational stirring at 37 ºC using 4.5 wt % of initial metal zinc of 2.5x 8 mm (d). 210

Figure 8.3. Influence of zinc metal pieces size on nascent hydrogen production expressed as mmol Zn^{2+} per g bio-oil. Comparison between using zinc metal pieces of 2.5x 8 mm and 2.5 x 80 mm under 37 ºC, rotational stirring and different initial concentrations of zinc metal: 4.5 wt % (a), 9 wt % (b) and 13.5 wt %(c)..... 211

Figure 8.4. Influence of the initial amount of zinc metal on nascent hydrogen production expressed as mmol Zn^{2+} per g bio-oil. Comparison between using 1.5 wt % of initial zinc metal, 3 wt % of initial zinc metal 4.5 wt % of initial zinc metal, 9 wt % of initial zinc metal and 13.5 wt % of initial zinc metal under 37 ºC using zinc metal pieces of 2.5 x 8 mm and stirring types: orbital stirring (a) and rotational stirring (b)different initial concentrations of zinc metal: 4.5 wt % (a), 9 wt % (b) and 13.5 wt %(c)..... 212

Figure 8.5. Influence of the initial amount of zinc metal on bio-oil acidity expressed as pH. Comparison of using 1.5 wt % of initial zinc metal, 3 wt % of initial zinc metal, 4.5 wt % of initial zinc metal, 9 wt % of initial zinc metal and 13.5 wt % of initial zinc metal under 37 ºC using zinc metal pieces of 2.5 x 8 mm and stirring types: orbital stirring (a) and rotational stirring (b). 214

Figure 8.6. Influence of agitation on bio-oil acidity expressed as pH. Comparison of non-stirring and orbital stirring at 20 ºC using zinc metal pieces of 2.5x 8 mm with different initial weights of initial zinc metal: 1.5 wt % (a), 3 wt % (b) and 4.5 wt %. And comparison between orbital stirring and rotational stirring (-o-) at 37 ºC using 4.5 wt % of initial metal zinc of 2.5x 8 mm (d) 214

Figure 8.7. Influence of agitation on bio-oil acidity expressed as pH. Comparison of experiments carried out at 20 ºC and 37 ºC using orbital stirring and zinc size of 2.5x 8 mm under different initial weights of Zn: 1,5 wt % (a), 3 wt % (b), 4,5 wt % (c). 215

Figure 8.8. Influence of agitation on bio-oil acidity expressed as pH. Comparison of using zinc metal pieces of 2.5x 8 mm and 2.5 x 80 mm under 37 ºC, rotational stirring and different initial concentrations of zinc metal: 4.5 wt % (a), 9 wt % (b) and 13.5 wt % (c). 216

Figure 8.9. Evaluation of the fixed final point for the DAN test: DAN, AN raw bio-oil and AN treated bio-oil 217

Figure 8.10. DAN, Zn^{2+} and pH changes through 10 days of reaction time at 37 ºC, vertical rotation agitation, 4,5 wt % of initial Zn and 8 x 2.5 mm Zn size and pH of the blank at the same conditions. 218

Figure 8.11. Twenty most abundant bio-oil chemical compounds accordingly to area ratio and their percentage of variance at each reaction time relative to initial time (48 h, 96h, 144 h, 240 h)..... 228

List of tables

Table 1.1. Advantages, disadvantages and production status of different biofuels (2013)..... 8

Table 1.2. Typical product weight yield (dry wood basis) obtained by different thermal conversion processes..... 13

Table 1.3. Comparison of properties of wood, torrefied biomass, wood pellets and TOP pellets..... 22

Table 1.4. Torrefaction technology development at a commercial or demonstration stage. 25

Table 1.5. Some organic compound present in bio-oil classified in organic groups 29

Table 1.6. Properties of wood bio-oils and mineral oils: heavy fuel oil (HFO) and light fuel oil (LFO)..... 30

Table 1.7. Bio-oil characteristics, its causes and the effects of bio-oil properties on as a liquid biofuel..... 30

Table 1.8. Comparison of characteristics of bio-oil, catalytically upgraded bio-oil and crude oil. 42

Table 1.9. Principal characteristics of Phase III biorefineries. 45

Table 3.1 Calibration range of bio-oil quantified compounds..... 58

Table 3.2. Calibration range of bio-oil quantified compounds..... 59

Table 3.3. Torrefaction operational conditions tested for almond and olive pruning biomass treatment. 71

Table 3.4. Economic indicators definition for the cost-benefit economic analysis 72

Table 3.5. Evaluated implementation scenarios for torrefaction plant to produce torrefied pellets in Ascó municipality context. 73

Table 3.6. Cost values for the economic assessment..... 74

Table 3.7. Assessed logistic scenarios to supply agricultural waste biomass to torrefaction plant for moderate and intensive implementation scenarios..... 76

Table 3.8. BTG-BTL bio-oil physical and chemical properties (accordingly to BTG-BTL product data sheet). 77

Table 3.9. Performed experiments at different experimental conditions: initial weight of zinc metal (1.5, 3, 4.5, 9, 13.5 wt %), temperature (20 and 37 ºC), stirring type (no stirring (NS), Orbital shaker (OS) and vertical rotation shaker (RS)) and Zn size (2.5 x 8 mm and 2.5 x 80 mm). 83

Table 4.1. Raw biomass properties as received. (HHV: High heating value; LHV: Low heating value)..... 107

Table 4.2. Operational conditions and obtained fractions efficiency (solid, liquid and gas from the biomass torrefaction treatment. (*calculated by difference)..... 110

Table 4.3. Comparison of moisture content and low heating values (LHV) between raw and torrefied biomass. 112

Table 4.4. Characteristics of produced olive pruning waste torrefied pellet at 250 ºC and almond pruning waste torrefied pellets at 280 ºC and their comparison to European Pellet Standards (prEN 14961-2)..... 114

Table 4.5. Water and organic content, density, pH and concentration of some target compounds of olive pruning waste torrefaction liquid at 250 ºC and almond pruning waste torrefaction liquid at 280 ºC. 115

Table 4.6. Identified compounds on almond and olive torrefaction liquid. (RT: Retention time; m/z: mass to charge ration; n.i.: no identified) 119

Table 4.7. Economic analysis of the torrefaction plant implementation in a moderate production of torrefaction pellets scenario (AWB: agricultural waste biomass, NPV: net present value, IRR: internal rate of return, ROE: Return on equity). 128

Table 4.8. Economic analysis in a moderate scenario using dried biomass and farmers support. Pellet price of 233 €/t (BBT: benefits before taxes; BAT: benefit after taxes,NPV: net present value, IRR: internal rate of return). 130

Table 4.9. Economic analysis of the torrefaction plant implementation in an intensive production of torrefaction pellets scenario (AWB: agricultural waste biomass, NPV: net present value, IRR: internal rate of return, ROE: Return on equity)..... 132

Table 4.10 Percentages of improvement of economic efficiency of each considered scenario adding torrefaction liquid as a valuable product (AWB: agricultural waste biomass). 136

Table 6.1. Raw bio-oil properties. (* confidence interval at 95% of confidence level) 138

Table 6.2. Identified compounds and their retention time (RT), molecular weight (MW), molecular formula, area, relative standard deviation (RSD), as well as the area percentage of each compound relative of the total area. 151

Table 6.3. Classification of bio-oil identified compounds in chemical families.. 153

Table 6.4. List of selected compounds for the study of method precision and quantification, such as the tested internal standards, with their retention time (RT) and quantifying mass to charge ratio (m/z) for peak integration. 156

Table 6.5. Peak area average of each selected compounds and its relative standard deviation (RSD)..... 158

Table 6.6. Average of peak area ratio relative to toluene, 1,1,3,3-tetramethoxypropane and 1-octanol for each selected compound and its relative standard deviation (RSD). 159

Table 6.7. Calibration equation for each selected compound obtained to fit their area into a Linear Least Squares Regression model and concentration of each compound. 162

Table 6.8. Calibration equation for each selected compound obtained to fit the area ratio relative to toluene into a Linear Least Squares Regression model and concentration of each compound 168

Table 6.9. Calibration equation for each selected compound obtained to fit the area ratio relative to 1,1,3,3-tetramethoxypropane into a Linear Least Squares Regression model and concentration of each compound. 169

Table 6.10. Calibration equation for each selected compound obtained to fit the area ratio relative to 1-octanol into a Linear Least Squares Regression model and concentration of each compound. 170

Table 7.1. Bio-oil properties at 60 ºC over time. 179

Table 7.2. Effect of different weight percentages of bentonite on bio-oil properties through the upgrading process at 60 ºC. 180

Table 7.3. Effect of different weight percentages of HZSM-5 on bio-oil properties through the upgrading process at 60 ºC. 181

Table 7.4. Area ratio of the identified compounds of raw and upgraded bio-oil at different reaction times for 5 wt % of HZSM-5 experiments.. 185

Table 7.5. Area ratio of the identified compounds of raw and upgraded bio-oil at different reaction times for 10 wt % of HZSM-5 experiments.. 187

Table 7.6. Area ratio of the identified compounds of raw and upgraded bio-oil at different reaction times for 15 wt % of HZSM-5 experiments.. 189

Table 8.1. Variation percentage of bio-oil composition between raw and treated bio-oil by hydrogenation processes. 206

Table 8.2. pH and Zn^{2+} (mmol Zn^{2+}/g bio-oil) changes at 0,3, 6 and 8 days of reaction time for acid addition experiment and the blank. 220

Table 8.3. Bio-oil chemical compounds ordered by area ratio (AR) with it confidence interval (CI) and percentage of variance at each reaction time relative to initial time.. 223

Table 8.4. Bio-oil properties of untreated and treated bio-oil. 230

List of acronyms, abbreviations and notations

% wt	Weight percentage
AN	Acid Number
ANOVA	Analysis of Variance
ASTM	American Society for Testing and Materials Standards
BTG	Biomass Technology group BV
CENER	Spanish National Renewable Energy Centre
CHP	Combined heat and power
d.b.	Dry basis
DAN	Differential Acid Number
DIN	Deutsches Institut für Normung (German Institute of Standardisation)
ECN	Energy Research Centre of the Netherlands
EIC	Extracted Ion Chromatogram
FAAS	Flame Atomic Absorption Spectroscopy
FCC	Fluid Catalytic Cracking
FTIR	Fourier Transform Infrared
GC-MS	Gas Chromatography - Mass Spectrometry
GFN	Green Fuel Nordic
GPC	Gel permeation chromatography
HDO	Hydrotreating
HDS	hydrodesulphurization
HHV	High Heating Value
HPLC	High Performance Liquid Chromatography
HZSM-5	Protonated Zeolita Socony Mobil - 5
ICP-MS	Inductively coupled plasma - mass spectrometry
IRR	Internal Rate Return
LHV	Low Heating Value
m/z	Mass to charge
NMR	Nuclear magnetic resonance
NPV	Net Present Value
NREL	National Renewable Energy Laboratory of United States
NS	No stirring
OS	Orbital Shaker with horizontal circular movements
ROE	Return on equity
RS	Vertical rotation shaker
RSD	Relative Standard Deviation
t	tonne
TAN	Total Acid Number
TG	Thermogravimetry
TGA	Thermogravimetric analysis

List of acronyms, abbreviations and notations

TIC	Total Ion Chromatogram
UV	Ultraviolet-visible spectroscopy
AWB	Agricultural waste biomass
ZSM-5	Zeolita Socony Mobil - 5

Summary

Biomass use to produce a biofuels and bio-products from a renewable source is raising a high interest in recent years motivated by the opportunity of converting biomass residues or sub-product into a primary energy source, using a primary energy source at local and regional scale, improving the agro-forestry sector by the preservation and restoration of the environment and traditional landscapes, reducing forest fire risk and increasing energy diversification which helps to reduce fossil fuels dependency and to mitigate the global warning effects. In this direction, the main aim of this thesis is to add-value to agro-forestry biomass residues as enhanced biofuels by means of thermochemical biomass conversion processes in order to move towards a more sustainable energy model.

Adding value to agricultural waste biomass as torrefied pellets by means of torrefaction process is performed by means of a pilot scale test carried out in a rural region to demonstrate the technic-economic viability implementing of this process as a local strategy to make use of this residue moving towards a circular economy. First of all, a proper characterisation of the potential valuable agricultural waste biomass is performed, as well as the obtained torrefaction products. Results shows that produced torrefaction pellets characteristics are within the European law standards of pellets demonstrating they are marketable products. Torrefaction liquid is aqueous product with high contents of acetic acid and furfural making it a potential biodegradable pesticide or wood preservative. Regarding to the economic assessment of implementing this mobile torrefaction plant in a rural region is performed considering both moderate and intensive torrefied pellets production scenarios and different logistic scenarios of obtaining agricultural waste biomass as feedstock for the plant. Results shows that the viability of this process is highly dependent on the logistic scenario considered, being the transport and the chipping logistic operation the most influent ones. Intensive production scenario is more economically favourable than

moderate one, being the purchasable biomass prices between 37 and 88 €/t depending on the considered scenario.

Bio-oil is a liquid product produced by fast pyrolysis process of biomass with a great potential as liquid biofuel product and chemical platform to obtain bio-products, offering a great potential feedstock in biorefinery scenarios. Currently, bio-oil is a low value biofuel due to its corrosiveness, high viscosity, high oxygen content and low thermal and chemical instability. Because of that its stabilization and upgrading is required to obtain an enhanced product, even though bio-oil upgrading processes reduce the economic viability of bio-oil as a marketable product. In this context, two novel bio-oil upgrading processes are explored in order to obtain an enhanced bio-oil using reduced energy and resources cost upgrading process in comparison to conventional ones. Firstly, a proper bio-oil characterisation is performed, as well as it is assessed and reached a reliable quantitative analysis of bio-oil chemical compounds by means of GC-MS to achieve a further characterization of this product and to permit a proper monitoring of bio-oil properties changes during the upgrading processes. Then, it is tested a catalytic upgrading process using bentonite and zeolite HZSM-5 at 60 ºC to avoid the necessity of a bio-oil external heating due to bio-oil comes out of the fast pyrolysis at this temperature. The results shows an acidity reduction of treated bio-oil, although a reduced catalytic reaction is observed due to the quick deactivation of these catalysts at this temperature. Finally, novel hydrogenation procedures to hydrogenate bio-oil at ambient temperature and atmospheric pressures are explored including molecular hydrogen injection and in situ generation of nascent hydrogen both via metal oxidation using bio-oil as acidic medium and via water electrolysis contained in bio-oi. A Preliminary assessment of these procedures are performed resulting nascent hydrogen via zinc metal oxidation the simplest and more effective hydrogenation process in comparison to the other tested ones. Then, an extended study of this hydrogenation process is assessed at different experimental conditions. Results shows that nascent hydrogen is produced under all the tested conditions, being favoured at temperature, proper agitation and initial zinc metal concentrations

up to of 4.5 wt %. Moreover, it is observed that after 24-48h of reaction time bio-oil is converted into non-enough acidity medium to take place the nascent hydrogen generation. Also, it is observed a bio-oil phase separation which permits the elimination of the produced ion zinc which might suppose a problem for the combustion of this treated bio-oil. Bio-oil chemical changes are achieved by this hydrogenation process although they not imply a noticeable changes on bio-oil properties as biofuel. Despite that fact, i*n situ* nascent hydrogen production is a promising cheap and simple novel hydrogenation process.

In conclusion, this research shows the current and future potential of adding value to agro-forestry waste biomass by means of thermochemical processes as biofuels and bioproducts to move towards a bioeconomy strategy.

1

INTRODUCTION AND METHODOLOGY

1. Introduction

1.1. Demand of fuels

The world energy demand was $5.5 \cdot 10^{20}$ J in 2010 and it is predicted to increase to $6.6 \cdot 10^{20}$ J in 2020 and $8.6 \cdot 10^{20}$ J in 2040 [1]. Global energy supply is to a large extent based on fossil fuels. Over 80% of the world energy demand are met by fossil fuel combustion (oil, natural gas, coal) [2–4]. Coal gives about 28% of the world's consumed energy while crude oil-petroleum and natural gas provide about 32% and 20 % respectively [5]. Fossil fuels have been used to power our world for many decades providing us with power to light and heat our homes and industry, and with many products derived from them. Till now, fossil fuels had been fairly easily available and extractable, although the excessive use of these non-renewable sources within a human timescale are running out them, mainly oil and gas [6]. Moreover, their intensive use is causing negative effects on the environment, since their combustion is accompanied by emission of carbon dioxide and water vapour, contributing to the greenhouse effect and global warming of the Earth [7]. Furthermore, their combustion generates toxic sulphur and nitrogen oxides that contribute to the formation of acid rain, which pollutes the environment [8]. Because of these facts, increasing the use of renewable energy sources is necessary in order to diversify the energy sources reducing, thereby, the dependence of fossil fuels and its associated drawbacks. Consequently, the world is currently challenged to develop renewable energy and chemical sources to move towards a sustainable bio-based community. Thus, energy planning and technology improvement have become an important research and public agenda of most developed and developing countries. In this sense, the European commission adopted its strategy on the bioeconomy, understanding it as those economy based on biomass derived fuel, chemicals and materials, sustainably sourced and produced [9,10].

1.2. Overview of biomass as energy resource

Biomass is recognized as a renewable resource for bioenergy, biofuels and biochemicals production. The term biomass refers to the set of organic matter of vegetable or animal origin. This broad definition includes from forest residues to animal residues such as meat and bone meal. However, in this dissertation the term biomass is referred to lignocellulosic biomass which involves wood, forest and crops residues, residues of textile, pulp and paper, municipal paper waste, among others.

Lignocellulosic biomass, hence the name, is composted by three main polymeric components (Figure 1.1.): cellulose, hemicellulose and lignin. They constitute 97-99% of the total dry mass of wood, of which 65-75% are polysaccharides. Typically, woody materials consist of 40-60% cellulose; 20-40% hemicellulose and 10-25% lignin on dry basis [11]. The rest of the components are inorganic minerals and organic extractives. They comprise a large variety of chemical substances, such as terpenoids, fats and waxes, various types of phenolic compounds, as well as n-alkanes [12,13]. Cellulose is a high molecular-weight lineal polymer of β-(1,4)-D-glucopyranose units. Hemicellulose is the second major wood chemical constituent and has lower molecular weights than cellulose and it contains mainly glucose, galactose, mannose, xylose, arabinose and glucuronic acid. Lignin is a three dimensional, highly branched, polyphenolic substance that consists of phenylpropane units, which exhibit the p-coumaryl, coniferyl and sinapyl structures.

Understanding the lignocellulosic biomass chemical composition permits a better comprehension of biomass behaviour during its conversion process to biofuel or the

extraction of biochemical products. As example, in Figure 1.2, it is highlighted the possible extractable chemical products from lignocellulosic biomass.

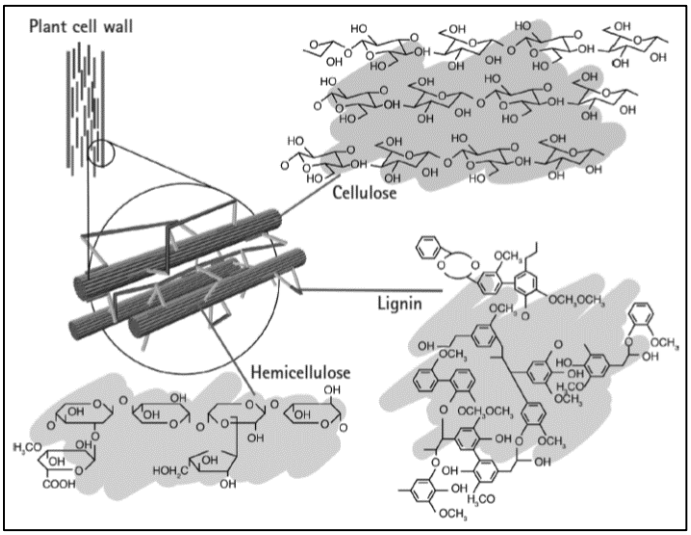

Source: [14]

Figure 1.1. Lignocellulosic biomass main components.

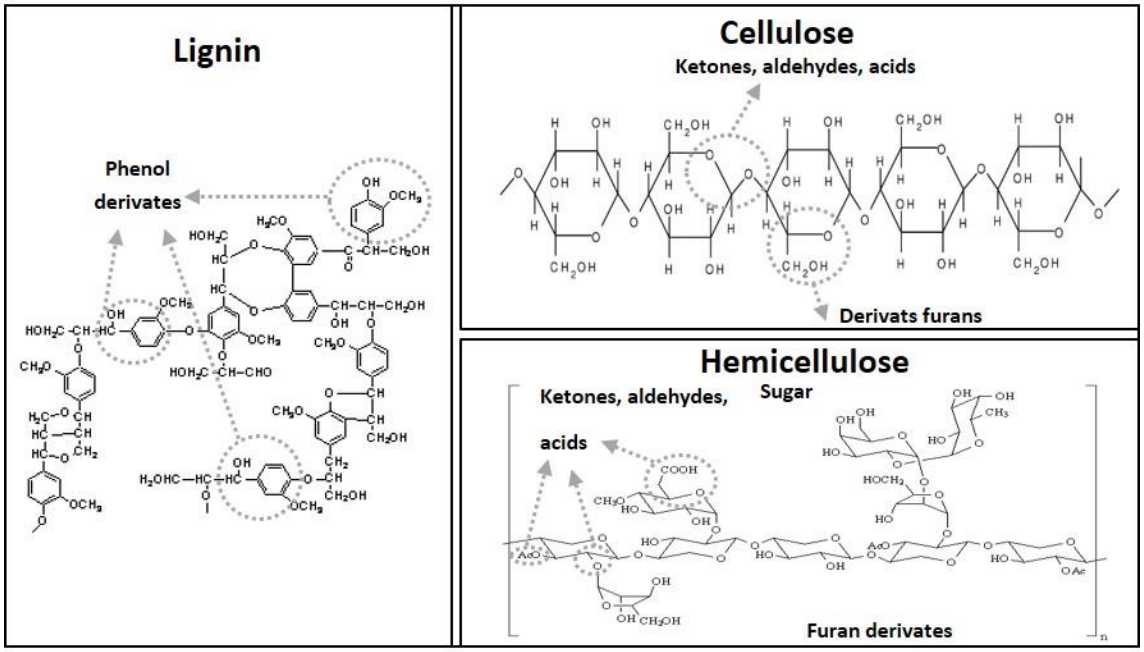

Figure 1.2. Biomass chemical structure and some possible extractable chemical products.

The advantages of using lignocellulosic biomass as renewable resource are numerous:

(1) Lignocellulosic biomass is abundantly available around the world [15]. The bioenergy captured each year by land plants is 3–4 times greater than human energy demands [16].

(2) It might be used as feedstock for production of liquid and solid biofuel for burning and/or gasification in order to generate heat, steam and electricity [11], as well as for the manufacturing of various bio-products and biochemical [17–19].

(3) Biomass as biofuel is considered CO_2-neutral fuel, which does not contribute to the greenhouse effect, due to biomass consumes the same amount of CO_2 from the atmosphere during growth as is released during its combustion [20].

(4) The use of lignocellulosic biomass, mainly agro-forestry residues, as biofuels feedstock minimize the competition of biofuel feedstock with the production of food and forestry products. Thus, it is reduced the risk of land use changes, deforestation and the socio-economic conflicts on this issue [21,22].

(5) Add value to lignocellulosic biomass as biofuels and bio-products might raising the economic activity of rural region. Furthermore, the use of forestry waste biomass as a renewable energy source might add value to this product boosting a proper forest management and reduce the forest fire risk.

Despite the main advantages of biomass use, it presents inherent problems when it is compared to fossil fuels resources as low bulk density, high moisture content, hydrophilic nature, and low calorific value render raw biomass difficult to use on a large scale. These limitations greatly impact logistics (mainly handling and transport) and final energy efficiency, which shall be avoid or minimized in order to use this renewable source. Because of that, many biomass conversion processes has been developed to convert biomass into a more suitable biofuel.

1.2.1. Biofuels

Biofuels refer to biomass and their refined products to be combusted for energy (heat or light) as an alternative of fossil fuels. Global production and utilisation of

bioenergy is in various solid, liquid, and gaseous biofuel forms. Recently, Guo et al. [16] reviewed biofuels history, status and perspectives classifying them into solid biofuels including firewood, wood chips, wood pellets and charcoal; liquid biofuels like bioethanol, biodiesel and bio-oil; and gas biofuels considering biogas and syngas. The advantages and disadvantages of these biofuels are briefed in Table 1.1. To sum up, solid biofuels are most available in source materials, most efficient in feedstock energy recovery, and most effective in conversion technology and production cost, but they are bulky, inconvenient to handle, low in energy density, and only applicable to solid fuel burners. Liquid biofuels are energy-dense, convenient to transport, and can substitute gasoline and petrol diesel; however, they are low in net energy efficiency, have stringent requirements for feedstock, and involve complicated conversion technology and high production cost. Gaseous biofuels can be produced from organic waste materials and residues using well- practiced techniques, yet there are fuel upgrading and by-product disposal challenges.

Table 1.1. Advantages, disadvantages and production status of different biofuels (2013).

Biofuels		Advantages	Disadvantages	Production
Solid	Firewood	Renewable, readily available, cheap, most energy efficient	Bulky, low in energy density; high hazardous emission from incomplete combustion; unsuitable for automated burners	$17 \cdot 10^8$ m^3
	Wood chips	More convenient to transport, handle and store than firewood; lower SO_2 and NOx emissions than coal upon combustion	Involves chipping cost; tends to decay during storage; bulkier and lower in energy density than coal; ash slagging and boiler fouling; unsuitable for precise combustion	$3{,}5 \cdot 10^8$ T
	Wood pellets	Convenient to transport, and handle and store, low SO_2 and NOx emissions; suitable for precise combustion	Higher processing cost; lower energy content than coal; only be used in solid fuel burners	$20 \cdot 10^6$ T
	Charcoal	Stable, high energy content, clean burning	High production cost; bulk, inconvenient for transport; cannot be used in liquid fuel and gas burners	$51 \cdot 10^6$ t
Liquid	bioethanol	Renewable substitute for gasoline; low combustion emissions; existing feedstock production system	Low net energy efficiency; corrosive to existing gasoline fuelling devices; competing with food and feed for source materials	$23 \cdot 10^6$ gal
	Biodiesel	Renewable substitute for petro diesel; existing feedstock production systems	Competes with food production; feedstock is limited to lipids; corrosive to existing diesel fuelling devices; substantial processing cost	$63 \cdot 10^8$ gal
	Bio-oil	Renewable feedstock; same conversion technology	Upgrading is needed prior to fuel uses; immature upgrading techniques	Pilot production $<1 \cdot 10^6$ gal
Gaseous	Biogas	From organic waste and residues, wide feedstock sources; fits the existing natural gas grid	Usually in rural areas; requires intensive feedstock collection and waste disposal	$25 \cdot 10^9$ m^3 CH_4
	Syngas	Mature production technology; as feedstock for industrial chemicals	Char and bio-oil as by-products; stringent requirements for feedstock	$4{,}5 \cdot 10^{11}$ m^3

Source: [16]

1.2.2. Biomass conversion processes

There are several available methods to convert biomass into biofuels and into chemicals including thermal, biological and physico-mechanical processes (Figure 1.3.). [23–26]. Biological processes are usually very selective and produce a small number of discrete products in high yields using biological catalysts. They include: fermentation to obtain products such as bioethanol or butanol; anaerobic digestion to produce biogas or hydrogen; and transesterification in order to generate biodiesel. Physico-mechanical conversion processes are generally needed to process biomass, which involve reducing the particle size (chipping, pulverisation, briquetting or pelletizing) and drying. Thermochemical processes are combustion, torrefaction, pyrolysis and gasification [27–31]. Combustion technologies produce about 90 % of the energy from biomass, converting biomass into several forms of useful energy. It is the most extended thermochemical process since it is used for household cooking and space heating mostly in developing countries, as well as, for industrial combustion and cogeneration plants, which generate electricity from steam-driven turbines [32]. Torrefaction, pyrolysis and gasification are thermal conversion processes based on biomass decomposition in presence or absence of oxygen.

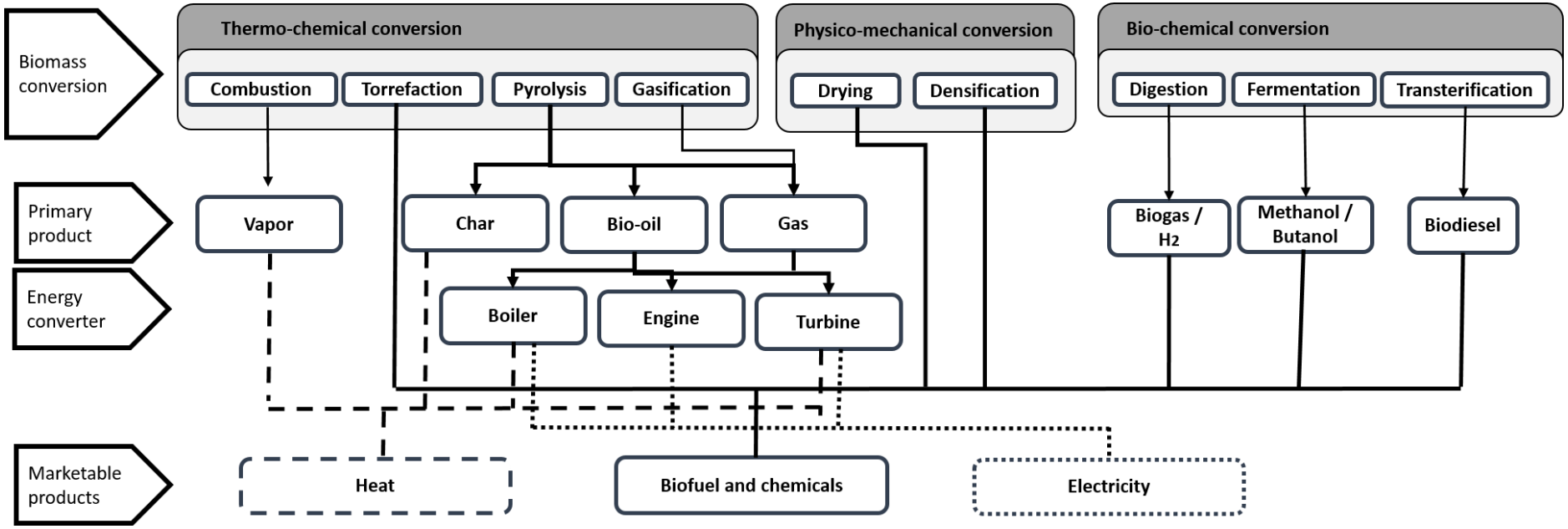

Source: adapted from [25,33]

Figure 1.3. Main conversion processes from biomass to secondary energy carriers

Lignocellulosic biomass thermal decomposition depends on the individual roles of its main components: Hemicellulose, cellulose and lignin. Lignocellulosic biomass decomposition can be divided into the following 4 ranges (Fig. 1.4.): (1) <200 °C where moisture elimination occurs (2) 200-315 °C where predominantly hemicellulose is decomposed; (3) 315-400 °C where cellulose decomposition take place; and (4) >400 °C lignin descomposes. Figure 1.4. shows a Thermogravimetry analysis (TGA) of the three main biomass components where it is represented the loss of mass (wt %) versus the temperature in absence of oxygen. This figure demonstrates the different behaviour of biomass components with temperature. When the mass loss rate (wt % / ºC) is calculated (DTGA), decomposition peaks of hemicellulose and cellulose can be clearly observed. From this decomposition, three main products (gas, liquid and solid) are always produced, but the yield of each fraction varies over temperature. An example is shown in Figure 1.5., where it is observed the products yields distribution obtained from pine wood pyrolysis as function of the reactor temperature. Thus, reactor temperature is crucial operational parameter to obtain mainly a solid, a liquid or a gas product, as well as the composition of these product. According to operational reactor temperature, Table 1.2. indicates the product distribution obtained from different processing modes, showing the considerable flexibility achievable by changing process conditions. Torrefaction is performed at lower temperatures between 200 – 300 º C where is mainly obtained a solid with enhanced properties as fuel in comparison to raw biomass [34] Gasification is carried out at higher temperatures between 750-900 ºC in presence of oxygen obtaining a synthesis gas as main product. Pyrolysis is performed at temperature around 500 ºC in absence of oxygen. Pyrolysis can be mainly divided into slow pyrolysis and fast pyrolysis depending on the operation conditions that are used. [35]. Slow pyrolysis is carried out at slow heating rates between 5-30 min and it has been applied for thousands of years mainly for the production of charcoal [36–38]. Fast pyrolysis is carried out at faster heating rate and the generated vapours are condensed to obtain mainly a brownish liquid called bio-oil that might be used as liquid fuel or as chemical platform [23,35,39].

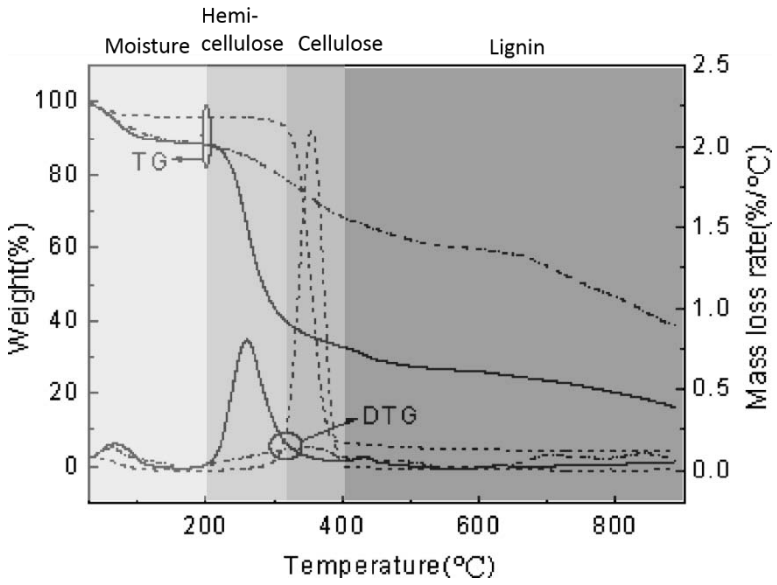

Source: Adapted from [40]

Figure 1.4. Decomposition curves of three main compounds of lignocellulosic biomass: hemicellulose (—); cellulose (- - -) and lignin (····).

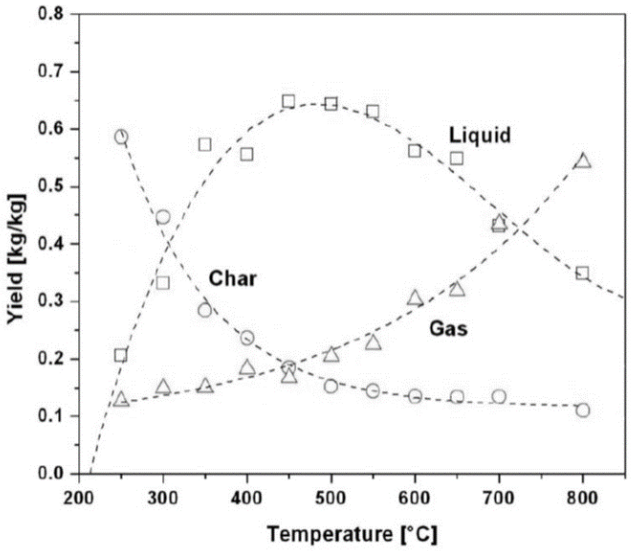

Source: [41]

Figure 1.5. Product yields obtained from pyrolysis of pine wood as a function of the reactor temperature: liquid fraction (□), solid fraction (○) and gas fraction (Δ).

Table 1.2. Typical product weight yield (dry wood basis) obtained by different thermal conversion processes.

Conversion process	Operational conditions	Liquid	Solid	Gas
Torrefaction	200 - 300 ºC 15-120 min solids residence time ~ 10-60 min	0% unless condensed then up to 5%	80% solid	20%
Fast pyrolysis	~ 500 ºC hot vapour residence time ~ 1 s	75%	12% char	13%
Intermediate pyrolysis	~ 500 ºC Hot vapour residence time ~ 10-30 s	50% in 2 phases	25% char	25%
Slow pyrolysis	~ 400 ºC 5-30 min	30%	35% charcoal	35%
Gasification	~ 750-900 ºC	5%	10% char	85%

Source: [42]

This dissertation is focused on the thermochemical conversion processes, particularly, torrefaction and fast pyrolysis processes. Torrefaction process has a special interest due to permit to enhance biomass physical and chemical properties to obtain a high energy density solid biofuel, closer to the properties of coal. Torrefied biomass can be densified converting it into a convenient energy carrier in terms of transport, storage and handling. The potential market of torrefied pellets is expected to be large in a short-term as a solid bio-fuel for domestic, commercial and industrial heat generation and as a co-firing fuel with pulverised coal in Combined Heat and Power plants (CHP) and metallurgical processes to replace partially coal use. Regarding to pyrolysis process, its concerns is focused on bio-oil, the main fraction of this process, since it is a storable and easily transportable liquid biofuel. Its use as industrial fuel in boilers of district heating and CHP plants are already in demonstration and industrial stage of development. However, bio-oil can be a potential resource and platform for producing transport fuels and chemicals with higher added value. However, commercialisation of bio-oil for fuels and chemicals production is limited due to its notoriously undesirable characteristics that are needed to be upgraded. Figure 1.6. shows the development stages of the

different added value products of torrefaction and pyrolysis process for its marketability along the time.

Further information on these processes are detailed in the following sections.

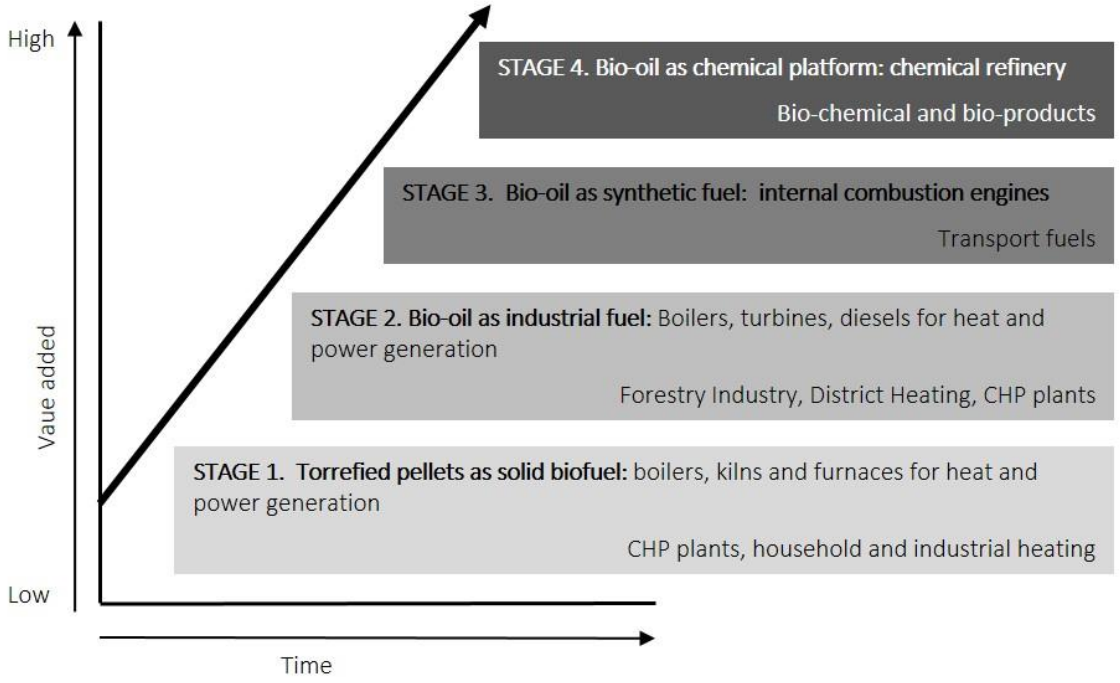

Source: Adapted from [35]

Figure 1.6. Development stages of pyrolysis and torrefaction products regarding to their potential use.

1.3. Torrefaction

Torrefaction is a biomass thermal pre-treatment process carried out with the aim of enhance raw biomass characteristics (high moisture, low calorific value, hygroscopic nature and low bulk density) to obtain an improved solid biofuel which performs better for combustion boilers, co-firing and gasification purposes [43,44]. Many reviews on this issue are published [14,34,45,46].

The torrefaction process consists on heating biomass with or without presence of oxygen at atmospheric pressure and temperature range of 200-300 ºC for residence times of 15-120 min after a proper drying and chipping process of the raw biomass (Figure 1.7.). The degree of torrefaction can be described by the colour changes of raw biomass, from brown at 150 ºC to black at 300ºC (Figure 1.8.).

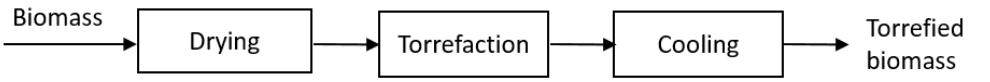

Source: [47]

Figure 1.7. Scheme of the basic torrefaction process

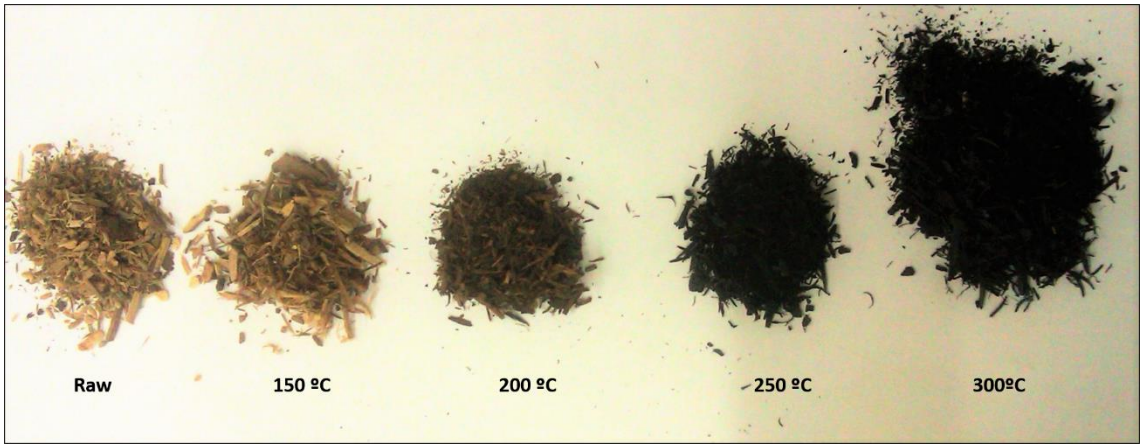

Figure 1.8. Colour changes during the torrefaction process.

Process temperature has influence on the degree of lignocellulosic biomass decomposition, and consequently, on the distribution of fractions yield and their composition. Three different fractions are produced during the torrefaction process (as well as on all the thermochemical processes): (1) a solid fraction, called torrefied biomass, is the primary product of this process (2) liquid fraction which consists on condensable volatile organic compounds; (3) non-condensable gases. The higher the reactor temperature is, the higher biomass decomposition occurs; which results into a higher yield to liquid and gas fraction in detriment of solid one [48]. A typical mass and energy balance for woody biomass torrefaction is that 70% of the mass is retained as a solid product, containing 90% of the initial energy content. The other 30% of the mass is converted into torrefaction gas and volatiles, which contains only 10% of the energy of the biomass [49]. The major decomposition reactions affect the hemicellulose while lignin and cellulose also decompose but to a lesser degree [40,45]. Liquid and gas products produced at low torrefaction temperature contain mainly hemicellulose decomposition products while at higher temperature will appear also cellulose and lignin decomposition ones.

Torrefaction time is another important operational parameter ranging from several minutes [50,51] to several hours [52]. An increase of residence time raises the carbon content and energy density of the solid phase. However, thermal degradation of biomass is rapid at torrefaction time less than 1 h and became very slow beyond this time [53].

The flexibility, moisture, particle size and composition of torrefaction feedstock also have an important role on reaction mechanisms, kinetics and duration of the process [43,50,54].

Many studies are carried out torrefying a wide variety of biomasses at different operational conditions which are listed in Chen et al. [45].

1.3.1. Torrefaction products

In this section, there are detailed the characteristics and applications of the different torrefaction products.

a. *Torrefied biomass*

Torrefied biomass is a solid fuel with enhanced physical and chemical properties in comparison to raw biomass. The benefits accomplished by torrefaction in solid fraction are: higher heating value and energy density; lower atomic O/C and H/C ratio; low moisture content; higher hydrophobicity; improved grindability and reactivity; and more uniform properties of biomass [34,46]. Thus, it is achieved a high energy density solid biofuel with reduced volume in comparison to raw biomass, making it easy to handle, storage and transport. Figure 1.9. shows a summary of changes in biomass properties before and after the torrefaction.

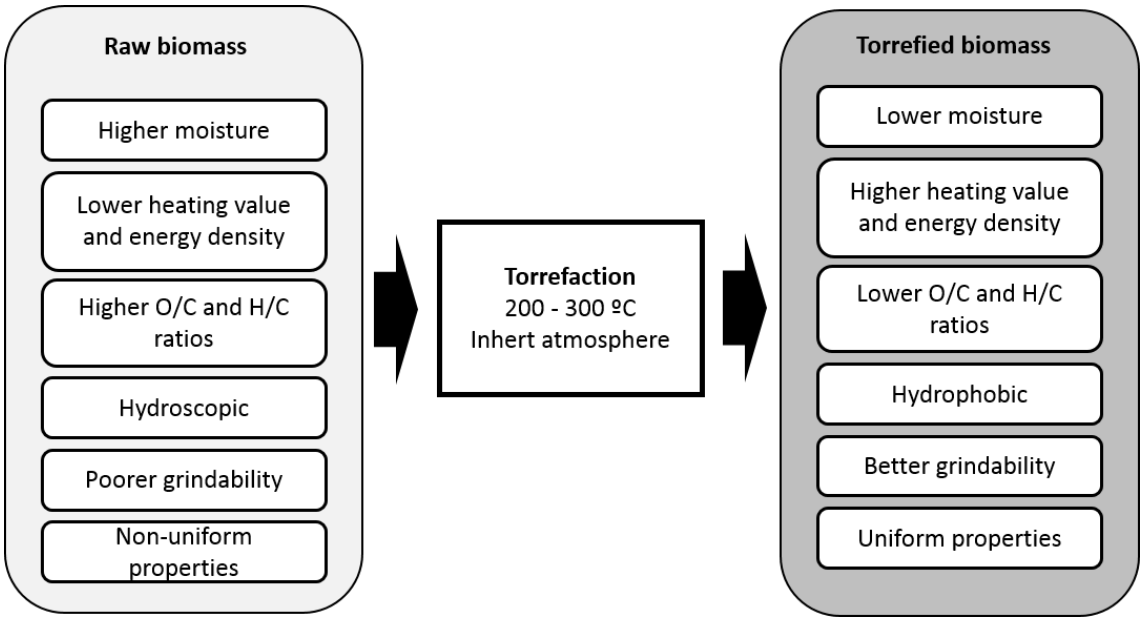

Source: [45]

Figure 1.9. A schematic of property variation of biomass undergoing torrefaction

The analysis and knowledge of torrefied biomass characteristic permit to understand the benefits of torrefaction process and enumerate the possible applications of this product. Because of that torrefied biomass properties and its applications are outlined below.

Torrefied biomass properties

Torrefied biomass properties achieved during the torrefaction process are detailed below.

Torrefied biomass contents a 1-3 wt % of moisture depending on the torrefaction conditions [55]. Torrefied biomass low moisture content reduces the high energy loss in the course of burnings, increasing the energy efficiency and reducing the burning emissions. Moreover, its transportation is less expensive, as a consequence of less moisture content.

Torrefaction changes the hydroscopic nature of biomass to hydrophobic removing OH groups and causing the loss of biomass capacity of form hydrogen bonds [56]. The hydrophobicity preserves the biomass for a long time without biological degradation.

Raw biomass becomes more porous through the torrefaction process when mass loss occurs. That results in a significant reduction of volumetric density, typically between 180-300 kg/m^3, depending on initial biomass density and torrefaction conditions [57]. Despite bulk density reduction, energy density increases from 18-23 MJ/Kg to 20-24 MJ/Kg [58,59] owing to a carbon content rise and oxygen content reduction. Biomass loses relatively more oxygen and hydrogen than carbon when it is decomposed into mainly water, CO and CO_2. This process decreases hydrogen-to-carbon ratio (H/C) and oxygen- to-carbon (O/C) ratios which results in less smoke and water vapour formation and reduced energy loss during composition and gasification processes.

Torrefied biomass is easier to grind and pulverize in comparison to raw biomass [60]. Grind torrefied biomass is required to facilitate its injection to boilers or blast furnaces and its fast combustion. During the torrefaction, the breakdown of hemicellulose and cellulose changes biomass microstructure giving rise to the improved grindability of torrefied biomass [49].

Due to the high variety of raw biomass feedstock, obtaining a uniform solid product implies an advantage for its potential applications. Torrefied biomass is an uniform solid taking into account the particle size distribution, sphericity and surface area) in comparison to untreated biomass [61].

Torrefied biomass pelletability

Beside the properties previously mentioned, one of the most appreciate properties of torrefied biomass as its pelletability. Torrefied biomass pelletisation has been considered by several researchers [47,62–64] due to the obtained product joint the advantages of torrefied biomass (low moisture content, high energy content, resistance against biological degradation and good grindability) and biomass pellet (facilitate its storage, handling and reduce the transportation cost). Energy Research Centre of the Netherlands (ECN) described a process called TOP process which combines torrefaction and pelletisation processes to obtained a TOP pellet [47] (Figure 1.10.). In

Table 1.3., it is compared the characteristics of this TOP pellet with conventional pellet, torrefied biomass and raw biomass. As it can be observed, torrefied pellet energetic density is increased in a 70-80 % in comparison to conventional ones. Moreover, the quality of conventional biomass pellets strongly depends on the variability of feedstock quality due to differences in the type of raw materials, tree species, climatic and seasonal variations, storage conditions and time [59] while torrefied pellets have an uniform composition.

The pelletability of torrefied biomass is demonstrated [43,47,65]. Torrefied biomass pelletability is assessed by their lignin content due to it is considered the basic binding agent [43]. In general, higher amounts of lignin improve binding and reduce the severity of process conditions. The torrefaction process opens more lignin active sites by breaking down hemicellulose matrix and forming fatty unsaturated structures, which creates better binding [45].

Potential applications of torrefied biomass

Torrefied biomass properties make this product an enhanced biofuel in comparison to raw biomass, which might substitute or reduce the use of fossil fuels use in order to diminish our dependency on them and lessen their use associated environmental problems. Thus, potential applications of torrefied biomass include:

- High-quality smokeless solid fuels for industrial, commercial and domestic applications.
- Solid fuel for co-firing directly with pulverized coal at electric power plants and metallurgical processes to replace partially coal. Actually, chip biomass and conventional biomass pellets are used for this purpose. However, the inherent differences between coal and biomass only permit a 5-15 % of the total input to the boiler supposing, in general, substantial modification to the boilers and losing boiler efficiency. That is because of the higher moisture and low energy content of biomass fuels compared to coal. In this way, torrefied biomass is more similar to coal and, consequently, more suitable for co-firing applications [66].

- Solid fuel for gasification to generate synthesis gas or syngas (H_2 + CO_2) from fuels in an oxygen deficient environment. Using torrefied biomass instead of raw one, might permit to improve the gasification efficiency and diminish the tar formation because of its high heating value and low volatiles content [51].
- An upgraded feedstock for fuel pellets, briquettes and other densified biomass fuels.

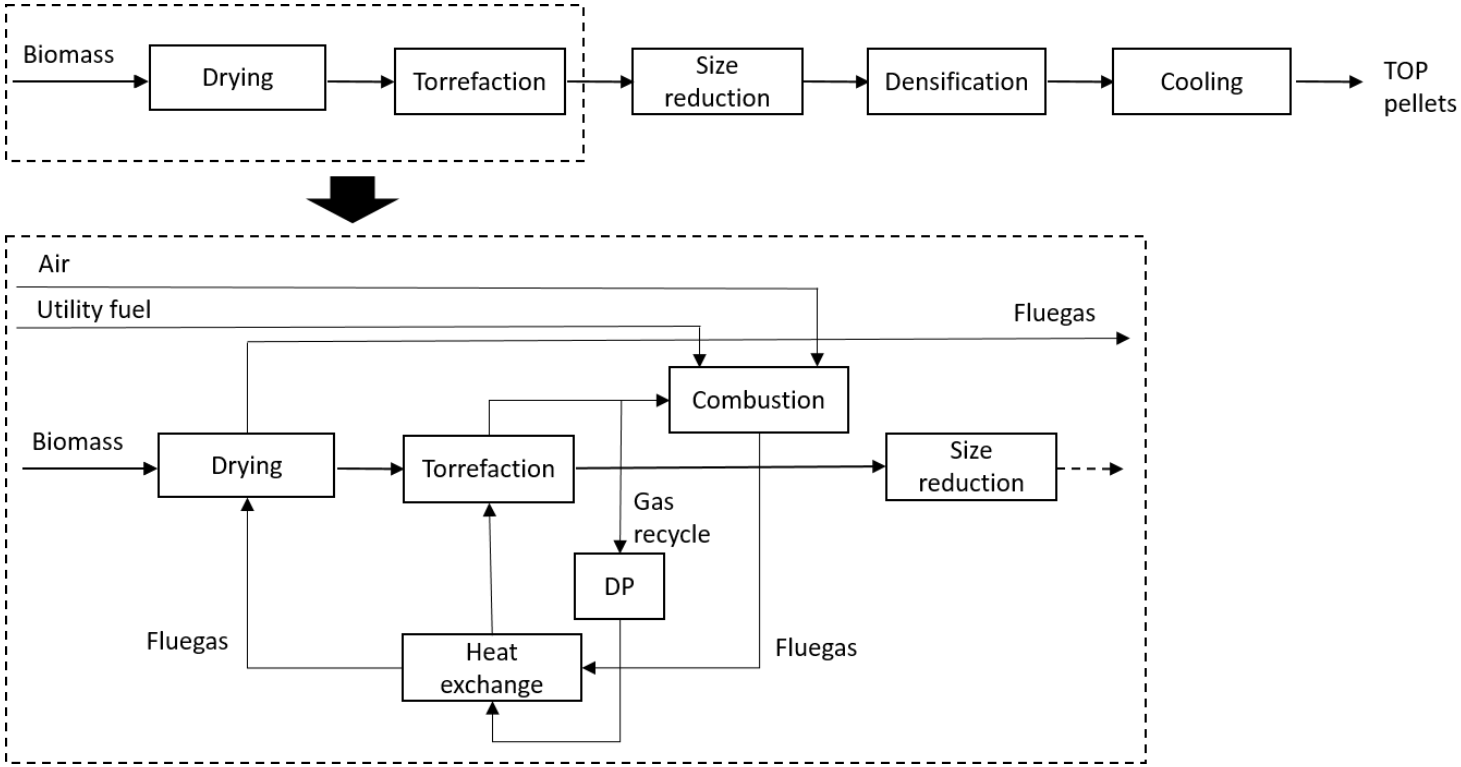

Source: [47]

Figure 1.10. Scheme of the basic TOP process.

Table 1.3. Comparison of properties of wood, torrefied biomass, wood pellets and TOP pellets

Properties	Unit	Wood	Torrefied biomass	Wood pellets		TOP pellets	
				Low	high	low	high
Moisture content	% wt	35	3	10	7	5	1
Calorific value (LHV)							
as received	MJ/kg	10.5	19.9	15.6	16.2	19.9	21.6
dry	MJ/kg	17.7	20.4	17.7	17.7	20.4	22.7
Mass density (bulk)	kg/m^3	500	230	500	650	750	850
Energy density (bulk)	GJ/m^3	5.8	4.6	7.8	10.5	14.9	18.4
Pellet strength		-	-	good		very good	
Dust formation		moderate	high	limited		Limited	
Hygroscopic nature		water uptake	hydrophobic	swelling/water uptake		poor swelling/hydrophobic	
Biological degradation		possible	impossible	Possible		impossible	
Seasonal influences (noticeable for end-user)		high	poor	Moderate		poor	
Handling properties		normal	normal	Good		good	

Source: [47]

b. *Torrefaction liquid*

Torrefaction liquid is a brown or dark liquid resulting of condensing the condensable gases generated by the biomass thermal decomposition. The main condensable product of torrefaction is water released during the raw biomass drying process when moisture evaporates and during dehydration reactions between organic molecules. Torrefaction liquid contains condensable organics produced during raw biomass devolatilisation as acetic acid, alcohols, aldehydes and ketones [48,67]. The type and amount of condensable organics depends on the feedstock composition and the operational conditions of the torrefaction process, mainly the temperature [48,67]. At low temperatures (200-240 ºC), acetic acid, methanol, furfural and 1-hydroxy-propane are the main compounds which are degradation products of hemicellulose [68,69]. At higher temperature also cellulose and lignin starts to decompose resulting in presence of phenols, aldehydes and ketones in the torrefaction liquid (see Figure 1.2.).

Torrefaction studies are not been focused on the potential utilisation of torrefaction liquid. However, Fagernas et al. [67] stated that torrefaction liquid might be

used with similar proposes of wood distillates from the slow pyrolysis process of charcoal production called wood vinegars or pyroligneous acids. These liquids are used in agriculture as fertilizer and growth-promoting agent [70], as effective fungicides [71], biodegradable pesticides [72,73] and wood preservatives [74] among others. Moreover, torrefaction liquid organic compounds are among the value-added chemicals that might be obtained from thermochemical conversion of lignocellulosic biomass presented recently by de Wild [19]. Thus, torrefaction liquid might be a valuable product by itself as fertilizer, fungicide or wood preservative or as a chemical platform to extract individual organic compounds. However, extraction of value-added chemical from such a complex liquids are not well developed and further investigations on it will be needed [67], becoming the other torrefaction liquid applications more feasible at short-term. Taking into account torrefaction liquid potential uses, it might be considered a future marketable product which will increase the economic efficiency of the torrefaction process.

c. *Gas fraction*

The non-condensable gas products comprise primarily CO, CO_2 and small amounts of CH_4 [48,49]. Toluene, benzene and low molecular weight hydrocarbons are also detected. The gas product typically contains less than 10 % of the energy of biomass. Because of the low heating value of the gas product, its application is limited [45].

1.3.2. Technology development of torrefaction process

A wild range of different torrefaction reactor technologies are under development at pilot-scale plants at research institutes and universities as Energy research Centre of the Netherlands (ECN), the Spanish National Renewable Energy Centre (CENER) and BioEndev (Sweden). All this reactor technologies are “proven technology” in other applications, such as combustion, pyrolysis or gasification [75]. At commercial scale, torrefaction technology is currently in its early phase. Several technology companies and their industrial partners are gradually moving towards its commercial market

introduction such as Torpell, 4Energy Invest, Torr-Coal and Thermya, reviewed by Chew and Doshi [34]. An overview of reactor technologies that are applied for torrefaction at commercial or demonstration stage are presented in Table 1.4, as well as, their technology suppliers. Some providers claimed that they have reached commercial production, although the current general view is that demonstration plants have technical problems that have delayed their commercial operation [76].

Table 1.4. Torrefaction technology development at a commercial or demonstration stage.

Developer	Technology	Supplier	Status	Location	Production capacity (t/a)	Product
Topell Energy (NL)	Torbed (fluidized bed reactor)	Torftech (UK)	commercial demo plant	Duiven (NL)	60000	Torrefied pellet
Renogen / 4EnergyInvest (NL)	Rotatory drum reactor	Stramproy Group (NL)	commercial operation	Amel (BE)	?	Co-generation power plant
Renogen / 4EnergyInvest (NL)	Rotatory drum reactor	Stramproy Group (NL)	commercial operation	Amel (BE)	38000	Torrefied pellets
Renogen / 4EnergyInvest (NL)	Rotatory drum reactor	Stramproy Group (NL)	commercial operation	Ham (BE)	38000	Co-generation power plant
Torr-Coal (NL)	Rotatory drum reactor	Unknown	-	Dilsen-Stokkem (BE)	35000	
AREVA	Compacting moving bed	Thorspyd (Thermya)	-	Urnieta (SP)	20000	
AREVA	Compacting moving bed	Thorspyd (Thermya)	-	Mazingarbe (FR)	20000	
Unknown	Rotatory drum reactor	Andritz (AT) / ECN (NL)	Industrial Demo plant	Sdr. Stenderup (DK)	700000	Torrefied pellets
Unknown	ABC reactor (rotatory drum reactor)	Andritz	Industrial Demo plant	Frohnleiten (AT)	50000-250000	Briquettes
New biomass energy	screw reactor	new biomass energy	Commercial operation	Mississipi (USA)	40000 (up to 160000)	Torrefied pellets

Source: adapted from [77] and updated

1.4. Fast pyrolysis

Fast pyrolysis is a high temperature thermochemical process performed with the aim of producing mainly a dark brown liquid, called bio-oil which might be used as liquid biofuel and as chemical platform to obtain biochemical products.

Fast pyrolysis process consists in decomposes biomass feedstock heating it rapidly under inert environment, atmospheric pressure, temperature around 500 ºC and residences time of less than 2 seconds to generate mostly vapours and aerosols. After a cooling and condensation step, bio-oil is formed. A fast pyrolysis process requires a feedstock drying its feedstock typically to less than 10 wt % of water content in order to minimise the water in the liquid product and a feedstock grinding process to sufficiently small particle to ensure rapid reaction. Rapid and efficient separation of solids (char) is required, usually using a cyclone, as well as rapid quenching and collection of the liquid product with a condenser. Figure 1.11 shows a scheme of the basic fast pyrolysis process.

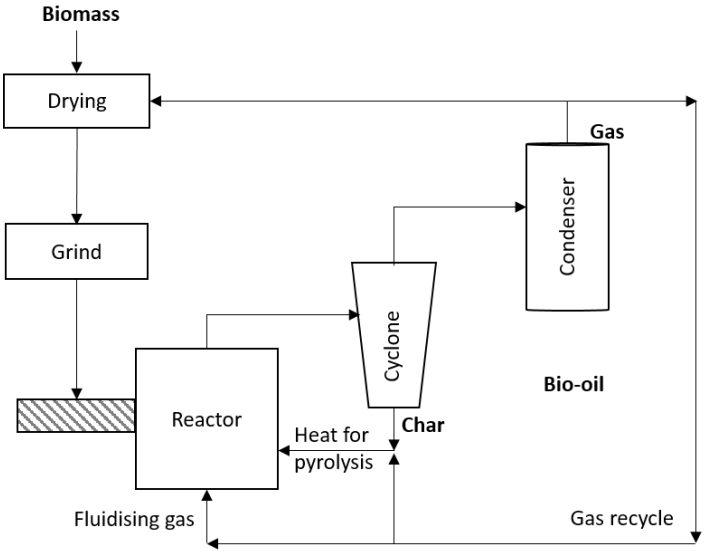

Source: [35]

Figure 1.11. Scheme of the basic fast pyrolysis process

The key features of fast pyrolysis and bio-oil have been reviewed by several researchers [30,35,38,78–80].

Temperatures around 500 ºC permit the maximisation of liquid yields for most biomasses, being bio-oil the main product. Biochar (solid fraction) and non-condensable gases are by-products of the process. In a typical mass balance of woody biomass pyrolysis, 50-70% of the mass is retained as bio-oil, 10-30 % of the mass is converted into biochar and the other 15-20 % of the mass is non-condensable gases. This last fraction only contents 5% of the raw biomass [81].

Biomass particle exposure at temperature below 500 ºC needs to be minimised not to favour biochar formation. Because of that, it is required very high heating rates and high heat transfer rates at the biomass particle, which is reached grinding biomass feedstock of typically less than 3 mm of particle size.

Short hot vapours residence times of typically less than 2s are required to minimise secondary reaction which implies rapid cooling systems, as well as, rapid removal of product char and ash to this vapours to minimise its cracking. Char acts as vapour cracking catalyst so rapid and effective separation from the pyrolysis product vapours is essential. Cyclones, hot vapour filtration and pressure filtration of the liquid are used with this aim.

1.4.1. Fast pyrolysis products

Characteristics and applications of the different fast pyrolysis products are detailed in this section.

a. *Bio-oil*

Bio-oil, also referred to as biomass pyrolysis liquid, pyrolysis oils or bio-crude oil, is a dark and thick liquid with smoky odour. It is a complex mixture of compounds that are derived from the depolymerisation of cellulose, hemicellulose and lignin. The physico-chemical properties of bio-oil are well documented in the literature [38,42,79,82–87].

Chemically, it comprises quite a lot of water, more or less solid particles and hundreds of organic compounds that belong to acid, alcohols, ketones, aldehydes,

phenols, ethers, ester, sugars furans, nitrogen compounds and multifunctional compounds (Table 1.5.). Over 300 organic compounds have been identified in different bio-oils, most of them in low concentrations. However, complete chemical characterisation of bio-oil is almost impossible due to the complexity of the sample. Moreover, bio-oil chemical composition depends a lot from the converted feedstock and pyrolysis process operation parameters. Bio-oil contains compounds with very different polarities: highly polar compounds (water, acid and alcohols), less polar once (esters, ethers and phenolic) and non-polar compounds (hexane and other hydrocarbons)[38] . These compounds are no completely mutual soluble, because of that bio-oil can be considered as a microemulsion where water and water soluble molecules form a continuous phase with dispersed micelles of water insoluble compounds [87].

Table 1.5. Some organic compound present in bio-oil classified in organic groups

Organic groups	Compounds
Acids	Formic, acetic, propanoic, hexanoic, benzoic, etc
Esters	Methyl formate, methyl propionate, butyrolactone, methyl n-butyrate, velerolactone, etc.
Alcohols	Methanol, ethanol, 2-propene-1-ol, isobutanol, etc
Ketons	Acetone, 2-butanone, 2-butanone, 2-pentanone, 2-cyclopentanone, 2,3 pentenedione, 2-hexanone, cyclo-hexanone, etc.
Aldehydes	Formaldehyde, acetaldehyde, 2-butenal, pentanal, ethanedial, etc.
Phenols	Phenol, methyl substituted phenols.
Alkenes	2-methyl propene, dimethylcyclopentene, alpha-pinene, etc.
Aromatics	Benzene, toluene, xylenes, nphthalenes, phenanthrene, fluoranthrene, chrysene, etc
Nitrogen compounds	Ammonia, methylamine, pyridine, methylpyridine, etc
Furans	Furan, 2-methyl furan, 2-furanone, furfural, furfural alcohol, etc
Guaiacols	2-methoxy phenol, 4-methyl guaiacol, ethyl guaiacol, eugenol, etc.
Syringols	Methyl syringol, 4-ethyl syringol, propyl syringol, etc.
Sugars	Levoglucosan, glucose, fructose, D-xylose, D-arabinose, etc.
Miscellaneous oxygenates	Hydroxyacetaldehyde, hydroxyacetone, dimethyl acetal, acetal, methyl cyclopentenolone, etc

Source: adapted from [30]

As can be seen, bio-oil is totally different from petroleum fuels in chemical composition, which will result in the vast difference in the fuel properties between them (Table 1.6.). Bio-oil is a low-grade liquid fuel when compared with fossil oils due to the complex multiphase structure; high content of oxygen, water, solids and ashes; low heating value; high viscosity and surface tension; low pH value; poor ignition and combustion properties; and chemical and thermal instability. Despite of that, bio-oil is less toxic and more biodegradable than fuel oil. Due to its poor chemical and thermal stability, chemical reactions continue to occur during its recovery, storage and transport which change bio-oil physical and chemical properties including viscosity increase, phase separation, increase in average molecular weight and varying chemical composition [88]. This process is known as aging process. Bio-oil properties are listed in Table 1.7. indicating their causes and effects on bio-oil properties as liquid biofuel. Bio-oil upgrading is required to enhance these properties, many efforts has been carried out on this issue (see section 1.4.2).

Table 1.6. Properties of wood bio-oils and mineral oils: heavy fuel oil (HFO) and light fuel oil (LFO)

Analysis	Typical bio-oil	HFO 180/420 (*)	LFO motor / heating EN590 (
Water wt %	20-30	0	0
Water and sediment. vol %		0.5 max	0.02 max
Solid wt %	below 0.5		
Ash (wt %)	0.01-0.1[a]	0.08 max	0.01 max
C (wt %)	54-58	85	
H (wt %)	5.5-70	11	
O (wt %)	35-40	1	
N (wt %)	below 0.4	0.4	0.02
S (wt %)	below 0.05	1 max	0.001 max
Stability	Unstable [b]		
Viscosity 40ºC (cSt)	15-35 [c]	180/420 max a 50 ºC	2.0-4.5
Density 15ºC (kg/L)	1.10-1.30 [c]	0.99/0.995 max	0.845 max
Flash point (ºC)	40-110[d]	65 min	60min
Pour point (ºC)	-9-36	15 max	-5min
LHV (MJ/kg)	13-18[c]	40.6 min	42.6
pH	2-3		
Distillability	Non-distillable	Distillable	Distillable

Source: [84,89]

Table 1.7. Bio-oil characteristics, its causes and the effects of bio-oil properties on as a liquid biofuel.

Characteristics	Cause	Effects
Colour	· Cracking of biopolymers and char	·Discolouration of some products such as resins
Water content	· Pyrolysis reactions · Feedstock water	· Complex effect on viscosity and stability · Increased water lowers heating value and density
Acidity	Organic acids from biopolymer degradation	Corrosion of vessels and pipework
High viscosity	Chemical composition of bio-oil	· Variable with time · Greater temperature influence than hydrocarbons · Gives high pressure drop increasing equipment cost · High pumping cost and poor atomisation
High oxygen content	·Biomass composition	·Poor stability · non-miscibility with hydrocarbons
Low miscibility with hydrocarbons	·Highly oxygenated nature bio-oil	Difficult integration into a refinery due not to mix with any hydrocarbon
Low H:C ratio	·Chemical composition of bio-oil	Upgrading to hydrocarbons is more difficult

Table 1.7. (Continued). Bio-oil characteristics, its causes and the effects of this properties on its properties as a liquid fuel

Characteristics	Cause	Effects
Chlorine content	·Contaminants in biomass feed	Catalyst poisoning in upgrading
Low heating value	· high water content · High oxygen content ·low H:C ratio	· less efficiency of furnace and boiler devices
Nitrogen content	· Contaminants in biomass feed · High nitrogen feedstock such as proteins in waste	· Unpleasant smell · Catalyst poisoning in upgrading
Solids content	· Char content due to incomplete solid separation · Particulates from reactor such as sand · Particles from feed contamination during harvesting.	· Aging of bio-oil Sedimentation · act as catalysts · can increase particulate carry over · Erosion and corrosion · Filter and engine injector blockage
Alkali metals content	· High ash feed. · Incomplete solid separation · Nearly all alkali metals report to char so not a big problem.	· Catalyst poisoning · Deposition of solids in combustion · Erosion and corrosion · Slang formation · Damage to turbines
Aging	· Continuation of secondary reaction including polymerisation · Bo-oil poor stability	· Slow increase in viscosity from secondary reaction such as condensation ·Potential phase separation
Poor distillability	·Reactive mixture of degradation products	· Bio-oil cannot be distilled. · Liquid begins to react at below 100 ºC and substantially decompose above 100 ºC
Material incompatibility	·Phenolic and aromatics	Destruction of seals and gaskets
Phase separation or inhomogeneity	· High feed water, · High ash in feed · Poor char separation	· Phase separation · Layering · Poor mixing · Inconsistency in handling, storage and processing
Smell or odour	·Aldehydes and other volatile organics, many from hemicellulose	while not toxic, the smell is often objectionable
Toxicity	·Chemical composition of bio-oil	· Human toxicity is possible but small · Eco-toxicity is negligible
Temperature sensibility	Incomplete reactions	· Irreversible decomposition of liquid into two phase above 100 ºC · Irreversible viscosity increase above 60 ºC Potential phase separation above 60 ºC
Instability	· Incomplete reaction · High oxygen content	· ageing during storage,
Low solubility in water	Bio-oil microemulsion structure	Phase separation: aqueous and organic phase

Source: [42]

Bio-oil characterisation

In order to determine fuel quality and chemical applications for bio-oil, it is important to assess and develop reliable analytical methods which permit a proper characterisation of raw bio-oil and upgraded one [90]. Due to the differences between bio-oil and mineral oil properties, standard fuel oil analysis for mineral oils are not always suitable as such for bio-oils. Research analysing physical properties of bio-oil has been carried our since the 1980s [91–94]. Several round robin tests have been performed in order to verify the relevant analytical procedures for bio-oil analysis [95–97]. Based on these round robin tests, the following conclusions were drawn: liquid sample handling plays a very important role, the precision of carbon and hydrogen content analysis by standard methods is good. Oxygen by difference is more accurate than by direct determination, water analysis by Karl fisher titrations is accurate but should be calibrated by water addition method and accuracy of density is good. High variations were obtained for nitrogen, viscosity, pH, solids, water insoluble and stability should be improved. Oasmaa and Peacocke [90,91,98] studies tested the applicability of standard fuel oil method developed for mineral oil to bio-oil and, when it is necessary, they modified them for their adaptation. They published guidelines for pyrolysis liquids producers and end-users to determine the fuel oil quality of bio-oil. Present consensus from end users on significant liquid properties for combustion applications are stability, homogeneity, water, lower heating value, viscosity, liquid density, solids content and to a limited extent chemical composition. For non-fuel applications, other properties may of interest as number of phases, pH and detailed chemical composition [98].

In general, most of the analytical methods described for mineral oils can be used as such but the accuracy of the analysis can be improved by minor modifications. However, a complete and detailed chemical characterisation of whole bio-oil is one of the remaining research issues due to the high complexity of bio-oil chemical composition. Many analytical techniques have been combined to obtain an inclusive analysis of bio-oil composition. Garcia-Perez at al. [99] reported and discussed the techniques used to analyse the chemical composition of bio-oil including GC-MS (volatile

compounds), high performance liquid chromatography (HPLC), HPLC/electrospray MS (nonvolatile compounds), Fourier transform infrared (FTIR) spectroscopy, gel permeation chromatography (GPC) (molecular weight distributions), Ultraviolet-visible spectroscopy (UV), UV-Fluorescence, nuclear magnetic resonance (NMR), thermogravimetry (TG) analysis . Bio-oil fractionation is widely used to separate bio-oil into groups of compounds to facilitate the analysis [100,101].

Bio-oil potential applications

Bio-oil has many potential applications, as it is shown in Figure 1.12. Their potential applications are reviewed by Czernik and Bridgwater [38,83,84,102], which mainly include:

- The use of bio-oil to substitute mineral oil or diesel in many static application including boilers, furnaces, engines and turbines for electricity generation and heat. The application of bio-oil for heat and power generation is possible and usually only requires minor modification of the existing equipment as demonstrated by the tests in boilers, diesel engines and turbines.
- Bio-oil will be used as future transportation fuel. However, more research is needed in the areas due to bio-oil have high oxygen content and instability which hider the use of bio-oil with this aim. Because of that, upgrading and stabilisation processes of bio-oil are required which still poses several technical challenges and is not currently economically attractive (see section 1.4.2.).
- Bio-oil might be used as chemical platform to produce chemicals [17,18,35,103]. There are many substances that can be extracted from bio-oil, such as phenols used in the resins industry, volatile organic acids in formation of de-icers, levoglucosan, hydroxylaldehyde and some additives applied in the pharmaceutical, fibre synthesis or fertilizing industry and flavouring agents in food products. However, their amount are small and isolation of specific single compounds is rarely practical or economic since it is usually required complex separation techniques. Because of that, using whole bio-oil as fertilizer or wood preservative and/or using bio-oil major separable

fractions [100] as liquid smoke or wood resins are the most advanced processes to achieve bio-oil bio-chemical products.

- Because of that, the development of technologies for producing products from the whole bio-oil or from its major, relatively easy separable fractions is the most advanced. Whole bio-oil might be used as fertilizer or wood preservative and its major fractions as liquid smoke or for wood resins.

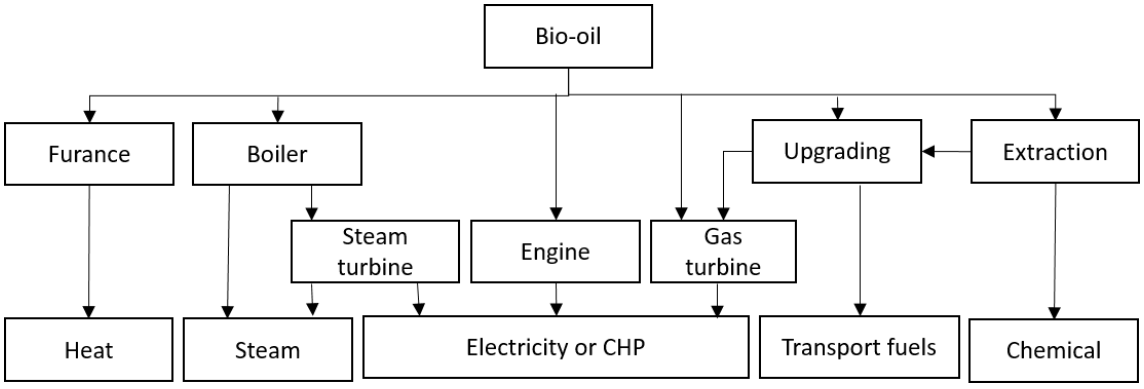

Source: [104]

Figure 1.12. Scheme of bio-oil potential applications.

b. *Biochar*

Char is the solid by-product of fast pyrolysis process [105–107]. This solid is carbon-rich product in comparison to other solid biofuels giving it a high LHV about 32MJ/kg and volatilities content between 15 and 45 wt % [108]. In addition, char also comprises various inorganic species as alkali and alkaline cations which are contained in feedstock are concentrated on bio-char. They may cause slagging, deposition and corrosion problems in combustion. Moreover, unconverted organic solids and carbonaceous residues produced on thermal decomposition of the organic components, in particularly lignin, might be present. Biochar produced during fast pyrolysis are very fine powders and it is very porous, both caused by the rapid devolatilisation of the biomass.

As well as bio-oil, biochar physico-chemical properties are governed by the pyrolysis conditions (heating temperature and duration) and the original feedstock. Possible applications depends on these properties [105–107].

Biochar potential applications

Biochar can be used for various industrial applications which are discussed as follows [30]:

- It might be used as a solid fuel to provide pyrolysis process required energy to make the process self-sufficient.
- The char could be used as a solid fuel in boilers.
- It can be converted into a brickets alone or mixed obtaining a high efficiency fuel in boilers.
- The char could be used for the production of activated carbon.
- Its use as carbon feedstock for making carbon-nanotubes may be explored.
- It can be used further for the gasification process to obtain hydrogen rich gas by thermal cracking with the advantage that alkali metals in the char can be controlled.

Moreover, biochar might be used for other applications as [105]:

- Decontamination of pollutants and bioremediation due to its adsorption capacity of pesticides, heavy metals and hydrocarbons.
- Carbon sequestration due to its recalcitrant character.

c. *Pyrolysis gas*

The pyrolysis gas is formed by the non-condensable gases formed in the pyrolysis process. As example, pyrolysis gas of pine wood at 550 º C contains carbon dioxide (~33 wt %), carbon monoxide (43 wt %), methane and other hydrocarbons (~17 wt %), hydrogen (7 wt %) and minor amounts of higher gaseous organics and water vapour [41]. It has a LHV of around 11 MJ/m^3 because of that it might be used burned jointly with biochar to provide the energy required for the pyrolysis process [41,108].

1.4.2. Bio-oil upgrading processes

Bio-oil upgrading is required to improve bio-oil properties to enhance bio-oil as a liquid biofuel and to obtain a more stable product. The aim of upgrading processes is to obtain a stable final product as transport fuel or fuel for boilers and furnaces or just an intermediate product which can be the feedstock for a biorefinery (see section 1.5.). The key to improve bio-oil properties for these purposes includes viscosity and acidity reduction, as well as the elimination of chemical instability by means of reducing bio-oil oxygen content and removing the solid content.

So far, extensive studies have been focused on this issues and the state-of-art of bio-oil upgrading has been extensively reviewed [42,86,109–112]. Many upgrading processes have been tested. The more significant ones are briefly described in this section. Upgrading process can be broadly classified into chemical and physical methods.

Physical methods include:

- Filtration: hot-vapour filtration can reduce the ash and char content in bio-oil, reducing the catalytic effect of these components, as well as posterior problems of blockage and corrosion in the end-user application of bio-oil [113]. Filtration of bio-oil in liquid phase results difficult due to bio-oil physicochemical nature, and usually requires very high pressure drops and self-cleaning filters.
- Solvent addition. Polar solvents are used to homogenise and reduce the viscosity of bio-oils. Moreover, the addition of polar solvent, especially methanol, slow down the aging process [92].
- Emulsion: bio-oil is not miscible with hydrocarbon fuels but they can be emulsified with diesel oil with the aid of surfactants [114,115].

Chemical methods as:

- Esterification: bio-oil compounds as carboxylic acids and aldehydes can react with alcohols and are converted into esters and acetals, respectively. These reactions

reduce acidity, improve volatility and heating value, as well as lead a better miscibility with diesel fuels [86,116,117],

- Hydrotreating. Hydrotreating consist in provoking bio-oil reaction with hydrogen rejecting oxygen as water in the presence of heterogeneous catalysts in order to reducing bio-oil oxygen content obtaining an energy dense and non-corrosive product, such as naphtha [118].
- Catalytic cracking. In catalytic cracking, oxygen is rejected as CO, CO_2 and H_2O using typically zeolites catalysts, also with the aim of reducing bio-oil oxygen content.
- Catalytic fast pyrolysis. It is the integration of fast pyrolysis and catalytic upgrading in one single reactor. In catalytic pyrolysis condition, biomass is thermally decomposed to volatiles (vapours) that pass over a catalyst bed, converting the vapours into stable and deoxygenated compounds [112].

Among upgrading processes, the most prospective ones are those which oxygen containing functional groups of bio-oil are removed. The upgrading processes focused on these aim are hydrotreating and catalytic cracking which are further describes below. Due to the high diversity of compounds in bio-oil, a complex reaction network takes place during both processes including cracking, decarbonylation, decarboxylation, hydrocracking, hydrodeoxygenation, hydrogenation, and polymerisation [119–121]. Examples of these reactions are given in Figure 1.13. Besides these, carbon formation is also significant in both processes. Formation of carbon (char, tar and coke) through polymerisation and polycondensation reactions constitute a pronounced problem in these upgrading processes due to their deposition on catalyst causes the blockage of

the catalyst pores and its deactivation [122,123]. This complexity makes difficult the control, evaluation and understanding of upgrading processes behaviour.

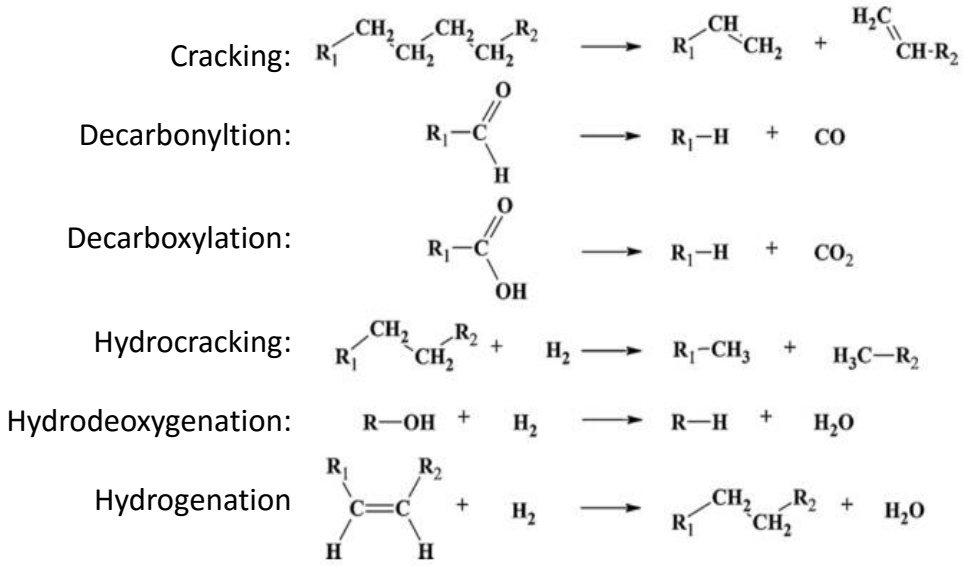

Source: [111]

Figure 1.13. Examples of reactions associated with catalytic bio-oil upgrading.

a. *Hydrotreating (HDO)*

Hydrotreating process aim is to reject oxygen as water by catalytic reaction at temperature ranging from 250-450 ºC under high pressure hydrogen atmosphere (75-300 bar) [29,124–127]. The high pressure increases the hydrogen solubility in the oil, facilitate hydrogen availability by catalyst and decrease carbon formation in the reactor [111,126].

Hydrotreating is a well-known process due to its development to a large extent has been extrapolated from hydrodesulphurisation (HDS) process from the refinery industry, used in the elimination of sulphur from organic compounds [82,128].

Hydrogenation and hydrodeoxygenation are the main reactions [129,130]. A complete bio-oil deoxygenation might achieve an energy dense and non-corrosive product, such as naphtha, with oxygen content less than 2 wt % [118] and maximum yield of 56–58 wt % [128]. Although a complete bio-oil deoxygenation is rarely achieved due to the span of reactions taking place, hydrotreated bio-oil has low content of oxygen

resulting in a decreased O/C ratios, increased H/C ratios, both raising bio-oil calorific value [111].

Regarding to the catalysts used for this upgrading process, the originally ones tested in the 1980s and 1990s were based on sulfided CoMo or NiMo supported on alumina or aluminosilicate using similar process conditions to those used in the desulfursation of petroleum fraction [131–133]. However, these catalysts have the disadvantage of potential deactivation if sulfur is absent in the feed [82]. More recently, attention turned to precious metals catalysts such as palladium (Pd) and ruthenium (Ru) on less susceptible supports[134–137]. Wildschut et al. [126] showed that both yields and the degree of deoxygenation are higher when noble metal catalysts were used instead of the traditional CoMo and NiMo catalysts.

The main barriers presented by this process are: the high cost of hydrogen consumption and the poor bio-oil thermal stability at elevated temperatures. Polymerisation/condensation reactions take place when bio-oil submitted at high temperatures, leading to heavy tar and coke formation. Even when stored for long periods or heated in the absence of catalysts, bio-oil tends to polymerize [11]. The formation of high carbon yields provokes the rapidly deactivation of upgrading catalysts [8–10] and reduce the upgraded bio-oil yields.

Many research efforts are being carried out in order to reduce hydroprocessing main drawbacks.

On one hand, due to the high bio-oil instability at high temperatures, many researchers posted for a two stages hydrotreating strategy. The first stage consist in stabilise bio-oil at milder hydroprocessing conditions (< 300 ºC) to avoid polymerisation of oxygen-containing compounds and the consequent catalyst deactivation [135,138,139]. This process is called mild hydrodeoxygenation process. Recently, Rover et al. [140] stated that low-temperature, low-pressure mild-hydrodeoxygenation process is possible to produce a stable and low viscosity product at high yields. Moreover, in the few last years, physical stabilisation processes are also considered for this first stage [141]. The second

stage consists in finishing hydrocarbon product production via high temperature hydroprocessing for further oxygen removal. Although partially successful, carbon yields under these conditions are still relatively modest and rapid coking of catalysts is still a problem [140].

On the other hand, bio-oil hydrotreating can be applied not only on whole bio-oil, but also on its fractions [138]. Phase separation might occurs during the pyrolytic process, during bio-oil storage or be prompt by water addition, resulting into a bottom heavy phase and top light phase. The heavy phase separated portion might be upgraded to obtain an enhanced biofuel while the light phase might be used as feedstock for hydrogen production or as chemical platform[142,143]. One of the barriers of this process is the low yields of improved product obtained, making it a non-feasible process for commercial applications.

Moreover, many researchers are been using model compounds to somewhat simplify the upgrading process permitting a better understanding of reactions that take place during the process [120,144–146]. Thereupon, this information will facilitate the development of new catalyst compositions, improve their activity, selectivity, and stability under hydrotreating conditions, reduce catalyst fabrication cost and move them to the industrial-scale. Recently, Ruddy et al. [147] published a report focus on model compound studies to develop catalysts for HDO approaches.

Therefore, further work is necessary to develop new hydrotreating processes that permit the reduction of energy requirements as temperature and hydrogen consumption, the reduction of carbon yields to increase upgraded bio-oil yields and explore new catalysts, as well as its recuperation and regeneration.

b. *Catalytic cracking*

Catalytic cracking rejects the oxygen of bio-oil oxygenated compounds by their cracking as mainly CO, CO_2 and H_2O. This operation is performed at temperatures between 350-650 ºC at atmospheric pressure and hydrogen is not required [111,118,127].

Catalytic cracking is related to Fluid Catalytic Cracking (FCC) [127]. However, catalytic cracking is not as well developed at present in comparison to HDO due to it is not possible to extrapolate this bio-oil upgrading process from FCC in the same degree [37,128,148].

In catalytic cracking the primary reactions are cracking ones, although decarboxylation, decarbonylation and dehydration reactions producing CO, CO_2 and H_2O also are significant (Figure 1.13.) [127]. The decomposition reactions occurring in catalytic cracking are accompanied by oligomerisating reactions, which in the end produces a mixture of light aliphatic hydrocarbons (C1–C6) and larger aromatic hydrocarbons (C6–C10) [149]. As well as hydrotreating process, the formation of carbon (char, tar and coke) through polymerisation and polycondensation reactions constitutes operational problem since they deposit on catalyst casing the blockage of the catalyst pores and its deactivation [122,123].

Catalytic upgrading process can be carried out on the vapours within or close coupled to the pyrolysis process, or they can be decoupled to upgrade either the liquids or re-vaporised liquids. For this application, several catalysts have been investigate such as metal oxides, mesoporous materials and shape-selectivity zeolites (HY, Beta-Y, ZSM-5) [123,144,149–158]. In the choice of catalysts, the availability of their acid sites is important since their affect the selectivity of the system. A mostly aromatic hydrocarbon product is obtained when strong acid-shape selective HZSM-5 is used, whereas mostly aliphatic hydrocarbons are produced when HY zeolites and mesoporous materials are used [119]. Many acid sites give a high yield of aromatic hydrocarbons, but they also lead to a high affinity for carbon formation. [122]. Among these tested catalysis, zeolites, particularly H-ZSM5, have been successfully used due to its high efficiency for reducing oxygenated compounds and improving aromatic hydrocarbon yields. This is because of ZSM-5 has many acid sites, high surface area, shape selectivity, and appropriate pore diameter. However, the high amounts of coke generated by ZSM-5 have been reported [159–162]. Therefore, the idea of adding transition metals into zeolite framework to

minimize the coke formation and to promote the formation of hydrocarbons have been explored [163–168].

Thus, the main weakness of catalytic cracking process is the high carbon yields and the consequent high catalyst deactivation. Because of that, the future research on this field needs to be focus on studying the mechanisms of catalyst deactivation and the design of new and more efficient catalysts that minimises their deactivation and achieves higher hydrocarbon yields. Moreover, similarly to hydrotreating processes, modelling reactions and bio-oil fractionation strategies to reach this aim are being carried out.

c. *Comparison between hydrotreating and catalytic cracking.*

Comparing upgraded bio-oil by means of hydrotreating and zeolite cracking processes (Table 1.8.), it is seen that the oxygen content decreases after both methods: to <5 wt% and to 13–24 wt% after hydrotreating and zeolite cracking respectively. Consequently, hydrotreated bio-oils have higher calorific value and pH compared to zeolite cracking. The increase of HHV of hydrotreated bio-oil is also caused by the addition of hydrogen. Furthermore, the viscosity at 50 ºC of the hydrotreated bio-oil decreases, which improves flow characteristics and is advantageous in further processing. Moreover, hydrotreated bio-oil can be produced in a larger yield and in a higher fuel grade compared to zeolite cracking oil due to less coke is generated. Generally, hydrotreated bio-oil properties approaches the characteristics of the crude oil more than those of the zeolite cracking oil. Despite that fact, the requirement of working with hydrogen at high pressures (30–140 bar) and its high cost makes this process industrially unattractive. In this sense, catalytic cracking has a great interest due to the advantages of operating at atmospheric pressure for both security and economic reasons [42].

Table 1.8. Comparison of characteristics of bio-oil, catalytically upgraded bio-oil and crude oil.

	Bio-oil	Hydrotreating	zeolite cracking	crude oil
Oil yield (wt %)	100	21-65	12-28	-
Water phase yield (wt %)	-	13-49	24-28	-
Gas yield (wt %)	-	3-15	6-13	-
Carbon yield (wt %)	-	4-26	26-39	-
Water (wt %)	15-30	1,5	-	0,1
pH	2,8-3,8	5,8	-	-
Density (kg/L)	1,05-1,25	1,2	-	0,86
Viscosity 50ºC (cP)	40-100	1-5	-	180
HHV (MJ7kg)	16-19	42-45	21-36	44
C (wt %)	55-65	85-89	61-79	83-86
O (wt %)	28-40	<5	13-24	<1
H (wt %)	5-7	10-14	2-8	11-14
S (wt%)	< 0,05	<0,005	-	<4
N (wt %)	< 0,4	-	-	<1
Ash (wt %)	<0,2	-	-	0,1
H/C	0,9-1,5	1,3-2,0	0,3-1,8	1,5-2,0
O/C	0,3-0,5	<0,1	0,1-0,3	0

Source: [111]

1.4.3. Fast pyrolysis development technology

Fast pyrolysis technology is a relatively mature technology and it is close to commercialisation stage, but bio-oil upgrading process is still in laboratory and pilot scale [110]. Several reactors have been investigated on a laboratory scale and pilot scale [110,169,170], being fluid beds, circulating fluid bed and auger pyrolysis strong technologies with and high market attractiveness.

Up to now, bio-oil commercial operation has only been achieved for food and flavouring products [171]. A few companies are currently moving forward bio-oil commercialisation of bio-oil for energy applications, reviewed by Lehto et al. [89]. Forschungszentrum Karlsruhe (KIT), Biomass Technology Group BV (BTG), Fortum together with Metso and Green Fuel Nordic (GFN) probably have today the most advanced initiatives in pursuing larger scale operations in European Union [169]. At industrial scale, bio-oil combustion tests are carried out showing that bio-oil is technically suitable for replacing heavy fuel oil in burner to produce heat and Combined

Heat and Power (CHP), specifically in district heating applications. However, some modifications are needed to be made to the existing combustion units [89].

Fortum bio-oil plant located in Joensuu (Finland) is based on fast pyrolysis technology and is the first of its kind in the world on an industrial scale. The plant produces around 50000 t/y and is planned to be in full production phase in the autumn 2015. It is fed with wood-chips and industrial by products from the local forest industry. The bio-oil plant was integrated to CHP plant in 2013 to replace the use of heavy and light fuel oils in its heat production with Fortum's bio-oil. Joensuu CHP produces heat for the inhabitants of Joensuu (covers roughly 95% of district heat needed) and electricity for the national grid. [172]

1.5. Biorefinery

According to National Renewable Energy Laboratory of United States (NREL), "a biorefinery is a facility that integrates conversion processes and equipment to produce fuels, power, and chemicals from biomass"[173]. The biorefinery concept is analogous to today's petroleum refineries, which produce multiple fuels and products from petroleum. A biorefinery uses renewable resources that contribute less to environmental pollution whereas petroleum uses non-renewable resources. The objective of a biorefinery is to optimise the use of resources and minimise wastes, thereby maximising benefits and profitability. Thus, industrial biorefineries are the most promising route to bio-based industry and bioeconomy [24]. The transition from fossil fuels refinery to biorefinery economy would require large investments in new infrastructure to produce, store, and deliver biorefinery products to end users.

Three different types of biorefineries are described in literature [174–176]:

- Phase I biorefineries. They use one only feedstock, have fixed processing capabilities (single process) and have a single major product. They are already in operation and are proven to be economically viable. Example of this biorefinery are biodiesel

production through transesterification, pulp and paper mills and corn grain-to-ethanol plants.

- Phase II biorefineries. They can only process one feedstock, but they are capable of producing various end products (energy, chemicals and material) and thus responds to marked demand, prices, contract obligation and the plant's operating limits. Examples of this type of biorefineries are the plants which use corn starch to produce a range of chemical products.

- Phase III biorefineries. They are able to produce a variety of energy and chemical products and also use various types of feedstocks and processing technologies to produce the multiplicity of industrial products. They are also called integrated biorefineries. Different types of phase III biorefineries are summarised in Table 1.9. Combining higher value products with higher calorific value fuels production and using any combination of conversion technologies has the greatest potential for making fuels, chemicals and materials, and power making the overall process more competitive.

Table 1.9. Principal characteristics of Phase III biorefineries.

Biorefinery type	Feedstock	Principal technologies	Phase of development
Green biorefinery	Wet biomass: green grasses and green crops	Pre-treatment, pressing, fractionation, separation, digestion	Pilot plant (and R&D)
Whole crop biorefinery	Whole crop (including straw) and cereals (wheat, maize, etc.)	Dry or wet milling, biochemical conversion	Pilot plant (and Demo)
Lignocellulosic biorefinery	Lignocellulosic-rich biomass. E.g. Mischanthus, wood, etc	Pre-treatment, chemical and enzymatic hydrolysis , fermentation, separation	R&D/Pilor plant (EC), Demo (US)
Two platform concept biorefinery	All types of biomass	Combination of sugar platform (biochemical conversion) and syngas platform (thermochemical conversion)	Pilot plant
Thermochemical biorefinery	All types of biomass	Thermochemical conversion: torrefaction, pyrolysis, gasification, HTU, products separation, cataytic synthesis	Pilot plant (R&D and Demo)
Marine biorefinery	Aquatic biomass: microalgae and macroalgae	Cell disruption, product extraction and separation	R&D (and Pilot plant)

Source: [177]

Biorefineries are also classified by their function meaning that they are defined by their biomass transformation process and/or the products obtained. Seven different types are defined by Demirbas [24]: Fast pyrolysis-based biorefineries, gasification based refineries, sugar-based refineries, green biorefinerey, oilseed biorefinery and lignocellulosic biorefinery [178,179]. In Figure 1.13, an integrated a fast pyrolysis biorefinery scheme is shown.

Although the biorefinery concept has been widely discussed and defined, there is a need for further development of demonstration plants, which will require cross-sector collaborations and attract the necessary investors for the construction of full-scale biorefinery [176].

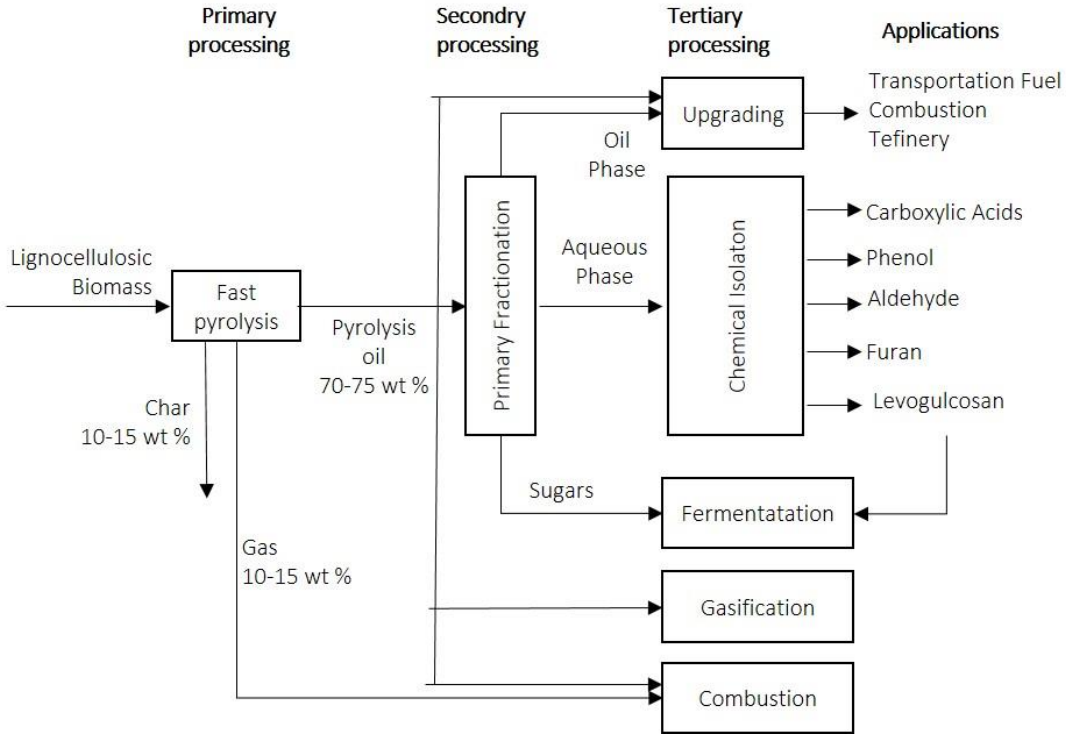

Source: [110]

Figure 1.14. Fast pyrolysis biorefinery scheme.

2. Motivations and objectives

2.1. Motivation

Biomass use raises a high interest in last years motivated by the opportunity of producing biofuels and chemical bioproducts from a renewable source. The use of renewable energies are encouraged by national, reginal and European plans and polices. This interest lies on the global necessity of fostering new renewable energy sources and increasing energy diversification which helps to reduce fossil fuels dependency and to mitigate the global warning effect. Moreover, the use of agro-forestry biomass with this aim is attractive, not only for the use of a primary energy source at local and regional scale, but also for the possibility of converting a biomass residue or sub-product into a primary energy source which adds value to this product with no high added value up to now.

The use of this type of biomass as renewable energy source in Catalonia region has an important role to play. Catalonia has a high potential of forest resources due to its forest extension (around 34 % of its area). Since eighties, Catalan economy has switched to a service economy causing an abandonment of the countryside and a decrease of forest biomass harvesting. This is resulting in an increase of forest areas and its carelessness, causing negative side effects such as a rise in forest fire risk. Thus, adding value to biomass might improve the agro-forestry sector by the preservation and restoration of the environment and traditional landscapes.

In this context, it is raising the necessity of a technologic advance towards biomass conversion processes that permit biomass to be an economically viable renewable resource for efficient energy utilities and production of bio-based products. Biomass can be transformed into a liquid, solid and/or gas biofuels by means of the current available thermochemical technologies at commercial scale. However, it is necessary to obtain new marketable added-value products from these technologies.

Torrefied pellets are a marketable added-value energy product obtained from biomass torrefaction process. Their production at local scale permits to make use of residual biomass generated in the rural zone converting it into a renewable source and reducing the logistic cost of the process and making it more economically viable. At the same time, the obtained product might be used in the local thermal installation, closing the cycle of resources and product in terms of circular economy. With this motivation, pilot scale tests should be carried out to demonstrated the technical and economic viability of this process in a rural area to facilitate the social acceptance of this technologies and demonstrate the viability of a this kind of bioeconomy project as a short-term strategy that combines an environmental friendly project with the aim of boosting the local economy by, not only creating jobs and diversifying the market of agricultural biomass

Bio-oil, pyrolysis main product, has received extensive recognition from international energy organisation around the world for their characteristics as liquid biofuel. However, much work is needed on its stabilisation and upgrading before its commercialisation and utilisation as transport fuel. Although many efforts are carried out on this issue as it is highlighted in the introduction, it is required to develop new upgrading processes that not only permit obtaining a higher quality product, but also a more environmental and economic sustainable processes. Moreover, bio-oil is considered as chemical platform to extract chemical bio-products. As a long-term strategy, production of bioenergy and bio-based products from bio-oil might be integrated into a biorefinery system, in an analogous to today's petroleum refineries but using biomass as feedstock instead of fossil fuels.

Thus, this project stems from the necessity of developing an energy production sustainable strategy with the potential of reducing the environmental impact of producing energy, as well as favouring the economic and social development of our society.

2.2. Objectives

The main aim of this dissertation is to add-value to agro-forestry biomass residues as enhanced biofuels by means of thermochemical biomass conversion processes in order to move towards a more sustainable energy model.

In order to achieve this main aim, two objectives are outlined:

- To study the viability of implementing a torrefaction process to add value to agricultural waste biomass into torrefied pellets in a rural region.
- To novel bio-oil upgrading processes to achieve a more economically viable enhanced bio-oil as liquid biofuel.

  This objective is translated into several secondary objectives:

  - To reach a reliable quantitative analysis of bio-oil chemical compounds by means of GC-MS to achieve a further characterisation of this product.
  - To assess bentonite and zeolite HZSM-5 as catalysts at low temperatures to improve bio-oil properties allowing the reduction of the energy cost of the conventional catalytic cracking upgrading processes.
  - To explore new hydrogenation procedure to hydrogenate bio-oil at ambient temperature and atmospheric pressure in order to reduce the high energy and hydrogen supply cost of conventional hydrotreating bio-oil upgrading processes.

3. Experimental Section

This chapter describes the methodology followed in this dissertation. Several methods and experiments are used and design in order to fulfil the objectives of this study, which can be grouped in three main groups.

i. Analytical methods used to characterise the raw and torrefied biomass, as well as the raw and treated bio-oil.

ii. Experimental design to study the viability of implementing a torrefaction process to add value to agricultural waste biomass as torrefied pellets in rural regions, which corresponds to Part II of this dissertation.

iii. Experimental design of new and improved bio-oil upgrading processes to reduce its economic cost, both energetic and resources, which corresponds to Part III of this thesis.

3.1. Analytical methods

The following section detailed the analytical methods used to characterise raw and torrefied biomass used and obtained in the torrefaction pilot project, as well as to characterise the raw and treated bio-oil obtained from the new and improved bio-oil upgrading processes. The analytical methods to characterise the solid samples are carried out by external laboratories. Liquid characterisation analysis are carried out in the laboratories of the research which has been started-up within this thesis work. In each results chapter is specified the used analytical method.

3.1.1. Thermogravimetric analysis

Thermogravimetric analysis (TGA) permits to study the thermal degradation of lignocellulosic biomass (see section 1.2.2.). It is used to characterise raw biomass. This

technique is based on continuous recording of mass loss as function of temperature. TGA is carried out with a thermobalance Mettler TGA/SDTA851e heating the sample from 30 ºC to 1000 ºC with a heating ratio of 10 ºC/min in a nitrogen atmosphere

This analysis is carried out by an external accredited laboratory from Thermal Analysis Service of Institut de Ciència dels Materials de Barcelona.

3.1.2. Calorific value

The amount of heat produced when the fuel is burned completely is determined by IKA 5000 bomb calorimetric. 1.2 g of sample is combusted in calorimetric bomb.

There are two values for combustion heat: higher heating value (HHV) and lower heating value (LHV). The difference between them is equal to the vaporisation heat of the water formed by the combustion of the fuel. The HHV is determined by measuring the temperature increase in the water jacket and then calculated from the energy balance for the system (DIN 51900) by the bomb calorimeter. The lower heating value (LHV) is calculated from the HHV and the hydrogen content (ASTM 529192) by Equation 3.1. The hydrogen content is determined by elemental analysis (see section 3.1.3.).

$$LHV\ \left(\frac{J}{g}\right) = HHV\ \left(\frac{J}{g}\right) - 218.13 \cdot H\ (wt\ \%) \qquad \text{Equation 3.1}$$

The combustion heat is analysed in raw and torrefied biomass, as well as in raw and treated bio-oil.

This analysis is carried out by an external laboratory from Unitat de Medi Ambient of Parc Científic de Barcelona.

3.1.3. Elemental analysis

Elemental analysis of carbon, hydrogen and nitrogen is performed by means of a Thermo Scientific Flash 2000 elemental analyser. They are determined simultaneously as gaseous products: carbon dioxide, water vapour and nitrogen. Oxygen is calculated

by difference. The sample is combusted at 1200 ºC in an oxygenated atmosphere and quantified by gas chromatography.

This analysis is used to characterise raw and torrefied biomass, as well as raw and treated bio-oil.

This analysis is carried out by an external accredited laboratory at Servei d'Analisi Química de la Universitat Autònoma de Barcelona.

3.1.4. Immediate analysis.

Immediate analysis gives the moisture, ash, volatile content and fixed carbon of a solid sample. They are calculated from the loss in mass after being heated up in a muffle Hobersal model HD-150 at different temperatures. The sample is dried at a temperature of 105 to 110 °C in a current of nitrogen up to constant weight to analyse moisture content and at 805 ºC to determine ash content. Fixed carbon is calculated by difference. In this thesis work, raw biomass is also characterised by this analysis.

This analysis is carried out by an external accredited laboratory from Unitat de Tècniques Separatives i Síntesi de Pèptids of Parc Científic del Barcelona.

3.1.5. Inductively coupled plasma mass spectrometry (ICP-MS)

Agilent ICP-MS model 7500ce is used to determine metals traces content in biomass ashes.

Firstly, metals extraction from the solid sample is required. Because of that, samples are digested with concentrated HNO_3 and HCl in a heating plate with magnetic stirring. Trace metal content is determined by ICP-MS semi-quantitative analysis by means of a response molar curve versus atomic weight.

This analysis is carried out by an external accredited laboratory at Servei d'Anàlisis Química de la Universitat Autònoma de Barcelona.

3.1.6. Gas chromatography - Mass Spectrometry (GC-MS)

A Gas Chromatography-Mass spectrometry (GC-MS) analysis is set up to analyse the chemical composition of torrefaction liquid, raw bio-oil and treated bio-oil. Once the method is set up, it is assessed its precision and used to develop a reliable quantification method.

The used instrument is a Thermo Trace GC Ultra coupled with a DSQ II single quadrupole Mass Spectrometer and a Triplus AS autosampler from ThermoFischer Scientific (Figure 3.1.).

Figure 3.1. Gas Chromatograph TRACE GC ULTRA coupled to a DSQ II Mass Spectrometer and a TRIPLUS AS autosample from ThermoFisher Scientific.

Hereafter, it is detailed the GC-MS used method and the methodology used to perform the precision method and quantification study.

GC-MS method

Before each day of analysis, few parameters of control to ensure the proper instrument operation are tested. The absence of air leaks in the system is controlled performing an air/water spectrum in a mass-to-charge (m/z) range of 10 to 100. It is, also, checked the full scan spectrum in a mass-to-charge range from 50 to 650 to ensure

the absence of background peaks caused by column contamination. The detector proper response is controlled by the injection of a calibration gas (perfluorotributylamine, FC-34). Finally, a diagnostics test is run to check the electronic internal components as power supply system, vacuum system, heater system, detector and lens.

The method used is adapted from Puy [180]. The used capillary column is a DB-Petro (100 m x 0.25 mm ID x 0.50 µm film thickness) with helium as carrier gas with an initial flow of 2.3 mL/min for 84 min, an increasing flow rate from 0.2 to 1.8 mL/min and kept at 1.8 mL/ min until the end of the analysis. The oven temperature is programmed at 40 ºC (4 min), a first heating rate of 1 ºC/ min to 55 ºC, a second one of 2 ºC/ min to 185 ºC, a third one of 10 ºC/min to 250 ºC hold 60 min. The total run time is 120 min. The injector, the ion source and the transfer line temperatures are kept constant at 300 ºC, 230 ºC and 280 ºC, respectively. A sample volume of 1 µL is injected applying 1:7 split mode with a SGE syringe of 10 µL and conical needle of 50 mm. The bio-oil samples are injected by triplicate, taking into account that the first injection of each day of analysis is rejected due to is not reproducible. After a solvent delay of 8 min, a full mass spectrum is acquired. The MS is operated in positive electron ionisation mode and a mass-to-charge range from 30 to 500 is scanned. The voltage applied to the multiplier detector is 1275 V in order to obtain the Total Ion Chromatograms (TICs) in a full-scan acquisition method. A quantifying mass-to-charge ratio (m/z) for each compound is used to produce an Extracted Ion Chromatogram (EIC) wherein the integration of peak area of analytes is performed. In this way, some interferences with each analyte and the other compounds do not occur or are reduced. The identification of peaks is based on computer matching of the mass spectra with the NIST library. Xcalibur is the software used for data processing.

Due to bio-oil is really thick sample, it is necessary a cycle of cleaning to avoid the syringe plugging. It consists in rinsing the syringe 5 times with 5 µL of methanol, 5 times

with 5 µL of acetone and 15 times with 9 µL of methanol. Moreover, before each injection, the syringe is conditioned 5 times with methanol and 3 times with the sample.

To obtain the chromatographic conditions specified above, a previous optimisation of them was carried out. The optimized parameters were the heating rates to obtain the best peak separation with the minimum run time, the injector temperatures testing 250 ºC, 275 ºC and 300 ºC, the used liner and the sample dilution checking 1:5, 1:10 and 1:40.

Sample preparation, before its analysis, consists in diluting bio-oil with methanol (1:10) and filtering to eliminate possible solids. At each sample, it is added one or more internal standards: 100 mg/L toluene, 200 mg/L, 1,1,3,3-tetramethoxypropane and 200 mg/L of 1-octanol. The used internal standard is specified in each experimental section. The use of internal standard permits the comparison of bio-oil composition between sample and between days by means of the calculated area ratio of each compound which is the area of the target compound relative to the area of the internal standard.

Precision study

A study of method precision is carried out by means of One-way Analysis of Variance (ANOVA) with a confidence interval of 95 %. Method precision is assessed by its instrumental, intraday and interday precision. The instrumental precision is evaluated by a sequence of repeated injections of the same aliquot and calculating the Relative Standard Deviation (RSD) of the three replicate of each aliquot for each compound. Intraday precision (or repeatability) is expressed as the precision under the same operating condition over a short period of time and assessed by an One Way ANOVA test for each compound with a confidence interval of 95 % between the three different analysed aliquots in the same day. Interday precision is determined to evaluate the influence of analyse bio-oil samples in different days. Ten days elapsed between analysis and different aliquots are analysed. Thus, One Way ANOVA test between peak

area values obtained in these two days are calculated. Moreover, it is evaluated the effect of using an internal standard on the method precision. Three different internal standards are tested: toluene, 1,1,3,3-tetramethoxypropane and 1-octanol. The area ratio of each compound and its RSD for all the aliquots are calculated to perform the study of the method precision using internal standards. The area ratio is the area of the selected compound relative to the area of the internal standard.

For this purpose, three aliquots of the bio-oil vessel are sampled and analysed by triplicate. After 10 days, another aliquot is sampled and analysed. Each aliquot is sampled after a proper bio-oil homogenisation that consists of a 10 min mixing of the sample vessel [90]. A proper homogenisation of the sample is crucial for a food reproducibility of the analysis and more important when the sample is as complex as bio-oil. Before each analysis, the different internal standards are added to bio-oil samples (100 mg/L toluene, 200 mg/L, 1,1,3,3-tetramethoxypropane and 200 mg/L of 1-octanol) and this mix is diluted with methanol (1:10). After that, this dilution is filtered. Bio-oil samples are analysed by GC-MS by triplicate, taking into account that the first injection of each day of analysis is rejected due to is not reproducible.

Quantitative assessment

Among the identified compounds, some target compounds are selected for their quantification including the most abundant compounds according to the chromatogram peak area and their added value considering almost one of each chemical family. They are quantified by means of four different calibration methods using three different internal standard (toluene, 1,1,3,3-tetramethoxypropane and 1-octanol) and without them. Moreover, an one-way ANOVA test with a confidence interval of 95 % is performed to carry out a comparative assessment of the results obtained from these four calibration methods.

For calibration standards, a methanol stock solution for each selected compound is prepared and six standards with different concentrations of each selected compound are prepared. The concentration rang of each compound is chosen by using successive approximation until it becomes considerably slim and contains the quantified value. The obtained calibration range for each compound is shown in Table 3.1. Stock and standard solutions are kept in the refrigerator until use.

Table 3.1 Calibration range of bio-oil quantified compounds

Compound	Range of calibration (mg/L)
2-propen-1-ol	20 to 70
2-butanone	10 to 250
Acetic acid	2000 to 7000
Furfural	50 to 50.0
2(5H)furanone	400 to 900
2,5-dimethoxy-tetrahydrofuran	25 to 150
3-methyl-1,2-Cyclopentanedione	300 to 800
2-methoxy-4-propyl	50 to 200
Vanillin	500 to 1000
Levoglucosan	2000 to 7000

The used reagents for the bio-oil chemical compounds quantification, as well as their purity and brand are listed in Table 3.2.

Table 3.2. Calibration range of bio-oil quantified compounds

Reagent	Purtiy	Brand/supplier
2-propen-1-ol	≥ 99%	Sigma-Aldrich
2-butanone	≥ 99%	Janssen Chimica
Acetic acid	≥ 99.5 %	Panreac
Furfural	≥ 99%	Sigma-Aldrich
2(5H)furanone	0.98	Sigma-Aldrich
2,5-dimethoxy-tetrahydrofuran	0.98	Sigma-Aldrich
3-methyl-1,2-cyclopentanedione	≥ 99%	Sigma-Aldrich
2-methoxy-4-propyl-phenol	≥ 99%	Sigma-Aldrich
Vanillin	≥ 99%	Sigma-Aldrich
Levoglucosan	≥ 99%	Sigma-Aldrich
Toluene	≥ 99.5 %	Panreac
1,1,3,3-tetramethoxypropane	≥ 99%	Sigma-Aldrich
1-octanol	0.95	J.T. Baker

3.1.7. pH

The pH of liquid products obtained from thermochemical conversion of biomass are measured by means of a Solvotrode electrode with c(LiCl) = 2 mol/L for non-aqueous media purchased by Metrohm (Figure 3.2.). Solvotrode electrode is a pH glass electrode

with ground-joint diaphragm recommended for measuring the pH in organic solvents. The separable ground-joint diaphragm guarantees stable potentials and is easy to clean.

Figure 3.2. pHmeter picture and Solvotrode electrode.

3.1.8. Total Acid Number (TAN)

Total Acid Number (TAN) is used to measure the acidity of both raw and treated bio-oil indicating the concentration of acidic constituents in them. TAN is analysed by an acid–base titration using a Crison micro TT 2050 potentiometer to determine the end point (Figure 3.3.).

Figure 3.3. Crison micro TT 2050 potentiometer for Total Acid Number titration.

TAN is defined as the amount of potassium hydroxide (KOH) in milligrams that is needed to neutralise the acidic groups present in one gram of bio-oil (Equation 3.2.). It is known that bio-oil acidic groups are carboxylic acids, phenols, alcohols and sugars, and that it is possible to quantify the amount of these groups by means of TAN test without interferences of other compounds [181]. The Amercian Society for Testing and Material (ASTM) has published a standard test method to measure TAN for petrochemical applications, which can be used for measuring the acidity of fast pyrolysis bio-oils and their upgrading products [181]. ASTM D664 measures acidic constituents of an oil using a potentiometric titration to determine the end point.

$$\mathrm{TAN} = \frac{(V_{\mathrm{KOH\ at\ EP}} \cdot [\mathrm{KOH}] \cdot MW_{\mathrm{KOH}})}{\mathrm{g\ bio-oil}} \qquad \text{Equation 3.2.}$$

0.25 g of bio-oil are dissolvent in 20 mL of a solvent mixture of toluene (50%), isopropyl alcohol (49.5%) and water (0.5%)[90]. Both solvents are purchased from Panreac. Potassium hydroxide 0.1N in isopropanol (Sigma-Aldrich) is then titrated into the solution using an automatic burette. The potentiometer output is monitored while the KOH is titrated into the solution. Due to the used device is not specific for TAN determination, potentiometer and automatic burette parameters adjustment are performed. The titration starts after 1 min of agitation. Titrant additions are carried out in “normal weaken” mode and the accepted reading values to obtain the TAN titration curve are those obtained with a maximum dispersion of 3 mV in 15 s. As an example, in Figure 3.4., it is shown a TAN titration curve. Despite the inflexion point in the titration curve is no pronounced due to the buffered system that bio-oil is, it is detectable.

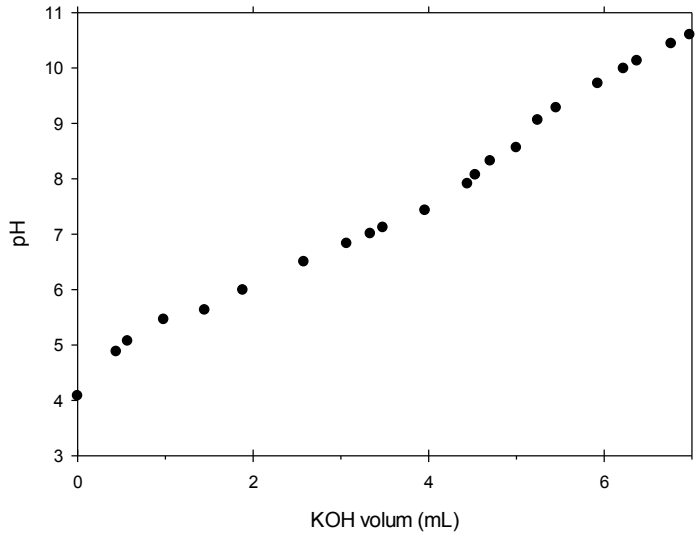

Figure 3.4. TAN titration curve.

3.1.9. Differential Acid Number (DAN)

Differential Acid Number (DAN) is a test developed within this thesis work to assess the number of acidic groups neutralized o reduced through an upgrading process reaction time.

Differential Acid Number (DAN) is defined as the difference between the Acid Number (AN) calculated as the amount of potassium hydroxide (KOH) in mmol needed to achieve a set pH per gram of raw bio-oil ($AN_{\text{raw bio-oil}}$) and the Acid Number (mmol KOH needed to achieve the same pH) per gram of treated bio-oil (Equation 3.3.)

$$\mathrm{DAN} = \mathrm{AN}_{\text{raw bio-oil}} - \mathrm{AN}_{\text{treated bio-oil}} \qquad \text{Equation 3.3.}$$

The concept of DAN comes from Total Acid Number test (TAN). TAN is used as a fast and simple method to measure the bio-oil acidity neutralizing the acidic groups in one gram of bio-oil using potentiometric titration to detect the titration end point [181]. However, it is sometimes difficult to distinguish easily the end point in TAN test due to bio-oil is a much buffered system. Because of that, in this work, DAN test is defined due to it is not necessary to distinguish the end point because a final point is defaulted

facilitating the analysis. However, it must be taken into account that the whole bio-oil acidity is not measured with DAN, neither with TAN, since it does not represent all the acidic components that might be found in bio-oil due to it is not affected by extremely weak acids that have a dissociation constant of less than 10^{-9} [90].

The analytical process of DAN test is similar to TAN one, adding bio-oil into a solvent mixture of toluene (50 %), isopropyl alcohol (49.5 %) and water (0.5 %) (ASTM D664) to dissolve the sample and titrated with a 0.1 M KOH in isopropyl alcohol[90]. DAN is analysed using a Crison micro TT 2050 potentiometer to determine the volume of KOH necessary to achieve the established pH.

To perform DAN test, it is necessary to set a final pH point. With this aim, it is performed four DAN tests at different default final points between 9 and 12 in order to study the possible effect of the set final point on DAN values. The study is performed with a hydrotreated bio-oil by the nascent hydrogen generated using 4.5 wt % of Zn of 2.5 x 8 mm at 37 ºC with vertical rotation shaker and at 5 days of reaction time; and its raw bio-oil. The hydrotreating process is further described in section 3.3.4. The obtained results are shown in section 8.5.

3.1.10. Water content

Water content of liquid samples are analysed by volumetric Karl Fischer titration (ASTM E 203) using 716 DMS Titrino (Metrohm) and 665 Dosimat (Metrohm) (Figure 3.5.).

Figure 3.5. 716 DMS titrino and 665 Dosimat for Karl Fischer titration.

The water content is determined by an amperometric titration at constant current. This current is passed between a double platinum-wire electrode (Metrohm), and the change in potential (mV) is measured during the titration. With the progress of titration, the value indicated by the potentiometer in the circuit decreases suddenly from a polarisation state of several hundred (mV) to the non-polarisation state, but it returns to the original state within several seconds. At the end of titration, the non-polarisation state persists for a certain time (usually, longer than 30 seconds). The end point of titration is determined when this electric state attains.

The solvent and titrant agents used are: Aquametric-solvent which is a solution of sulfur dioxide and imidazole in methanol and Aquametric-Titrant 5 which contains a solution of iodine in methanol with a precisely defined concentration. Both purchased

from Panreac. The titration reaction is shown in Equation 3.4. Methanol is a good working medium as it allows for a rapid and stoichiometric course of reaction, it gives a sensitive and reliable indication of the end point and bio-oil dissolves easily in it. A base as imidazole is added for buffering the titration system due to water titration produces acids that must be neutralized.

$$H_2O + I_2 + SO_2 + CH_3OH + 3\ C_3H_4N_2 \rightarrow [C_3H_4N_2]SO_4CH_3 + 2\ [C_3H_4N_2] \qquad \text{Equation 3.4.}$$

The followed procedure is: (1) 20 mL of solvent are added to the titration vessel by means of the 665 Dosimat to reduce the solvent humidification. (2) pre-titration of the solvent to dryness to remove not only the residual water that was in the solvent, but also the adherent moisture in the cell, on the walls of the cell and the electrode. The atmosphere of the cell is also dried of moisture. (3) About 60 mg of bio-oil is added opening the vessel for as short time as necessary to reduce the intrusion of atmospheric moisture to an absolute minimum. (4) The titration of water is started immediately to achieve a stable end point. (5) Finally, the spent working medium should be removed from the cell or subsequent titrations are possible until a maximum of 28 mL of titrant during the subsequent titrations.

For calibration, between 30 and 200 mg of Sodium tartrate dihydrate (Panreac) are titrated following the above explained process obtaining a calibration range of 5-30 mg of water.

3.1.11. Flame Atomic Absorption Spectroscopy (FAAS)

Perkin–Elmer atomic absorption spectrometer model 2100 equipped with 10-cm burner (Figure 3.6.) is used to quantify Zn^{2+} in bio-oil samples and the purity of zinc metal. The radiation source is a zinc hollow-cathode lamp. The analysis is performed at wavelength of 213.8 nm and under optimized operating conditions by FAAS with an air-acetylene flame.

For Zinc metal purity analysis, an acidic digestion of the metal is required. 1 g of zinc metal is digested with 25 mL of HNO_3 solution of 17.5 %. Then, the obtained solution is filtered to remove possible solid particles and diluted with methanol to obtain 1 litre of solution. The blank is prepared with 25 mL of the same nitric acid and diluted up to 1 litre.

For the analysis, bio-oil samples are dissolved in methanol (1:10) and, when it is necessary, further diluted until it fits in the calibration curve values.

In both cases, the calibration range is between 0.1 and 3 mg/L. The standards are prepared from a stock of 1000 mg/L of Zinc solution in nitric acid (Sigma-Aldrich) dissolved in methanol.

Figure 3.6. Perkin–Elmer flame atomic absorption spectrophotometer.

3.2. Experimental design of part II: adding value of agricultural waste biomass as torrefied pellet woody crop.

Part II of this dissertation describes the results of a pilot project carried out to assess the technical-economic viability of implementing a torrefaction process to add value to agricultrual waste biomass as torrefied pellets in a rural region. This pilot project consists in different stages including the description of implementation study zone, the biomass potential assessment, the logistic costs of biomass supply to torrefaction plant, and the technical and economic viability of producing torrefied pellets as added vale

product. The work team constituted to carry out this pilot project is composed by Inèdit Innovació S.L., Energies Tèrmiques Bàsiques S.L. and Universitat Autònoma de Barcelona, with the collaboration of Ascó local government. Each work team member is responsible of one or more stages of this project.

The part of this project carried out within this thesis works is the characterisation of raw biomass and the different torrefaction products, as well as the torrefied pellets as final valuable product. Moreover, it is carried out an overall economic assessment. In this section, it is described the methodology followed to carry out these stages of the pilot project, as well as the main methodology and results obtained in other stages of the project that are required to perform and understand this work.

3.2.1. Implementation zone and its biomass potential

The pilot project is carried out in Ribera d'Ebre region which is located in the south of Catalonia (Spain) (Figure 3.7.). It is constituted of different municipalities, including Ascó municipality where is located the semi-industrial pilot plant of Energies Tèrmiques Bàsiques.

The main uses of land of this region are pastureland, agricultural land, forestry and industrial land (Figure 3.8.). The traditional economic activity of this region is the agriculture, currently with a cultivable area of around 28.000 hectares. Its high extension of cultivable land, jointly with its forestry area (22.000 hectares), makes this region a good candidate to assess its potential of biomass and its value addition. Moreover, it is important to highlight that agricultural biomasses are more accessible than forestry ones due to most of forestry areas are located in lands with slopes superior to 20 %. Taking into account that fact, only agricultural waste biomass (AWB) is considered as valuable biomass for this study including pruning waste of fruit trees (pear tree, apple tree, peach tree, cherry tree, etc), nut trees (almond tree, hazelnut tree, walnut tree),

other fruit trees (carob tree, mulberry tree, etc), citrus fruit trees (orange tree, mandarin tree), olive trees and grapevine.

The AWB potential of the whole Ribera d'Ebre region is 29703 t d. b./ year. Regarding to Ascó municipality where is located the plant, the AWB potential is 2525 t d. b. / year. Fruit tree crops have the higher biomass potential, followed by olive tree crop, nut tree crop, vineyard and mixture of crops.

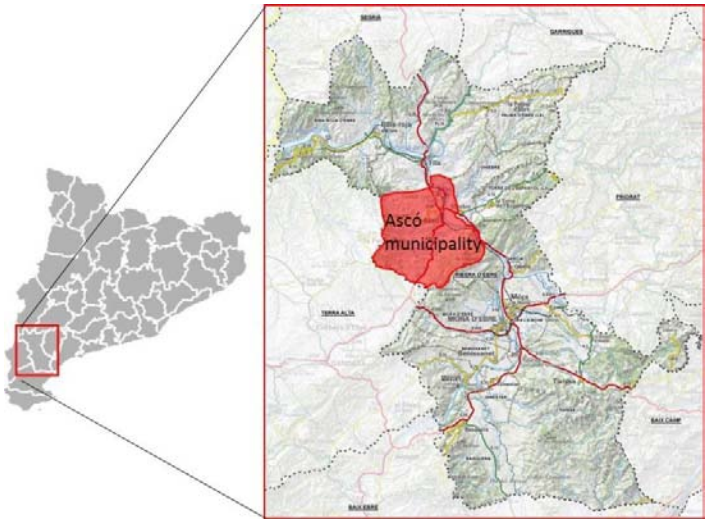

Figure 3.7. Pilot project implementation area.

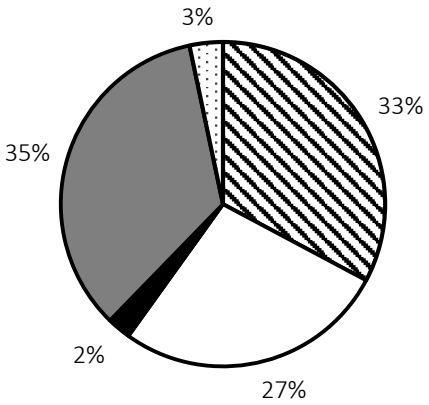

Figure 3.8. Uses of land of Ribera d'Ebre region. Agricultural land (▨); forestry land (□); industrial and urban land (■); pastureland (▩); others (⁙).

3.2.2. Semi-industrial pilot plant

Energies Tèrmiques Bàsiques SL is a company dedicated to thermochemical conversion of different biomass types, from forestry biomass to residues as municipal waste, CDR and CRS. One of the aims of this company is to produces added value products from biomass residues which suppose two advantages: convert a residue in a source and obtain a profitable product by the thermochemical process itself. Moreover, it is an innovative company focused on the research and development of new processes and products.

This company developed a thermochemical biomass convention pilot plant that can operate at 30 kg/h based on torrefaction and pyrolysis technologies, wherein it is carried out the pilot project in Ribera d'Ebre region (Figure 3.9.). Moreover, Energies Tèrmiques Bàsiques own a small scale pelletiser of 1 t/h of maximum capacity. Currently, this plant is further developed into a patented demonstration plant with a capacity of more than 100 kg/h and it foresees, in the following months, to develop an industrial plant of 1 t/h capacity. These biomass adding value plants are modular and transportable, with the aim of obtaining added –value products (solid, liquid or gaseous) in situ from the different types of biomasses.

Figure 3.9. Picture of Energies Tèrmiques Bàsiques biomass conversion plant.

3.2.3. Adding value to Agricultural Waste Biomass (AWB) as torrefied pellets by Energies Tèrmiques Bàsiques SL plant.

In this stage of the project, it is performed a pilot-test of adding value to AWB in the torrefaction plant. Ascó local government lends municipal smallholdings to harvest olive pruning waste, almond pruning waste, cherry pruning waste and obtain olive stone in order to use them as feedstock for the torrefaction plant tests.

After a proper characterisation of these feedstock biomasses, they are treated in the torrefaction plant at different operational condition to select the optimum ones for each biomass type. The torrefaction products (solid and liquid) are recovered and characterised. The torrefaction tested runs are shown in Table 3.3. Potential uses of each of these products are evaluated. The torrefied biomass is pelletised and the obtained pellets are characterised to assess their quality.

Table 3.3. Torrefaction operational conditions tested for almond and olive pruning biomass treatment.

Waste biomass	Temperature (ºC)	Biomass loading (kg/h)	Chip size (mm)	Drying biomass temperature (ºC)	Screw conveyor velocity (Hz)
Almond pruning	255	17.2	4	180	40
	280	15.2	4	180	40
	290	13.6	4	180	40
	295	15.6	4	180	40
Olive pruning	220	16.8	4	180	40
	250	13.8	4	180	40
	270	14.1	4	180	40

3.2.4. Economic assessment

The economic viability of implementing a torrefaction plant to add value to AWB as torrefied pellets in Ascó municipality context is evaluated. The economic assessment is carried out by means of a cost-benefit analysis. Three main investment indicators are used: Net Present Value (NPV), internal rate of return (IRR) and return on equity (ROE). They are summarized in Table 3.4. For the economic analysis, it is considered two main implementation scenarios taking into account the plant capacity (1 t d.b. / h) and the operational hours of the plant being 8 and 16 h which corresponds to one and two work shifts (Table 3.5.).

Table 3.4. Economic indicators definition for the cost-benefit economic analysis

Indicators	Formula	Variables	Value
Net present value (NPV)	$NPV = \sum_{k=1}^{n} \frac{F_k}{(1+i)^k} - I_0$ Where: Fk= PSI – TFC – TVC – T – F + A	n: plant useful life time k: the year of the cash flow i: interest rate I_0: investment cost F_k: net cash flow at year k PSI: product selling income TFC: Total fix costs TVC: total variable costs T: taxes F: Fare A is the amortisation	NPV > 0. Project may be accepted NPV < 0 Project may be rejected NPV = 0 Project adds no monetary value
Internal Rate of Return (IRR)	$NPV = \sum_{k=1}^{n} \frac{F_k}{(1+i)^k} - I_0 = 0$	NPV: Net present value k: the year of the cash flow I_0: investment cost F_k: net cash flow at year k.	IRR > r. Project may be accepted IRR < r. Project may be rejected
Return on equity (ROE)	$ROE = \frac{NPV}{I_0}$	ROE: return on equity	ROE> 1. Investment costs are recovered.

Table 3.5. Evaluated implementation scenarios for torrefaction plant to produce torrefied pellets in Ascó municipality context.

Variables		Moderate scenario	Intensive scenario
Biomass ($t_{30\ wt\ \%\ wet\ basis}$ / year)		2288	4576
Biomass ($t_{50\%\ wet\ basis}$ / year)		2640	5280
Plant capacity ($t_{dry\ basis}$ /h)		1	1
Operating hours (h)		8	16
Operating days a year (days)		220	220
Torrefaction efficiency (wt %)		80	80
Plant useful life time (years)		15	15
Staff	Quality and production manager	1	1
	Supply and warehousing manager	1	1
	Marking and sale manager	1	1
	Operator	2	4

The economic assessment is carried out considering that the benefits of the plant are those obtained from pellet selling. The considered fix costs are amortisation of the investment cost and insurance costs while the variable costs are maintenance cost, AWB cost, energy cost and salaries. Cost values are obtained from the pilot-test carried out in Ascó municipality. The different cost values are shown in Table 3.6.

Table 3.6. Cost values for the economic assessment

		Units	Moderate scenario	Intensive scenario
Investment costs				
Torrefaction plant		€	600000	
Pelletisation unit		€	300000	
Interest rate		%	5	
Plant and pelletizer life time		Years	15	
Fixed costs				
Amortisation		€	900000	
Insurance cost		%	1% the fixed assets	
Variable costs				
Staff	quality and production manager	€/y	25855	
	supply and warehousing manager	€/y	24840	
	marketing and Sales manager	€/y	24840	
	Operator	€/y	31270	62540
Maintenance		%	3 % of initial investment cost	
Energy consumption	Consume	kWh	25	
	Energy cost	€/kWh	0.1	
	Correction coefficient		1.5	
Cost of biomass			depends on the logistic scenario	

Furthermore, the logistic costs of biomass supply to torrefaction plant are quantified by Inèdit Innovació SL and Energies Tèrmiques Bàsiques SL considering different logistic scenarios within the Ribera d'Ebre context. Logistic scenarios are taking into account the different logistic operations required and the different options to perform them (Table 3.7.). The logistic operation considered for this process are biomass extraction, biomass drying process, chipping process and chips transport, storage and feeding cost, which are outlined below.

Biomass extraction includes the pruning and collection of AWB in the field.

Biomass drying process is required for two months since torrefaction plant feedstock must be wood chips of maximum 30 wt % w. b. while AWB extracted has a moisture content of 50 wt %. Two logistic scenarios are considered: (1) to dry harvested biomass in the field and (2) to dry biomass in a warehouse located near to the torrefaction plant since many farmers do not want to dry the biomass at the field for fear to pest spreading.

The biomass chipping process is considered to be carried out in the field where the AWB is generated using a mobile wood chipper in all considered scenarios because it is easier to transport chipped biomass than the entire one. Moreover, two logistic scenarios are considered based on the ownership of the mobile wood chipper. Mobile wood chipper might be: (1) rented to a forestry service company or (2) bought and amortized by the torrefaction plant management company.

Wet or dried biomass chips are considered to be transported from the yield to the warehouse by means of a tractor with a trailer of 8 m^3 which is considered to be rented to a forestry service company, bought and amortized by the torrefaction plant management company or might be lent by the famers**.**

Biomass storage is considered to be carried out in a warehouse located next to the torrefaction plant. Biomass storage is required to ensure the feeding of torrefaction plant a whole year and to dry wet chips to a 30 wt % of water content for two month in some considered scenarios.

Feeding plant cost includes the transport of dried biomass chips from the warehouse to the plant by means of a forklift truck with a loader of 1.5 t of capacity bough by the torrefaction plant management company.

Table 3.7. Assessed logistic scenarios to supply agricultural waste biomass to torrefaction plant for moderate and intensive implementation scenarios

Biomass extraction	Pruning and collection of AWB in the fields.					
Biomass drying process	Warehouse			Field		
Chipping in the field	Wet biomass[a]			Dried biomass[b]		
Wood chipper ownership	Forest service company	Plant management company		Forest service company	Plant management company	
Transport devices ownership	Forest service company	Plant management company	Support of farmers	Forest service company	Plant management company	Support of farmers
Biomass storage	Warehouse					
Plant feeding device	Torrefaction plant management company					

[a] wet biomass at 50 wt % wet basis; [b] dried biomass at 30 wt % wet basis

3.3. Experimental design of Part III: Bio-oi characterisation and upgrading.

The following section outlines the experimental methodology used to explore new and improved bio-oil upgrading processes to reduce their current cost. It comprises: (1) BTG-BTL bio-oil product description, (2) bio-oil catalytic upgrading process experimental design and (3) bio-oil hydrogenation processes experimental design.

3.3.1. BTG-BTL bio-oil

The bio-oil used in this dissertation is purchased from BTG-BTL (Figure 3.10.). It is pine wood bio-oil produced by BTG-BTL fast pyrolysis technology based on a rotating cone reactor.

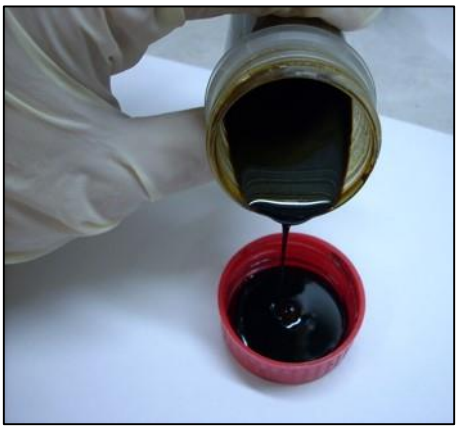

Figure 3.10. BTG-BTL bio-oil

The purchased bio-oil has the following physical and chemical properties, according to BTG-BTL product data sheet (Table 3.8.).

Table 3.8. BTG-BTL bio-oil physical and chemical properties (accordingly to BTG-BTL product data sheet).

Properties	Values
Boiling point	< 100 ºC
Pour point	- 20 ºC
Flash point	> 62 ºC
Density	1150-1200 Kg /m^3
Viscosity (20ºC)	60-2250 cSt
Viscosity (50ºC)	10-30 cSt
pH	2.5-3.5
Auto ignition temperature	>500 ºC
Decomposition temperature	>150 ºC

3.3.2. Bio-oil catalytic upgrading process

Firstly, it is assessed a bio-oil catalytic upgrading using zeolite ZSM-5 and bentonite under atmospheric pressure and at 60 ºC (bio-oil temperature at the outlet of the pyrolysis process). The used zeolite is a ZSM-5 in hydrogen form (HZSM-5) that has a SiO_2/Al_2O_3 ratio of 500 ± 70, a particle size of 2 – 8 µm, a surface area of 400 m^2/ g and pore size of 5.3 x 5.6 Å. The used bentonite is a Total-sorb product certificated as an oil absorber type III-R with a particle size below 0.25 mm. These HZSM-5 and bentonite are respectively purchased from Across Organics and MYTA S.A.

The upgrading process is performed using raw bio-oil and different weight percentages of catalyst (bentonite or HZSM-5) in a three-neck flask equipped with a thermometer, reflux condenser and magnetic stirrer (Figure 3.11.). The tested percentages are 0, 5, 10, 15 and 20 wt % of reaction solution for both catalysts. Temperature is maintained at 60 ºC during all the process. Reactions are sampled every 2 h interval and samples are centrifuged at 4500 rpm for 15 min to separate the catalyst from the treated bio-oil. Raw and treated bio-oil are characterised by means of pH, TAN, water content and chemical composition to observe the changes in bio-oil properties during the upgrading process (see section 3.1.). In Figure 3.12.a., it is shown a scheme of the upgrading process.

Figure 3.11. Picture of experimental set-up for assessment of the catalytic upgrading process.

Moreover, the catalyst lifetime is tested. With this aim, pH changes are followed in the first 90 min of the upgrading process in order to study when the catalyst deactivation takes place. Moreover, the effect of catalyst replacement over the process is studied replacing the HZSM-5 by a new one every 15 min of reaction time adding 10 wt % of HZSM-5 to a raw bio-oil in the equipped three bottle flask at 60 ºC (Figure 3.12. b.). A total of three consecutive substitutions of HZSM-5 are performed. The catalyst is removed by centrifugation, replaced by a new one and mixed vigorously.

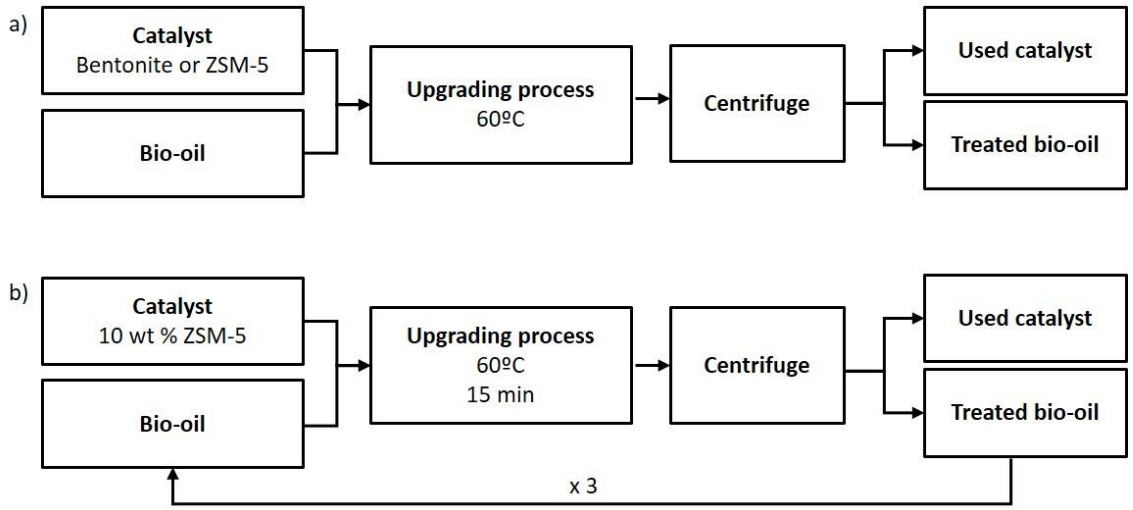

Figure.3.12. Scheme of: a) overall upgrading experiment and (b) and catalyst replacement experiment.

3.3.3. Hydrogenation processes: preliminary assessment

Secondly, three different hydrogenation processes under ambient temperature and atmospheric pressure are considered to explore new ways to hydrogenate bio-oil which reduces the high energy and hydrogen supply cost of conventional hydrotreating processes. These hydrogenation processes include molecular hydrogen injection and in situ production of nascent hydrogen by means of water electrolysis and via metal oxidation in an acidic medium.

Molecular hydrogen injection

Molecular hydrogen is injected by means of a needle directly in 35 g of bio-oil poured in a round bottom flask equipped with a magnetic stirrer and covered with a septum. The hydrogen is stored inside a balloon and this is connected to the needle. Also, another needle is inserted to the septum as gas outlet (Figure 3.13.). In this way, it is not generated pressure inside the round bottom flask. Before molecular hydrogen injection, the air inside the round bottom flask is released to ensure hydrogen atmosphere. Treated bio-oil is sampled after 5 days of reaction time and analysed by GC/MS.

Figure 3.13. Molecular hydrogen experimental set-up scheme.

Electrolytic nascent hydrogen

To generate electrolytic nascent hydrogen, electrolysis of water contained in bio-oil is carried out decomposing it into oxygen (O_2) and hydrogen gas (H_2). A potential difference of 31.6 V is applied between two platinum electrodes. At negatively charged cathode, reduction of the hydrogen cations of the medium are reduced to form hydrogen gas. At positively charged anode, oxygen gas is generated by oxidation (Equation 3.5. and 3.6).

$$\text{Cathode (reduction): } 2\ H_2O\ (l) + 2e^- \rightarrow H_2(g) + 2\ OH^-(aq) \qquad \text{Equation 3.1.}$$

$$\text{Anode (oxidation): } 4\ OH^-(aq) \rightarrow O_2(g) + 2\ H_2O(l) + 4\ e^- \qquad \text{Equation 3.6.}$$

Both half reactions are needed to take place separately joined by a salt bridge, due to hydrogen is only desired to be injected in bio-oil for hydrogenate it. Usually, individual half-cells are separated by a porous membrane which act as salt bridge. The bio-oil contact with this membrane can clogging it porous and impeding its function as salt bridge. In order to avoid this inconvenient, the anode is placed into a syringe which contains KCl 3M. The syringe tip is equipped with a compacted paper filter which plays as a salt bridge without allowing the bio-oil flow and can be changed easily if it becomes clogged. Bio-oil is stirred by a magnetic stirrer during the whole experiment. Figure 3.14. shows a picture of the experiment.

Bio-oil is sampled after 6h of reaction time, the sample is analysed by GC-MS.

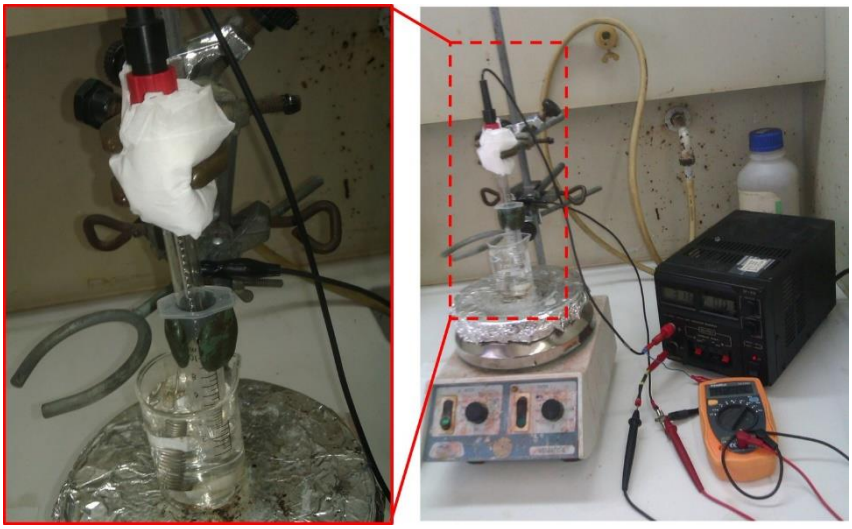

Figure 3.14. Picture of the electrolytic nascent hydrogen production experimental set-up.

Nascent hydrogen via metal oxidation in acidic medium

Nascent hydrogen is produced via metal oxidation using bio-oil as the acidic medium required to occur the reaction showed in Equation 3.6. Two metals are tested with this aim: zinc and aluminium.

$$2\,H^{+} + Me \rightarrow Me^{2+} + 2H\bullet \qquad \text{Equation 3.6.}$$

In order to evaluate which is the most effective metal to generate nascent hydrogen using bio-oil as acidic medium, three covered vessels are prepared containing 35 g of bio-oil with 2.5 wt % of aluminium in the first one, 2.5 wt % of Zinc in the second one and without metal in the third one to use it as a blank. The experiment is carried out at atmospheric pressure and without agitation for 44 days of reaction time. A sample of each vessel is analysed by GC-MS analysis to study the bio-oil composition changes that take place during the hydrogenation process.

3.3.4. *In situ* generation of nascent hydrogen via zinc oxidation.

Among the preliminarily assessed hydrogenation processes, *in situ* generation of nascent hydrogen via zinc oxidation to its ion form using bio-oil as acidic medium is selected to be further developed and studied. This study consist of adding zinc metal

pieces to a raw bio-oil in a covered vessel under different experimental conditions in order to assess the feasibility of generate nascent hydrogen under different operational conditions and select which are the optimum ones.

A set of 15 experiments under different experimental conditions are carried out (Table 3.9.). The different tested variables are the initial weight of Zn, the stirring type, the temperature and different size of metal pieces (Figure 3.15.). 1.5, 3, 4.5, 9, 13.5 wt % of reaction solution are the studied initial weight of Zn. The tested temperatures are 20 ºC (ambient temperature) and 37 ºC. Three different agitation types are studied: no stirring (NS), orbital shaker with horizontal circular movements (OS) at 150 rpm and vertical rotation shaker (RS) at 35 rpm. Finally, two different size of metal pieces are tested: 2.5 x 80 mm and 2.5 X 8 mm of thin sheet of Zn. For each experimental condition, a blank without zinc metal addition is carried out in the same way as the experiments.

Table 3.9. Performed experiments at different experimental conditions: initial weight of zinc metal (1.5, 3, 4.5, 9, 13.5 wt %), temperature (20 and 37 ºC), stirring type (no stirring (NS), Orbital shaker (OS) and vertical rotation shaker (RS)) and Zn size (2.5 x 8 mm and 2.5 x 80 mm).

Experiment	Initial Zn (wt %)	Temperature (ºC)	Stirring type	Zn size
1	1.5	20 ºC	NS	2.5 X 8 mm
2	3	20 ºC	NS	2.5 x 8 mm
3	4.5	20 ºC	NS	2.5 x 8 mm
4	1.5	20 ºC	OS	2.5 x 8 mm
5	3	20 ºC	OS	2.5 x 8 mm
6	4.5	20 ºC	OS	2.5 x 8 mm
7	1.5	37 ºC	OS	2.5 x 8 mm
8	3	37 ºC	OS	2.5 x 8 mm
9	4.5	37 ºC	OS	2.5 x 8 mm
10	4.5	37 ºC	RS	2.5 x 8 mm
11	9	37 ºC	RS	2.5 x 8 mm
12	13.5	37 ºC	RS	2.5 x 8 mm
13	4.5	37 ºC	RS	2.5 x 80 mm
14	9	37 ºC	RS	2.5 x 80 mm
15	13.5	37 ºC	RS	2.5 x 80 mm

Figure 3.15. Picture of the shakers used and the pieces of Zn: orbital shaker with horizontal circular movements (a); Vertical rotation shaker (b); Zn pieces of 2.5 x 8 mm (c); Zn pieces of 2.5 x 80 mm.

To test the zinc reaction, bio-oil is sampled at 0, 1, 2, 4, 6, 8, 13, 17, 22 days of reaction time. For each sample, it is analysed the pH and the concentration of Zn^{2+} (mmol Zn^{2+} /g bio-oil) as an indirect measurement of the hydrogen nascent generated which can be stoichiometrically calculated.

After the selection of the optimum tested conditions, three experiments are carried out under these conditions to assess: (1) the reaction progress at the first 10 d of reaction time and its influence on bio-oil properties.; (2) bio-oil acidity influence on the possibility of carrying out the zinc oxidation reaction; (3) bio-oil phase separation and its influence on zinc ion distribution.

Nascent hydrogen production under optimum tested condition.

After the selection of the optimum tested conditions, an additional experiment is carried out under these conditions to study the reaction progress up to 10 days of reaction time. For each sample, not only the amount of Zn^{2+} and pH are analysed in order to follow the nascent hydrogen production, but also bio-oil properties changes by means of bio-oil acidity by DAN analysis, chemical composition by GC-MS, elemental composition and calorific value.

Influence of bio-oil acidity on nascent hydrogen generation

It is known that the metal oxidation to its ion requires an acidic medium to occur, because of that it is important to assess the influence of bio-oil acidity on the nascent hydrogen generation. This influence is studied by means of an experiment carried treating 30 g of bio-oil under the optimum tested conditions for 3 days. After that time, concentrated acid (H_2SO_4 18M in methanol) is added to bio-oil to reacidify the treated bio-oil up to a pH value of 2.2 (pH of raw bio-oil). After the reacidification, bio-oil is subjected to the optimum tested conditions for extra 5 days. A blank is tested under the same conditions without acid addition. To follow both reactions, bio-oil is sampled at 0, 3, 6 and 8 days of reaction time. For each sample, the pH and the amount of Zn^{2+} (mmol Zn^{2+} /g bio-oil) is analysed to assess the nascent hydrogen production.

Phase separation influence on ion zinc distribution

Bio-oil phase separation might occur during the hydrotreating process, which might suppose some advantages for this hydrogenation process due to the presence of ion zinc in the treated bio-oil is undesirable to its use as fuel. In this sense, separating aqueous phase where it is supposed to be solved the Zn^{2+} from the organic phase which has more energetic value might permit the elimination of this ion. Because of that, it is interesting to study the Zn^{2+} distribution on water and oil phases when phase separation occurs after some reaction time. An experiment in a vessel with 30 g of bio-oil and under

the optimum tested conditions is carried out during 7 days of reaction time. After this time, the sample is centrifuged at 5000 rpm for 30 minute to obtain a clear interphase. Both phases are separated and weighted and the Zn^{2+} content is analysed in each phase.

Finally, in order to reduce the Zn^{2+} content in the oil phase, a liquid-liquid extraction of the Zn^{2+} present in this phase with water is performed. With this aim, 7 g of oil phase are mixed with 7 g of water. The mixture is stirred vigorously with a spatula to ensure a good contact between liquids. After that, the sample is centrifuged at 5000 rpm for 30 minutes to obtain a clear interphase. The oil phase is separated and its Zn^{2+} content is analysed.

References of Part I

[1] Haberl H, Erb K-H, Krausmann F, Running S, Searchinger TD, Kolby Smith W. Bioenergy: how much can we expect for 2050? Environ Res Lett 2013;8:031004.

[2] Hossain KA. Global Energy Consumption Pattern and GDP. Int J Renew Energy Technol Res 2012;1:23–9.

[3] International Energy Agency. Annual Report. 2012.

[4] BP. Statistical Review of World Energy. 2013.

[5] Ioelovich M. Recent Findings and the Energetic Potential of Plant Biomass as a Renewable Source of Biofuels – A Review. Bioresource 2015;10:1879–914.

[6] Shafiee S, Topal E. When will fossil fuel reserves be diminished? Energy Policy 2009;37:181–9.

[7] Schneider SH. The Greenhouse effect: Science and Policy. Science (80-) 1989;243:771–81.

[8] Singh A, Agrawai M. Acid rain and its ecological consequences. J Envirnomental Biol 2008;2919:15–24.

[9] EuropaBio. Boosting the EU bioeconomy. 2008.

[10] Commission E. Communication from the Commission “Innovating for Sustainable Growth: A Bioeconomy for Europe” {SWD(2012) 11 final}. 2012.

[11] McKendry P. Energy production from biomass (Part 1): Overview of biomass. Bioresour Technol 2002;83:37–46.

[12] Di Blasi C, Signorelli G, Di Russo C, Rea G. Product Distribution from Pyrolysis of Wood and Agricultural Residues. Ind Eng Chem Res 1999;38:2216–24.

[13] Li S, Xu S, Liu S, Yang C, Lu Q. Fast pyrolysis of biomass in free-fall reactor for hydrogen-rich gas. Fuel Process Technol 2004; 85:1201–11.

[14] Tumuluru JS, Sokhansanj S, Wright CT, Hess JR, Boardman RD. A Review on Biomass Torrefaction Process and Product Properties. Symp. Thermochem. Convers., 2011.

[15] Ramage J, Scurlock J. Biomass. In: Boyle G, editor. Renew. Energy power ofr a Sustain. Futur., Oxford University Press; 1996, p. 37–82.

[16] Guo M, Song W, Buhain J. Bioenergy and biofuels: History, status, and perspective. Renew Sustain Energy Rev 2015;42:712–25.

[17] Todd Werpy T, Petersen P. Top Value Added Chemicals from Biomass Volume I —

Results of Screening for Potential Candidates from Sugars and Synthesis Gas Top Value Added Chemicals From Biomass Volume I : Results of Screening for Potential Candidates. 2004.

[18] Holladay JE, White JF, Bozell JJ, Johnson D. Top Value-Added Chemicals from Biomass Volume II — Results of Screening for Potential Candidates from Biorefinery Lignin. 2007.

[19] de Wild P, Reith H, Heeres E. Biomass pyrolysis for chemicals. Biofuels 2012;2:185–208.

[20] Jahirul M, Rasul M, Chowdhury A, Ashwath N. Biofuels Production through Biomass Pyrolysis —A Technological Review. Energies 2012;5:4952–5001.

[21] Rathmann R, Szklo A, Schaeffer R. Land use competition for production of food and liquid biofuels: An analysis of the arguments in the current debate. Renew Energy 2010;35:14–22.

[22] Ajanovic A. Biofuels versus food production: Does biofuels production increase food prices? Energy 2011;36:2070–6.

[23] Demirbas. Biomass resource facilities and biomass conversion processing for fuels and chemicals. Energy Convers Manag 2001;42:1357–78.

[24] Demirbas MF. Biorefineries for biofuel upgrading: A critical review. Appl Energy 2009;86:151–61.

[25] Faaij A. Modern Biomass Conversion Technologies. Mitig Adapt Strateg Glob Chang 2006;11:335–67.

[26] Yaman S. Pyrolysis of biomass to produce fuels and chemical feedstocks. Energy Convers Manag 2004;45:651–71.

[27] McKendry P. Energy production from biomass (Part 2): Conversion technologies. Bioresour Technol 2002;83:47–54.

[28] Bridgwater A. Renewable fuels and chemicals by thermal processing of biomass. Chem Eng J 2003;91:87–102.

[29] Huber GW, Iborra S, Corma A. Synthesis of transportation fuels from biomass: chemistry, catalysts, and engineering. Chem Rev 2006;106:4044–98.

[30] Goyal HB, Seal D, Saxena RC. Bio-fuels from thermochemical conversion of renewable resources: A review. Renew Sustain Energy Rev 2008;12:504–17.

[31] Serrano-Ruiz JC, Dumesic J a. Catalytic routes for the conversion of biomass into liquid hydrocarbon transportation fuels. Energy Environ Sci 2011;4:83.

[32] Koppejan J, van Loo S. Biomass combustion: an overview. In: Bridgwater A,

Houfbauer H, van Loo S, editors. Therm. biomass Convers., CPL press; 2009.

[33] Turkenburg WC. Renewable Energy Technologies. In: Goldemberg J, editor. World energy Assess. energy Chall. Sustain., vol. 3, United Nations Development Programme; 2000, p. 220–72.

[34] Chew JJ, Doshi V. Recent advances in biomass pretreatment – Torrefaction fundamentals and technology. Renew Sustain Energy Rev 2011;15:4212–22.

[35] Bridgwater AV, Peacocke GVC. Fast pyrolysis processes for biomass. Renew Sustain Energy Rev 2000;4:1–73.

[36] Bridgwater a. An overview of fast pyrolysis of biomass. Org Geochem 1999;30:1479–93.

[37] Bridgwater AV. Catalysis in thermal biomass conversion. Appl Catal A Gen 1994;1-2:5–47.

[38] Mohan D, Pittman, CU, Steele PH. Pyrolysis of Wood/Biomass for Bio-oil: A Critical Review. Energy & Fuels 2006;20:848–89.

[39] Basu P. biomass gasification and pyrolysis: practical design and theory. Elsevier Inc.; 2010.

[40] Yang H, Yan R, Chen H, Zheng C, Lee DH, Uni V, et al. In-Depth Investigation of Biomass Pyrolysis Based on Three Major Components : Hemicellulose , Cellulose and Lignin 2006:388–93.

[41] Wang X, Kresten SRA, Prins W, Van Swaaij PMW. Biomass Pyrolysis in a Fluidized Bed Reactor. Part 2: Experimental Validation of Model Results. Ind Eng Chem Res 2005:8786–95.

[42] Bridgwater A V. Review of fast pyrolysis of biomass and product upgrading. Biomass and Bioenergy 2012;38:68–94.

[43] Tumuluru JS, Sokhansanj S, Hess JR, Wright CT, Boardman RD. A review on biomass torrefaction process and product properties for energy application. Ind Biotechnol 2011.

[44] Tumuluru JS, Hess JR, Boardman RD, Wright CT, Westover TL. Formulation, Pretreatment, and Densification Options to Improve Biomass Specifications for Co-Firing High Percentages with Coal. Ind Biotechnol 2012;8:113–32.

[45] Chen W-H, Peng J, Bi XT. A state-of-the-art review of biomass torrefaction, densification and applications. Renew Sustain Energy Rev 2015;44:847–66.

[46] van der Stelt MJC, Gerhauser H, Kiel JH a., Ptasinski KJ. Biomass upgrading by torrefaction for the production of biofuels: A review. Biomass and Bioenergy

2011;35:3748–62.

[47] Bergman PCA. Combined torrefaction and pelletisation The TOP process. 2005.

[48] Prins MJ, Ptasinski KJ, Janssen FJJG. Torrefaction of wood. Part 2. Analysis of products. J Anal Appl Pyrolysis 2006;77:35–40.

[49] Bergman PC a, Boersma a R, Zwart RWR, Kiel JH a. Torrefaction for biomass co-firing in existing coal-fired power stations. Energy Res Cent Netherlands ECN ECNC05013 2005:71.

[50] Peng JH, Bi HT, Sokhansanj S, Lim JC. A Study of Particle Size Effect on Biomass Torrefaction and Densification 2012.

[51] Prins MJ, Ptasinski KJ, Janssen FJJG. More efficient biomass gasification via torrefaction. Energy 2006;31:3458–70.

[52] Wannapeera J, Fungtammasan B, Worasuwannarak N. Effects of temperature and holding time during torrefaction on the pyrolysis behaviors of woody biomass. J Anal Appl Pyrolysis 2011;92:99–105.

[53] Chen W-H, Kuo P-C. A study on torrefaction of various biomass materials and its impact on lignocellulosic structure simulated by a thermogravimetry. Energy 2010;35:2580–6.

[54] Peng JH, Bi XT, Sokhansanj S, Lim CJ. Torrefaction and densification of different species of softwood residues. Fuel 2013;111:411–21.

[55] Bergman PCA, Kiel JHA. Torrefaction for biomass upgrading. 14th Eur. Biomass Conf. Exhib., 2005, p. 17–21.

[56] Pastorova I, Arisz P, Boon JJ. Preservation of D-glucose oligosaccharides in cellulose chars. Carbohydr Res 1993;248:151–65.

[57] Oliveira-Rodrigues T, Rousset P. Effects of torrefaction on energy proper- ties of eucalyptus grandis wood. Cerne 2009;15:446–52.

[58] Bergman P, Boersma A, Kiel J, Prins M, Ptasinski K, Janssen F. Torrefied biomass for entrained-flow gasification of biomass.Report ECN-C- 05-026. Petten: 2005.

[59] Uslu A, Faaij a. PC, Bergman PC a. Pre-treatment technologies, and their effect on international bioenergy supply chain logistics. Techno-economic evaluation of torrefaction, fast pyrolysis and pelletisation. Energy 2008;33:1206–23.

[60] Arias B, Pevida C, Fermoso J, Plaza MG, Rubiera F, Pis JJ. Influence of torrefaction on the grindability and reactivity of woody biomass. Fuel Process Technol 2008;89:169–75.

[61] Phanphanich M, Mani S. Impact of torrefaction on the grindability and fuel

characteristics of forest biomass. Bioresour Technol 2011;102:1246–53.

[62] Agar D, Gil J, Sanchez D, Echeverria I, Wihersaari M. Torrefied versus conventional pellet production – A comparative study on energy and emission balance based on pilot-plant data and EU sustainability criteria. Appl Energy 2015;138:621–30.

[63] Peng JH, Bi HT, Lim CJ, Sokhansanj S. Study on density, hardness, and moisture uptake of torrefied wood pellets. Energy and Fuels 2013;27:967–74.

[64] Järvinen T, Agar D. Experimentally determined storage and handling properties of fuel pellets made from torrefied whole-tree pine chips, logging residues and beech stem wood. Fuel 2014;129:330–9.

[65] Ciolkosz D, Pennsylvania T, Wallace R, Hamilton BA. A review of torrefaction for bioenergy feedstock. Biofuels, Bioprod Biorefining 2011;5:317–29.

[66] Tumuluru JS, Wright CT, Kenney KL, Hess JR, Lawrence DL. A Technical Review on Biomass Processing : densification, preprocessing, modeling and optimization. Biomass 2010;0300.

[67] Fagernäs LI, Kuoppala E, Arpiainen V. Composition, utilization and economic assessment of torrefaction condensates. Energy & Fuels 2015:150331150901001.

[68] Branca C, Di Blasi C, Galgano A, Broström M. Effects of the Torrefaction Conditions on the Fixed-Bed Pyrolysis of Norway Spruce 2014.

[69] Khazraie Shoulaifar T, Demartini N, Willför S, Pranovich A, Smeds AI, Virtanen TAP, et al. Impact of torrefaction on the chemical structure of birch wood. Energy and Fuels 2014;28:3863–72.

[70] Tiilikkala K, Fagernäs L, Tiilikkala J. History and use of wood pyrolysis liquids as biocide and plant protection product. Open Agric J 2010;4:111–8.

[71] Jung KH. Growth inhibition effect of pyroligneous acid on pathogenic fungus, Alternaria mali, the agent of Alternaria blotch of apple. Biotechnol Bioprocess Eng 2007;12:318–22.

[72] Lindqvist I, Lindqvist B, Tiilikkala K, Hagner M, Penttinen OP, Pasanen T, et al. Birch tar oil is an effective mollusc repellent: Field and laboratory experiments using Arianta arbustorum (Gastroboda: Helicidae) and Arion lusitanicus (Gastroboda: Arioni- dae). Agric Food Sci 2010;19:1–12.

[73] Hagner M., Pasanen T., Lindqvist B., Lindqvist I., Tiilikkala K., Penttinen OP., et al. Effects of birch tar oils on soil organisms and plants. Agric Food Sci 2010;19:13–23.

[74] Lande S, Westin M, Schneider MH. Eco-efficient wood protection. Furfurylated wood as alternative to traditional wood preservationNo Title. Manag Environ Qual Int J 2004;15:529–40.

[75] Kleinschmidt CP. Overview of international developments in torrefaction, IEA Bioenergy Torrefaction workshop. Graz (Austria): 2011.

[76] Wilén C, Jukola P, Sipil K, Verhoeff F, Kiel J. Wood torrefaction – pilot tests and utilisation. 2013.

[77] Meijer C and. Overview of European torrefaction landscape. 2012.

[78] Balat M, Balat M, Kırtay E, Balat H. Main routes for the thermo-conversion of biomass into fuels and chemicals. Part 1: Pyrolysis systems. Energy Convers Manag 2009;50:3147–57.

[79] Huber GW, Iborra S, Corma A. Synthesis of transportation fuels from biomass: chemistry, catalysts and engineering. Chem Rev 2006;106:4044–98.

[80] Akhtar J, Saidina Amin N. A review on operating parameters for optimum liquid oil yield in biomass pyrolysis. Renew Sustain Energy Rev 2012;16:5101–9.

[81] Laird DA, Brown R, Amonette J, Lehmann J. e pyrolysis platform for coproducing bio-oil and biochar. Biofuels, Bioprod Biorefin 2009;3:547–62.

[82] Huber GW, Corma A. Synergies between bio- and oil refineries for the production of fuels from biomass. Angew Chem Int Ed Engl 2007;46:7184–201.

[83] Chiaramonti D, Oasmaa A, Solantausta Y. Power generation using fast pyrolysis liquids from biomass. Renew Sustain Energy Rev 2007;11:1056–86.

[84] Czernik S, Bridgwater A V. Overview of Applications of Biomass Fast Pyrolysis Oil. Energy & Fuels 2004;18:590–8.

[85] Radovanovic M, Venderbosch RH, Prins W, van Swaaij WP. Some remarks on the viscosity measurement of pyrolysis liquids. Biomass and Bioenergy 2000;18:209–22.

[86] Qi Z, Jie C, Tiejun W, Ying X. Review of biomass pyrolysis oil properties and upgrading research. Energy Convers Manag 2007;48:87–92.

[87] Lu Q, Wen-Zhi L, Xi-Fen Z. Overview of fuel properties of biomass fast pyrolysis oils. Energy Convers Manag 2009;50:1376–83.

[88] Meier D, Faix O. State of the art of applied fast pyrolysis of lignocellulosic materials - A review. Bioresour Technol 1999;68:71–7.

[89] Lehto J, Oasmaa A, Solantausta Y, Kytö M, Chiaramonti D. Review of fuel oil quality and combustion of fast pyrolysis bio-oils from lignocellulosic biomass. Appl Energy 2014;116:178–90.

[90] Oasmaa A, Peacocke C. Properties and fuel use of biomass-derived fast pyrolysis liquids. A guide. 2010.

[91] Oasmaa A, Leppämäki E, Koponen P, Levander J, Tapola E. Physical characterization of biomass-based pyrolysis liquids. Application of standard fuel oil analyses. Espoo, Tech Res Cent Finl 1997.

[92] Diebold J, Czernik S. Additives to lower and stabilize the viscosity of pyrolysis oils during storage. Energy Fuels 1997;11:1081–91.

[93] McKinley J. Biomass liquefaction: centralised analysis. Final report:23216-4-6192. Ottawa, Canada.: 1989.

[94] Chum H, McKindley J. Report on the characterization of biomass pyrolysis liquid products workshop. In: Bridgwater A V., Kuester JL, editors. Reserach therochmical biomass Convers., Springer Netheralnds; 1988, p. 1177–80.

[95] Elliott DC, Oasmaa A, Meier D, Preto F, Bridgwater A V. Results of the IEA round robin on viscosity and aging of fast pyrolysis bio-oils: Long-Term tests and repeatability. Energy and Fuels 2012;26:7362–6.

[96] Oasmaa a, Meier D. Norms and standards for fast pyrolysis liquids1. Round robin test. J Anal Appl Pyrolysis 2005;73:323–34.

[97] Meier D. New Methods for chemical and physical characterization and round robin testing. Fast pyrolysis biomass a Handb. 2nd ed., Newbury: CPL Press; 1999.

[98] Oasmaa A, Peacocke C. A guide to physical property characterisation of biomass-derived fast pyrolysis liquids. Vtt Publ 2001.

[99] Garcia-perez M, Garcia-nunez JA, Lewis T, Kruger C, Kantor S. Methods for Producing Biochar and Advanced Bio-fuels in Washington State. Part 3: Literature Review of Technologies for Product Collection and Refining. Third Proj Report Dep Biol Syst Eng Cent Sustain Agric Nat Resour Washingt State Univ Pullman, WA 2012:129.

[100] Garcia-Perez M, Chaala A, Pakdel H, Kretschmer D, Roy C. Characterization of bio-oils in chemical families. Biomass and Bioenergy, vol. 31, 2007, p. 222–42.

[101] Oasmaa A, Kuoppala E, Solantausta Y. Fast Pyrolysis of Forestry Residue. 2. Physicochemical Composition of Product Liquid. Energy & Fuels 2003;17:433–43.

[102] Oasmaa a., Peacocke C, Gust S, Meier D, McLellan R. Norms and Standards for Pyrolysis Liquids. End-User Requirements and Specifications. Energy & Fuels 2005;19:2155–63.

[103] Gallezot P. Conversion of biomass to selected chemical products. Chem Soc Rev 2012;41:1538–58.

[104] Bridgwater a. V, Toft a. J, Brammer JG. A techno-economic comparison of power production by biomass fast pyrolysis with gasification and combustion. vol. 6.

2002.

[105] Jindo K, Mizumoto H, Sawada Y, Sanchez-Monedero M a., Sonoki T. Physical and chemical characterizations of biochars derived from different agricultural residues. Biogeosciences Discuss 2014;11:11727–46.

[106] Özçimen D, Ersoy-Meriçboyu A. Characterization of biochar and bio-oil samples obtained from carbonization of various biomass materials. Renew Energy 2010;35:1319–24.

[107] Brewer CE, Schmidt-Rohr K, SatrioR JA, Brown RC. Characterization of Biochar from Fast Pyrolysis and Gasification Systems. Environ Prog Sustain Energy 2009;28:386–96.

[108] Vamvuka DÃ. Bio-oil , solid and gaseous biofuels from biomass pyrolysis processes — An overview. Int J Energy Res 2011;35:835–62.

[109] Chen D, Zhou J, Zhang Q, Zhu X. Evaluation methods and research progresses in bio-oil storage stability. Renew Sustain Energy Rev 2014;40:69–79.

[110] Butler E, Devlin G, Meier D, McDonnell K. A review of recent laboratory research and commercial developments in fast pyrolysis and upgrading. Renew Sustain Energy Rev 2011;15:4171–86.

[111] Mortensen PM, Grunwaldt J-D, Jensen P a., Knudsen KG, Jensen a. D. A review of catalytic upgrading of bio-oil to engine fuels. Appl Catal A Gen 2011;407:1–19.

[112] Yang Z, Kumar A, Huhnke RL. Review of recent developments to improve storage and transportation stability of bio-oil. Renew Sustain Energy Rev 2015;50:859–70.

[113] Pattiya A, Suttibak S. Production of bio-oil via fast pyrolysis of agricultural residues from cassava plantations in a fluidised-bed reactor with a hot vapour filtration unit. J Anal Appl Pyrolysis 2012;95:227–35.

[114] Chiaramonti D, Bonini M, Fratini E, Tondi G, Gartner K, Bridgwater A V. Development of emulsions from biomass pyrolysis liquid and diesel and their use in engines — Part 1 : emulsion production. Biomass and Bioenergy 2003;25:85–99.

[115] Ikura M, Stanciulescu M, Hogan E. Emulsification of pyrolysis derived bio-oil in diesel fuel. Science (80-) 2003;24:221–32.

[116] Zhang Q, Chang J, Wang T, Xu Y. Upgrading Bio-oil over Different Solid Catalysts. Energy & Fuels 2006;20:2717–20.

[117] Mahfud F, Melincabrera I, Manurung R, Heeres H. Biomass to FuelsUpgrading of Flash Pyrolysis Oil by Reactive Distillation Using a High Boiling Alcohol and Acid Catalysts. Process Saf Environ Prot 2007;85:466–72.

[118] Dickerson T, Soria J. Catalytic fast pyrolysis: A review. Energies 2013;6:514–38.

[119] Adjaye JD, Bakhshi NN. Production of hydrocarbons by catalytic upgrading of a fast Part I: Conversion over various catalysts. Fuel Process Technol 1995;45:161–83.

[120] Adjaye JD, Bakhshi NN. Catalytic conversion of a biomass-derived oil to fuels and chemicals ii: chemical kinetics, parameter estimation and model predictions. Biomass and Bioenergy 1995;8:265–77.

[121] Wildschut BJ. Pyrolysis Oil Upgrading to Transportation Fuels by Catalytic Hydrotreatment. 2009.

[122] Huang J, Long W, Agrawal PK, Jones CW. Effects of Acidity on the Conversion of the Model Bio-oil Ketone Cyclopentanone on H−Y Zeolites. J Phys Chem C 2009;113:16702–10.

[123] Guo X, Zheng Y, Zhang B, Chen J. Analysis of coke precursor on catalyst and study on regeneration of catalyst in upgrading of bio-oil. Biomass and Bioenergy 2009;33:1469–73.

[124] de Miguel Mercader F, Groeneveld MJ, Kersten SR a., Way NWJ, Schaverien CJ, Hogendoorn J a. Production of advanced biofuels: Co-processing of upgraded pyrolysis oil in standard refinery units. Appl Catal B Environ 2010;96:57–66.

[125] Elliott DC, Hart TR, Neuenschwander GG, Rotness LJ, Zacher AH. Catalytic Hydroprocessing of Biomass Fast Pyrolysis Bio-oil to Produce Hydrocarbon Products. Environ Prog Sustain Energy 2009;28:441–9.

[126] Venderbosch RH, Ardiyanti AR, Wildschut J, Oasmaa A, Heeres HJ. Stabilization of biomass-derived pyrolysis oils. J Chem Technol Biotechnol 2010;85:674–86.

[127] Corma A, Huber G, Sauvanaud L, Oconnor P. Processing biomass-derived oxygenates in the oil refinery: Catalytic cracking (FCC) reaction pathways and role of catalyst. J Catal 2007;247:307–27.

[128] Bridgwater a. V. Production of high grade fuels and chemicals from catalytic pyrolysis of biomass. Catal Today 1996;29:285–95.

[129] Li NT, Ompsett G, Huber G. Renewable high-octane gasoline by aqueous- phase hydrodeoxygenation of C5 and C6 carbohydrates over Pt/Zirconium phosphate catalyst. ChemSusChem 2010;3:1154–7.

[130] Li N, Huber GW. Aqueous-phase hydrodeoxygenation of sorbitol with Pt/SiO2-Al2O3: Identification of reaction intermediates. J Catal 2010;270:48–59.

[131] Elliott DC. Historical Developments in Hydroprocessing Bio-oils. Energy & Fuels 2007;21:1792–815.

[132] Parapati DR, Guda VK, Penmetsa VK, Tanneru SK, Mitchell B, Steele PH. Comparison of Reduced and Sulfided CoMo/c-Al2O3 Catalyst on Hydroprocessing of Pretreated Bio-Oil in a Continuous Packed-Bed Reactor. Environ Prog Sustain Energy 2015;34:1174–9.

[133] Parapati DR, Guda VK, Penmetsa VK, Steele PH, Tanneru SK. Single Stage hydroprocessin gof pyrolysis oil in a continuous packed-bed reactor. Environ Prog 2014;33:726–31.

[134] de Miguel Mercader F, Groeneveld MJ, Kersten SR a., Geantet C, Toussaint G, Way NWJ, et al. Hydrodeoxygenation of pyrolysis oil fractions: process understanding and quality assessment through co-processing in refinery units. Energy Environ Sci 2011;4:985.

[135] Wildschut J, Mahfud FH, Venderbosch RH, Heeres HJ. Hydrotreatment of Fast Pyrolysis Oil Using Heterogeneous Noble-Metal Catalysts. Ind Eng Chem Res 2009;48:10324–34.

[136] Wildschut J, Melián-Cabrera I, Heeres HJ. Catalyst studies on the hydrotreatment of fast pyrolysis oil. Appl Catal B Environ 2010;99:298–306.

[137] Capunitan J a., Capareda SC. Hydrotreatment of corn stover bio-oil using noble metal catalysts. Fuel Process Technol 2014;125:190–9.

[138] Elliott DC, Hart TR, Neuenschwander GG, Rotness LJ, Olarte M V., Zacher AH, et al. Catalytic hydroprocessing of fast pyrolysis bio-oil from pine sawdust. Energy and Fuels 2012;26:3891–6.

[139] Elliott DC, Baker EG. Process for upgrading biomass pyrolyzates, 1989.

[140] Rover MR, Hall PH, Johnston P a., Smith RG, Brown RC. Stabilization of bio-oils using low temperature, low pressure hydrogenation. Fuel 2015;153:224–30.

[141] Elliott DC, Wang H, French RJ, Deutch S, Iisa K. Hydrocarbon Liquid Production from Biomass via Hot-Vapor Filtered Fast Pyrolysis and Catalytic Hydroprocessing of the Bio-oil. Energy & Fuels 2014:140814202117009.

[142] Marker TL, Petri JA. Gasoline and diesel production from pyrolytic lignin produced from pyrolysis of cellulosic waste. Patent 7,578,927, 2009.

[143] Sanna A, Vispute TP, Huber GW. Hydrodeoxygenation of the aqueous fraction of bio-oil with Ru/C and Pt/C catalysts. Appl Catal B Environ 2015;165:446–56.

[144] Adjaye JD, Bakhshi NN. Catalytic conversion of a biomass-derived oil to fuels and chemicals I: Model compound studies and reaction pathways. Biomass and Bioenergy 1995;8:131–49.

[145] Elliott DC, Hart TR. Catalytic hydroprocessing of chemical models for bio-oil. Energy

and Fuels 2009;23:631–7.

[146] Wang H, Male J, Wang Y. Recent advances in hydrotreating of pyrolysis bio-oil and its oxygen-containing model compounds. ACS Catal 2013;3:1047–70.

[147] Ruddy D a., Schaidle J a., Ferrell III JR, Wang J, Moens L, Hensley JE. Recent advances in heterogeneous catalysts for bio-oil upgrading via "ex situ catalytic fast pyrolysis": catalyst development through the study of model compounds. Green Chem 2014;16:454.

[148] Kersten SRA, van Swaaij WPM, Lefferts L, Seshan K. Options for catalysis in the Thermochemical conversion of biomass into fuels. In: Centi Ga, Sant R van S, editors. Renewables From Feed. to Energy Prod., Wiley; 2007, p. 119–46.

[149] Vitolo S, Bresci B, Seggiani M, Gallo M. Catalytic upgrading of pyrolytic oils over HZSM-5 zeolite: behaviour of the catalyst when used in repeated upgrading–regenerating cycles. Fuel 2001;80:17–26.

[150] Vitolo S, Seggiani M, Frediani P, Ambrosini G, Politi L. Catalytic upgrading of pyrolytic oils to fuel over different zeolites. Fuel 1999;78:1147–59.

[151] Adjaye JD, Bakhshi NN. Production of hydrocarbons by catalytic upgrading of a fast pyrolysis bio-oil. Part II: Comparative catalyst performance and reaction pathways. Fuel Process Technol 1995;45:185–202.

[152] Gayubo AG, Valle B, Aguayo T, Bilbao J. Attenuation of Catalyst Deactivation by Cofeeding Methanol for Enhancing the Valorisation of Crude Bio-oil. Energy & Fuels 2009;23:4129–36.

[153] Valle B, Gayubo AG, Alonso A, Aguayo AT, Bilbao J. Hydrothermally stable HZSM-5 zeolite catalysts for the transformation of crude bio-oil into hydrocarbons. Appl Catal B Environ 2010;100:318–27.

[154] Triantafyllidis K, Iliopoulou E, Antonakou E, Lappas a, Wang H, Pinnavaia T. Hydrothermally stable mesoporous aluminosilicates (MSU-S) assembled from zeolite seeds as catalysts for biomass pyrolysis. Microporous Mesoporous Mater 2007;99:132–9.

[155] Zhu X, Mallinson RG, Resasco DE. Role of transalkylation reactions in the conversion of anisole over HZSM-5. Appl Catal A Gen 2010;379:172–81.

[156] Gong F, Yang Z, Hong C, Huang W, Ning S, Zhang Z, et al. Selective conversion of bio-oil to light olefins: controlling catalytic cracking for maximum olefins. Bioresour Technol 2011;102:9247–54.

[157] Park HJ, Jeon J-K, Suh DJ, Suh Y-W, Heo HS, Park Y-K. Catalytic Vapor Cracking for Improvement of Bio-Oil Quality. Catal Surv from Asia 2011;15:161–80.

[158] Katikaneni S, Adjaye J, Bakhshi N. Performance of aluminophosphate molecular sieve catalysts for the production of hydrocarbons from wood-derived and vegetable oils. Energy & Fuels 1995:1065–78.

[159] Lu Q, Zhang Z-F, Dong C-Q, Zhu X-F. Catalytic Upgrading of Biomass Fast Pyrolysis Vapors with Nano Metal Oxides: An Analytical Py-GC/MS Study. Energies 2010;3:1805–20.

[160] Lu Q, Zhang Y, Tang Z, Li W, Zhu X. Catalytic upgrading of biomass fast pyrolysis vapors with titania and zirconia/titania based catalysts. Fuel 2010;89:2096–103.

[161] Mihalcik DJ, Mullen C a., Boateng A a. Screening acidic zeolites for catalytic fast pyrolysis of biomass and its components. J Anal Appl Pyrolysis 2011;92:224–32.

[162] Aho A, Kumar N, Eränen K, Salmi T, Hupa M, Murzin DY. Catalytic pyrolysis of woody biomass in a fluidized bed reactor: Influence of the zeolite structure. Fuel 2008;87:2493–501.

[163] French R, Czernik S. Catalytic pyrolysis of biomass for biofuels production. Fuel Process Technol 2010;91:25–32.

[164] Cheng Y-T, Jae J, Shi J, Fan W, Huber GW. Production of Renewable Aromatic Compounds by Catalytic Fast Pyrolysis of Lignocellulosic Biomass with Bifunctional Ga/ZSM-5 Catalysts. Angew Chemie Int Ed 2012;51:1387–90.

[165] Vichaphund S, Aht-ong D, Sricharoenchaikul V, Atong D. Catalytic upgrading pyrolysis vapors of Jatropha waste using metal promoted ZSM-5 catalysts: An analytical PY-GC/MS. Renew Energy 2014;65:70–7.

[166] Vichaphund S, Aht-ong D, Sricharoenchaikul V, Atong D. Production of aromatic compounds from catalytic fast pyrolysis of Jatropha residues using metal/HZSM-5 prepared by ion-exchange and impregnation methods. Renew Energy 2015;79:28–37.

[167] Veses a., Puértolas B, Callén MS, García T. Catalytic upgrading of biomass derived pyrolysis vapors over metal-loaded ZSM-5 zeolites: Effect of different metal cations on the bio-oil final properties. Microporous Mesoporous Mater 2015;209:189–96.

[168] Du Z, Ma X, Li Y, Chen P, Liu Y, Lin X, et al. Production of aromatic hydrocarbons by catalytic pyrolysis of microalgae with zeolites: Catalyst screening in a pyroprobe. Bioresour Technol 2013;139:397–401.

[169] Meier D, Van De Beld B, Bridgwater A V., Elliott DC, Oasmaa A, Preto F. State-of-the-art of fast pyrolysis in IEA bioenergy member countries. Renew Sustain Energy Rev 2013;20:619–41.

[170] Venderbosch RH, Prins W. Fast pyrolysis technology development. Biofuels, Bioprod Biorefining 2010;4:178–208.

[171] Underwood G, Graham R. Method of using fast pyrolysis bio-oils as liquid smoke. 4,876,108, 1989.

[172] Fortum. http://www.fortum.com/en/energy-production/combined-heat-and-power/finland/pages/default.aspx (accessed October 10, 2015)

[173] Laboratory NRE. Conceptual biorefinery. http://www.nrel.gov/biomass/biorefinery.html (accessed October 10, 2015).

[174] Fernando S, Adhikari S, Chandrapal C, Murali N. Biorefineries: Current Status, Challenges, and Future Direction. Energy & Fuels 2006;20:1727–37.

[175] Kamm B, Kamm M. Principles of biorefineries. Appl Microbiol Biotechnol 2004;64:137–45.

[176] Clark JH, Deswarte FEI. Introduction to chemicals from biomass. Wiley Series in Renewable Resources. John Wiley & Sons, TJ International, Padstow, Cornwall.; 2008.

[177] Van Ree R, Annevelink B. Status Report Biorefinery. 2007.

[178] Devappa RK, Rakshit SK, Dekker RFH. Forest biorefinery: Potential of poplar phytochemicals as value-added co-products. Biotechnol Adv 2015;33:681–716.

[179] Joelsson E, Wallberg O, Börjesson P. Integration potential, resource efficiency and cost of forest-fuel-based biorefineries. Comput Chem Eng 2015;82:240–58.

[180] Puy Marimon N. Integrated sustainability analysis of innovative uses of forest biomass . Bio-oil as an energy vector. 2010.

[181] Oasmaa A, Elliott DC, Korhonen J. Acidity of Biomass Fast Pyrolysis Bio-oils. Energy & Fuels 2010;24:6548–54.

II

ADDING VALUE OF AGRICUTRAL WASTE BIOMASS AS TORREFIED PELLETS

4. Adding value of agricultural waste biomass as torrefied pellets

The results of the pilot project carried out to study the viability of recovering agricultural waste biomass (AWB) into a valuable solid product as torrefied pellets by means of torrefaction process in Ribera d'Ebre are presented in this chapter.

4.1. Introduction of chapter 4: adding value of agricultural waste biomass as torrefied pellets

Biomass as a solid fuel is characterised by its high moisture content, low heating value , hygroscopic nature and large volume and low bulk density, which results in a low conversion efficiency, as well as difficulties in its collection, grinding, storage and transportation [1]. As it is stated in Chapter 1, torrefaction is a thermochemical process carried out at 200-300ºC under atmospheric conditions in absence of oxygen [2] that improve biomass properties to obtain a higher quality and more attractive solid biofuel. Torrefied biomass has higher calorific value, energy density, lower moisture content; higher hydrophobicity and improved grindability and reactivity in comparison to the original biomass [1]. The pelletisation of this torrefied solid result in a final product with further enhanced fuel properties due to torrefied pellets have low moisture content, low uptake of moisture, high energy content, resistance against biological degradation and good grindability [3–5]

The main product of torrefaction process is torrefied solid, already mentioned, which has been extensively studied [6,7], as well as its pelletisation due to its obtained a valuable and short term marketable product. However, liquid and gas fractions are also obtained during the process. These fractions are not very studied yet, although Fagernäs et al. [8] studied the yields and chemical composition of torrefaction liquid and assessed their potential uses to convert torrefaction liquid into a valuable product.

Torrefaction technology at commercial scale is currently in its early phase. To move toward its commercial market introduction, several technology companies and

their industrial partners are developing pilot and demonstration scale torrefaction plants to assess and proof the feasibility and benefits of this technology. In this context, Energies Tèrmiques Bàsiques S.L. is a company that has developed a pilot thermochemical conversion plant for processing different types of biomass which can operate at 30 kg/h. Currently, it is on a pre-commercial stage with a more than 100 kg/h capacity conversion plant that has successfully tested a wide range of biomass under continuous operation and it is planned to scale it up to 1 t/h industrial plant. These biomass adding value plants are modular and transportable, with the aim of obtaining added value products (solid, liquid or gaseous) in situ from the different types of biomasses.

Moving in this direction, a pilot project is performed to demonstrate the technical and economic viability of implementing a torrefaction process to add value of agricultural waste biomass as torrefied pellets in the torrefaction pilot plant developed by Energies Tèrmiques Bàsiques SL installed in a rural zone. The viability of this project in a rural zone might permit a local energy production and consume using a residue as a resource, moving toward the circular economy concept. Moreover, locating the torrefaction plant and performing the pilot test in the study zone might facilitate the acceptance of the use of this technology by local social agents and proper implementation of this type bioeconomy project as short term strategy.

This pilot project consists on many stages that permit to obtain a whole picture of the adding value process which encloses: (1) the biomass potential assessment of the study zone; (2) a pilot test to determine and calculate the real logistic requirements and costs of supply the valuable biomass to the plant (harvesting, chipping, transport and storage); (3) the installation of the semi-industrial pilot plant of Energies Tèrmiques Bàsiques SL for a year in an agricultural cooperative of Ascó municipality; (4) the characterisation and treatment of the valuable biomass in the semi-industrial plant, as well as the characterisation of the obtained torrefied products after the optimisation of the torrefaction process; (5) the pelletability assessment of

the obtained torrefied biomass; and (6) the economic viability of the torrefaction process to produce torrefaction pellets in Ribera d'Ebre context using the data obtained during the pilot test considering different scenarios of implementation.

This project is performed by a work team comprised by Inèdit Innovació S.L., Energia Tèrmica Bàsiques S.L. and Universitat Autònoma de Barcelona, with the collaboration of Ascó local government. Each work team member is responsible of one or more stages of the project. Among them, the characterisation of raw biomass, torrefaction products (solids and liquids) and torrefied pellets is performed within this thesis work, as well as the overall economic assessment. However, the results obtained from other stages of the project required to carry out this thesis work are also shown in this chapter.

The results obtained during this pilot project has been submitted (15.10.15) in a peer-reviewed scientific journal with the following reference:

Artigues A, Cañadas V, Puy N; Gasol C; Alier S; Bartrolí J. Torrefied pellets production from wood crop waste as valuable product in agricultural sector: techno-economical pilot test assessment. Biomass and Bioenergy (Under review).

4.2. Feedstock characterisation

From the assessment of the potential valuable agricultural waste biomass, it is concluded that fruit, olive and nut waste biomass have high potential of exploitation (section 3.2.1.). Because of that cherry pruning waste, almond pruning waste and olive pruning waste are characterised as feedstock to assess their possible use as feedstock for the torrefaction plant. The raw biomass characterisation is mandatory due to the quality of the torrefaction products depends on their composition and their thermal behaviour [2,9]. In Figure 4.1., it is shown a picture of each of these biomasses.

Figure 4.1. Pictures of potential valuable raw biomasses: cherry pruning waste (a); almond pruning waste (b); olive pruning waste (c).

These biomasses are characterised by means of elemental analysis, immediate analysis, calorific value, thermogravimetric analysis and ash composition analysis (see section 3.1). Characterization results are shown in Table 4.1. All biomasses have a very similar composition as it can be observed from the elemental analysis. They contain low concentrations of sulphur which implies the absence of sulphur oxides (SOx) during their combustion. Regarding to the immediate analysis, cherry tree pruning biomass has the highest ash content, which might affect the combustion boiler efficiency in comparison to olive pruning waste. The main element present in the biomass ashes is calcium. Other elements as magnesium, phosphorus, potassium and sodium (in this order) have high concentrations in the ash of all the biomasses. Moreover, the content of potentially toxic metals as nickel, copper, zinc, arsenic, cadmium and lead are in low quantities. This ash composition makes ashes a good candidates as quality fertilizer [10].

Comparing the calorific value of the different kinds of biomass, olive pruning waste has the highest calorific value, followed by cherry and almond pruning waste.

Table 4.1. Raw biomass properties as received. (HHV: High heating value; LHV: Low heating value)

		Almond pruning waste	Olive pruning waste	Cherry pruning waste
	N	0.24	0.26	0.3
	C	47.21	46.02	45.59
	H	5.87	5.92	5.92
	S	<0.1	<0.1	<0.1
	O[a]	46.68	47.79	48.19
	Mositure	7.6	7.27	8.27
	Volatiles	83.7	84.16	82.2
	Ash	0.98	0.84	1.26
	Fixed carbon[a]	7.72	7.74	8.27
HHV	(MJ/Kg)	17.42	18.98	17.54
LHV	(MJ/Kg)	16.13	17.67	16.24
	Na	3	0.6	0,9
	Mg	61	27	20
	P	53	23	13
	K	17	2	2
	Ca	364	442	405
	Ni	< 0.05	< 0.05	0,09
	Cu	0.2	0.2	0,3
	Zn	< 0.05	< 0.05	0,06
	As	< 0.05	< 0.05	< 0,05
	Cd	< 0.05	< 0.05	< 0,05
	Pb	< 0.05	< 0.05	< 0,05

Finally, it is carried out a ThermoGravimetric Analysis (TGA) which shows the biomass decomposition at different temperatures. This decomposition corresponds to the loss of mass of biomass when there is an increase of temperature.

TGA indicates the maximum temperature therein the torrefaction process must be carried out in order to eliminate moisture content and high volatile compounds without high weight losses, since a maximum efficiency of solid fraction is desirable. In Figure 4.2., it is shown the TGA curve for each potential valuable agricultural waste biomass. All biomasses have similar behaviour against temperature. Their decomposition started from 200 ºC and finished around 400 ºC. Cherry woody waste biomass decomposition profile is a bit different from the other two lignocellulosic biomasses. The devolatilisation rate is slower between 200-250 ºC, at higher temperatures the profile is really similar however it is moved around 50 ºC at the right

side. Moreover, a decomposition peak is observed for olive and cherry pruning waste biomass between 250 ºC and 300 ºC and 300 ºC -350 ºC, respectively, but not for almond pruning waste biomass.

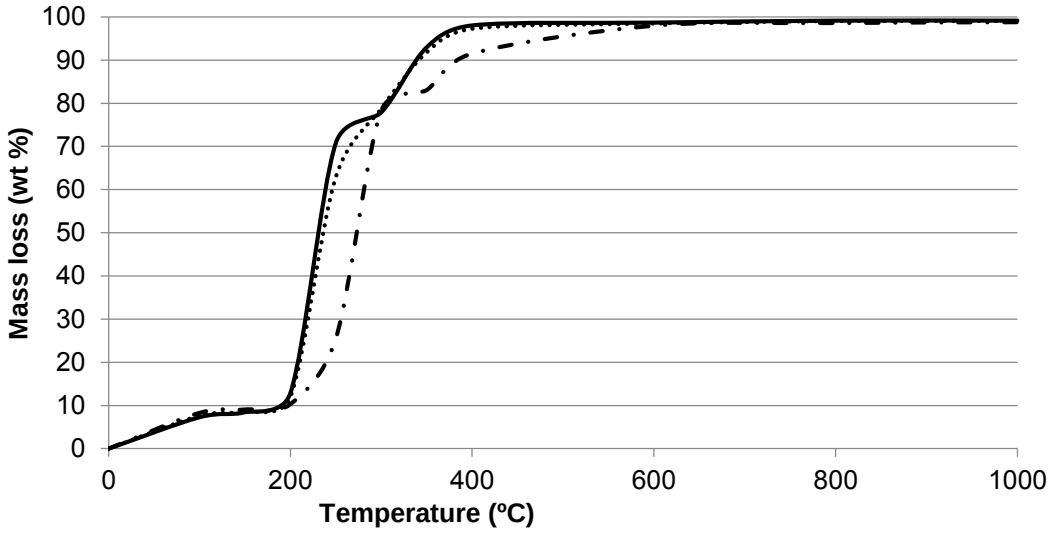

Figure 4.2. Thermogravimetric analysis of biomass coming from Ascó: almod wood (•••); cherry wood (-•–); olive wood (—).

To sum up, all lignocellulosic biomasses might be treated in the torrefaction plant. From the TGA results, it is considered that the tested temperatures for biomass torrefaction in the plant are between 200 - 300 ºC.

4.3. Optimum operational conditions to treat agricultural waste biomass in the torrefaction plant.

Taking into account the obtained results from the characterisation of the different feedstock, the operational conditions of the torrefied plant are optimised by Energies Tèrmiques Bàsiques.

The first optimised parameter is the wood chip size of biomass feedstock. The chip size is a crucial parameter to ensure the heat transfer inside the biomass particles. The smaller is the chip size, the higher is the heat intake into the biomass. However, generate small chips has a higher energetic consume and reduce biomass fibre size to enable a proper pelletisation of the obtained torrefied biomass. Because of that, it is important to select an appropriate chip size to balance out these three parameters: heat transfer, cost of chipping process and suitable particle shape for pelletisation. Consequently, it is carried out preliminary experiments with chips of 3, 4 and 5 mm of different types of biomass resulting in a compromise chip size of 4 mm. Figure 4.3. shows raw biomasses pictures and the grinded biomass at 4mm to observe their differences.

Figure 4.3. Comparison between raw and grinded biomass: almond pruning waste (a); olive pruning waste (b).

After biomass pre-treatment optimisation, different runs at diverse temperatures are performed to test the optimum operational conditions of each feedstock. The operational conditions of each run are specified in section 3.2.3. The obtained fractions efficiency for each run and biomass is shown in Table 4.2. The optimum torrefaction conditions are those that maximise the solid fraction and achieve improved biomass properties in comparison to the feedstock biomass.

Table 4.2. Operational conditions and obtained fractions efficiency (solid, liquid and gas from the biomass torrefaction treatment. (*calculated by difference)

Biomass	Temperature (ºC)	Biomass load (kg/h)	Solid fraction (wt %)	Liquid fraction (wt %)	Gas fraction (*) (wt%)
Cherry pruning waste	230	15.6	92.8	2.9	4.3
	250	14.7	91.3	4.1	4.6
	265	15.6	83.7	11.5	4.8
	280	12.8	84.4	12.5	3.1
Almond pruning waste	250	17.2	88.3	7	4.7
	280	15.2	87.3	7.8	4.9
	290	13.6	86.5	8.8	4.7
	295	15.6	84.6	9.6	5.8
Olive pruning waste	220	16.8	83.9	16.1	0
	250	13.8	76.1	10.9	13
	270	14.1	63.8	12.8	23.4

As it is observed in Table 4.2., each type of biomass has a different behaviour inside the reactor.

Firstly, it is compared the solid yield at the same reactor temperature (250 ºC) from the three different raw biomassess. For cherry pruning waste biomass, the recovered torrefied solid fraction is around 91 wt % while for almond and olive pruning waste is a 3 % and 8 % lower, respectively. Olive pruning waste wood has the lowest solid recovery due to there is a decomposition peak at this temperature that almond and cherry biomass do not have. Consequently, this biomass treatment at this temperature generates more volatiles which mainly are non-condensable gases and the condensable ones increase the liquid fraction yield. Because of that, the liquid and gas fraction obtained from olive pruning waste biomass treatment are higher in comparison to almond pruning waste biomass.

The solid fraction yields produced from almond pruning waste treatment are higher than 85 wt % in all the tested temperatures, even when the reactor temperature is around 300 ºC. Thus, this biomass can be treated at temperatures up to 300 ºC with a loss of mass of maximum 15 wt %. Cherry pruning biomass, at temperatures between 260-280 ºC has higher loss of mass in comparison to almond pruning waste, although it is only around 15 wt %. However, at temperatures between

200-250 ºC, the solid recovery is higher than in almond pruning waste treatment. Therefore, this biomass can be treated at temperatures up to 300 ºC being between 200-250 ºC the optimum ones. For olive pruning waste biomass, the yields to solid fraction is highly dependent on the reactor temperature. Among the tested conditions, the maximum solid yield is achieved at 220 ºC. At 270 ºC, it is reduced a 24 %. Because of that olive pruning waste ideal operational temperatures are between 220 – 250 ºC.

Regarding to the liquid fraction, the results shows an increase of liquid fraction to detriment of solid phase with the increase of temperature, as it is expected.

4.4. Characterisation of torrefaction products and their applications.

In this section, the properties of the obtained torrefaction products from the optimum runs of each biomass are assessed. Furthermore, the pelletability of the torrefied biomass is also evaluated.

With these aims, the optimum conditions for olive and almond pruning waste biomass are selected and a complete characterisation of the obtained torrefaction products are performed. Characterised products are those reached to treat olive pruning waste at 250 ºC and almond pruning waste at 280 ºC.

In this work the gas fraction is not characterised due to it contains mainly CO, CO_2 and small amounts of CH_4 [11] resulting in a low heating value product with limited applications.

4.4.1. Torrefied biomass

The solid fraction called torrefied biomass is characterised by means of its calorific value and its moisture content. Comparing torrefied biomass and raw biomass (Table 4.3.), it is observed that the calorific value of each torrefied biomass is higher than those for each raw biomass. There is an increase of calorific value of 6 and 7% for olive pruning waste and almond pruning waste, respectively. The moisture of raw biomasses are reduced between 85-90% during the torrefaction process. Thus, it is

achieved a torrefied biomass with reduced moisture content and higher calorific value, which is the aim of this thermic treatment. Apart from that, torrefied biomass presents other advantages in front of raw biomass as it hydrophobicity and high resistance against biological degradation [6,7].

Table 4.3. Comparison of moisture content and low heating values (LHV) between raw and torrefied biomass.

	Raw biomass		Torrefied biomass	
	Almond pruning waste	Olive pruning waste	Almond pruning waste	Olive pruning waste
LHV (MJ/kg)	14.45	15.27	15.35	17.65
Moisture (wt %)	18.34	18.18	0.71	1.08

Common torrefied biomass applications include: high-quality smokeless solid fuels for industrial, commercial and domestic applications; solid fuel for co-firing directly with pulverized coal at electric power plants and an upgraded feedstock for fuel pellets, briquettes, and other densified biomass fuels [12]. In this work, it is studied its pelletisation in order to obtain torrefied pellets.

4.4.2. Torrefied biomass pelletisation

The feasibility of pelletise the obtained and characterised torrefied biomasses is assessed in this section. The achieved torrefied pellets are evaluated by calorific value, moisture content and ash content (see section 3.1)

The pelletisation process has been carried out by means of a small scale pelletiser of 150 Kg/h of maximum capacity. Torrefied biomass is pelletised achieving torrefied pellets from both biomasses (Figure 4.4.). Their characteristics are shown in Table 4.4. The obtained pellets of both biomasses have similar length and diameter, around 18.5 mm and 6 mm approximate. Pelletisation process increases LHV in comparison to torrefied biomass, around a 18 % for almond pruning waste and 13 %

for olive pruning waste. What is more, LVH increase of almond pruning waste torrefied pellets and olive pruning waste torrefied pellets relatively to raw biomass is around 25 % and 30%, respectively. Regarding to moisture content, almond pruning waste torrefied pellet has a water content of 4.3 wt % while for olive pruning waste torrefied pellet is 4.7 wt %. The ash content of produced pellets are low in both cases. The characteristics of produced torrefied pellets are compared to the European Pellet Standards A1, A2, A3 accordingly to European law pr-EN 14961-2. According to this legislation, both produced torrefied pellets are in category A1-A2 in relation to size (diameter and length), moisture, apparent density and calorific value. However, regarding to the ash content, they are in category A3.

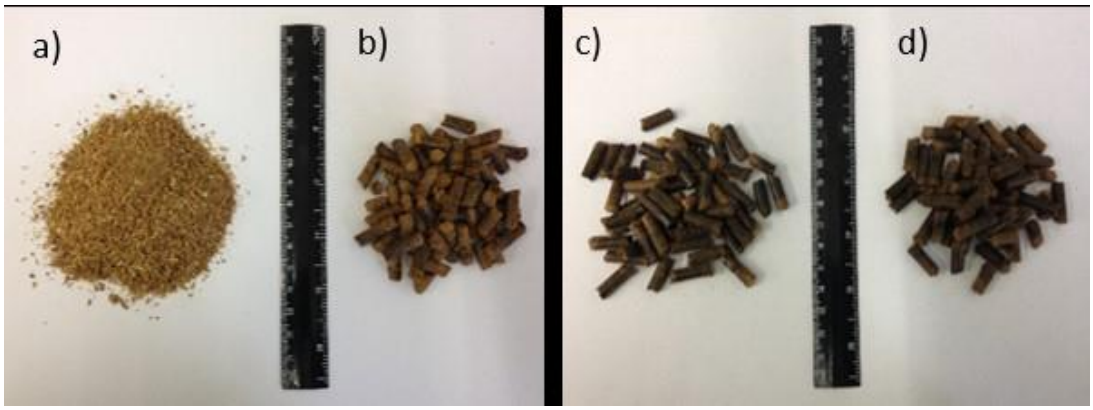

Figure 4.4. Picture of almond pruning waste (a); pellet of raw almond pruning waste (b); torrefied pellets of almond pruning waste at 280 ºC (c); and torrefied pellet of olive pruning waste at 250 ºC (d).

Table 4.4. Characteristics of produced olive pruning waste torrefied pellet at 250 ºC and almond pruning waste torrefied pellets at 280 ºC and their comparison to European Pellet Standards (prEN 14961-2).

Properties	Units	Almond torrefied pellet	Olive torrefied pellet	A1	A2	A3
Diameter	Mm	6.08 ± 0.08	6.08 ± 0.12	D06: 6 ± 1	6 ± 1	6 ± 1
Length	Mm	18.71 ± 1.22	18.54 ± 1.57	3.15 ≤ L ≤ 40	3.15 ≤ L ≤ 40	3.15 ≤ L ≤ 40
				Max. 45 mm		Max. 45 mm
Moisure	wt %	4.3	4.7	≤ 10	≤ 10	≤ 10
Ashes	wt %	1.37	1.19	A0.5: ≤ 0.5	A1.0: ≤ 1.0	A3.0: ≤ 3.0
				A0.7: ≤ 0.7		
Bulk density	kg/m^3	633	655	≥ 600	≥ 600	≥ 600

To sum up, the obtained torrefied biomass pellets are marketable products of the torrefaction plant, with enhanced calorific value in comparison to raw biomass. They are densified product easily transportable with higher calorific value in comparison to non-pelletised torrefied biomass that comply with the standards for European legislation. Thus, these products might be sold and/or be used directly in domestic and municipal boiler of the study zone consuming a local produced energy from a residue converted into a resource of the same zone, reaching a more sustainable energy model moving towards a circular economy.

4.4.3. Liquid of torrefaction

Torrefaction liquids obtained from the torrefaction of almond pruning waste at 280 ºC and olive pruning waste at 250 ºC are also characterised by means of pH, water

content, density and chemical composition, as well as, the quantification of the most abundant chemical compounds (see section 3.1.)

Both liquids are very aqueous and it is observed emulsion formation in these products which indicates the presence of organic compounds in them (Table 4.5.). When the torrefaction operational temperature is high, more torrefied liquid is obtain and it contains more organic compounds in comparison to liquids produced at lower temperatures. This can be observed in the colour of the torrefaction liquid, it is dark brownish when the torrefaction process is carried out at high temperatures and light brownish when it is performed at low temperatures (Figure 4.5.).

Table 4.5. Water and organic content, density, pH and concentration of some target compounds of olive pruning waste torrefaction liquid at 250 ºC and almond pruning waste torrefaction liquid at 280 ºC.

		Olive torrefaction liquid	Almond torrefaction liquid
Water content (wt %)		88.2 ± 0.9	85.6 ± 0.1
Organic matter content (wt %)*		11.8	14.4
Density at 20 ºC		1000.2	1004.1
pH		3.3	4.0
Concentration (mg/L)	Acetic acid	42.6 ± 0.9	17 ± 2
	Furfural	3.6 ± 0.5	0.42 ± 0.04
	Phenol	0.76 ± 0.06	0.9 ± 0.1
	3-methyl-2-cyclopenten-1-one	0.8 ± 0.2	1 ± 0.2

* Calculated by difference.

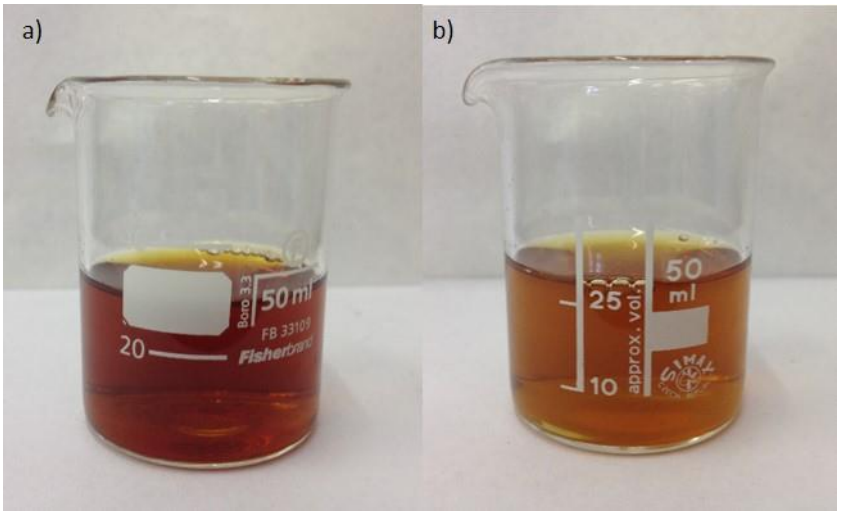

Figure 4.5. Picture of liquid fraction produced: at 280 ºC from almond pruning waste (a) and at 250 ºC from olive pruning waste (b).

Both liquids are acidic due to high content of organic acids. What is more, the main compound of both liquids are acetic acid with concentrations as high as 42.6 ± 0.9 g/L of olive torrefaction liquid and 17 ± 2 g/L of almond one, making olive liquid more acidic than almond one (Table 4.5.).

Regarding to the complete chemical characterisation, torrefaction liquids contain only few majority compounds and many minority compounds, as it is observed in Total ion Chromatogram (TIC) (Figure 4.6.). In Table 4.6., the identified compounds are listed with its identification ion and retention time, as well as, its area and percentage of area relative to the total peak area. The main identified compounds are quantified by means of external calibration, which results are shown in Table 4.5.

For olive pruning torrefaction liquid, the main compounds according to the chromatogram area are acetic acid, 1-hydroxy-2-propanone, furfural, formic acid and phenol. Fagernäs et al [8] reported that the main compounds of torrefied liquids at temperatures between 105-240 ºC are acetic acid and furfural, which is consistent with the obtained results for liquid torrefaction of olive pruning waste at 250 ºC. The liquid fraction with acetic acid and furfural as main compounds have a potential use as pesticides, herbicides, fungicide, insecticide and repellent [13–15].

Regarding to almond pruning torrefaction liquid, its main compounds accordingly the chromatogram area are also acetic acid, 1-hydroxy-2-propanone, phenol, furfural and 2,6-dimethoxy phenol. This liquid is obtained at higher temperatures because of that contained higher amount of organic matter. This liquid has less concentration of acetic acid and furfural, and consequently more concentration of other compounds from different chemical families. Because of that, it might not be suitable for the same purposes as the fraction collected at low temperatures [8]. Its potential use might be as wood preservative in wood protection [16]. Moreover, it might be extracted of some added-value compounds present in the liquid [17].

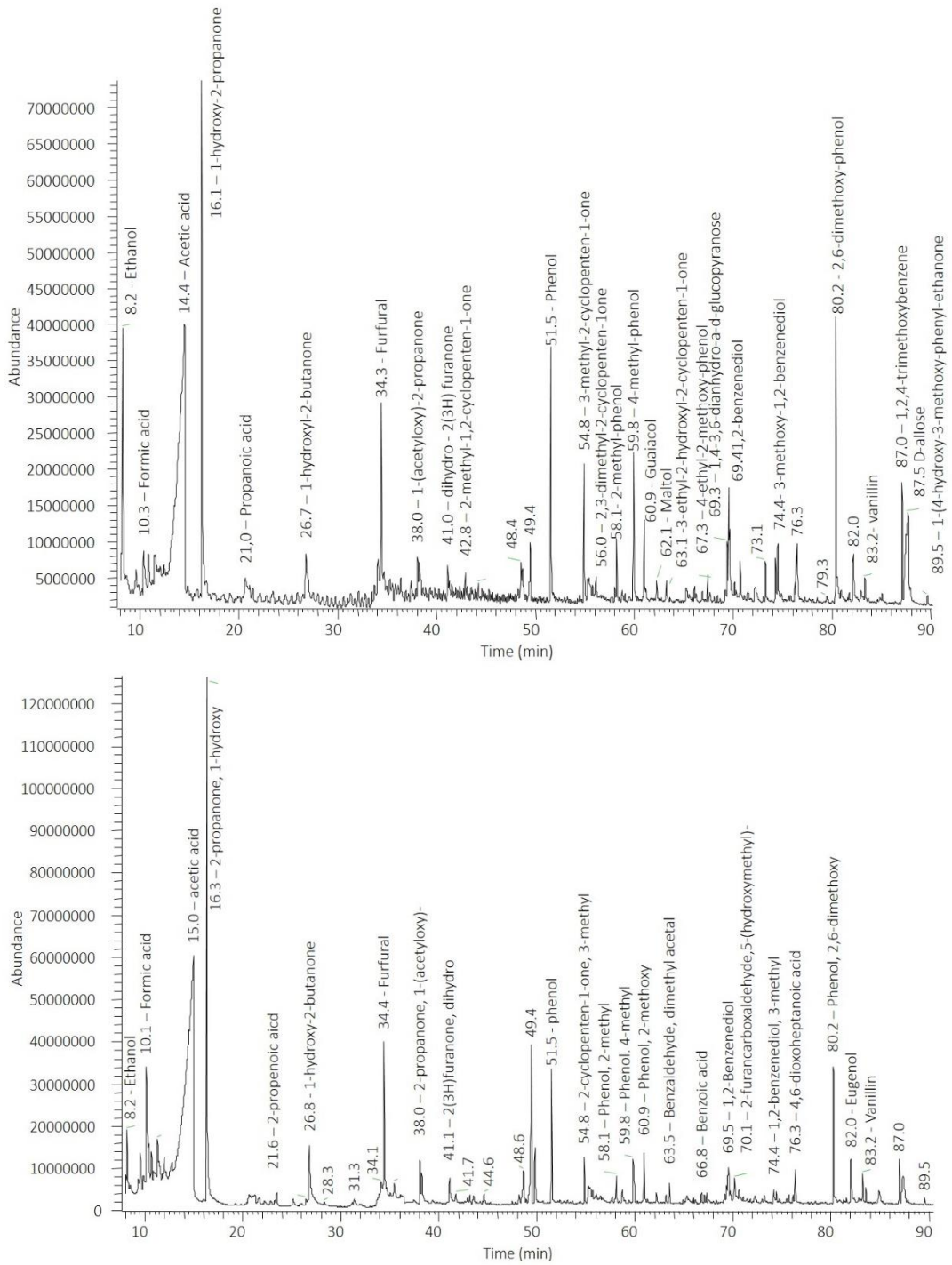

Figure 4.6. Total Ion Chromatogram of torrefaction liquids from almond pruning waste (a) and olive pruning waste (b).

Table 4.6. Identified compounds on almond and olive torrefaction liquid. (RT: Retention time; m/z: mass to charge ration; n.i.: no identified)

Compound	m/z	RT (min)	Almond Torrefaction liquid			Olive torrefaction liquid		
			Area	RSD (%)	Area (%)	Area	RSD (%)	Area (%)
Ethanol	45	8,2	75589946	6	5,4	41704259	13	1,9
Acetic acid methyl ester	74	9,5	4553966	8	0,3	676070	8	0,0
Formic acid	45	10,3	16773378	4	1,2	93642423	9	4,2
Acetic acid	60	14,4	388804769	3	27,8	1008934043	8	45,3
2-propanone, 1-hydroxy	43	16,2	207647495	5	14,9	398574795	5	17,9
Propanoic acid	74	21,0	19451573	3	1,4	26997938	10	1,2
2-propenoic acid	72	21,7	n.i.	-	-	13299919	6	0,6
1,2:3,4-diepoxy-butane	55	25,1	n.i.	-	-	14654440	8	0,7
1-hydroxy-2-butanone	57	26,7	13221278	5	0,9	23405095	8	1,1
Furfural	95	34,3	78211813	0	5,6	102964985	3	4,6
1-(acetyloxy)-2-propanone	43	38,0	27843258	6	2,0	42384463	8	1,9
2-furanmethanol	98	38,1	15121306	2	1,1	19961754	4	0,9
Dihydro-2(3H)furanone	42	41,0	6022579	3	0,4	6699665	4	0,3
2-methyl-1,2-cyclopenten-1-one	96	42,8	6179351	8	0,4	n.i.	-	-
5-methyl-2-furancarbocaldehyde,	110	48,6	5676299	11	0,4	n.i.	-	-
Furan, tetrahydro-2,5-dimethoxy	101	43,2	n.i.	-	-	6105752	6	0,3
1,2 cyclopenten-1-one, 2-hydroxy	98	44,6	n.i.	-	-	7602189	5	0,3
2,3-pentanedione	57	48,1	n.i.	-	-	3633748	3	0,2
Phenol	94	51,5	91487155	1	6,5	75254201	3	3,4
3-methyl-2-cyclopenten-1-one	112	54,8	31067208	8	2,2	17881425	5	0,8
2,3-dimethyl-2-cyclopenten-1-one	67	56,0	3676847	9	0,3	1368788	4	0,1
3-ethyl-2-hydroxy-2-cyclopenten-1-one	126	57,9	1833953	0	0,1	n.i.	-	-
2-methyl-phenol	108	58,1	8927379	11	0,6	7390522	6	0,3
Hydroxymethylcyclopropane	44	58,7	n.i.	-	-	7266176	11	0,3

Table 4.6. (Continued). Identified compounds on almond and olive torrefaction liquid. (RT: Retention time; m/z: mass to charge ration; n.i.: no identified)

Compound	m/z	RT (min)	Almond Torrefaction liquid			Olive torrefaction liquid		
			Area	RSD (%)	Area (%)	Area	RSD (%)	Area (%)
4-methyl-phenol,	107	59,8	39821809	5	2,9	24918768	7	1,1
2-methoxy-phenol	124	60,9	14844166	1	1,1	15052516	6	0,7
Maltol	126	62,1	7471585	1	0,5	6250500	6	0,3
3 ethyl-2-hydroxy-2-cyclopenten-1-one	126	63,1	3430621	1	0,2	1851129	3	0,1
dimethyl acetal-benzaldehyde	121	63,5	n.i.	-	-	13304669	17	0,6
2-4-dimethyl-phenol	107	66,0	2792011	9	0,2	1684865	3	0,1
2,3-dimethyl-phenol	107	66,1	775377	4	0,1	509576	13	0,0
Benzoic acid	105	66,8	2874387	7	0,2	6419005	6	0,3
2,3-dihydroxybenzaldehyde	138	67,1	n.i.	-	-	3399677	8	0,2
4-ethyl-2-methoxy-phenol	107	67,3	9121483	7	0,7	n.i.	-	-
3,5-dimethyl-phenol	122	67,5	1484052	4	0,1	n.i.	-	-
1,4-3,6-dianhydro-a-d-glucopyranose	69	69,3	13857642	6	1,0	8262073	5	0,4
1,2-benzenediol	110	69,4	74735387	7	5,3	38990469	6	1,8
2-methoxy-4-methyl-phenol	123	69,5	6433771	4	0,5	4678016	4	0,2
Dianhydromannitol	86	69,7	n.i.	-	-	3962983	11	0,2
2,3-anhydro-d-mannosan	71	70,0	1306750	8	0,1	n.i.	-	-
5-(hydroxymethyl)-2-furancarboxaldehyde	126	70,1	2640960	6	0,2	13254318	8	0,6
2,3-anhydro-d-mannosan	71	70,6	3473165	7	0,2	1720566	5	0,1
3-methyl-1,2-benzenediol	139	74,2	201137	8	0,0	n.i.	-	-
3-methoxy-1,2-benzenediol	140	74,4	16316581	1	1,2	5203898	5	0,2
2-acetoxy-5-hydroxyacetophenone	137	75,7	1520731	3	0,1	3078183	4	0,1
4-ethyl-2-methoxy-phenol	137	76,1	5420417	3	0,4	3718308	2	0,2
4-methyl-1,2-benzenediol	124	76,2	11415264	2	0,8	n.i.	-	-
4,6-dioxoheptanoic acid	141	76,4	n.i.	-	-	13461957	1	0,6
2,6-dimethoxy-phenol	154	80,2	59522160	2	4,3	52833301	1	2,4

Table 4.6. (Continued). Identified compounds on almond and olive torrefaction liquid (RT: Retention time; m/z: mass to charge ration; n.i.: no identified)

		RT	Almond Torrefaction liquid			Olive torrefaction liquid		
Compound	m/z	(min)	Area	RSD (%)	Area (%)	Area	RSD (%)	Area (%)
4,5-dimethyl-1,3-benzenediol	138	80,8	2435161	2	0,2	n.i.	-	-
Eugenol	164	81,6	795918	1	0,1	1371955	3	0,1
4-ethyl-1,3-benzenediol	123	82,8	4104249	6	0,3	n.i.	-	-
Vanillin	151	83,2	6601010	6	0,5	12250016	9	0,6
4-hydroxy-benzeneethanol	107	84,8	n.i.	-	-	18004402	6	0,8
1,2,4-trimethoxybenzene	168	86,9	30021690	2	2,1	19068241	2	0,9
D-allose	60	87,4	66909861	9	4,8	28517817	7	1,3
2-methoxy-4-(1-propenyl)-phenol	164	87,8	1429094	5	0,1	1158305	9	0,1
1-(4-hydroxy-3-methoxy`-phenyl)-ethanone	151	89,5	3157635	10	0,2	3913834	10	0,2

Although the market for torrefaction liquid is currently undeveloped, it is a valuable product which might be sell to new applications in future as for example biodegradable pesticides or wood preservative in wood protection [8]. Moreover, torrefaction liquid might be used as pellet additive up to 2 wt % of pellet according to European legislation. Thus, it might be achieved even a more compact pellet with a higher calorific value of the initial torrefied pellet. Thus, the economic efficiency of the torrefaction process might be enhance if liquid fraction might be considered valuable product.

4.5. Logistic costs of biomass supply to the plant

The quantification of logistic cost of biomass supply to torrefaction plant is necessary to posteriorly assess the economic viability of this agricultural waste biomass value addition process. These costs are calculated based on the experimental data obtained from the pilot test carried out in a municipal smallholding. This part of the pilot project is carried out by Inèdit Innovació SL and Energies Tèrmiques Bàsiques SL. The main conclusions obtained to afterward understand the performed economic assessment are explained in this section.

Figure 4.7. shows the total logistic cost of biomass and the cost of each logistic operation required (biomass extraction, chipping process, transport, storage and plant feeding) considering the different options to perform them in both considered implementation scenario, described in section 3.2.4.

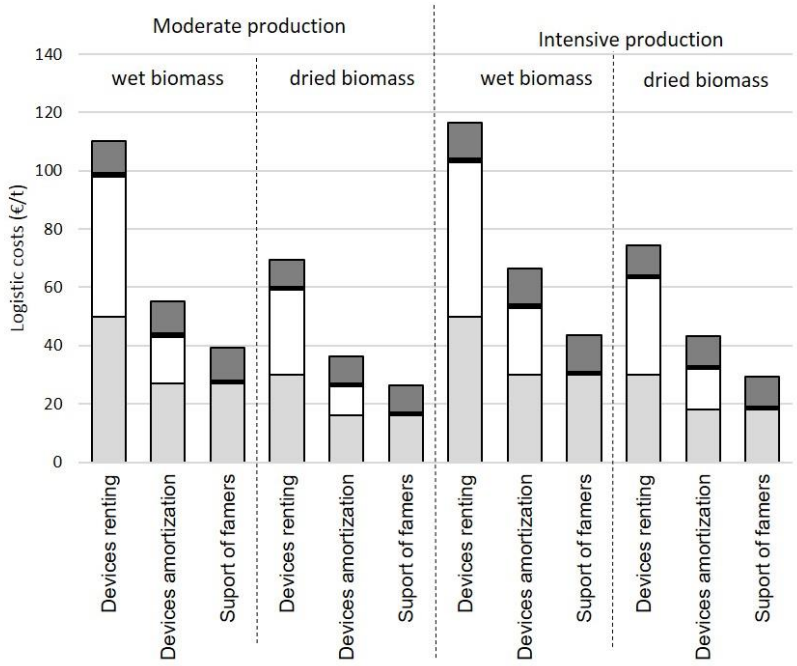

Figure 4.7. Logistic costs for each considered scenario: chipping cost ( ), transport co ( ), storage cost ( ) and feeding plant cost ( ).

Biomass extraction costs which include the pruning and collection of agricultural waste biomass are not included in the total logistic cost since it is considered that the farmer assumes them. That is because the farmer will perform this task to enhance the efficiency and productivity of its crop, both this residue is used or not. What is more, their recovery means a benefit of not having to burn the biomass in the field in an area with a fairly high fire-risk.

The chipping process cost is one of the highest logistic costs and it is highly dependent on the considered scenario. To chip dried biomass at 30 wt % is cheaper than to chip wet biomass at 50 wt % due to the wood chipper yield obtained during the pilot test are 0.9 t wet biomass /h and 1.5 t dried biomass/h. Regarding to the ownership of the wood chipper, renting it is expensive than buying and amortizing it due to the high renting price of this device. Moreover, in intensive scenarios, it is required to buy two wood chippers instead of one due to it is needed more biomass. Because of that, the chipping process cost is higher in intensive production scenarios in comparison to the moderate ones when chipping device is bought.

Transport chipped biomass from the field to the warehouse has a high cost really dependent on the considered scenario. In moderate scenario, it is considered that 2288 t biomass $_{(30\ wt\ \%\ moisture)}$ are required to feed the plant. Thus, the plant can be supplied by the agricultural waste biomass produced in Ascó municipality (2525 t biomass $_{(30\ wt\ \%\ moisture)}$/year), where the plant is located. Because of that it is considered that an average distance radio of 10 km from the field to the torrefaction plant. However, to supply the torrefaction plant in intensive scenario is required the Ascó municipality produced AWB and 1291 t biomass $_{30\ wt\ \%\ of\ moisture}$ obtained from other municipalities of Ribera d'Ebre region. In this case, it is considered that an average distance radio from the field to the torrefaction plant is of 20 km. Because of that biomass transport cost is higher in intensive scenarios in comparison to moderate ones, as can be observed in Figure 4.7. Moreover, in Figure 4.7, it is observed that transport wet chipped biomass has a higher cost than transport dried biomass due to wet biomass take up more volume and require more tractor trips for its transport. Moreover, rent the tractor and trailer to a forestry service company increases the transportation cost in comparison to buy and amortize them. In intensive scenario, two transport devices are required due to double amount of biomass is transported. Because of that, the cost of transport in intensive scenario when the transport devices are owned by the torrefaction plant management company is higher than in moderate scenario. Furthermore, the transportation cost is not considered in scenarios where the transportation is carried out by the farmers support.

Regarding to storage cost to guarantee biomass availability to feed the plant, it has less importance on overall logistic cost. The cost of biomass storage is higher when the initial storage chips are wet due to they take up more space in comparison to the dried ones.

Finally, The feeding plant cost is the same for all the scenarios due to the feedstock must be in all cases dried biomass at 30 wt % and the cost of its feeding is only the amortization cost of buying the forklift truck with a loader to transport it.

To sum up, the logistic costs vary from 28 € / t to 115 € / t depending on proposed logistic operation, being the transport and chipping processes the higher logistic costs (except when the transport is carried out by the support of the farmers). In general, logistic costs increase when wet biomass is handled and when it is rented the logistic devices. Moreover, biomass cost is higher in the intensive production scenario.

4.6. Economic analysis for torrefaction plant implementation

In this section, it is evaluated the economic viability of torrefaction pellet production by means of the torrefaction plant in Ribera d'Ebre context with the data obtained during the pilot test. The economic analysis applied is a cost-benefit analysis by means of Net Present Value (NPV), internal rate of return (IRR) and Effective Rate of Return (ERR), summarized in Table 3.4. in section 3.2.4. Two main implementation scenarios are considered for benefit-cost economic analysis: moderate pellet production and intensive pellet production (see section 3.2.4.).

Torrefied pellet is considered the marketable product of the torrefaction plant. Two different torrefaction pellet sale price are considered for the economic analysis: 206 €/t and 233 € /t. 206 €/t is the average price of conventional wood pellet sale price in 2014 accordingly to AVEBIOM data [18]. The average high calorific value of this conventional pellet is around 17 MJ/kg. Taking into account, that torrefied pellet has a low heating value of approximately 19 MJ/kg , it is considered that this price might be increase a 13 % comparing the calorific value of conventional and torrefied pellet, resulting in a selling price of 233 € / t.

4.6.1. Economic analysis of the torrefaction plant implementation in a moderate torrefaction pellets production scenario.

The economic analysis of the torrefaction plant implementation in a moderate production pellets scenario is shown below. This scenario comprises the production of

torrefied pellets using 2288 t biomass $_{30\ \%\ of\ moisture}$ available in Ascó municipality from agricultural waste biomass.

The values of the calculated economic indicators (NPV, IRR and ROE) taking into account different logistic costs, in moderate scenario, are shown in Table 4.7. Moreover, it is calculated the maximum biomass cost accepted for each scenario which is that makes NPV=0 (Figure 4.8.)

Economic analysis results show that the viability of the torrefaction plant implementation depends on the used logistic process, meaning the biomass cost. It is considered viable those scenarios with positive values of NPV and IRR. However, any of the moderate production scenarios has a ROE value higher than 1, which implies that in any case it is recovered the investment cost of the plant in 15 years. The only exception is the scenarios with a pellet price of 233 € / t with logistics with the support of farmer pre-treating dried biomass.

Taking into account the scenarios that considered the current pellet price, torrefaction plant implementation is not viable both pre-treating dried or wet biomass when chipping and transport devices are rented. It is viable when it is bought the logistic required devices except when wet biomass is chipped. Furthermore, the implementation is always viable when the transport is carried out with the support of farmers. Considering an increase of torrefied pellet price, all scenarios are viable with one exception: when it is chipped wet biomass with rented devices.

To sum up, the only viable moderate scenario that permits to recover the investment cost of the plant in 15 years is that uses dried biomass (30% of moisture), purchases a chipper and performs transport operation with farmers support, as well as pellet selling price of 233 €/t. This scenario is viable due to NPV value (911387 €) and IRR value (17.71 %) are positive and its ROE value is 1.01 which indicated that initial inversion is recovered during plant lifetime. In this case, the purchase price of biomass to the farmer might be 50 € / t. Table 4.8. shows the results obtained from the economic analysis for this scenario, as example.

Table 4.7. Economic analysis of the torrefaction plant implementation in a moderate production of torrefaction pellets scenario (AWB: agricultural waste biomass, NPV: net present value, IRR: internal rate of return, ROE: Return on equity).

Pellet selling price (€)	AWB moisture	Logistic scenarios	NPV	IRR (%)	ROE	AWB cost (€/t)	màx. AWB cost (€/t)	Viability
206	Wet[a]	Devices renting	-1125444	-	-1.25	110		NO
		Devices amortization	-70456	3.82	-0.08	55	51	NO
		Support of farmers	236450	8.67	0.26	39		SI
	Dried[b]	Devices renting	-162528	2.19	-0.18	69		NO
		Devices amortization	386066	10.82	0.43	36	59	SI
		Support of farmers	552307	13.09	0.61	26		SI
233	Wet[a]	Devices renting	-766365	-15.03	-0.85	110		NO
		Devices amortization	288624	9.43	0.32	55	70	SI
		Support of farmers	595530	13.67	0.66	39		SI
	Dried[b]	Devices renting	196552	8.08	0.22	69		SI
		Devices amortization	745146	15.61	0.83	36	81	SI
		Support of farmers	911387	17.71	1.01	26		SI

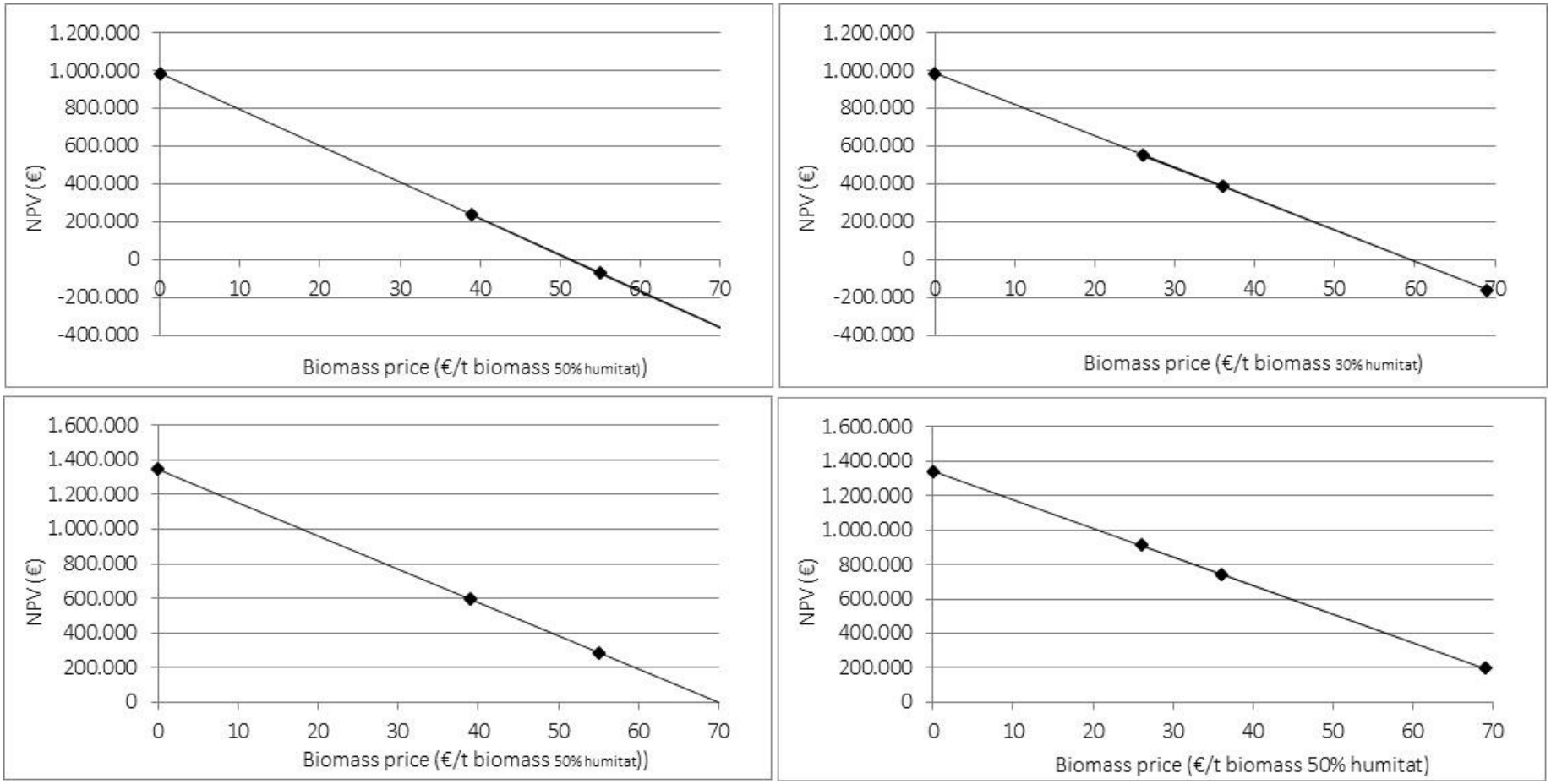

Figure 4.8. Estimation of the maximum biomass cost (€/t) of: biomass 50% of moisture in moderate scenario with pellet selling price of 206 €/t (a); biomass 30% of moisture in moderate scenario with pellet selling price of 206 €/t (b); biomass 50% of moisture in moderate scenario with pellet selling price of 233 €/t (c); biomass 30% of moisture in moderate scenario with pellet selling price of 233 €/t.

Table 4.8. Economic analysis in a moderate scenario using dried biomass and farmers support. Pellet price of 233 €/t (BBT: benefits before taxes; BAT: benefit after taxes,NPV: net present value, IRR: internal rate of return).

		Year														
		1st	2nd	3rd	4th	5th	6th	7th	8th	9th	10th	11th	12th	13th	14th	15th
Investment costs																
Torrefaction plant	€	*600.000*	*600.000*	*600.000*	*600.000*	*600.000*	*600.000*	*600.000*	*600.000*	*600.000*	*600.000*	*600.000*	*600.000*	*600.000*	*600.000*	*600.000*
Pelletisation unit	€	*300.000*	*300.000*	*300.000*	*300.000*	*300.000*	*300.000*	*300.000*	*300.000*	*300.000*	*300.000*	*300.000*	*300.000*	*300.000*	*300.000*	*300.000*
Total	€	900.000	900.000	900.000	900.000	900.000	900.000	900.000	900.000	900.000	900.000	900.000	900.000	900.000	900.000	900.000
Fixed costs																
Amortization	€/year	*60.000*	*60.000*	*60.000*	*60.000*	*60.000*	*60.000*	*60.000*	*60.000*	*60.000*	*60.000*	*60.000*	*60.000*	*60.000*	*60.000*	*60.000*
Insurance	€/year	*3.000*	*3.000*	*3.000*	*3.000*	*3.000*	*3.000*	*3.000*	*3.000*	*3.000*	*3.000*	*3.000*	*3.000*	*3.000*	*3.000*	*3.000*
Total	€/year	*63.000*	*63.000*	*63.000*	*63.000*	*63.000*	*63.000*	*63.000*	*63.000*	*63.000*	*63.000*	*63.000*	*63.000*	*63.000*	*63.000*	*63.000*
Variable costs																
Staff	€/year	*106.805*	*106.805*	*106.805*	*106.805*	*106.805*	*106.805*	*106.805*	*106.805*	*106.805*	*106.805*	*106.805*	*106.805*	*106.805*	*106.805*	*106.805*
Maintenance	€/year	*27.000*	*27.000*	*27.000*	*27.000*	*27.000*	*27.000*	*27.000*	*27.000*	*27.000*	*27.000*	*27.000*	*27.000*	*27.000*	*27.000*	*27.000*
energy consumption	€/year	*6.600*	*6.600*	*6.600*	*6.600*	*6.600*	*6.600*	*6.600*	*6.600*	*6.600*	*6.600*	*6.600*	*6.600*	*6.600*	*6.600*	*6.600*
biomass cost	€/year	*59.488*	*59.488*	*59.488*	*59.488*	*59.488*	*59.488*	*59.488*	*59.488*	*59.488*	*59.488*	*59.488*	*59.488*	*59.488*	*59.488*	*59.488*
Total		*199.893*	*199.893*	*199.893*	*199.893*	*199.893*	*199.893*	*199.893*	*199.893*	*199.893*	*199.893*	*199.893*	*199.893*	*199.893*	*199.893*	*199.893*
Total cost	€/year	*262.893*	*262.893*	*262.893*	*262.893*	*262.893*	*262.893*	*262.893*	*262.893*	*262.893*	*262.893*	*262.893*	*262.893*	*262.893*	*262.893*	*262.893*
unit cost	€/t	*143,63*	*143,63*	*143,63*	*143,63*	*143,63*	*143,63*	*143,63*	*143,63*	*143,63*	*143,63*	*143,63*	*143,63*	*143,63*	*143,63*	*143,63*
BBT	€/year	*163.590*	*163.590*	*163.590*	*163.590*	*163.590*	*163.590*	*163.590*	*163.590*	*163.590*	*163.590*	*163.590*	*163.590*	*163.590*	*163.590*	*163.590*
BAT	€/year	*114.513*	*114.513*	*114.513*	*114.513*	*114.513*	*114.513*	*114.513*	*114.513*	*114.513*	*114.513*	*114.513*	*114.513*	*114.513*	*114.513*	*114.513*
Flux de caixa	€/year	*174.513*	*174.513*	*174.513*	*174.513*	*174.513*	*174.513*	*174.513*	*174.513*	*174.513*	*174.513*	*174.513*	*174.513*	*174.513*	*174.513*	*174.513*
NPV	**€**	*166.203*	*158.289*	*150.751*	*143.572*	*136.736*	*130.224*	*124.023*	*118.117*	*112.493*	*107.136*	*102.034*	*97.175*	*92.548*	*88.141*	*83.944*
IRR	**%**	*17,71%*	*17,71%*	*17,71%*	*17,71%*	*17,71%*	*17,71%*	*17,71%*	*17,71%*	*17,71%*	*17,71%*	*17,71%*	*17,71%*	*17,71%*	*17,71%*	*17,71%*

4.6.2. Economic analysis of the torrefaction plant implementation in an intensive torrefaction pellets production scenario

The values of the economic indicators calculated considering different logistic scenarios in the context of an intensive production of torrefied pellet are shown in Table 4.9. The maximum cost of biomass is calculated taking into account the cost that makes NPV=0 (Figure 4. 9.)

The results of the economic analysis in an intensive production scenarios are more economically favourable in comparison to moderate scenarios. When it is pretreated wet biomass and the logistic devices are rented, the NPV and IRR values are negative at both considered pellet price, being non-viable scenarios. All the other considered scenarios are viable taking into account the NPV and IRR values. Moreover, unlike moderate scenario, all of them have a ROE value higher than 1 except when pellet is sold at 206 € / t, wet biomass is chipped and it is bought the logistic devices. The viable scenarios with ROE value higher than one permit to recover the initial investment in less than 15 years.

The difference between the maximum cost of biomass and the logistic biomass cost is the maximum purchase price of biomass maintaining the economic viability. This price might be between 37 and 88 €/t, depending on the scenario.

Table 4.9. Economic analysis of the torrefaction plant implementation in an intensive production of torrefaction pellets scenario (AWB: agricultural waste biomass, NPV: net present value, IRR: internal rate of return, ROE: Return on equity).

Pellet selling price (€)	AWB moisture	Logistic scenarios	NPV	IRR (%)	ROE	AWB cost (€/t)	màx. AWB cost (€/t)	Viability
206	Wet[a]	Devices renting	-1039473	-	-1.15	117		NO
		Devices amortization	878688	17.30	0.98	67	90	SI
		Support of farmers	1761042	27.76	1.96	44		SI
	Dried[b]	Devices renting	988662	18.67	1.10	74		SI
		Devices amortization	2019354	30.69	2.24	43	103	SI
		Support of farmers	2484828	35.87	2.76	29		SI
233	Wet[a]	Devices renting	-321314	-0.90	-0.36	117		NO
		Devices amortization	1596847	25.88	1.77	67	109	SI
		Support of farmers	2479201	35.81	2.75	44		SI
	Dried[b]	Devices renting	1706822	27.14	1.90	74		SI
		Devices amortization	2737514	38.65	3.04	43	125	SI
		Support of farmers	3202987	43.73	3.56	29		SI

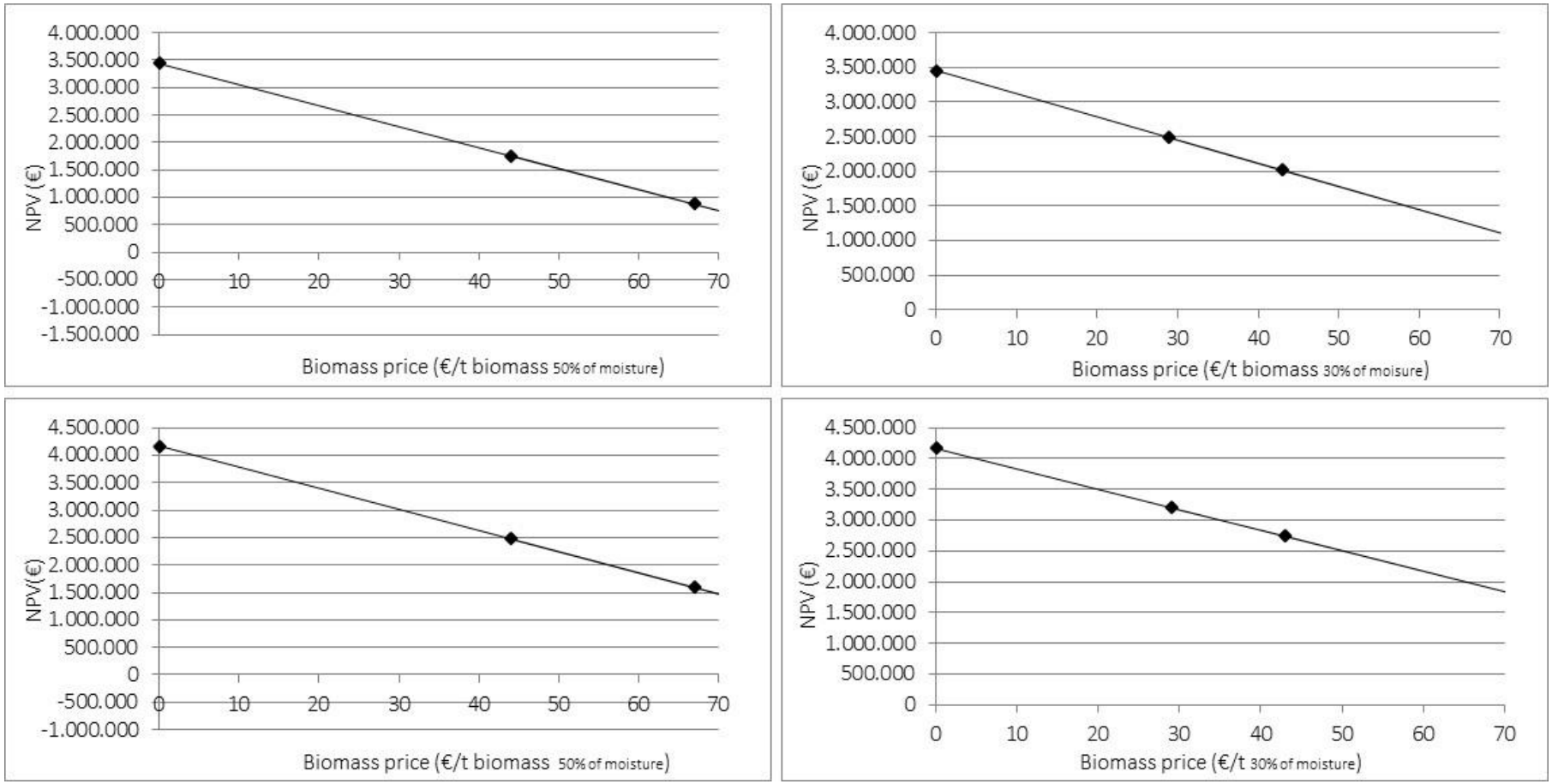

Figure 4.9. Estimation of the maximum biomass cost (€/t) of: biomass 50% of moisture in moderate scenario with pellet selling price of 206 €/t (a); biomass 30% of moisture in moderate scenario with pellet selling price of 206 €/t (b); biomass 50% of moisture in moderate scenario with pellet selling price of 233 €/t (c); biomass 30% of moisture in moderate scenario with pellet selling price of 233 €/t

To sum up, viable moderate scenario that permits to recover the investment cost of the plant in 15 years are:

- Intensive implementation scenario using wet biomass (50% of moisture) purchasing a chipper and performing transport operation with farmers support; and considering pellet selling price of 206 €/t.
- Moderate implementation scenario using dried biomass (30% of moisture), renting the chipper and tractor with trailer and considering pellet selling price of 206 €/t.
- Moderate implementation scenario using dried biomass (30% of moisture), purchasing and amortizing the chipper and tractor with trailer; and considering pellet selling price of 206 €/t.
- Moderate implementation scenario using dried biomass (30% of moisture), purchasing a chipper and performing transport operation with farmers support; and considering pellet selling price of 206 €/t.
- Moderate implementation scenario using wet biomass (50% of moisture), purchasing and amortizing the chipper and tractor with trailer; and considering pellet selling price of 233 €/t.
- Moderate implementation scenario using wet biomass (50% of moisture), purchasing a chipper and performing transport operation with farmers support; and considering pellet selling price of 233 €/t.
- Moderate implementation scenario using dried biomass (30% of moisture), renting the chipper and tractor with trailer and considering pellet selling price of 233 €/t.
- Moderate implementation scenario using dried biomass (30% of moisture), purchasing and amortizing the chipper and tractor with trailer; and considering pellet selling price of 233 €/t.
- Moderate implementation scenario using dried biomass (30% of moisture), purchasing a chipper and performing transport operation with farmers support; and considering pellet selling price of 233 €/t.

4.6.3. Sensitivity analysis of including torrefaction liquid as torrefaction by-product.

Even though, the main purpose of the plant is to produce torrefied pellets, there is the possibility of valuing the torrefaction liquid as a biodegradable pesticide or wood preservative in wood protection. Because of that, a sensitivity analysis is performed considering torrefaction liquid a torrefaction by-product. With this aim, it is considered that the torrefaction liquid selling price will be 100 €/t, 250 €/t and 400 €/t according to the values stablished by Fagernas et al. [8] and that the liquid fraction yield of torrefaction process is 10 wt %. Results show that consider torrefaction liquid as a torrefaction by-product increases the economic efficiency of the process. Table 4.10. shows the percentages of improvement of economic efficiency of each considered scenario adding torrefaction liquid as a valuable product. This enhancement depends on the scenario considered, achieving an increase of economic efficiency up to 31 % in moderate scenario and up to 14 % in intensive production scenario.

Table 4.10 Percentages of improvement of economic efficiency of each considered scenario adding torrefaction liquid as a valuable product (AWB: agricultural waste biomass).

Pellet selling price (€)	AWB at the field	Logistic scenarios	Torrefaction liquid selling price		
			100 €/t	250 €/t	400 €/t
Moderate scenario					
206	Wet[a]	Devices renting	-1 %	-3 %	-5 %
		Devices amortization	-22 %	-54 %	-87 %
		Support of farmers	6 %	16 %	26 %
	Dried[b]	Devices renting	-9 %	-23 %	-38 %
		Devices amortization	4 %	10 %	16 %
		Support of farmers	3 %	7 %	11 %
233	Wet[a]	Devices renting	-2 %	-5 %	-8 %
		Devices amortization	5 %	13 %	21 %
		Support of farmers	3 %	6 %	10 %
	Dried[b]	Devices renting	8 %	19 %	31 %
		Devices amortization	2 %	5 %	8 %
		Support of farmers	2 %	4 %	7 %
Intensive scenario					
206	Wet[a]	Devices renting	-3 %	-7 %	-12 %
		Devices amortization	3 %	9 %	14 %
		Support of farmers	2 %	4 %	7 %
	Dried[b]	Devices renting	3 %	8 %	12 %
		Devices amortization	2 %	4 %	6 %
		Support of farmers	1 %	3 %	5 %
233	Wet[a]	Devices renting	-9 %	-24 %	-38 %
		Devices amortization	2 %	5 %	8 %
		Support of farmers	1 %	3 %	5 %
	Dried[b]	Devices renting	2 %	4 %	7 %
		Devices amortization	1 %	3 %	4 %
		Support of farmers	1 %	2 %	4 %

4.7. Conclusions of Chapter 4: Adding value to agricultural waste biomass as torrefied pellets

Technical and economic viability of implementing a torrefaction process to add value of agricultural waste biomass as torrefied pellets is assessed by means of a pilot project carried out in a rural zone using a semi-industrial pilot plant located in the region. This project has been carried out by a group team which involves Energies Tèrmiques Bàsiques S.L., Inedit innovació S.L. and Chemistry Department of Química de la UAB. Within this thesis work, the characterisation of raw materials and the

obtained products from the torrefaction plant are carried out, as well as the economic assessment of the overall project. Thus, the pilot test project conclusions drawn within this thesis work are outlined below.

A complete biomass characterisation of almond tree, cherry tree and olive tree pruning waste is achieved permitting to assess the viability of treated each type of biomass in the torrefaction plant to obtain an enhanced torrefied product. From characterisation results, it is concluded that all the characterised AWB might be treated in the torrefaction plant at temperatures between 200-300 ºC.

Moreover, the characterisation of torrefaction products obtained by the treatment of olive pruning waste biomass at 250 ºC and almond pruning waste biomass at 280 ºC is also reached. It is concluded that this torrefaction process permits to achieve an enhanced solid biofuel with higher calorific value and lower moisture, being olive wood torrefied biomass more energetic than almond wood torrefied biomass. The enhancement of calorific value on the torrefied biomass is between 6-15 % in comparison to raw biomass and torrefied pellet has a calorific value between 13-18 % higher than torrefied pellets. Therefore, torrefaction process can enhance the calorific value of the product up to 25-30 % depending on the raw biomass used and the operational conditions. Furthermore, the characteristics of torrefied pellets produced by Energies Tèrmiques Bàsiques plant are within the European law standards of pellets demonstrating they are marketable pellet. Regarding to torrefied liquid, its characterisation is achieved permitting to assess the potential uses of this liquid.

Torrefaction liquid is not a potential biofuel due to its watery nature, although it is a good candidate to obtain bio-chemicals and bio-products. Torrefaction liquids obtained at higher temperatures contains more organic compounds even if the main compounds of this liquids are acetic acid and furfural making it a potential biodegradable pesticides or wood preservative.

The overall economic costs, at short term, of implementing this technology to add value to agricultural regions considering to different scenarios is assessed. The

intensive production of torrefied pellets is a more economically favourable scenario than the moderate production one. The purchase biomass price might be between 37 and 88 €/t, depending on the considered scenario. The economic efficiency of the overall process might be increased when the torrefaction liquids can be also recovered.

On the whole, technical and economic feasibility of implementing a torrefaction process to add value to biomass in the Ribera d'Ebre is demonstrated as long as public-private partnership is established and the social stakeholders from the area are involved in the project. Thus, this project is a clear example of a state-of-the-art bioeconomy project, since it combines an environmental friendly project with the aim of boosting the local economy by, not only creating jobs and diversifying the market of agricultural biomass, but also using the products in the local thermal installation, closing the cycle of resources and products in terms of circular or green economy.

Above and beyond the specific finding, performing more pilot projects of this kind in different rural areas might permit to promote and make public this technology and their products, as well as its benefits in the implementation zone, with the aim of facilitate the implementation of this kind of technologies in a near future.

References of Part II

[1] Chen W-H, Peng J, Bi XT. A state-of-the-art review of biomass torrefaction, densification and applications. Renew Sustain Energy Rev 2015;44:847–66.

[2] Prins MJ, Ptasinski KJ, Janssen FJJG. Torrefaction of wood. Part 1. Weight loss kinetics. J Anal Appl Pyrolysis 2006;77:28–34.

[3] Peng JH, Bi HT, Lim CJ, Sokhansanj S. Study on density, hardness, and moisture uptake of torrefied wood pellets. Energy and Fuels 2013;27:967–74.

[4] Tumuluru JS, Hess JR, Boardman RD, Wright CT, Westover TL. Formulation, Pretreatment, and Densification Options to Improve Biomass Specifications for Co-Firing High Percentages with Coal. Ind Biotechnol 2012;8:113–32.

[5] Järvinen T, Agar D. Experimentally determined storage and handling properties of fuel pellets made from torrefied whole-tree pine chips, logging residues and beech stem wood. Fuel 2014;129:330–9.

[6] van der Stelt MJC, Gerhauser H, Kiel JH a., Ptasinski KJ. Biomass upgrading by torrefaction for the production of biofuels: A review. Biomass and Bioenergy 2011;35:3748–62.

[7] Chew JJ, Doshi V. Recent advances in biomass pretreatment – Torrefaction fundamentals and technology. Renew Sustain Energy Rev 2011;15:4212–22.

[8] Fagernäs LI, Kuoppala E, Arpiainen V. Composition, utilization and economic assessment of torrefaction condensates. Energy & Fuels 2015:150331150901001.

[9] Prins MJ, Ptasinski KJ, Janssen FJJG. Torrefaction of wood. Part 2. Analysis of products. J Anal Appl Pyrolysis 2006;77:35–40.

[10] Demeyer a., Voundi Nkana JC, Verloo MG. Characteristics of wood ash and influence on soil properties and nutrient uptake: An overview. Bioresour Technol 2001;77:287–95.

[11] Bergman PC a, Boersma a R, Zwart RWR, Kiel JH a. Torrefaction for biomass co-firing in existing coal-fired power stations. Energy Res Cent Netherlands ECN ECNC05013 2005:71.

[12] Tumuluru JS, Sokhansanj S, Hess JR, Wright CT, Boardman RD. A review on biomass torrefaction process and product properties for energy application. Ind Biotechnol 2011.

[13] Ntalli NG, Vargiu S, Menkissoglu-Spiroudi U, Caboni P. Nematicidal carboxylic acids and aldehydes from Melia azedarach fruits. J Agric Food Chem 2010;58:11390–4.

[14] Hagner M. Potential of the Slow Pyrolysis Products Birch Tar Oil, Wood Vinegar and Biochar in Sustainable Plant Protection − Pesticidal Effects, Soil Improvement and Environmental Risks. Lahti (Finland): 2013.

[15] Liu WW, Zhao LJ, Wang C, Mu W, Liu F. Bioactive evaluation and application of antifungal volatiles generated by five soil bacteria. Acta Phytophylacica 2009;36:97–105.

[16] Lande S, Westin M, Schneider MH. Eco-efficient wood protection. Furfurylated wood as alternative to traditional wood preservation. Manag Environ Qual Int J 2004;15:529–40.

[17] de Wild P, Reith H, Heeres E. Biomass pyrolysis for chemicals. Biofuels 2012;2:185–208.

[18] Avebiom 2015. http://www.avebiom.org/es/ind-precios-biomasa (accessed October 9, 2015).

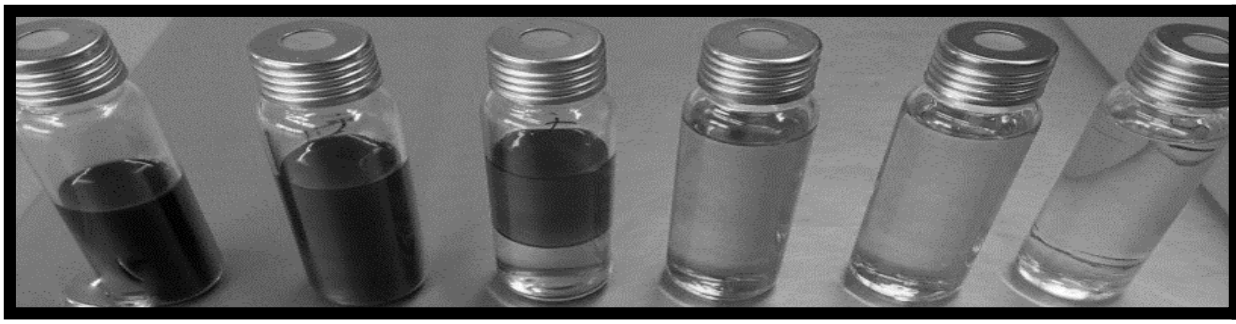

III

BIO-OIL CHARACTERISATION AND UPGRADING

5. Introduction of Part III: bio-oil characterisation and upgrading

In chapter 4, it is demonstrated that torrefied pellets are a short-term marketable solid bio-fuel with many associated benefits as increasing energy diversification, boosting the rural economy and fostering forest management and conservation. With the same aims but as a longer term strategy, bio-oil has awaked a great interest in the last years thanks to not only its potential as liquid biofuel, but also as chemical platform to obtain bio-products.

Bio-oil is a liquid product obtained from biomass fast pyrolysis processes, as it has been stated in Chapter 1. Bio-oil is a complex mixture of water and hundreds of organic compounds products from the defragmentation of the lignin, cellulose and hemicelluloses of biomass. These compounds are acids, aldehydes, ketones, alcohols, esters, sugars, furans, phenols, guaiacols, syringols, nitrogen containing compounds, as well as large molecular oligomers [1]. The chemical composition of bio-oil depends on the nature of the biomass and the fast pyrolysis conditions employed [2,3]. These diversity of oxygenated compounds makes bio-oil a promising chemical platform for obtaining value-added chemicals [4,5], such as phenols used in the resins industry, volatile organic acids in formation of de-icers, levoglucosan, hydroxyacetaldehyde and some additives applied in the pharmaceutical, fibre synthesizing or fertilizing industry and flavouring agents in food products [4,6]. Moreover, bio-oil is a promising liquid biofuel that contains negligible amounts of ash and it has an energetic density 5–20 times higher than the original biomass. However, it has some properties which set up many obstacles to their application as biofuel, such as corrosiveness, high viscosity, high oxygen content and low thermal stability [2,3]. Because of that, bio-oil upgrading is necessary to improve bio-oil properties to achieve a stable final product that might be used as transport fuel, fuel for boilers or biorefinery feedstock. Many upgrading processes are reported in literature (see section 1.4.2.), being hydrotreating and catalytic cracking the most prospective ones [7]. The aim of both processes is to reduce

bio-oil oxygen content resulting in a decreased O/C ratio and increased H/C which mainly achieves an increase of its heating value and its stability [7,8].

Hydrotreating upgrading processes are carried out at 250 ºC and 450 ºC and pressures between 75 and 300 bar with hydrogen supply. It can achieve enhanced bio-oil yields of 21-65 wt % which contains less than 5 wt % of oxygen released as water [7,9,10]. Catalytic cracking is carried out at softer operational conditions, temperatures of 350 ºC - 650 ºC and under atmospheric pressure without hydrogen supply [10,11]. Nonetheless, the improved bio-oil yields are lower (around 12-28 wt %) and its oxygen content is 13-24 wt % released as CO, CO_2 and H_2O [7]. Both processes usually requires the use of catalysts as sulfided CoMo and NiMo supported on alumina or aluminosilicates and novel metals for hydrotreating process [12–14]; and zeolites and mesoporous materials for catalytic cracking. The high energy and operational costs of these processes reduce the economic viability of obtained product. In this context, further research toward a more environmental friendly bio-oil upgrading processes with low energy and operational cost are needed.

Moreover, insights in the molecular composition of the crude and upgraded bio-oil are highly desirable as useful information to better understand the molecular processes taking place during the fast pyrolysis and upgrading processes. This information is crucial to develop efficient processes delivering products that meet the required product properties for their use as fuels or chemical platform. Many analytical techniques have been combined to obtain an inclusive qualitative analysis of bio-oil composition (see section 1.4.1.a). High resolution chromatographic techniques (GC-MS and HPLC-MS) are the most common techniques used to characterise chemically bio-oils, although a complete characterisation of bio-oil cannot be achieved due to it is not possible to detect the high molecular mass compounds derived from the lignin decomposition [15]. Among them, GC-MS techniques are the most used ones since they permit the identification of the chromatographic peaks, and therefore, the identification of bio-oil composition by means of a computer matching of the mass spectra with a library to identify the peaks [16].They permit to identify the content of phenols and

furans, which account for around 10-15 wt. % [17,18], as well as carboxylic, fatty, and resin acids content in bio-oils [19]. However, GC-MS chromatographic separation results in an overlap of compounds due to the high complexity of bio-oil. Because of that, more recently, multidimensional GC-MS analysis of bio-oil is also used to improve bio-oil chromatographic resolution [20–23], and consequently, increase the number of identified products.

GC-MS analysis, apart from permitting the identification of volatile bio-oil compounds, also allows their quantification [16]. With this aim, relative quantification of bio-oil composition has been reported as the average percentage of the total area from each individual peak and totalling the area of compounds[18,24], a method that does not show the real concentration of the compounds since the area of the peaks is not directly proportional to the concentration of the compound. Despite that fact, it permits to have a global idea of the most abundant compounds in a simple way since the quantification of each individual compound is tedious. Nevertheless, a detailed quantification of bio-oil can be carried out by means of an internal standards calibration method [16], where a calibration curve for each single quantified compounds is required. Regarding to quantification of single compounds, further work is needed due to the best of our knowledge, only few publications are addressed to this issue [17,25,26] and any of them is addressed to assess the reliability of the method itself.

Taking into account these necessities, the following chapters are addressed to move towards molecular insights in the molecular composition of raw and upgraded bio-oil, as well as the development of a reduced energy cost bio-oil upgrading processes that permits not only the enhancement of bio-oil properties for its potential application, but also reduce the economic cost of these processes to achieve a more economically viable product. Thus, in Chapter 6, it is developed a reliable quantitative analysis of main bio-oil compounds by Gas Chromatography coupled to Mass Spectrometry (GC-MS) in order to reach a further characterisation and better comprehension of bio-oil composition to better assess the potential use of bio-oil as a chemical platform and biofuel. In Chapter 7, catalytic upgrading processes at 60 ºC and using bentonites and zeolites as catalysts

are assessed. Different hydrogenation processes as molecular hydrogen and nascent hydrogen generated electrochemically and by metal oxidation performed at 20 ºC and 37 ºC are explored on Chapter 8 in order to reduce the economic and operational cost of conventional hydrotreating upgrading processes.

6. Bio-oil characterisation

In present chapter, a complete characterisation of purchased BTG-BTL bio-oil is characterised by means of acidity (TAN and pH), water content and qualitative chemical composition. Taking into account that bio-oil properties depend on different factors as the raw biomass, the fast pyrolysis operational conditions and time of storing, it is mandatory to perform a complete characterisation bio-oil in order to understand better this product and to follow bio-oil upgrading processes developed in the following chapters. To achieve a proper bio-oil characterisation, a start-up the required analytical methods is performed for first time in the research group where this thesis work is accomplished. Moreover, the present chapter describes a reliable quantitative analysis of main bio-oil compounds by Gas Chromatography-Mass Spectrometry (GC-MS) in order to reach a further characterisation and better comprehension of bio-oil composition to better assess the potential use of bio-oil as a chemical platform and fuel. After a complete chemical characterisation of bio-oil, it is selected those compounds that are going to be quantified by means of different calibration methods testing three different internal standards. A statistical analysis is used to study the precision of this method, as well as to compare the different tested calibration methods.

The results showed in this chapter have been published in a peer-reviewed scientific journal with the following reference:

Artigues A, Puy N, Bartrol J, Fabregas E. Comparative Assessment of Internal Standards for Quantitative Analysis of Bio-oil Compounds by Gas Chromatography / Mass Spectrometry Using Statistical Criteria. Energy & Fuels 2014; 28:3908–15

Thanks to the obtained reliable chemical characterisation, some bio-oil samples obtained from the co-pyrolysis of biomass and waste tyres by Instituto de Carboquímica de Zaragoza (ICB-CSIC) where analysed as a punctual collaboration with this research group. From this collaboration, it has been published the following paper:

Martínez JD, Veses A, Mastral AM, Murillo R, Navarro M V., Puy N, Artigues A, Bartrolí J and García T. Co-pyrolysis of biomass with waste tyres: Upgrading of liquid bio-fuel. Fuel Process Technol 2014; 119:263–71.

6.1. Bio-oil characterisation results

6.1.1. Bio-oil acidity and water content

Bio-oil acidity is an important parameter to take into account due to it is the main reason of bio-oil corrosiveness, especially at elevated temperatures [27], making its reduction mandatory for bio-oil use as biofuel in conventional devices. It is measured by means of pH and TAN (see section 3.1.7 and 3.1.8). The obtained pH and TAN results (Table 6.1.) are within typical values reported, 2 - 3 pH units and 70 - 100 mg KOH / g bio-oil, respectively [28]. Measured pH value is slightly lower than the specified in BTG-BTL product data sheet (See Table 3.8.). pH and TAN values show the high acidic nature of the bio-oil, derived mainly (60 – 70 %) from the volatile acids and from other groups like phenolics (5–10 %) and fatty and resin acids (< 5 %), since there are no inorganic acids in bio-oil [28].

Table 6.1. Raw bio-oil properties. (* confidence interval at 95% of confidence level)

pH	TAN* (mg KOH/ g bio-oil)	Water* (wt %)
1.9	80 ± 3	23 ± 1

Water content is also a crucial parameter to assess bio-oil properties. The presence of water has both negative and positive effects on bio-oil properties. On one hand, high water content causes serious drawbacks as low high heating value, increase in ignition delay and, in some cases, decrease of combustion rate compared to conventional fuel oils [12,29]. On the other hand, water improves bio-oil flow characteristics (reduces the oil viscosity), which is beneficial for fuel pumping and atomization [2]. Measured bio-oil water content (Table 6.1.) is also within the typically

values (15 – 30 wt %)[12,28] resulting from the original moisture in the feedstock and as a product of the dehydration reactions occurring during fast pyrolysis [29].

6.1.2. Bio-oil chemical composition.

Reaching a bio-oil complete chemical composition is necessary to further understand this product properties and to assess possible posterior upgrading processes and chemical products recovery. Owing to bio-oil composition depends on many factors as raw biomass type, fast pyrolysis operational conditions and storage time, determining bio-oil chemical composition of each bio-oil is necessary. BTG-BTL bio-oil chemical composition is not included in the product specifications because of that its characterisation is mandatory to develop this thesis work.

With this aim, a bio-oil sample is filtered and diluted with methanol (1:10) and analysed to GC/MS by triplicate following the method described in section 3.1. An example of bio-oil Total Ion Chromatogram (TIC) is shown in Figure 6.1. From the TIC, a total of 45 compounds among the more than 200 detected are identified by a probability match > 800 by comparison with spectra from the NIST mass spectral library. These 45 identified compounds correspond to 63 % of the area of the TIC since they are the main bio-oil compounds. The identified compounds are listed in Table 6.2. The compounds with higher peak area are: levoglucosan (15.1 %), acetic acid (8.4 %), 2-methoxy-4-methyl-phenol (5.3 %), guaiacol (3.5 %), 1-hydroxy-2-propanone (3.5 %), 4-(acetyloxy)-3-methoxy-benzaldehyde (3.2 %) and hydroxyacetaldehyde (2.3 %).

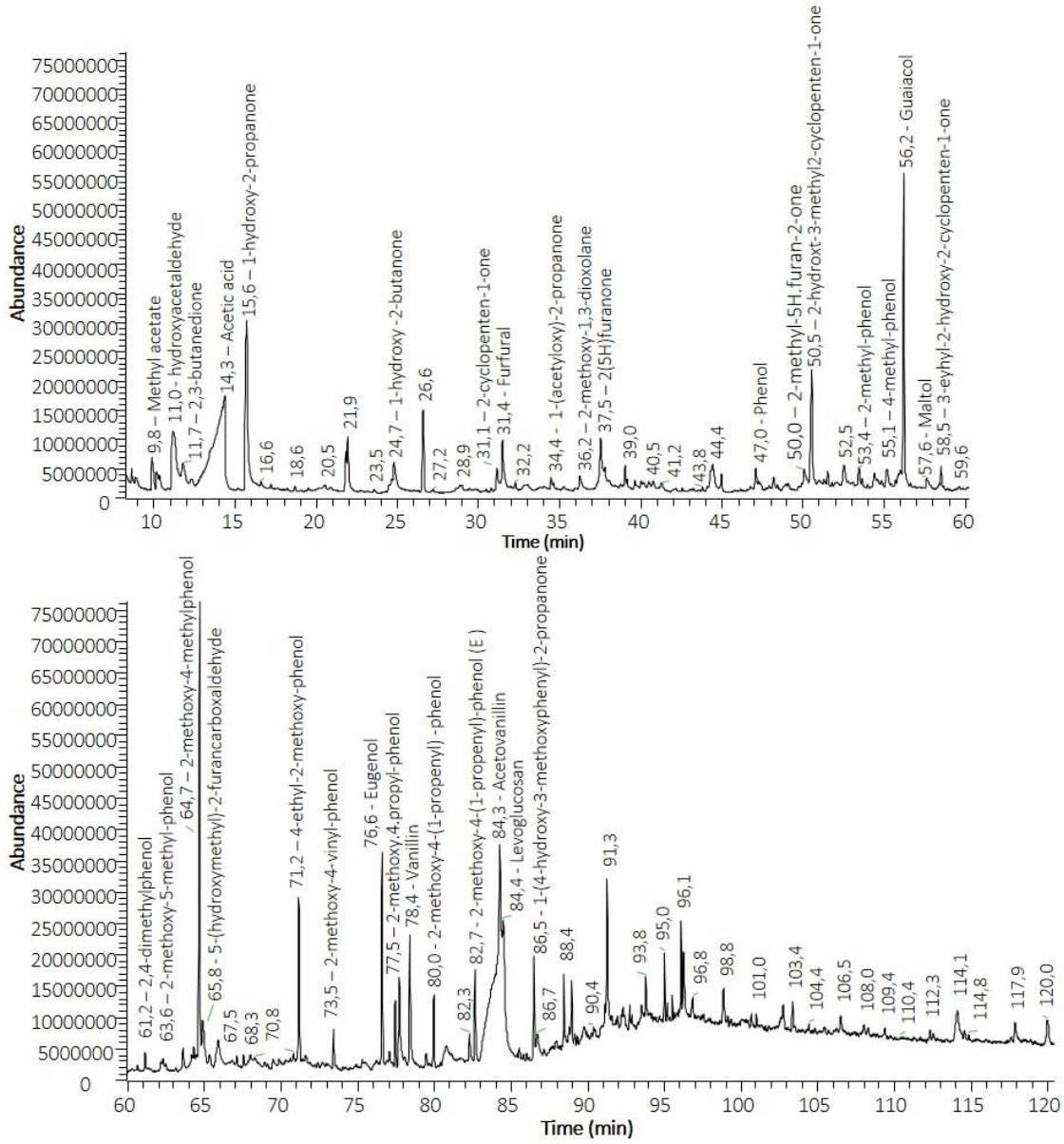

Figure 6.1. Total Ion Chromatogram (TIC) from a bio-oil sample showing the retention time and the main identified compounds.

Table 6.2. Identified compounds and their retention time (RT), molecular weight (MW), molecular formula, area, relative standard deviation (RSD), as well as the area percentage of each compound relative of the total area.

Compound	RT (min)	MW	Formula	Area	RSD (%)	% Area
Methyl acetate	9.8	74.08	$C_3H_6O_2$	47028681	1	0.5
Formic acid	10.1	46.03	CH_2O_2	22649734	4	0.2
1,3-cyclopentadiene	10.3	66.10	C_5H_6	18429014	1	0.2
2-propen-1-ol	11.0	58.08	C_3H_6O	2802483	2	0.0
Hydroxyacetaldehyde	11.0	60.05	$C_2H_4O_2$	204669689	5	2.3
2,3-butanedione	11.7	86.09	$C_4H_6O_2$	54968756	0.3	0.6
2-butanone	12.3	72.11	C_4H_8O	11383534	6	0.1
Acetic acid	14.3	60.05	$C_2H_4O_2$	759559932	5	8.4
1-hydroxy-2-propanone	15.6	74.08	$C_3H_6O_2$	313539938	8	3.5
1-hydroxy-2-butanone	24.7	88.11	$C_4H_8O_2$	80684713	6	0.9
2-cyclopenten-1-one	31.1	82.10	C_5H_6O	31781177	6	0.4
Furfural	31.4	96.08	$C_5H_4O_2$	74117033	9	0.8
1-(acetyloxy)-2-propanone	34.4	116.12	$C_5H_8O_3$	24192478	1	0.3
2-methoxy-1,3-dioxolane	36.2	104.10	$C_4H_8O_3$	31696994	4	0.3
2(5H)furanone	37.5	84.07	C4H4O2	98423438	6	1.1
2,5-dimethoxy-tetrahydrofuran	37.8	132.16	$C_6H_{12}O_3$	38882466	3	0.4
3-methyl-2,5-furandione	40.0	112.08	$C_5H_4O_3$	23989756	6	0.3
2,5 Hexanedione	40.1	114.14	$C_6H_{10}O_2$	19410386	6	0.2
1,2 cyclopentanedione	40.7	98.10	$C_5H_6O_2$	22255505	6	0.2
Phenol	47.1	94.11	C_6H_6O	50266091	9	0.6
4-methyl-5H-furan-2-one	50.0	98.10	C_5H_6O2	45351130	1	0.5
2-hydroxy-3-methyl-2-cyclopenten-1-one	50.5	112.13	$C_6H_8O_2$	157193622	4	1.7
2-methyl-phenol	53.4	108.14	C_7H_8O	35775868	0.3	0.4
4-methyl-phenol	55.1	108.14	C_7H_8O	35957224	3	0.4
Guaiacol	56.2	124.14	$C_7H_8O_2$	317726612	0.9	3.5
Maltol	57.6	126.11	$C_6H_6O_3$	26021491	5	0.3
3-ethyl-2-hydroxy-2-cyclopenten-1-one	58.5	126.15	$C_7H_{10}O_2$	35729012	7	0.4
2.4-dimethyl-phenol	61.2	122.16	$C_8H_{10}O$	17369899	6	0.2
2.3-dihydroxybenzaldehyde	62.3	138.12	$C_7H_6O_3$	40251323	8	0.4
2-methoxy-5-methyl-phenol	63.6	138.16	$C_8H_{10}O_2$	25152261	5	0.3
2-methoxy-4-methyl-phenol	64.7	138.16	$C_8H_{10}O_2$	482110939	9	5.3
5-(hydroxymethyl)-2-furancarboxaldehyde	65.8	126.11	$C_6H_6O_3$	72060011	6	0.8

Table 6.2. (Continued). Identified compounds and their retention time (RT), molecular weight (MW), molecular formula, area, relative standard deviation (RSD), as well as the area percentage of each compound relative of the total area.

Compound	RT (min)	MW	Formula	Area	RSD (%)	% Area
4-(2-propenyl)-phenol	68.9	134.18	$C_9H_{10}O$	11626584	9	0.1
3-methyl-1,2-benzenediol	69.5	124.14	$C_7H_8O_2$	17468706	6	0.2
4-ethyl-2-methoxy-phenol	71.2	152.19	$C_9H_{12}O_2$	142975027	3	1.6
4-methyl-1,2 benzenediol	71.7	124.14	$C_7H_8O_2$	36579951	6	0.4
2-methoxy-4-vinyl-phenol	73.5	150.17	$C_9H_{10}O_2$	39784167	9	0.4
Eugenol	76.6	164.20	$C_{10}H_{12}O_2$	176981088	4	2.0
2-methoxy-4-propyl-phenol	77.5	166.23	$C_{10}H_{14}O_2$	131744693	4	1.5
Vanillin	78.4	152.15	$C_8H_8O_3$	139874619	7	1.5
2-methoxy-4-(1-propenyl) – phenol	80.0	164.20	$C_{10}H_{12}O_2$	54091086	10	0.6
2-methoxy-4-(1-propenyl)-phenol (E)	82.7	164.20	$C_{10}H_{12}O_2$	35349940	7	0.4
4-(acetyloxy)-3-methoxy-benzaldehyde	84.3	194.18	$C_{10}H_{10}O_4$	286997858	5	3.2
Levoglucosan	84.4	162.14	$C_6H_{10}O_5$	1364692409	6	15.1
1-(4-hydroxy-3-methoxyphenyl)-2-propanone	86.5	180.20	$C_{10}H_{12}O_3$	78919028	4	0.9

Functional groups distribution in bio-oil is divided into mostly sugars, acids, esters, ketones, aldehydes, furan, alcohols and phenols. The same functional groups have been reported [30,31]. The identified compounds are classified into these chemical families in Table 6.3. In Figure 6.2., it is represented the percentage of the summation of all the compound areas of the same chemical family related to the total area.

Table 6.3. Classification of bio-oil identified compounds in chemical families.

Acids and esters	Phenols and alcohols
Acetic acid	2-methoxy-4-methyl-phenol
Methyl acetate	Guaiacol
Formic acid	Eugenol
	4-ethyl-2-methoxy-phenol
Sugar	2-methoxy-4-propyl-phenol
Levoglucosan	2-methoxy-4-(1-propenyl) –phenol
	Phenol
Aldehyde	2-methoxy-4-vinyl-phenol
4-(acetyloxy)-3-methoxy-benzaldehyde	4-methyl-1,2-benzenediol
Hydroxyacetaldehyde	4-methyl-phenol
Vanillin	2-methyl-phenol
Furfural	2-methoxy-4-(1-propenyl)-phenol (E)
5-(hydroxymethyl)-2-furancarboxaldehyde	2-methoxy-5-methyl-phenol
2,3-dihydroxybenzaldehyde	3-methyl-1,2-benzenediol
2-methoxy-4-vinyl-phenol	2,4-dimethyl-phenol
	4-(2-propenyl)-phenol
Furan	2-propen-1-ol
2(5H)furanone	
4-methyl-5H-furan-2-one	**Ketone**
2,5-dimethoxy-tetrahydrofuran	1-hydroxy-2-propanone
3-methyl-2,5-furandione	2-hydroxy-3-methyl-2-cyclopenten-1-one
	1-hydroxy-2-butanone
	1-(4-hydroxy-3-methoxyphenyl)-2-propanone
Other	2,3-butanedione
2-methoxy-1,3-dioxolane	3-ethyl-2-hydroxy-2-cyclopenten-1-one
Maltol	2-cyclopenten-1-one
1,3-cyclopentadiene	1-(acetyloxy)-2-propanone
	1,2 cyclopentanedione
	2,5 Hexanedione
	2-butanone

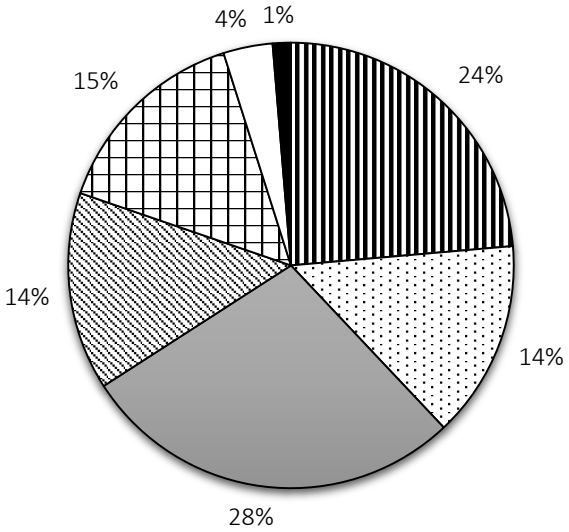

Figure 6.2. Percentage of the summation of all compounds areas from the same chemical family related to the total area: Sugar (▥); acid and esters (⬚); phenols and alcohols (□), ketones (▨), aldehydes (▦), furans (□) and others (■).

6.2. Quantitative assessment of bio-oil chemical composition

In this section, it is described a reliable quantitative analysis of main bio-oil compounds by GC-MS. The complete chemical bio-oil characterisation underlines the complexity of the sample which is a mix of hundreds of compounds. Because of that, the evaluation of the quantification method is carried out with the most abundant bio-oil compounds accordingly to their peak area and those that present especial interest as added value products. Their quantification is carried out by means of different calibration methods testing three different internal standards. A statistical analysis including one-way ANOVA test and t-test are used to study the precision of this method, as well as to compare the different calibration methods using different internal standards.

6.2.1. Selection of the quantified bio-oil compounds.

Once it is reached a completed chemical characterisation of bio-oil, the most abundant compounds accordingly to the chromatogram area and those that might have an interest as added value products are selected for their quantification. It is considered that almost one compound of each chemical family is selected for quantification. Quantification of whole bio-oil would be experimentally very hard and expensive due the high complexity of bio-oil, because of that the necessity of selecting target compounds for this study.

As it is observed in Figure 6.1. of Section 6.1.2., bio-oil TICs are very complex and there are overlapping peaks. These interferences hinder a proper integration of the selected compounds peaks and, therefore, a proper quantification of them. Because of that, it is crucial to choose a quantifying mass-to-charge ratio (m/z) for each compound that reduce or eliminate these interferences allowing a faultless integration.

The selected compounds for the quantitative analysis and the method precision study are listed in Table 6.4., as well as, their retention time and the quantifying mass to charge ratio.

Apart from selecting the compounds to quantify, it is important to select a proper internal standard for the quantification method. An internal standard should reacts to variation in the chromatographic condition in exactly the same way as the analyte so that its response varies to the same degree. Owing to the bio-oil complexity, selecting an internal standard that fulfill this premise for all the varied selected compounds is challenging. Because of that, three different internal standards with different functional groups which do not have interferences with the bio-oil compounds are selected and tested to study the most suitable one. The tested internal standards are toluene, 1,1,3,3-tetramethoxypropane and 1-octanol. Table 6.4. also lists the tested internal standards, their retention times and the quantifying mass to charge ratio.

Table 6.4. List of selected compounds for the study of method precision and quantification, such as the tested internal standards, with their retention time (RT) and quantifying mass to charge ratio (m/z) for peak integration.

	RT	m/z
Selected compounds		
2-propen-1-ol	11.0	57
2-butanone	12.3	43
Acetic acid	14.3	60
Furfural	31.4	95
2(5H)furanone	37.5	55
2,5-dimethyoxy-tetrahydrofuran	39.1	101
2-hydoxy-3-methyl-2-cyclopenten-1-one	50.5	112
2-methoxy-4-propyl-phenol	77.5	137
Vanilline	78.4	151
Levogucosan	84.4	60
Tested internal standards		
Toluene	26.5	91
1,1,3,3-tetramethoxypropane	51.6	75
1-octanol	55.3	164

6.2.2. GC-MS method precision study for bio-oil chemical characterisation

To ensure the suitability of the method to quantify bio-oil compounds, it is performed a precision study of the method considering the instrumental precision, the intraday precision and the interday precision for each selected compound. As it is defined in section 3.1.6, the instrumental precision is assessed by the precision obtained from three replicate of the same aliquot for each compound, intraday precision is the precision achieved under the same operating condition over a short period of time and interday precision evaluate the influence of analyse bio-oil samples in different days. Moreover, the influence of using an internal standard on the method precision is assessed being toluene, 1,1,3,3-tetramethoxypropane and 1-octanol the tested ones. Samples preparation and the statistical tests performed for this study are detailed in section 3.1.6.

To assess the instrumental precision, peak area average of each selected compound and its RSD is calculated (Table 6.4). Calculated RSD are less than 10 % for all

compounds and for all the aliquots, indicating a good instrumental precision of the runs. Regarding to the intraday precision, One Way Analysis of Variance (ANOVA) test shows no significant differences in peak areas between different aliquots analysed in the same day which means an acceptable repeatability of the method and no significant effect of bio-oil sampling whenever a proper homogenization of bio-oil vessel is carried out. ANOVA test is calculated to compare peak areas of the same compound at different days of analysis showing no significant differences between days except for furfural, 2(5H)-furanone and 2,5-dimethoxy-tetrahydrofuran. Although a good interday precision is achieved for the majority of the compounds, it is not an acceptable for some others probably due to the stability of the chromatographic column is not high enough. Column stability depends on the nature of the stationary phase, on the complexity of the chromatographic run and on the composition of the test samples. Due to the complexity of the method and the sample, problems on column stability might occur over a long period of time. However, a proper quantification analysis might be carried out if the calibration curve is performed the same day of the sample analysis due to it is achieved a good intraday precision.

Table 6.5. Peak area average of each selected compounds and its relative standard deviation (RSD)

	day 1						day 2	
	aliquot 1		aliquot 2		aliquot 3			
	Average (n=3)	RSD (%)	Average (n=3)	RSD (%)	Average (n=3)	RSD (%)	Average (n=3)	RSD (%)
2-propen-1-ol	2868224	6	2899068	1	2816769	1	2700082	3
2-butanone	5372496	3	5256107	3	5012921	8	5066275	3
Acetic acid	220655592	7	211479931	1	208922210	2	223463513	2
Furfural	25993327	19	23808535	5	19678893	6	13911930	7
2(5H)furanone	32392937	6	31922756	2	30017943	2	23334018	1
2,5-dimethyoxy-tetrahydrofuran	25423461	20	23359202	1	24373241	1	11368326	10
2-hydoxy-3-methyl-2-cyclopenten-1-one	36330149	6	36652257	5	34115182	4	35287319	1
2-methoxy-4-propyl-phenol	24474339	2	24876406	1	25085703	1	25596683	3
Vanilline	37897482	1	38924515	3	38877889	1	40521856	5
Levogucosan	411103389	0,2	429381572	2	424954928	0,4	404529876	2

Table 6.6. Average of peak area ratio relative to toluene, 1,1,3,3-tetramethoxypropane and 1-octanol for each selected compound and its relative standard deviation (RSD).

	day 1							
	aliquot 1		aliquot 2		aliquot 3		day 2	
	Average (n=3)	RSD (%)	Average (n=3)	RSD (%)	Average (n=3)	RSD (%)	Average (n=3)	RSD (%)
Area ratio relative to toluene								
2-propen-1-ol	0.11	7	0.11	2	0.104	1	0.09	3
2-butanone	0.20	5	0.19	2	0.18	7	0.18	5
Acetic acid	9	8	7.7	1	7.7	2	7.8	2
Furfural	0.9	9	0.9	5	0.73	5	0.48	5
2(5H)furanone	1.3	5	1.16	2	1.11	1	0.81	3
2,5-dimethyoxy-tetrahydrofuran	1.06	4	1.1	6	1.08	0.4	0.42	4
2-hydoxy-3-methyl-2-cyclopenten-1-one	1.42	0.3	1.3	5	1.26	3	1.23	3
2-methoxy-4-propyl-phenol	0.9	9	0.90	2	0.93	2	0.9	6
Vanilline	1.4	9	1.4	4	1.43	1	1.4	8
Levogucosan	15	9	16	3	15.7	1	14	5
Area ratio relative to 1,1,3,3-tetramethoxypropane								
2-propen-1-ol	0.018	9	0.018	1	0.0177	2	0.016	3
2-butanone	0.033	7	0.032	3	0.031	7	0.030	4
Acetic acid	1.4	10	1.30	1	1.3	4	1.3	3
Furfural	0.14	8	0.15	4	0.12	7	0.08	9
2(5H)furanone	0.20	8	0.197	1	0.19	4	0.140	2
2,5-dimethyoxy-tetrahydrofuran	0.16	9	0.144	2	0.153	3	0.07	8
2-hydoxy-3-methyl-2-cyclopenten-1-one	0.23	6	0.23	4	0.21	5	0.25	8
2-methoxy-4-propyl-phenol	0.15	3	0.153	1	0.158	1	0.153	1
Vanilline	0.24	5	0.24	3	0.24	3	0.24	4
Levogucosan	2.6	4	2.6	3	2.7	2	2.42	0.4
Area ratio 1-octanol								
2-propen-1-ol	0.29	5	0.29	5	0.31	3	0.162	5
2-butanone	0.55	5	0.53	3	0.54	7	0.30	5
Acetic acid	22	6	21	3	22.6	1	13	4
Furfural	2.4	7	2.4	3	2.1	2	0.83	3
2(5H)furanone	3.3	3	3.2	3	3.3	2	1.4	5
2,5-dimethyoxy-tetrahydrofuran	2.6	9	2.3	5	2.6	4	0.74	5
2-hydoxy-3-methyl-2-cyclopenten-1-one	3.7	2	3.7	3	3.69	0	2.1	5
2-methoxy-4-propyl-phenol	2.5	5	2.5	5	2.7	5	1.5	8
Vanilline	3.9	5	3.9	7	4.2	3	2.4	10
Levogucosan	42	4	43	7	46	4	24	7

Results obtained for the study of the method precision using internal standard are shown in Table 6.6. It is expected to obtain a higher method precision when an internal standard is used due to it should reduce the effect of the instrumental drift (possible deviation in the injection volume and possible variations in the performance of the detectors) in the final result. However, unexpectedly, the use of an internal standard does not have a high influence on the method precision due to the results are similar to those obtained with the method without internal standard, possibly due to there are not several instrumental drifts during the analysis. The instrumental and intraday precision are satisfactory for all compounds using either of the internal standards. However, the interday precision is good for all compounds except furfural, 2(5H)-furanone and 2,5-dimethoxy-tetrahydrofuran when toluene or 1,1,3,3-tetramethoxypropane are used. Regarding to 1-octanol, there are not an acceptable interday precision for any compound which mean that 1-octanol is more sensitive to changes in the column with time.

Even though a good precision is achieved for all compounds, there are two considerations to take into account. The first one is that levoglucosan boiling point is 380 ºC while the inlet temperature of the used method is 300 ºC. As a result, levoglucosan is not completely volatilised in this analysis. Consequently, the non-volatilised levoglucosan is retained in the liner glass wool reducing its lifetime and making the use of glass wool liner indispensable to prevent non-volatilised levoglucosan reaches into the column. Despite that fact, a good precision for this compound during the analysis is obtained, which can be explained by the fact that the volatilised fraction is always the same The second consideration is that there is a double peak of 2,5-dimethoxy-tetrahydrofuran in the TIC. It is possible that they correspond to a two different isomers of this compound and it is no possible to distinguish them with the software and the library used.

6.2.3. Bio-oil chemical composition quantitative analysis

Once the method precision is accepted, the selected compounds are quantified by different calibration methods testing three different internal standards (toluene, 1,1,3,3-tetramethoxypropane and 1-octanol). A comparative assessment of the use of these three internal standards for quantitative analysis is carried out. Moreover, it is evaluated the possible enhancement of interday precision of the method performing the calibration and sample analysis in the same day.

To perform the calibration, 6 standards with different concentrations of each selected compound are prepared (see Table 3.1. of section 3.1.6). In each standard, 100 mg/L toluene, 200 mg/L 1,1,3,3-tetramethoxypropane and 200 mg/L of 1-octanol are added as internal standards. Regarding to bio-oil samples preparation, bio-oil is diluted with methanol to 1:10 and it is added the three internal standards. Standards and the sample are analysed. Moreover, two quantification analysis are carried out in two different days performing both calibration curve and sample analysis each day of analysis in order to assess if the possible instability of the column might be solve.

a. *Quantification method without using internal standard*

First of all, it is carried out the quantification of bio-oil selected compounds without considering the use of an internal standard. With this aim, the standards peak area of each selected compound (without considering the internal standards) is plotted against its concentration in the standards. Then, the calibration curve data for each selected compound is fitted to a linear least squares regression model in order to obtain a calibration equation for each compound. Finally, sample peak area of each selected compounds is interpolate. The obtained results are shown in Table 6.7.

Table 6.7. Calibration equation for each selected compound obtained to fit their area into a Linear Least Squares Regression model and concentration of each compound. (SD: Standard deviation, RSD: relative standard deviation, CI: confidence interval at 95% of confidence level, R^2: correlation coefficient, wt %: weight percentage)

	Day 1					Day 2				
	y=bx+a		R^2	Concentration		y=bx+a		R^2	Concentration	
	b ± SD	a ± SD		wt % ± CI	RSD	b ± SD	a ± SD		wt % ± CI	RSD
2-propen-1-ol	107234 ± 4834	-868316 ± 232680	0.992	0.027 ± 0.004	7	114392 ± 2973	-1090327 ± 143115	0.997	0.029 ± 0.002	2
2-butanone	54122 ± 1438	-209308 ± 217815	0.997	0.07 ± 0.01	7	50631 ± 2173	-101168 ± 329088	0.993	0.09 ± 0.02	3
Acetic acid	41909 ± 1411	-9523152 ± 6893954	0.995	4.0 ± 0.3	1	46216 ± 1064	-23317845 ± 5195700	0.998	4.6 ± 0.2	2
Furfural	69290 ± 4845	2360320 ± 1470360	0.981	0.17 ± 0.05	1	96349 ± 5270	-502001 ± 1599282	0.988	0.13 ± 0.04	7
2(5H)furanone	59456 ± 1644	-15357129 ± 1172795	0.998	0.61 ± 0.02	8	64113 ± 3961	-21216379 ± 2658121	0.985	0.60 ± 0.05	5
2,5-dimethoxy-tetrahydrofuran	100317 ± 1087	-546084 ± 105869	0.999	0.078 ± 0.002	12	110699 ± 3776	-1573194 ± 367061	0.995	0.10 ± 0.01	8
3-methyl-1,2-cyclopentanedione	79644 ± 4420	-14279500 ± 2570729	0.988	0.46 ± 0.05	7	94587 ± 3266	-17776980 ± 1899593	0.995	0.48 ± 0.03	1
2-methoxy-4-propyl-phenol	393366 ± 5671	-3520198 ± 718295	0.999	0.054 ± 0.004	6	426528 ± 19976	-3679259 ± 2530073	0.991	0.06 ± 0.01	3
Vanillin	45854 ± 5168	2677177 ± 4045661	0.951	0.5 ± 0.1	6	64398 ± 5793	-9379329 ± 4534908	0.968	0.67 ± 0.07	4
Levoglucosan	68187 ± 2479	31639436 ± 12009980	0.995	3.8 ± 0.3	4	77391 ± 5858	-9180908 ± 28394232	0.977	4.6 ± 0.6	2

Regarding to the calibration, an acceptable linearity of the data is reached obtaining calibration curves with correlation coefficient around 0.99 for all the selected compound except for vanillin calibration curve which is around 0.95. Thus, it is considered that a proper calibration of each selected compound is achieved in both days of analysis. In Figure 6.3, it is shown the calibration curves of all compounds in day 1. Moreover, it is compared the regression slope of both days calibration curves for each selected compound by means of t-test statistical analysis showing significant differences between slope values for all compounds. Once more, it is demonstrated that the chromatographic procedure is unstable for long periods of time. However, it is expected that a successful quantification analysis should be carried out if the calibration curve is performed the same day of the sample analysis due to it is achieved a good intraday precision.

The quantitative analysis of all the selected compounds is achieved performing a calibration curve and a sample analysis at the same day. Regarding to the concentrations calculated in day 1, acetic acid and levoglucosan are the most concentrated compounds, with concentration as high as 4.0 ± 0.3 wt % and 3.8 ± 0.3 wt %, respectively. 2(5H)furanone, vanilline and 2-hydroxy-2-cyclopenten-1-one have substantial concentrations of 0.61 ± 0.02 wt %; 0.5 ± 0.1 wt % and 0.46 ± 0.05 wt %. Less concentrated compounds are furfural (0.17 ± 0.05 wt %) and 2,5-dimethoxytetrahydrofuran (0.078 ± 0.002 wt %); followed by 2-butanone (0.07 ±0.01 wt %), 2-methoxy-4-propyl-phenol (0.054 ± 0.004 wt %) and 2-propen-1-ol (0.027 ± 0.004 wt %). A t-test statistical analysis is carried out to compare the quantification values calculated for each compound in both days. The quantification values are not significantly different for any of the selected compounds except for acetic acid and levoglucosan. These two compounds have high concentration in bio-oil, consequently, they have large peaks in the chromatograms which supposes more interferences with

other compounds that may not be completely solved by quantifying mass-to-charge ratio. Although the obtained values for these compounds are statistically different, the values do not differ a lot (Table 6.7.). Thus, it can be concluded that performing the calibration curve and the sample analysis at the same day permits a successful quantification analysis solving the possible interday precision problems.

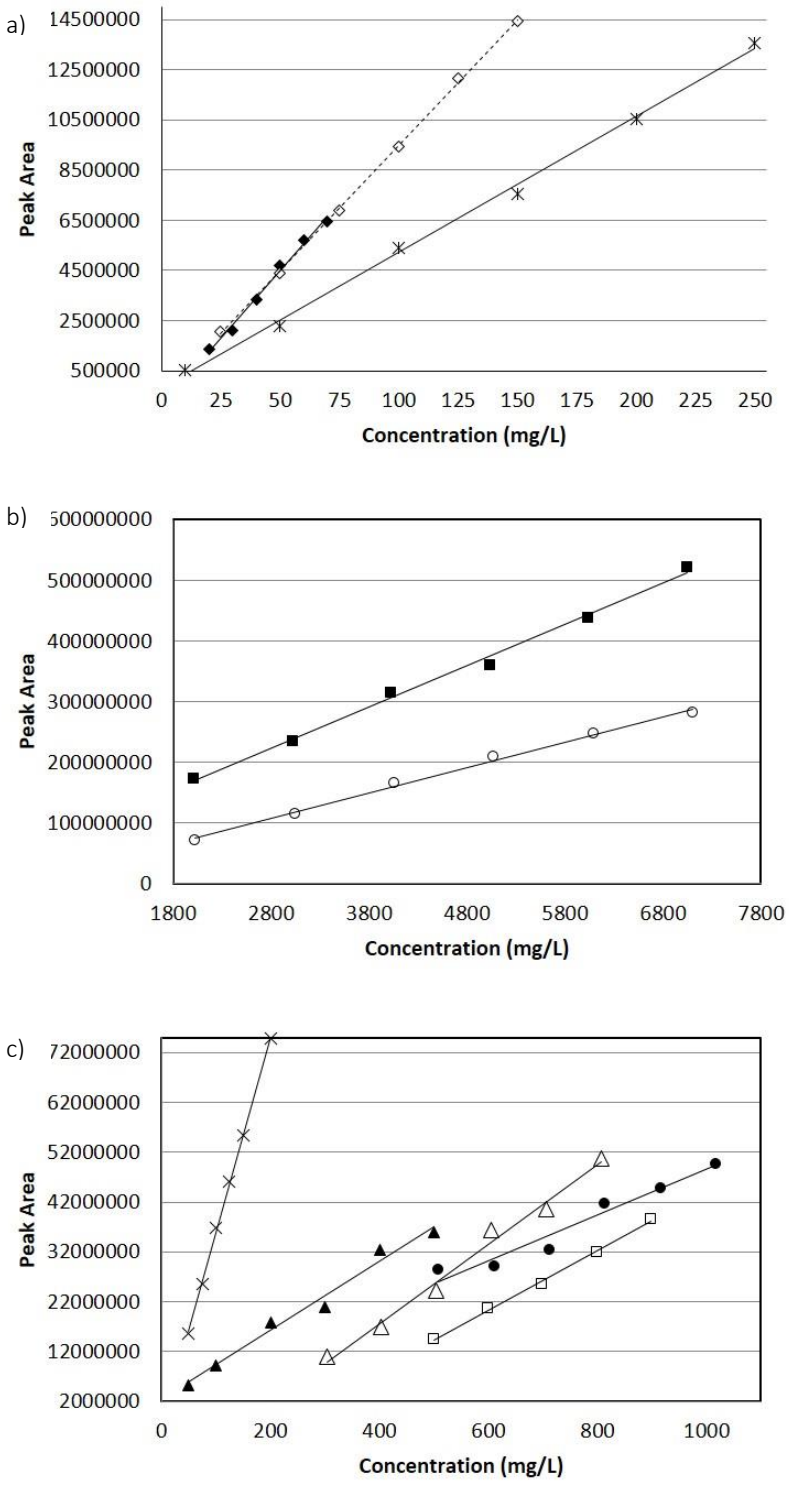

Figure 6.3. Calibration curves using the peak area of (a) 2-propanol (◆), 2-butanone (X), 2,5-dimethoxytetrahydrofuran (◇); b) acetic acid (○), levoglucosan (■); (c) 2-methoxy-4-propyl-phenol (×), furfural (▲),2-hydroxy-3-methyl-2-cyclopenten-1-one (△), vanilline (●) and 2(5H)furanone (□).

b. *Quantification method using internal standards*

Secondly, bio-oil quantification using different internal standard calibration methods is carried out in order to assess which is the most proper internal standard for bio-oil quantification method. To perform the calibration curve using toluene as internal standard, the standards area ratio relative to toluene of each selected compound is plotted against the concentration of the selected compounds in the standards. Then, calibration curves data of each selected compound is fitted to a linear least squares regression model in order to obtain toluene internal standard method calibration equation of each compound. Finally, the sample area ratio relative to toluene of each selected compound is interpolated. This methodology is repeated for the other two tested internal standards (1,1,3,3-tetramethoxypropane and 1-octanol). The obtained results are shown in Table 6.8., 6.9 and 6.10.

The calibration curves obtained for each selected compound with any of internal standard calibration methods used are linear. Their correlation coefficient (R^2) are slightly lower in comparison to the correlation coefficient of the calibration curve of calibration method without internal standard. Calibration curves using 1,1,3,3-tetramethoxypropane are the ones that have a better correlation coefficient in comparison to the other tested internal standards. Comparing the regression slopes of both days by a t-test for each selected compound, there are no significant differences in regression slopes of any of the tested internal standards except for 2-propenol and levoglucosan regression slopes when toluene is used as internal standard. The use of any of the tested internal standard enhanced the reproducibility of the calibration curves between days. That is because the use of an internal standard corrects the erratic variations of the chromatographic procedure from one run to the next, in other words, correct the short time instability of the chromatographic procedure. In conclusion, the quantitative analysis of all the selected compounds is achieved for any of the calibration methods tested provided that both calibration curve and sample analysis are performed in the same day.

Once more, it is compared the calculated concentration of each selected compound in day 1 and 2 by means of t-test analysis for each internal standard. There are no significant differences between days when toluene and 1,1,3,3-tetramethoxypropane are used as internal standard. Only acetic quantification is significant different between days when 1,1,3,3-tetramethoxypropane is used as internal standard. Regarding to 1-octanol internal standard method, there is not significant differences on calculated concentrations of 2-propen-1-ol, 2-butanone, 2,5-dimethoxy-tetrahydrofuran, 2-methoxy-4-propyl-phenol and vanillin, although there is significant differences of the other compounds. This result might be explained because 1-octanol might react to variation in the chromatographic condition in different way to some of the selected compounds. Because of that, it does not correct the chromatographic variation making unreproducible the quantification results. Therefore, it might be rejected as useful internal standard. About the other two internal standards, they have good reproducibility being both of them good candidates as internal standard for bio-oil chemical composition quantification method.

Table 6.8. Calibration equation for each selected compound obtained to fit the area ratio relative to toluene into a Linear Least Squares Regression model and concentration of each compound (SD: Standard deviation, RSD: relative standard deviation, CI: confidence interval at 95% of confidence level, R^2: correlation coefficient, wt %: weight percentage)

	Day 1					Day 2				
	y=bx+a		R^2	Concentration		y=bx+a		R^2	concentration	
	b ± SD	a ± SD		wt % ± CI	RSD	b ± SD	a ± SD		wt % ± CI	RSD
2-propen-1-ol	0.0278 ± 0.0002	-0.02 ± 0.01	0.971	0.036 ± 0.007	0	0.0028 ± 0.0002	-0.017 ± 0.008	0.984	0.035 ± 0.005	2
2-butanone	0.00142 ± 0.00003	-0.001 ± 0.004	0.998	0.10 ± 0.01	4	0.00127 ± 0.00002	0.003 ± 0.003	0.999	0.12 ± 0.01	5
Acetic acid	0.00108 ± 0.00009	-0.02 ± 0.42	0.974	5.9 ± 0.8	2	0.00111 ± 0.00009	-0.06 ± 0.43	0.975	6.1 ± 0.8	2
Furfural	0.0018 ± 0.0001	0.08 ± 0.03	0.981	0.27 ± 0.04	3	0.00124 ± 0.00006	0.004 ± 0.019	0.973	0.17 ± 0.05	5
2(5H)furanone	0.00151 ± 0.00007	-0.35 ± 0.05	0.993	0.81 ± 0.04	2	0.0017 ± .0001	-0.57 ± 0.09	0.983	0.71 ± 0.04	2
2,5-dimethoxy-tetrahydrofuran	0.0026 ± 0.0001	-0.006 ± 0.011	0.992	0.11 ± 0.01	8	0.0028 ± 0.0002	-0.03 ±0.02	0.983	0.13 ± 0.01	11
3-methyl-1,2-cyclopentanedione	0.0021 ± 0.0002	-0.3 ± 0.1	0.963	0.61 ± 0.09	5	0.0023 ± 0.0002	-0.4 ± 0.1	0.974	0.615 ± 0.061	2
2-methoxy-4-propyl-phenol	0.0101 ± 0.0005	-0.03 ± 0.07	0.990	0.08 ± 0.01	8	0.00102 ± 0.0008	0.03 ±0.09	0.977	0.07 ± 0.02	6
Vanillin	0.0011 ± 0.0002	0.17 ± 0.17	0.864	0.8 ± 0.2	10	0.0014 ± 0.0003	0.02 ± 0.25	0.821	0.9 ± 0.2	6
Levoglucosan	0.0011 ±0.0002	0.17 ± 0.17	0.864	6.0 ± 0.3	7	0.00184 ± 0.00000	0.740 ± 0.000	1	6.2 ± 0.0	5

Table 6.9. Calibration equation for each selected compound obtained to fit the area ratio relative to 1,1,3,3-tetramethoxypropane into a Linear Least Squares Regression model and concentration of each compound (SD: Standard deviation, RSD: relative standard deviation, CI: confidence interval at 95% of confidence level, R^2: correlation coefficient, wt %: weight percentage).

	Day 1					Day 2				
	y=bx+a		R^2	Concentration		y=bx+a		R^2	Concentration	
	b ± SD	a ± SD		wt % ± CI	RSD	b ± SD	a ± SD		wt % ± CI	RSD
2-propen-1-ol	0.00146 ± 0.00005	-0.013 ± 0.003	0.995	0.031 ± 0.003	6	0.00140 ± 0.00009	-0.008 ± 0.004	0.984	0.025 ± 0.005	3
2-butanone	0.00073 ± 0.00003	-0.004 ± 0.004	0.995	0.08 ± 0.01	5	0.00066 ± 0.00004	0.0001 ± 0.0054	0.989	0.08 ± 0.02	4
Acetic acid	0.00006 ± 0.00002	-0.18 ± 0.08	0.996	4.5 ± 0.2	2	0.00055 ± 0.00003	0.009 ± 0.132	0.990	4.2 ± 0.4	3
Furfural	0.00094 ± 0.00007	0.03 ± 0.02	0.981	0.20 ± 0.05	2	0.00124 ± 0.00006	0.004 ± 0.02	0.989	0.11 ± 0.03	9
2(5H)furanone	0.00082 ± 0.00004	-0.22 ± 0.03	0.993	0.66 ± 0.03	8	0.00090 ± 0.00007	-0.32 ± 0.05	0.982	0.58 ± 0.04	1
2,5-dimethoxy-tetrahydrofuran	0.00136 ± 0.00002	-0.009 ± 0.001	0.999	0.093 ± 0.002	10	0.00141 ± 0.00007	-0.015 ± 0.006	0.991	0.09 ± 0.01	8
3-methyl-1,2-cyclopentanedione	0.00109 ± 0.00006	-0.20 ± 0.03	0.988	0.52 ± 0.04	5	0.00116 ± 0.00004	-0.18 ± 0.02	0.995	0.45 ± 0.02	2
2-methoxy-4-propyl-phenol	0.0053 ± 0.0001	-0.06 ± 0.01	0.998	0.061 ± 0.005	6	0.0052 ± 0.0003	0.02 ± 0.04	0.982	0.05 ± 0.02	2
Vanillin	0.00064 ± 0.00006	0.01 ± 0.05	0.962	0.61 ± 0.07	6	0.0006 ± 0.0002	0.06 ± 0.14	0.754	0.6 ± 0.2	3
Levoglucosan	0.00064 ± 0.00006	0.01 ± 0.05	0.963	4.4 ± 0.4	5	0.00092 ± 0.00009	0.5 ± 0.5	0.958	4.1 ± 0.8	0.5

Table 6.10. Calibration equation for each selected compound obtained to fit the area ratio relative to 1-octanol into a Linear Least Squares Regression model and concentration of each compound (SD: Standard deviation, RSD: relative standard deviation, CI: confidence interval at 95% of confidence level, R^2: correlation coefficient, wt %: weight percentage).

	Day 1					Day 2				
	y=bx+a		R^2	Concentration		y=bx+a		R^2	Concentration	
	b ± SD	a ± SD		wt % ± IC	RSD	b ± SD	a ± SD		wt % ± IC	RSD
2-propen-1-ol	0.0075 ± 0.0006	-0.07 ± 0.03	0.971	0.034 ± 0.006	4	0.0067 ± 0.0005	-0.04 ± 0.02	0.982	0.026 ± 0.005	4
2-butanone	0.0038 ± 0.0002	-0.02 ± 0.03	0.985	0.09 ± 0.02	2	0.0032 ± 0.0002	-0.002 ± 0.026	0.988	0.08 ± 0.02	5
acetic acid	0.0030 ± 0.0003	-0.9 ± 1.3	0.969	5.2 ± 0.7	5	0.0027 ± 0.0002	-0.1 ± 0.7	0.987	4.4 ± 0.5	4
Furfural	0.0049 ± 0.0006	0.2 ± 0.2	0.940	0.2 ± 0.1	3	0.0060 ± 0.0003	0.009 ± 0.093	0.989	0.12 ± 0.03	3
2(5H)furanone	0.0042 ± 0.0005	-1.1 ± 0.3	0.961	0.74 ± 0.08	7	0.0043 ± 0.0003	1.6 ± 0.2	0.982	0.59 ± 0.04	2
2,5-dimethoxy-tetrahydrofuran	0.0070 ± 0.0005	-0.05 ± 0.05	0.982	0.11 ± 0.01	6	0.0068 ± 0.0004	-0.08 ± 0.03	0.989	0.09 ± 0.01	13
3-methyl-1,2-cyclopentanedione	0.0056 ± 0.0002	-1.0 ± 0.1	0.993	0.57 ± 0.04	2	0.0056 ± 0.0003	-0.9 ± 0.1	0.992	0.46 ± 0.03	3
2-methoxy-4-propyl-phenol	0.027 ± 0.002	-0.3 ± 0.2	0.980	0.07 ± 0.02	9	0.025 ± 0.002	0.05 ± 0.21	0.981	0.05 ± 0.02	8
Vanillin	0.0033 ± 0.0004	0.04 ± 0.3	0.936	0.8 ± 0.1	9	0.0031 ± 0.0009	0.2 ± 0.7	0.747	0.6 ± 0.2	7
Levoglucosan	0.0033 ± 0.0004	0.04 ± 0.34	0.964	5.3 ± 0.9	9	0.0044 ± 0.0005	2 ± 1	0.956	4.4 ± 0.8	8

c. *Comparative assessment of the different quantification methods*

Up to this point, it is compared the quantification values of all the selected compound obtained from the different quantification methods used (without internal standard, with toluene, with 1,1,3,3-tetramethoxypropane and with 1-octanol) and it is assessed which the best quantification method tested is.

A One Way Analysis of Variance is performed to compare the different quantification methods results between days showing significantly differences between them. What is more, it is observed that the calculated concentrations are greater when the area ratio relative to toluene is used for their calculation in comparison to the calculated one with the area ratio relative to 1-octanol, and this is greater than the calculated one with the area ratio relative to 1,1,3,3-tetramethoxypropane. What is more, the calculated concentration without using any internal standard is the lowest. Taking acetic acid quantification in day 1 as example, the concentration calculated using the area ratio relative to toluene is 5.9 ± 0.8 wt %, which is higher than the calculated one using 1-octanol (5.2 ± 0.7 wt %) and this is higher than the calculated one using 1,1,3,3-tetramethoxypropane (4.5 ± 0.2 wt %). All of them are higher that the calculated on without using internal standard which is 4.0 ± 0.3 wt %. Due to the real concentration of each compound is unknown, it is not possible to know which the more accurate method is. However, it is possible to assess the use of which internal standard achieve better reproducibility between days. With this aim, it is performed a scatterplot to graphically represent the correlation between quantification in day 1 and day 2 for each quantification method. It is also adjusted a linear regression to observe the strength of the **linear** relationship between both days.

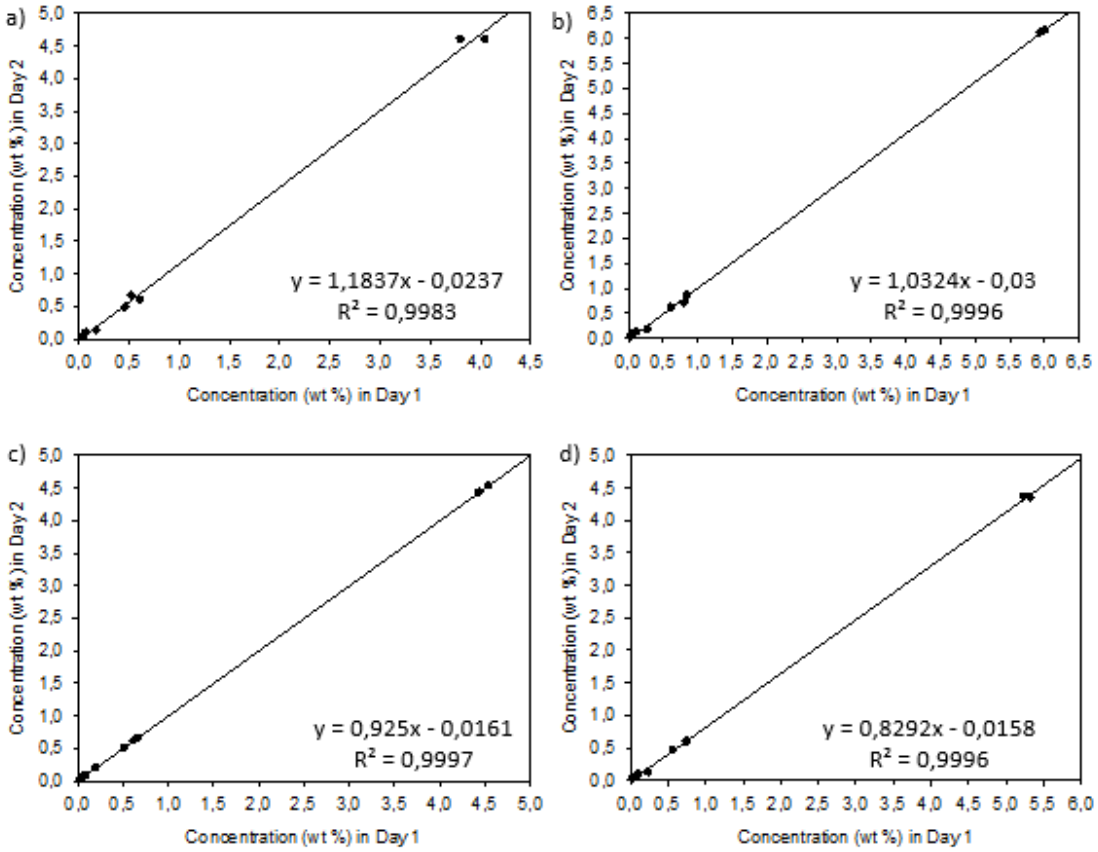

Figure 6.4. Strength of linearity between days for each external calibration method: without internal standard (a); toluene as internal standard (b); 1,1,3,3-tetramethoxypropane as internal standard (c); 1-octanol as internal standard (d).

The strength of linearity can be interpreted by the correlation coefficient (R^2) and by the regression slope. For all methods, the correlation coefficient between days are higher than 0.99. The closer the estimated correlation coefficient is to 1, the closer the two days concentration values are to a perfect linear relationship. It can be interpreted as there is a systematic error in all the quantification methods due to the quantification values are proportional for all the compounds in both days. Regarding to regression slope, regression slope value of 1 means that concentration values obtained in day 1 and day 2 are the same. Moreover, if the regression slope value is lower than 1, means that concentration values calculated in day 2 are systematically lower than those calculated in day 1, and vice versa. The regression slope value of correlate quantification method using toluene as internal standard between days is 1.0324 which means that quantification values are really close between them. Also, it shows that concentration

values calculated in day 2 are slightly higher than in day 1, being this method the more reproducible one between days. For the external calibration using 1,1,3,3-tetramethoxypropane, the regression slope value is 0.925 meaning, once more, that quantification values are so close between them and indicating they are slightly lower in day 2 in comparison to day 1. Regarding to calibration method without using internal standard and using 1-octanol as internal standards, the regression slope values are not so close to 1 being these two methods the less reproducible ones. These results are in concordance with the conclusion mentioned before. Calibration method without internal standard has less precision due to the instability of the chromatographic procedure is not corrected by the internal standards and calibration method using 1-octanol as internal standard is not suitable for all selected compounds.

To sum up, the best calibration method to quantify the selected compounds of bio-oil are those that use toluene as internal standard or 1,1,3,3-tetramethoxypropanone, although it is not possible to say which of them gives a more accurate quantification. In any case, the obtained values are similar if the data is compared, although the ANOVA test show significant differences due to the repeatability is really good making statistical really noticeable that differences between concentration values.

6.3. Conclusions of Chapter 6: Bio-oil characterisation

In this chapter, bio-oil characterisation is achieved by means of pH, TAN, water content and chemical composition using the analytical methods started up during this thesis work.

Furthermore, the reliability of the GC-MS analytical method used for the chemical characterisation of bio-oil is demonstrated by the assessment of its precision. Some target compounds are selected to carry out this precision test including the most representative compounds of each chemical family present in bio-oil (acids, alcohols, phenols, ketones, aldehydes and sugars). The selected compounds are 2-propen-1-ol, 2-butanone, acetic acid, furfural, 2(5H)furanone, 2,5-dimethyoxy-tetrahydrofuran, 3-methyl-1,2-cyclopentanedione, 2-methoxy-4-propyl, vanilline and levoglucosan. The acceptable method precision is supported by the good instrumental and intraday precision achieved. Interday precision is satisfactory for most of the target compounds selected, except furfural, 2(5H)furanone and 2,5-dimethody-tetrahydrofuran. Moreover, it is assessed the influence on the method precision of using or not using an internal standard (toluene, 1,1,3,3-tetramethoxypropane or 1-octanol). The obtained results are similar when toluene and 1,1,3,3-tetramethoxypropane are used as internal standards to those results obtained without using internal standard. However, the use of 1-octanol reduces the method precision due to it is more sensitive to changes in the column with time in comparison to the other internal standards.

Once it is proved the acceptable precision of analytical method, a quantification analysis of the bio-oil target compounds is carried out by means of the four different calibration methods (using toluene, 1,1,3,3-tetramethoxypropane and 1-octanol as internal standards, and without them). An acceptable linearity is obtain for all the selected target compounds and all the tested calibration methods allow the quantification of all of them although calibration curve are needed to be performed each day of analysis to solve the possible problems of interday precision.

The comparison between the results obtained by the different quantification methods by means of One Way Analysis of Variance shows that the calculated concentration of each compound depends on calibration method used. Because of that, it is carried out a study of the results correlation obtained in two different days of analysis. These results show that the best calibration method are those methods that use toluene as internal standard or 1,1,3,3-tetramethoxypropanone due to a better correlation of results between days is achieved, although it is not possible to say which of them gives a more accurate quantification. In any case, the obtained values are similar if the data is compared, although the ANOVA test shows significant differences due to the repeatability is really good making statistical really noticeable that differences between concentration values.

This bio-oil characterisation provides crucial information to design the new upgrading processes and evaluating the viability of extract added-value products from bio-oil. Moreover, the start-up of bio-oil characterisation methods will permit also the evaluation of bio-oil properties changes after an upgrading process, as well as monitoring the upgrading processes developed in the following chapters.

In the main, a proper characterisation of bio-oil might permit to have a further understanding of this product and a better comprehension of the effects of fast pyrolysis conditions and biomass type on the bio-oil composition; and to monitoring and further understanding the bio-oil upgrading processes.

7. Reduced energy cost bio-oil catalytic upgrading process

A study to improve bio-oil properties at low temperatures (60 ºC) using bentonite and HZSM-5 in order to reduce the energy cost of the conventional catalytic cracking upgrading processes is explained in this chapter. Particularly, the reduction of bio-oil acidity is the main purpose of this work due to its negative effect on the possible bio-oil applications as biofuel to generate energy and heat in boilers, furnaces and engines and as transportation fuel. Moreover, catalyst life time is tested.

7.1. Introduction of Chapter 7: reduced energy cost bio-oil catalytic upgrading process

As it is stated in section 1.4.1.a., bio-oil properties have drawbacks for its use as biofuel making mandatory their upgrading before its use as fuel in conventional devices. Catalytic cracking is one of the most prospective upgrading processes. However, the material and energy required for this process (between 350-650 ºC) reduce the economic viability of the obtained biofuel compared to fossil fuels which makes necessary the development of new upgrading processes with lower energy and environmental costs. Because of that, performing bio-oil upgrading at temperatures close to those at bio-oil comes out of the fast pyrolysis process (around 60 ºC) would allow the *in situ* upgrading of the bio-oil at the fast pyrolysis plant and, among other advantages, avoid the necessity of external heating to upgrade it. This process has not yet been explored in literature.

Bentonite and HZSM-5 zeolite are the used catalysts to perform the catalytic cracking process tested in this thesis work. ZSM-5 are crystalline alumina-silicate microporous materials with well-defined pore structures in the order of 5 – 12 Å forming regular and defined channels and pores [32,33]. These channels and pores give to ZSM-5 the ability to act as a molecular sieve, separating and storing molecules [34]. ZSM-5 zeolites are very selective and active catalysts due to their structure. The negative

charges in the network are compensated with cations or alkali metals like Na^+. Substitution of them for NH^{4+} by ion exchange and followed by a treatment of thermal decomposition generates an H^+ as compensation cation of the network. Thus, zeolites contain acid sites that promote acid-catalysed reactions and give selectivity based mainly on both spatial constraints [35] and attractive-repulsive interactions between adsorbed molecules and pore walls [36,37]. Therefore, shape selectivity and acid properties of zeolites are crucial properties for upgrading processes [7]. Bentonite is an alumina-silicate that could be used for upgrading processes, although it has not yet been addressed in this field. Bentonite consists in a sheet of octahedral alumina between two sheets of tetrahedral silica around 10 Å thick [38]. It has an amorphous structure that gives it less selectivity comparing to zeolite. It possesses acid sites, although some of them might be found buried in inaccessible sites which might lead to less acid-catalysed reactions [39]. Bentonites has been used as molecular sieve and for the esterification of carboxylic acids in reactions model [40] [41]. Despite of these disadvantages in comparison of zeolite, bentonite's natural origin, its abundance in most continents of the world and its low cost make it a strong candidate as adsorbent of phenols and pollutants [42].

7.2. Effect of bentonite and HZSM-5 on bio-oil properties

To study the effect of bentonite and HZSM-5 as catalysis, raw bio-oil is mixed with different weight percentages of catalyst at 60 ºC for up to 12 hours using a three neck flask equipped with a thermometer, reflux condenser and magnetic stirrer, as it has been described in section 3.3.2.

Prior to perform the bio-oil upgrading process, an initial run is carried out at 60 °C without catalyst to test possible changes on the bio-oil properties at 60 °C over the time. As it is shown in Table 7.1., bio-oil properties remain constant over time at 60 °C. Thus, no thermal effects can be observed on bio-oil properties at working temperature of 60 °C.

Table 7.1. Bio-oil properties at 60 ºC over time. (* confidence interval at 95% of confidence level)

Time (h)	pH	TAN* (mg KOH/g bio-oil)	Water content* (wt %)
0	2.0	80 ± 4	22 ± 1
2	2.0	81 ± 5	23 ± 2
4	2.1	86 ± 5	21 ± 1
6	2.0	85 ± 3	22 ± 2
8	1.9	83 ± 2	21 ± 1

First, the effect of bentonite on the bio-oil properties is studied. Bio-oil acidity decreases when bentonite is used (Table 7.2.). A pH raise of 0.6 pH units is observed using 15 wt % of bentonite in the first 2 h of reaction time, while pH enhancement of 0.3 pH units is achieved with 5 wt % and 10 wt % of bentonite. After the first 2 h of reaction time, no significant changes on pH value are observed in any of the different weight percentages of catalyst studied. Accordingly, TAN values decrease in all experiments around 6 mg KOH / g bio-oil in the first 2 h of reaction time and in all weigh percentages of catalyst under study. Hence, a reaction time of 2 h seems enough to decrease acidity at 60 ºC. Regarding to water content, no significant changes in water content are detected in all weight percentages of catalyst studied. Therefore, all percentages of bentonite have improved bio-oil acidity at the reaction conditions tested, being 15 wt % the most effective one.

Table 7.2. Effect of different weight percentages of bentonite on bio-oil properties through the upgrading process at 60 ºC. (* confidence interval at 95% of confidence level; n.a. = not available)

	Bentonite percentage								
	5 wt %			10 wt %			15wt %		
Time (h)	pH	TAN* (mg KOH/g)	Water* (wt %)	pH	TAN* (mg KOH/g)	Water* (wt %)	pH	TAN* (mg KOH/g)	Water* (wt %)
0	1.9	80 ± 5	23 ± 1	2.1	80 ± 11	22 ± 3	2.0	81 ± 3	22 ± 3
2	2.2	73 ± 6	22 ± 1	2.4	85 ± 6	24 ± 2	2.6	75 ± 2	23 ± 1
4	2.4	72 ± 1	24 ± 1	2.5	78 ± 7	25 ± 2	2.7	79 ± 3	22 ± 1
6	2.2	76 ± 5	21 ± 1	2.5	77 ± 6	25 ± 1	2.7	79 ± 5	22 ± 3
8	2.2	73 ± 4	22 ± 1	2.4	77 ± 5	22 ± 1	2.7	75 ± 8	23 ± 2
10	2.5	75 ± 3	22 ± 2	n.a.	n.a	n.a.	n.a.	n.a	n.a.
12	2.3	74 ± 2	22 ± 1	n.a.	n.a.	n.a.	n.a.	n.a.	n.a

Secondly, the upgrading process is carried out using HZSM-5 (Table 7.3.). A reduction of acidity is reached when HZSM-5 is used during the first 2 hours of reaction time. The most effective weight percentage of HZSM-5 are 10 wt %, 15 wt % and 20 wt %, which result in a pH increase in 0.7 pH units, while the increase is slightly lower when using 5 wt % (0.4 pH units). TAN values are reduced using 10, 15 wt % and 20 wt % while with 5 wt % of HZSM-5 it remains constant. As for bentonite upgrading processes, any significant changes are detected in water content in overall zeolite experiments. Therefore, it is considered that a minimum of 10 wt % of HZSM-5 is necessary to improve bio-oil acidity.

Table 7.3. Effect of different weight percentages of HZSM-5 on bio-oil properties through the upgrading process at 60 ºC. (* confidence interval at 95% of confidence level; n.a. = not available)

	HZSM-5 percentage											
	5 wt %			10 wt %			15 wt %			20 wt %		
Time (h)	pH	TAN (mg KOH/g bio-oil)	Water (wt %)	pH	TAN (mg KOH/g bio-oil)	Water (wt %)	pH	TAN (mg KOH/g bio-oil)	Water (wt %)	pH	TAN (mg KOH/g bio-oil)	Water (wt %)
0	1.9	80 ± 5	23 ± 1	2.1	78 ± 5	22 ± 5	2.0	85 ± 3	22 ± 4	2.1	77 ± 1	22 ± 3
2	2.3	80 ± 3	22 ± 2	2.7	75 ± 1	21 ± 1	2.7	78 ± 3	24 ± 3	2.7	67 ± 3	19 ± 8
4	2.3	80 ± 4	21 ± 6	2.7	75 ± 5	21 ± 1	2.9	70 ± 2	23 ± 1	2.7	70 ± 3	20 ± 7
6	2.4	84 ± 7	22 ± 3	2.7	73 ± 1	20 ± 1	2.7	71 ± 4	23 ± 6	n.a.	n.a.	n.a.

Bio-oil acidity reduction supposes a significant improvement of bio-oil, taking into account that the acidic nature of the bio-oil constitutes a problem of corrosion in conventional devices used for storage, transport and processing, as well as common construction materials when they are in contact with bio-oil [6,43]. Acidity reduction takes place with both bentonite and zeolite, which is observed by a pH raise and a TAN decrease. It is important to point out the connection between pH and TAN: a reduction of acidic constituents of bio-oil supposes an increase of the pH value. However, this relationship is not always direct due to TAN value comprises the weak and strong acidic components with dissociation constant of more than 10^{-9} [44] and a reduction of weak acids might not have an influence on pH value. Moreover, TAN analysis has presented some difficulties as low reproducibility, probably due to the reduced pH change at the equivalence point as a result of the large number of weak acids present in bio-oil.

Among the tested catalysts, HZSM-5 is the most effective one reducing the acidity of the bio-oil because it is possible to reduce the same acidity with less amount of catalyst. This can be explained by the more accessible acid sites and the regular structure of HZSM-5 in comparison of other silica-alumina catalysts [39] as it is bentonite.

Furthermore, it can be concluded that no significant changes on bio-oil properties are observed after 2 h of reaction time, making unnecessary to carry out the upgrading process for longer time. Longer reaction times result in carbon deposition (coke) and thereby catalyst deactivation which constitutes a problem in zeolite catalytic upgrading processes as it has been reported [7]. There are described mainly two ways of catalyst deactivation: the blockage of zeolite microporous and internal acid sites by high molecular weight formed to polymerization and polycondensation reactions [45,46] and the depositions of carbon on the walls of zeolite and in the macroporous [47]. Thus, a possible deactivation of the catalyst might explain the limited upgrading reaction at longer reaction times. The study of the possible causes of the limited reaction time of the catalyst working at 60 ºC is shown in section 7.4.

This acidity reduction might be caused by the reaction of volatile acids and phenolic groups (which render the acidic nature of bio-oil) during the upgrading process reducing their concentrations and consequently bio-oil acidity. Also, esterification reactions might explain the reduction of bio-oil acidity [40–42]. Moreover, it is reported that water content tends to increase in catalytic process due to the dehydration reaction during the catalytic processes [48] or due to the esterification reaction that might take place [49]. However, it is worth noting that no significant water increase has been observed when the upgrading process takes place at 60 ºC using nor bentonite nor zeolite, which indicates that these reactions are not the main responsible of the bio-oil acidity enhancement. Thus, a chemical characterisation of upgraded bio-oil and raw bio-oil is carried out in order to unravel the chemical changes that take place during this upgrading process.

7.3. Chemical changes in upgraded bio-oil using HZSM-5.

Since HZSM-5 has been shown as the most effective catalyst, the chemical composition of the upgraded bio-oil by HZSM-5 is compared to raw bio-oil composition in all catalyst percentages tested to study the chemical changes on the bio-oil during the upgrading process.

The chemical composition of raw bio-oil and treated bio-oil at different reaction is analysed by means of a GC-MS analysis using toluene as internal standard (see section 3.1.6). To carry out the comparison between treated and raw bio-oil, it is calculated the percentage of variance between the area ratio relative to toluene for each compound at determined reaction time (t_x) and the area ratio relative to toluene for each compound in raw bio-oil, following the Equation 7.1. Area ratio (AR) is defined as the area of the target compound relative to the area of the internal standard.

$$\%\ variance = \frac{(AR_{treated\ bio-oil})t_x - (AR_{raw\ bio-oil})}{(AR_{raw\ bio-oil})} \cdot 100 \qquad \text{Equation 7.1.}$$

The evaluation of the bio-oil chemical changes during the upgrading process is carried out, although its assessment is difficult due to due to the high diversity of compounds in the bio-oil and the span of potential reactions [7]. Table 7.4., Table 7.5., Table 7.6. listed all bio-oil identified compounds of raw and treated bio-oil at different reaction times for 5 wt %, 10 wt % and 15 wt % of HZSM-5 experiments, respectively. Moreover, they show the area ratio relative to toluene for each compound and reaction time. From the 49 identified compounds, 28 compounds tend to reduce their area ratio through the reaction time in all percentages of zeolite used, while in the remaining 21 no significant changes can be observed. Even so, cracking, decarbonylation, hydrocraking, hydrodeoxygenation, hydrogenation and polymerization have been reported as potential reactions to take place through the catalytic upgrading at 300 – 410 ºC [39,50], although there is no information in literature on reaction pathways for upgrading processes at 60 ºC.

Table 7.4. Area ratio of the identified compounds of raw and upgraded bio-oil at different reaction times for 5 wt % of HZSM-5 experiments. (m/z: mass to charge ratio; RT: retention time; * confidence interval at 95% of confidence level).

Compound	RT	m/z	Area Ratio * 5 wt % HZSM-5			
			0 h	2 h	4 h	6 h
Methyl acetate	9.1	43	1.0 ± 0.3	0.69 ± 0.05	0.63 ± 0.01	0.57 ± 0.04
Formic acid	9.3	46	1.1 ± 0.2	1.00 ± 0.04	0.95 ± 0.03	1.10 ± 0.02
1,3-cyclopentandiene	9.5	66	0.033 ± 0.001	0.033 ± 0.002	0.031 ± 0.002	0.036 ± 0.001
2-propen-1-ol	10.0	57	0.08 ± 0.01	0.073 ± 0.002	0.067 ± 0.002	0.073 ± 0.002
Hydroxy-acetaldehyde	10.3	31	5 ± 2	4.5 ± 0.7	4.3 ± 0.4	4.89 ± 0.04
2,3-butanedione	10.9	43	0.6 ± 0.3	0.59 ± 0.02	0.54 ± 0.02	0.56 ± 0.06
2-butanone	11.4	43	0.14 ± 0.06	0.10 ± 0.02	0.09 ± 0.01	0.09 ± 0.01
Acetic acid	13.5	60	4.3 ± 0.7	4.0 ± 0.1	3.82 ± 0.09	4.3 ± 0.2
2-butenal	14.0	70	0.02 ± 0.01	0.020 ± 0.002	0.0186 ± 0.0003	0.023 ± 0.002
1-hydroxy-2-propanone	14.6	43	7 ± 2	6.0 ± 0.4	5.9 ± 0.1	6.7 ± 0.7
1-hydroxy-2-butanone	23.3	57	0.7 ± 0.3	0.73 ± 0.02	0.67 ± 0.05	0.80 ± 0.03
2-cyclopenten-1one	29.6	82	0.35 ± 0.04	0.32 ± 0.01	0.31 ± 0.01	0.35 ± 0.02
Furfural	30.0	95	0.67 ± 0.07	0.60 ± 0.04	0.55 ± 0.03	0.63 ± 0.02
1-acetyloxy-2-propanone	33.0	43	0.27 ± 0.06	0.21 ± 0.03	0.19 ± 0.05	0.22 ± 0.04
2-methoxy-1.3-dioxolane	34.7	73	0.5 ± 0.1	0.51 ± 0.01	0.5 ± 0.1	0.5 ± 0.1
2(5H)furanone	35.9	55	1.2 ± 0.3	1.10 ± 0.03	1.06 ± 0.02	1.19 ± 0.02
2,5-dimethoxy-tetrahydro-furan	36.3	101	0.06 ± 0.02	0.06 ± 0.01	0.066 ± 0.008	0.06 ± 0.01
3-methyl-2,5-furandione	38.4	68	0.06 ± 0.01	0.06 ± 0.01	0.06 ± 0.02	0.08 ± 0.01
2,5-hexanedione	38.6	99	0.019 ± 0.003	0.016 ± 0.001	0.015 ± 0.003	0.018 ± 0.003
5-methyl-2(5H)furanone	38.9	43	0.03 ± 0.01	0.03 ± 0.02	0.03 ± 0.02	0.03 ± 0.03
1,2-cyclopentanedione	39.1	98	0.07 ± 0.01	0.08 ± 0.04	0.07 ± 0.03	0.08 ± 0.01
Phenol	45.5	94	0.23 ± 0.02	0.218 ± 0.002	0.19 ± 0.02	0.230 ± 0.005
4-methyl-5H-furan-2-one	48.4	69	0.28 ± 0.01	0.26 ± 0.01	0.25 ± 0.01	0.29 ± 0.04
2-hydoxy-3-methyl-2-cyclopenten-1-one	48.9	112	1.0 ± 0.1	0.89 ± 0.04	0.83 ± 0.03	0.94 ± 0.05
2,3-dimethyl-2-cyclopenten-1-one	49.9	67	0.05 ± 0.01	0.05 ± 0.01	0.05 ± 0.01	0.06 ± 0.01
2-methyl-phenol	51.9	108	0.08 ± 0.01	0.07 ± 0.01	0.07 ± 0.01	0.08 ± 0.01
4-methyl-phenol	53.5	107	0.17 ± 0.01	0.153 ± 0.003	0.15 ± 0.01	0.17 ± 0.01
Guaiacol	54.6	124	1.9 ± 0.1	1.8 ± 0.1	1.7 ± 0.2	1.9 ± 0.2
Maltol	56.0	126	0.26 ± 0.01	0.26 ± 0.01	0.24 ± 0.01	0.29 ± 0.01
3-ethyl-2-hydroxy-2-cyclopenten-1-one	56.9	83	0.06 ± 0.01	0.055 ± 0.004	0.054 ± 0.004	0.063 ± 0.001
2-4-dimethyl-phenol	59.5	107	0.08 ± 0.01	0.075 ± 0.004	0.072 ± 0.003	0.083 ± 0.003

Table 7.4. (Continued). Area ratio of the identified compounds of raw and upgraded bio-oil at different reaction times for 5 wt % of HZSM-5 experiments. (m/z: mass to charge ratio; RT: retention time; * confidence interval at 95% of confidence level).

Compound	RT	m/z	Area Ratio * 5 wt % HZSM-5			
			0 h	2 h	4 h	6 h
2,3-dihydroxybenzaldehyde	60.7	138	0.07 ± 0.01	0.066 ± 0.003	0.061 ± 0.002	0.071 ± 0.003
2-methoxy-5-methyl-phenol	62.0	123	0.103 ± 0.005	0.09 ± 0.01	0.09 ± 0.01	0.101 ± 0.001
2-methoxy-4-methyl-phenol	63.1	123	2.7 ± 0.1	2.5 ± 0.1	2.4 ± 0.3	2.70 ± 0.04
5-hydroxymethyl-2-furancarboxaldehyde	64.0	126	0.29 ± 0.02	0.28 ± 0.01	0.26 ± 0.01	0.31 ± 0.02
4-(2-propenyl)-phenol	67.3	134	0.016 ± 0.001	0.015 ± 0.001	0.014 ± 0.002	0.016 ± 0.001
3-methyl-1,2-benzenediol	67.8	124	0.16 ± 0.03	0.15 ± 0.01	0.14 ± 0.01	0.16 ± 0.01
4-ethyl-2-methoxy-phenol	69.5	137	1.35 ± 0.04	1.28 ± 0.07	1.2 ± 0.1	1.37 ± 0.02
4-methyl-1,2-benzenediol	69.9	124	0.26 ± 0.04	0.26 ± 0.02	0.24 ± 0.01	0.29 ± 0.02
2-methoxy-4-vinyl-phenol	71.8	150	0.24 ± 0.02	0.22 ± 0.02	0.20 ± 0.01	0.24 ± 0.01
Eugenol	74.9	75	0.95 ± 0.05	0.91 ± 0.03	0.86 ± 0.03	0.98 ± 0.04
2-methoxy-4-propyl-phenol	75.8	137	1.04 ± 0.06	1.00 ± 0.05	0.94 ± 0.02	1.06 ± 0.06
4-ethyl-1.3-benzenediol	76.3	123	0.23 ± 0.04	0.23 ± 0.02	0.20 ± 0.03	0.25 ± 0.02
Vanillina	76.7	151	0.95 ± 0.03	0.94 ± 0.06	0.88 ± 0.03	1.02 ± 0.08
2-methoxy-4-(1-propenyl)-phenol	78.3	164	0.34 ± 0.02	0.33 ± 0.01	0.31 ± 0.01	0.34 ± 0.01
2-methoxy-4(1-propenyl)-phenol (E)	81.0	164	0.57 ± 0.05	0.44 ± 0.04	0.42 ± 0.01	0.48 ± 0.02
Acetonvanilline	82.6	151	0.97 ± 0.09	0.97 ± 0.06	0.90 ± 0.01	1.04 ± 0.04
D-allose	83.0	60	7 ± 1	7.0 ± 0.6	6.8 ± 0.5	7.8 ± 0.4
1-(4-hydorxy-3-methoxypheny)-2-propanone	85.1	137	0.7 ± 0.1	0.75 ± 0.04	0.70 ± 0.02	0.80 ± 0.02

Table 7.5. Area ratio of the identified compounds of raw and upgraded bio-oil at different reaction times for 10 wt % of HZSM-5 experiments. (m/z: mass to charge ratio; RT: retention time; * confidence interval at 95% of confidence level).

Compound	RT	m/z	Area Ratio * 10 wt % HZSM-5			
			0 h	2 h	4 h	6 h
Methyl acetate	9.1	43	1.2 ± 0.1	0.79 ± 0.06	0.83 ± 0.04	0.73 ± 0.08
Formic acid	9.3	46	1.0 ± 0.1	0.91 ± 0.03	1.00 ± 0.03	0.92 ± 0.02
1,3-cyclopentandiene	9.5	66	0.038 ± 0.001	0.036 ± 0.001	0.038 ± 0.001	0.036 ± 0.001
2-propen-1-ol	10.0	57	0.087 ± 0.001	0.076 ± 0.001	0.082 ± 0.002	0.074 ± 0.001
Hydroxy-acetaldehyde	10.3	31	5 ± 1	4.3 ± 0.3	4.6 ±1.0	4.08 ± 0.11
2,3-butanedione	10.9	43	0.8 ± 0.1	0.76 ± 0.03	0.80 ± 0.06	0.74 ± 0.04
2-butanone	11.4	43	0.15 ± 0.02	0.09 ± 0.01	0.10 ± 0.01	0.10 ± 0.02
Acetic acid	13.5	60	4.5 ± 0.2	4.0 ± 0.1	4.37 ± 0.06	4.0 ± 0.0
2-butenal	14.0	70	0.025 ± 0.003	0.022 ± 0.001	0.0226 ± 0.0050	0.021 ± 0.003
1-hydroxy-2-propanone	14.6	43	7 ± 1	6.7 ± 0.5	7.5 ± 0.9	6.9 ± 0.5
1-hydroxy-2-butanone	23.3	57	0.8 ± 0.1	0.72 ± 0.07	0.75 ± 0.08	0.73 ± 0.06
2-cyclopenten-1one	29.6	82	0.33 ± 0.01	0.31 ± 0.01	0.34 ± 0.00	0.31 ± 0.01
Furfural	30.0	95	0.52 ± 0.04	0.47 ± 0.02	0.52 ± 0.04	0.46 ± 0.06
1-acetyloxy-2-propanone	33.0	43	0.26 ± 0.07	0.24 ± 0.08	0.22 ± 0.07	0.20 ± 0.07
2-methoxy-1,3-dioxolane	34.7	73	0.5 ± 0.1	0.44 ± 0.10	0.45 ± 0.01	0.46 ± 0.04
2(5H)furanone	35.9	55	1.18 ± 0.05	1.08 ± 0.06	1.19 ± 0.05	1.09 ± 0.04
2,5-di<methoxy-tetrahydro-furan	36.3	101	0.06 ± 0.04	0.04 ± 0.01	0.053 ± 0.004	0.06 ± 0.01
3-methyl-2,5-furandione	38.4	68	0.07 ± 0.01	0.06 ± 0.02	0.07 ± 0.01	0.07 ± 0.02
2.5-hexanedione	38.6	99	0.016 ± 0.005	0.013 ± 0.001	0.015 ± 0.001	0.014 ± 0.001
5-methyl-2(5H)furanone	38.9	43	0.02 ± 0.01	0.022 ± 0.004	0.023 ± 0.003	0.020 ± 0.005
1,2-cyclopentanedione	39.1	98	0.09 ± 0.03	0.97 ± 0.003	0.10 ± 0.03	0.08 ± 0.01
Phenol	45.5	94	0.19 ± 0.01	0.199 ± 0.024	0.20 ± 0.01	0.206 ± 0.015
4-methyl-5H-furan-2-one	48.4	69	0.25 ± 0.01	0.24 ± 0.03	0.24 ± 0.06	0.22 ± 0.04
2-hydoxy-3-methyl-2-cyclopenten-1-one	48.9	112	1.0 ± 0.1	0.98 ± 0.03	1.00 ± 0.09	0.97 ± 0.10
2,3-dimethyl-2-cyclopenten-1-one	49.9	67	0.07 ± 0.01	0.06 ± 0.01	0.07 ± 0.01	0.07 ± 0.01
2-methyl-phenol	51.9	108	0.074 ± 0.004	0.074 ± 0.005	0.079 ± 0.003	0.08 ± 0.01
4-methyl-phenol	53.5	107	0.17 ± 0.01	0.167 ± 0.015	0.18 ± 0.02	0.172 ± 0.003
Guaiacol	54.6	124	1.8 ± 0.1	1.8 ± 0.2	1.91 ± 0.04	1.8 ± 0.1
Maltol	56.0	126	0.24 ± 0.01	0.246 ± 0.004	0.26 ± 0.01	0.25 ± 0.04
3-ethyl-2-hydroxy-2-cyclopenten-1-one	56.9	83	0.06 ± 0.01	0.062 ± 0.002	0.064 ± 0.007	0.063 ± 0.005

Table 7.5. (Continued). Area ratio of the identified compounds of raw and upgraded bio-oil at different reaction times for 10 wt % of HZSM-5 experiments. (m/z: mass to charge ratio; RT: retention time; * confidence interval at 95% of confidence level).

Compound	RT	m/z	Area Ratio * 10 wt % HZSM-5			
			0 h	2 h	4 h	6 h
2-4-dimethyl-phenol	59.5	107	0.084 ± 0.004	0.081 ± 0.003	0.088 ± 0.004	0.082 ± 0.004
2,3-dihydroxybenzaldehyde	60.7	138	0.059 ± 0.004	0.060 ± 0.005	0.063 ± 0.002	0.060 ± 0.006
2-methoxy-5-methyl-phenol	62.0	123	0.100 ± 0.008	0.10 ± 0.01	0.10 ± 0.01	0.099 ± 0.006
2-methoxy-4-methyl-phenol	63.1	123	2.8 ± 0.2	2.7 ± 0.2	2.85 ± 0.05	2.70 ± 0.06
5-hydroxymethyl-2-furancarboxaldehyde	64.0	126	0.21 ± 0.01	0.21 ± 0.01	0.232 ± 0.004	0.20 ± 0.03
4-(2-propenyl)-phenol	67.3	134	0.014 ± 0.001	0.013 ± 0.002	0.015 ± 0.001	0.014 ± 0.001
3-methyl-1.2-benzenediol	67.8	124	0.12 ± 0.01	0.12 ± 0.01	0.135 ± 0.003	0.13 ± 0.01
4-ethyl-2-methoxy-phenol	69.5	137	1.32 ± 0.04	1.28 ± 0.05	1.4 ± 0.1	1.32 ± 0.06
4-methyl-1,2-benzenediol	69.9	124	0.22 ± 0.01	0.226 ± 0.004	0.25 ± 0.01	0.231 ± 0.004
2-methoxy-4-vinyl-phenol	71.8	150	0.25 ± 0.01	0.23 ± 0.01	0.25 ± 0.02	0.23 ± 0.01
Eugenol	74.9	75	0.94 ± 0.02	0.92 ± 0.05	1.00 ± 0.01	0.93 ± 0.02
2-methoxy-4-propyl-phenol	75.8	137	1.00 ± 0.07	1.00 ± 0.01	1.08 ± 0.02	0.98 ± 0.06
4-ethyl-1,3-benzenediol	76.3	123	0.19 ± 0.01	0.197 ± 0.002	0.22 ± 0.01	0.20 ± 0.01
Vanillina	76.7	151	1.01 ± 0.05	0.98 ± 0.04	1.06 ± 0.01	0.98 ± 0.02
2-methoxy-4-(1-propenyl)-phenol	78.3	164	0.33 ± 0.01	0.32 ± 0.01	0.35 ± 0.01	0.32 ± 0.00
2-methoxy-4-(1-propenyl)-phenol (E)	81.0	164	0.48 ± 0.07	0.41 ± 0.01	0.45 ± 0.02	0.41 ± 0.02
Acetonvanilline	82.6	151	1.07 ± 0.02	1.05 ± 0.03	1.16 ± 0.05	1.07 ± 0.02
D-allose	83.0	60	8.6 ± 0.4	8.2 ± 0.5	8.6 ± 0.3	8.2 ± 0.7
1-(4-hydorxy-3-methoxypheny)-2-propanone	85.1	137	0.75 ± 0.04	0.74 ± 0.01	0.81 ± 0.04	0.75 ± 0.03

Table 7.6. Area ratio of the identified compounds of raw and upgraded bio-oil at different reaction times for 15 wt % of HZSM-5 experiments. (m/z: mass to charge ratio; RT: retention time; * confidence interval at 95% of confidence level).

Compound	RT	m/z	Area ratio - 15 wt % HZSM-5 *			
			0 h	2 h	4 h	6 h
Methyl acetate	9.1	43	0.97 ± 0.04	0.58 ± 0.03	0.51 ± 0.02	0.46
Formic acid	9.3	46	1.0 ± 0.1	1.05 ± 0.04	0.99 ± 0.05	0.94
1,3-cyclopentandiene	9.5	66	0.032 ± 0.003	0.032 ± 0.001	0.032 ± 0.002	0.032
2-propen-1-ol	10.0	57	0.078 ± 0.004	0.071 ± 0.002	0.063 ± 0.002	0.058
Hydroxy-acetaldehyde	10.3	31	4.7 ± 0.5	3.7 ± 0.1	4.7 ± 0.5	3.58
2,3-butanedione	10.9	43	0.6 ± 0.1	0.58 ± 0.03	0.55 ± 0.03	0.51
2-butanone	11.4	43	0.13 ± 0.01	0.0745 ± 0.0002	0.070 ± 0.003	0.07
Acetic acid	13.5	60	4.1 ± 0.3	3.9 ± 0.1	3.76 ± 0.12	3.7
2-butenal	14.0	70	0.02 ± 0.01	0.020 ± 0.002	0.0185 ± 0.0042	0.019
1-hydroxy-2-propanone	14.6	43	6 ± 1	6.2 ± 0.4	5.9 ± 0.2	6.1
1-hydroxy-2-butanone	23.3	57	0.7 ± 0.1	0.65 ± 0.06	0.57 ± 0.10	0.65
2-cyclopenten-1one	29.6	82	0.32 ± 0.01	0.32 ± 0.01	0.29 ± 0.01	0.29
Furfural	30.0	95	0.58 ± 0.09	0.49 ± 0.05	0.43 ± 0.03	0.45
1-acetyloxy-2-propanone	33.0	43	0.24 ± 0.07	0.15 ± 0.06	0.11 ± 0.01	0.16
2-methoxy-1.3-dioxolane	34.7	73	0.5 ± 0.1	0.36 ± 0.02	0.4 ± 0.2	0.4
2(5H)furanone	35.9	55	1.10 ± 0.04	1.01 ± 0.05	0.97 ± 0.05	0.97
2,5-dimethoxy-tetrahydro-furan	36.3	101	0.06 ± 0.01	0.061 ± 0.005	0.060 ± 0.005	0.06
3-methyl-2.5-furandione	38.4	68	0.06 ± 0.01	0.06 ± 0.01	0.05 ± 0.01	0.06
2,5-hexanedione	38.6	99	0.016 ± 0.004	0.012 ± 0.002	0.010 ± 0.002	0.012
5-methyl-2(5H)furanone	38.9	43	0.03 ± 0.03	0.02 ± 0.02	0.02 ± 0.02	0.04
1,2-cyclopentanedione	39.1	98	0.08 ± 0.01	0.07 ± 0.02	0.07 ± 0.02	0.06
Phenol	45.5	94	0.20 ± 0.01	0.199 ± 0.019	0.18 ± 0.01	0.192
4-methyl-5H-furan-2-one	48.4	69	0.25 ± 0.03	0.24 ± 0.01	0.24 ± 0.04	0.18
2-hydoxy-3-methyl-2-cyclopenten-1-one	48.9	112	0.83 ± 0.04	0.83 ± 0.06	0.79 ± 0.07	0.86
2,3-dimethyl-2-cyclopenten-1-one	49.9	67	0.052 ± 0.001	0.05 ± 0.01	0.04 ± 0.01	0.05
2-methyl-phenol	51.9	108	0.07 ± 0.01	0.07 ± 0.01	0.063 ± 0.003	0.07
4-methyl-phenol	53.5	107	0.15 ± 0.01	0.146 ± 0.002	0.15 ± 0.01	0.15
Guaiacol	54.6	124	1.7 ± 0.1	1.7 ± 0.1	1.6 ± 0.2	1.6
Maltol	56.0	126	0.25 ± 0.02	0.25 ± 0.01	0.24 ± 0.03	0.23
3-ethyl-2-hydroxy-2-cyclopenten-1-one	56.9	83	0.06 ± 0.00	0.054 ± 0.002	0.051 ± 0.003	0.054
2-4-dimethyl-phenol	59.5	107	0.07 ± 0.00	0.071 ± 0.003	0.070 ± 0.003	0.073
2,3-dihydroxybenzaldehyde	60.7	138	0.06 ± 0.00	0.062 ± 0.002	0.061 ± 0.006	0.059
2-methoxy-5-methyl-phenol	62.0	123	0.092 ± 0.007	0.09 ± 0.01	0.08 ± 0.01	0.086
2-methoxy-4-methyl-phenol	63.1	123	2.4 ± 0.1	2.31 ± 0.05	2.2 ± 0.1	2.34
5-hydroxymethyl-2-furancarboxaldehyde	64.0	126	0.28 ± 0.02	0.27 ± 0.01	0.26 ± 0.03	0.26

Table 7.6. (Continued). Area ratio of the identified compounds of raw and upgraded bio-oil at different reaction times for 15 wt % of HZSM-5 experiments. (m/z: mass to charge ratio; RT: retention time; * confidence interval at 95% of confidence level).

Compound	RT	m/z	Area ratio - 15 wt % HZSM-5 *			
			0 h	2 h	4 h	6 h
4-(2-propenyl)-phenol	67.3	134	0.014 ± 0.001	0.013 ± 0.001	0.014 ± 0.002	0.0142
3-methyl-1,2-benzenediol	67.8	124	0.14 ± 0.00	0.15 ± 0.01	0.15 ± 0.02	0.15
4-ethyl-2-methoxy-phenol	69.5	137	1.23 ± 0.04	1.14 ± 0.11	1.17 ± 0.03	1.19
4-methyl-1,2-benzenediol	69.9	124	0.24 ± 0.02	0.26 ± 0.01	0.26 ± 0.03	0.26
2-methoxy-4-vinyl-phenol	71.8	150	0.23 ± 0.02	0.19 ± 0.01	0.19 ± 0.03	0.20
Eugenol	74.9	75	0.87 ± 0.02	0.83 ± 0.02	0.84 ± 0.04	0.85
2-methoxy-4-propyl-phenol	75.8	137	0.97 ± 0.03	0.93 ± 0.02	0.93 ± 0.06	0.95
4-ethyl-1,3-benzenediol	76.3	123	0.20 ± 0.04	0.22 ± 0.01	0.22 ± 0.03	0.22
Vanillina	76.7	151	0.90 ± 0.06	0.89 ± 0.03	0.90 ± 0.09	0.88
2-methoxy-4-(1-propenyl)-phenol	78.3	164	0.31 ± 0.02	0.30 ± 0.01	0.30 ± 0.02	0.31
2-methoxy-4(1-propenyl)-phenol (E)	81.0	164	0.52 ± 0.05	0.37 ± 0.03	0.37 ± 0.06	0.37
Acetonvanilline	82.6	151	0.94 ± 0.02	0.93 ± 0.03	0.9 ± 0.1	0.92
D-allose	83.0	60	7.3 ± 1.0	7.5 ± 0.3	7.0 ± 0.7	6.8
1-(4-hydorxy-3-methoxypheny)-2-propanone	85.1	137	0.71 ± 0.03	0.71 ± 0.02	0.7 ± 0.1	0.7

The identified acids (Figure 7.1.) (acetic acid and formic acid) reduce their area ratio between 5 – 10 %. Regarding to alcohols (Figure 7.2.), 2-propen-1-ol and phenols tend to reduce their amount. Although this tendency it is not very pronounced, it is important due to the conversion of acids and phenols contributes to the reduction of acidity and increment of calorific value of raw bio-oil. Esterification reactions might take place to convert acid and alcohols into esters during this upgrading process, as it is described by esterification model reaction at low temperature (353 K) and atmospheric pressure in a similar equipment as the used one in this study, although using solid acid catalysts as $SO_4^{2-}/SiO^{2-}TiO^2$ or $SO_4^{2-}/ZrO^{2-}TiO_2$ [49]. However, no significant formation of esters has been observed in the upgraded samples. What is more, the presence of esters in the raw bio-oil (methyl acetate) is reduced between 40 – 50 % of its area ratio when the upgrading process takes place, and the higher reduction of this ester is observed using 15 wt % of HZSM-5 (Figure 7.1.). The deoxygenation of acids and esters is a proposed pathway to produce long-chain aldehydes and ketones with water release at temperatures of 300 – 410 ºC [50]. In conclusion, no significant deoxygenation or esterification reactions take place during the upgrading process, owing to the negligible

increase of water content and the neither formation of aldehydes and ketones in upgraded bio-oil.

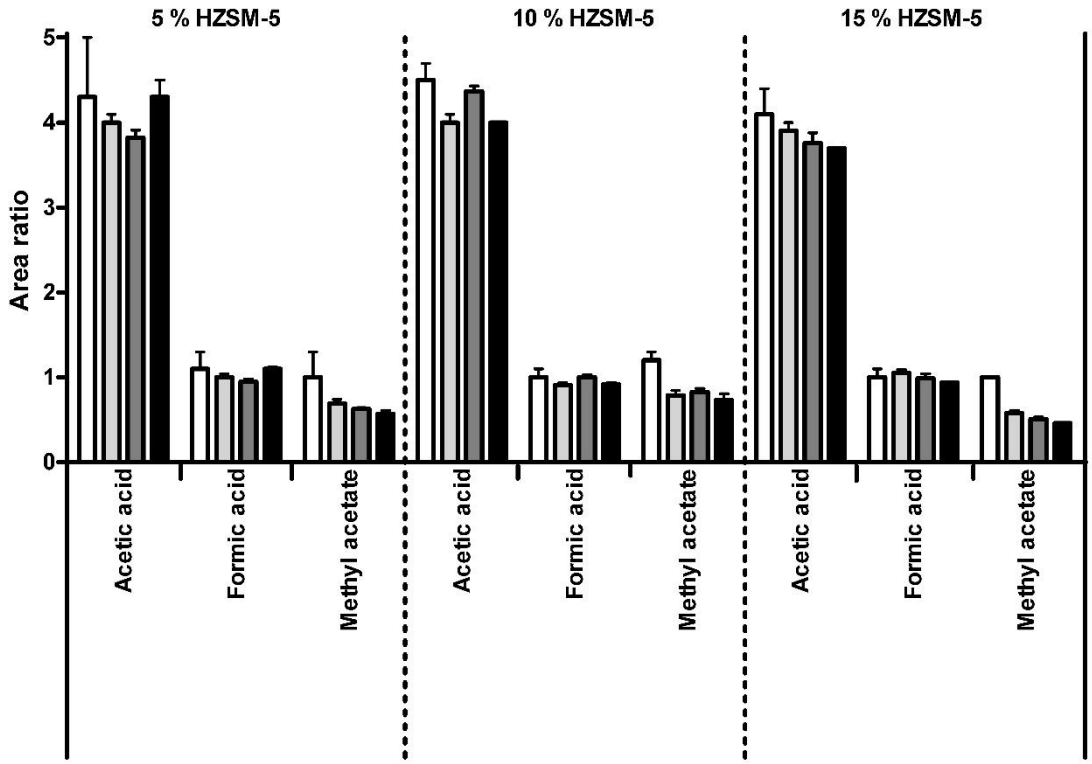

Figure 7.1. Area ratio of acid and esters through the upgrading process at 60 ºC for 5, 10, 15 wt % of HZSM-5: 0 h □, 2h ▒, 4h ▓, 6 h ■.

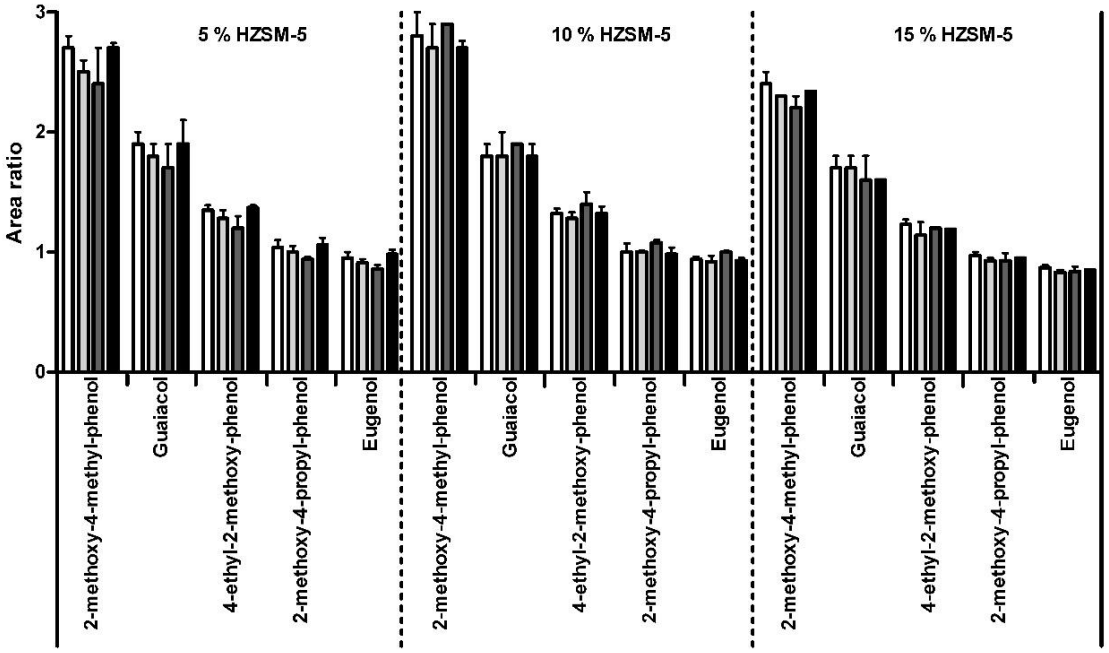

Figure 7.2. Area ratio of alcohols through the upgrading process at 60 ºC for 5, 10, 15 wt % of HZSM-5. : 0 h □, 2h □, 4h ■, 6 h ■

Regarding to aldehydes (**Figure 7.3** 7.3.), hydroxyl-acetaldehyde, furfural and vanillin (the main ones) tend to reduce their amount during the upgrading process. For example, hydroxyl-acetaldehyde reduces its amount up to a 23 % of its area ratio. Ketones (Figure 7.4.) (for instance 1-hydroxy-2-propanone, 2(5H)furanone, 2-hydoxy-3-methyl-2-cyclopenten-1-one, acetovanilline and 1-hydroxy-2-butanone) also tend to reduce their area ratio during the upgrading process. Deoxygenation and decarboxylation are the described reactions for aldehyde and ketones conversion to alkenes [50]. Besides, the polymerization of aldehydes under acidic conditions is also proposed in literature [51], as well as the condensation of some ketones by releasing water at room temperatures [45]. Although the reduction of some of these compounds is observed, no significant production of higher molecular weight compounds can be observed, and consequently, none of these reactions have an important role in the upgrading process.

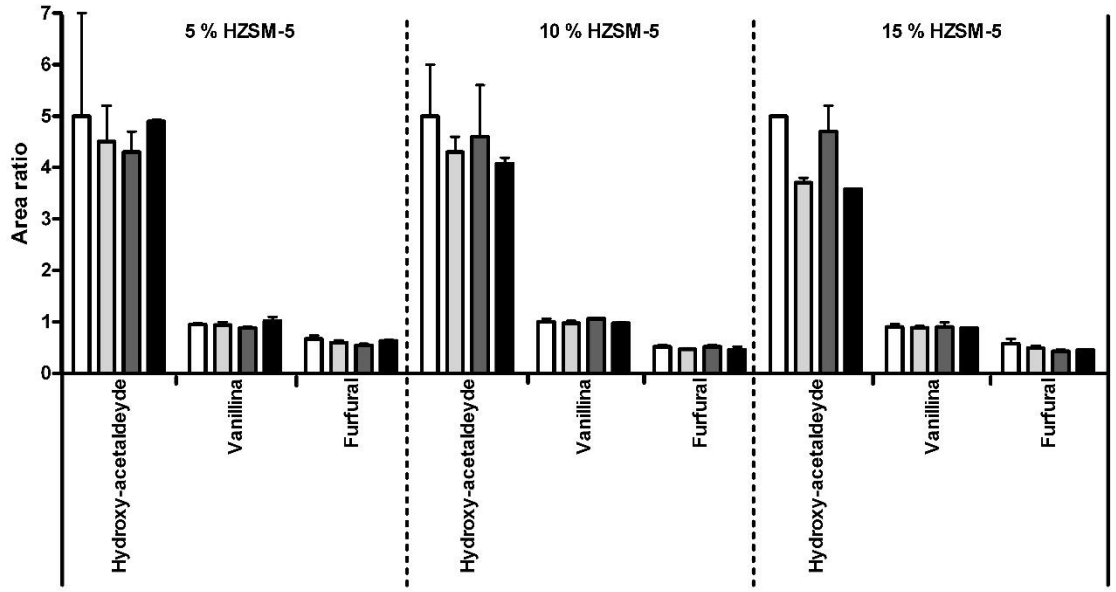

Figure 7.3. Area ratio of aldehydes through the upgrading process at 60 ºC for 5, 10, 15 wt % of HZSM-5: 0 h □, 2h □, 4h ■, 6 h ■.

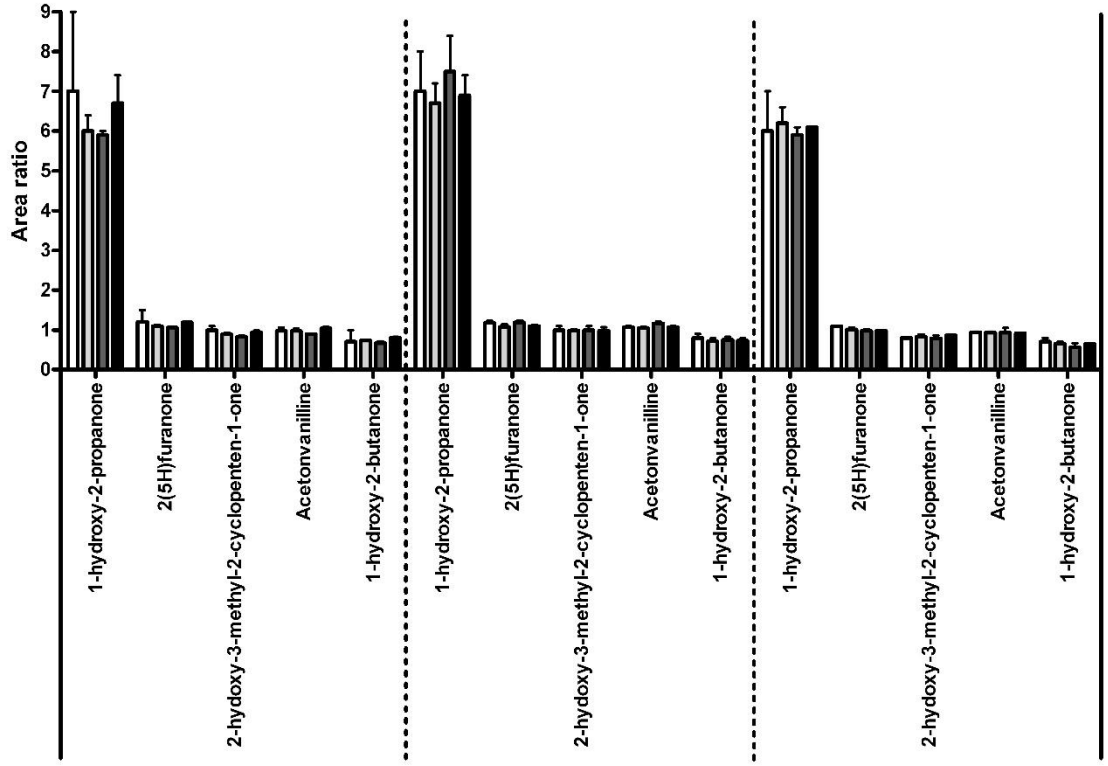

Figure 7.4. Area ratio of ketones through the upgrading process at 60 ºC for 5, 10, 15 wt % of HZSM-5: 0 h □, 2h □, 4h ■, 6 h ■.

Furthermore, no significant changes are observed in the hydrocarbon presence (Table 7.4.), cracking reactions at high temperature (370 ºC) are the responsible of hydrocarbon production [52].

As a result, it can be concluded that low temperatures might limit the influence of catalytic reactions [45]. Although HZSM-5 could catalyse reaction at low temperatures, bio-oil could blocks catalyst porous and prevents HZSM-5 catalytic capacity due to its high viscosity at 60 ºC. Thus, the reduction of bio-oil acidity might be caused by the acid-base interaction between bio-oil compounds and the catalyst acid sites. Moreover, the reduction of some bio-oil compounds might be explained by their deposit on the catalyst surface or porous and might be the potential coke precursors that cause the subsequent deactivation of the catalyst [53].

7.4. HZSM-5 time life study

The limited bio-oil upgrading might be caused by the deactivation of the catalyst over the process. To assess when the catalyst deactivation takes place, it is followed the pH changes every 15 min during the first 90 min of reaction time, as it has been described in section 3.3.2.

For this experiment, 10 wt % of HZSM-5 to raw bio-oil in the equipped three-neck bottle flask at 60 ºC is used due to it is the most efficient weight percentage of HZSM-5 at the working conditions because it is possible to reduce the same acidity as 15 wt % and 20 wt % with less amount of HZSM-5 (Figure 7.3.). Results (Fig. 7.5.) show that bio-oil acidity reduction takes place in the first 15 min since after this time pH remains constant. Thus, it is confirmed that possible HZSM-5 deactivation at this work conditions take place in less than 15 min of reaction time since bio-oil acidity is not further reduced after this time.

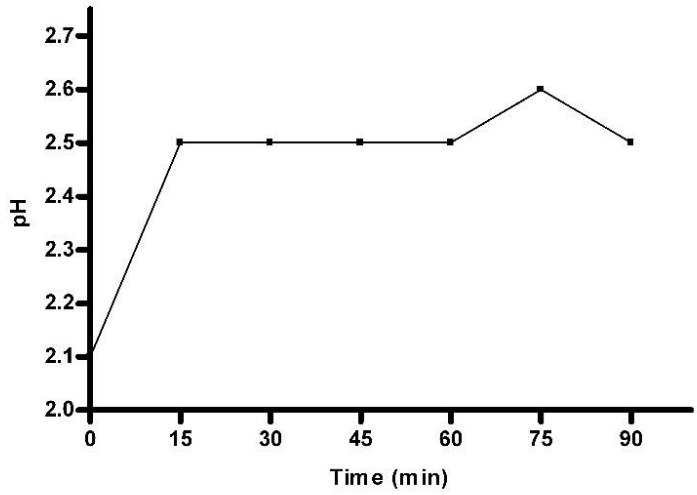

Figure 7.5. pH changes for 2 h of reaction time using 10 wt % of HZSM-5.

In order to confirm that the limited reaction is caused by the catalyst deactivation, a study of the effect of replacing the catalyst over the process is carried out. With this aim, an experiment using 10 % of HZSM-5 with consecutive replacements of HZSM-5 every 15 min is performed (see section 3.3.2). Results are shown in Table 7.7. At 15 min of reaction time, pH increases 0.7 units, TAN values decreases 6 mg KOH/g bio-oil and water content is constant. These results are consistent with the previous results obtained with 10 wt % of HZSM-5 (Table 7.3.). After 15 min of reaction time from the first HZSM-5 replacement, pH value raises 0.9 units and TAN decreases 7 mg KOH/g bio-oil. After three HZSM-5 replacements, a pH increase of 1.3 units is achieved comparing to the raw bio-oil (from 2.1 to 3.4 pH units). Once more, water content is constant through the process. Although a fourth consecutive replacement of HZSM-5 is also performed, a proper sampling was not possible due to the high viscosity of the upgraded bio-oil. Thus, replacement of HZSM-5 permits a further bio-oil acidity reduction, although this improvement is lower after each replacement in comparison to the previous one. That fact confirmed that HZSM-5 deactivation takes place at the first 15 min reaction time since after being replaced bio-oil acidity is further reduced.

Table 7.7. Effect of consecutive zeolite replacement using 10 wt % of HZSM-5 on bio-oil properties through the upgrading process at 60 ºC (* confidence interval at 95% of confidence level)

Time	pH	TAN* (mg KOH/g bio-oil)	Water* (wt %)
0 min	2.1	84 ± 4	22 ± 1
15 min	2.8	78 ± 1	23 ± 4
		zeolite replacement	
0 min	2.8	78 ± 1	23 ± 4
15 min	3.0	79 ± 3	23 ± 1
		zeolite replacement	
0 min	3.0	79 ± 3	23 ± 1
15 min	3.2	79 ± 3	22 ± 2
		zeolite replacement	
0 min	3.2	79 ± 3	22 ± 2
15 min	3.4	80 ± 1	22 ± 4

Since it is assumed that an acid-base reaction takes place with the zeolite and the bio-oil from the GC-MS results, a bio-oil titration using a 6 M NaOH solution in methanol is carried out to assess this hypothesis. It results in a titration curve of a weak acid and a strong base because acetic acid is the main acid in bio-oil. The curve shows a rapid pH increase until pH 3.4, followed by a pH stabilization that indicates the formation of an acid buffer zone that is broken at pH 6. When comparing the results achieved with the HZSM-5 replacements, it can be observed that the pH value is 3.4, which concurs with the beginning of the buffer zone obtained in the titration curve. Thus, it can be assumed that further replacements of HZSM-5 would not allow an additional acidity reduction due to the presence of the buffer in the bio-oil solution.

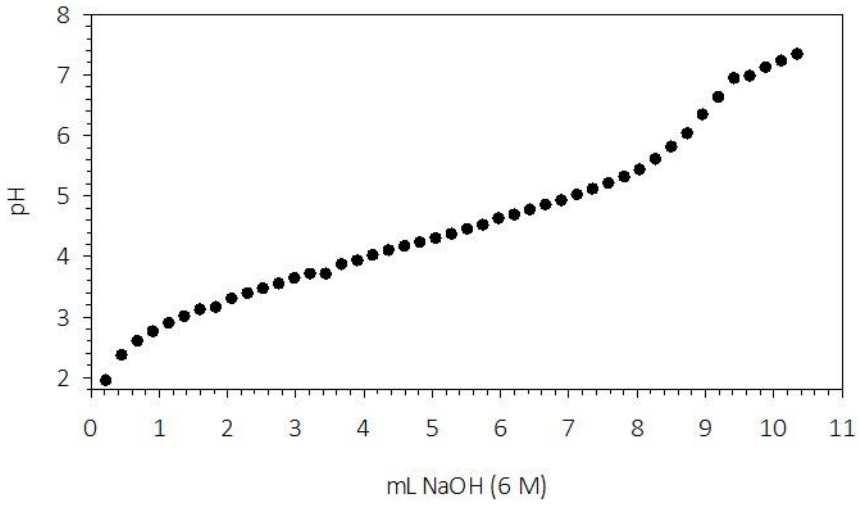

Figure 7.6. Bio-oil titration curve using NaOH (6M) solution

7.5. Conclusions of Chapter 7: reduced energy cost bio-oil catalytic upgrading process

The use of bentonites and zeolites as catalysts at 60 ºC is tested in order to reduce the economic costs of the conventional catalytic upgrading processes usually performed at 350-650 ºC, since bentonite and zeolite are low cost catalysts and operating at 60 ºC avoids the necessity of a bio-oil external heating since it is the bio-oil temperature at the outlet of the fast pyrolysis process. Different concentrations of catalyst are tested at this operational conditions permitting to reduce bio-oil acidity and, consequently, its associated negative effects on bio-oil for its uses as a biofuel to generate energy and heat with conventional devices. Comparing the different concentrations of the catalysts tested, 15 wt % of bentonite and 10 wt % of HZSM-5 are the most effective amounts of catalyst, increasing bio-oil pH value from 2.1 to 2.6 – 2.7 and reducing TAN from 81 to 75 and from 78 to 75 mg KOH /g bio-oil, respectively. Therefore, HZSM-5 is more efficient catalyst due to fewer amounts are required to obtain higher acidity reduction, although bentonites are cheaper and more environmental friendly catalyst due to its a high abundant natural origin product.

In order to study the possible reaction pathways that provoke this acidity reduction, a GC-MS analysis of HZSM-5 treated bio-oil is performed. It is observed a reduction of some oxygenated compounds such as acids, alcohols and aldehydes and no significant changes in hydrocarbon and sugar content are noted. However, non-detected formation of new compounds and no significant changes in water content suggest that low temperatures limit the influence of catalytic reactions. Thus, the acidity reduction might be caused by the acid-base interaction or adsorption of bio-oil compounds to the catalyst causing an earlier deactivation of the catalyst.

Moreover, HZSM-5 possible deactivation is assessed by means of the replacement of the catalyst every 15 min of reaction time since after 15 min of reaction time non acidity reduction is observed under the working conditions applied. After three catalyst replacement, further acidity enhancement of 1.3 pH units are obtained. Further replacements of HZSM-5 would not allow an additional acidity reduction owing to the presence of a buffer in the bio-oil solution.

To sum up, both catalyst operating at the tested conditions reduces bio-oil acidity, although operational temperatures of 60 ºC provoke a quick deactivation of the catalyst hindering its catalytic function. Because of that, it is necessary to find other bio-oil upgrading processes to enhance bio-oil properties using reduced energetic cost upgrading processes. Moving to this direction, in the following chapter, different hydrogenation processes are tested at ambient temperature and atmospheric pressure to reduce the economic costs of the conventional hydrotreating processes.

8. Reduced cost bio-oil hydrogenation processes

Different hydrogenation processes performed at ambient temperature and atmospheric pressure are preliminarily assessed in this chapter including molecular hydrogen and nascent hydrogen generated electrochemically and via metal oxidation. Furthermore, a more extent study of the feasibility of generating *in situ* nascent hydrogen in bio-oil by means of the oxidation of Zn metal using bio-oil as acidic medium is performed. Finally, the effect of this hydrotreating process on bio-oil properties is evaluated.

8.1. Introduction of Chapter 8: reduced cost bio-oil hydrogenation processes

Apart from catalytic cracking, one of better developed bio-oil upgrading process is bio-oil hydrogenation to reduce bio-oil oxygen content in order to enhance bio-oil properties as biofuel. Molecular hydrogen injection is extensively used to upgrade bio-oil, as it is described in Chapter 1. Hydrotreating process is usually performed at temperature between 200 - 400 ºC and pressures of 100-200 bar [13,54]. This process requires high consume of energy and high cost of hydrogen consumption. Because of that, the economic viability of the process is low. Taking into account this fact, nascent hydrogen is considered as a possible alternative to hydrogenate bio-oil at ambient temperature and atmospheric pressure, which has not yet been explored in literature.

Molecular hydrogen has a high bond energy, making it very stable and non-reactive under ambient conditions. High energy supply is needed to enable its reaction. Nascent hydrogen is hydrogen at its “moment of birth” and is considered to be especially reactive [55,56]. Nascent hydrogen is naturally produced on a metal surface upon oxidation in solution or may be electrolytically generated by the reduction of hydrogen ions on certain cathode materials [57]. Although nascent hydrogen exists transiently, its lifetime is long enough to affect chemical reactions [55,57,58]. There are different

theories to explain nascent hydrogen high reactivity [56]: 1) nascent hydrogen at the moment of liberation exists as a single atoms and hence it is more reactive; 2) The enhanced activity of nascent hydrogen is related to the size of bubbles produced. The nascent hydrogen at the moment of its liberation is in the form of very minute bubbles having a high internal pressure. The smaller the bubbles of the gas are, the greater is the pressure of hydrogen inside the bubbles, and consequently, high reducing power; 3) its activity may be explained on the basis of association of energy when electrons are transferred from metals of low electronegativity to H^+ ions in order to change its valence from +1 to 0. Moreover, molecular hydrogen has high diffusivity, it is easily ignited and it presents considerable hazards, particularly on the large scale. The use of *in situ* produced nascent hydrogen may reduce these difficulties due to no gas storage and no pressure vessels will be required.

In this thesis work, it is studied the feasibility of generate *in situ* nascent hydrogen in bio-oil by two ways: electrochemically and via metal oxidation.

Nascent hydrogen can be produced electrochemically by means of water electrolysis. Water electrolysis is the decomposition of water into H_2 and O_2 due to an electric current being passed through the water, following the reaction shown in equation 3.5. (see section 3.3.3). Thus, bio-oil water content (around 30 wt %) might be reduced at the same time nascent hydrogen is generated. What is more, this produced nascent hydrogen might simultaneously reduce bio-oil compounds and consequently bio-oil oxygen content. In this way, the main advantage of this process is the reduction of bio-oil water content simultaneously to the production of nascent hydrogen which might imply an increase of calorific value. However, electrolysis also produces oxygen gas which is not convenient for bio-oil upgrading process due to might increase bio-oil oxygen content by the oxidation of bio-oil compounds. Because of that, it is important to design an experimental methodology that permits the separation between the cathode and the anode of this redox reaction which is described in section 3.3.3.

The second commonly used method to produce nascent hydrogen is the reaction of metals, such as Mg, Al, Fe or Zn with an acid or amphoteric metals (Al and Zn) with alkali solution [55–58]. It is widely known that bio-oil is an acidic liquid with pH around 2.5 [28]. Because of that, bio-oil is expected to provide the necessary acidity to permit the metal oxidation reaction, and consequently, to generate nascent hydrogen. This method might permit the reduction of bio-oil acidity together with nascent hydrogen generation. Aluminium and Zinc are the selected metals to carry out this test. Thus, the proposed reaction to generate nascent hydrogen (H•) in bio-oil via metal oxidation are shown in equation 8.1. and 8.2. Both metals have high standard reduction potentials of – 1.68 V for aluminium and -0.76 V for zinc, which makes possible the spontaneity of the redox reaction. Moreover, Aluminium is the most abundant metal in the Earth's crust while zinc is the 24th most abundant. Both of them are extendedly used in many important industrial sectors as metallurgic, automotive sector, food industry, pharmaceutical, aerospace industry and construction sector. This fact makes both metals easily available and cheap.

$$2\,H^{+} + Zn \rightarrow Zn^{2+} + 2\,H\bullet \qquad \text{Equation 8.1.}$$

$$3\,H^{+} + Al \rightarrow Al^{3+} + 3\,H\bullet \qquad \text{Equation 8.2.}$$

The drawback of this method of producing nascent hydrogen is the metal ions release to the medium (bio-oil) which might be undesirable for bio-oil combustion.

Finally, it is also explored the possible effect of molecular hydrogen injection at ambient temperature and atmospheric pressure on bio-oil properties.

Thus, firstly four different hydrogenation processes performed at ambient temperature and atmospheric pressure are preliminarily assessed including molecular hydrogen injection directly to bio-oil and nascent hydrogen generated electrochemically and via zinc and aluminium oxidation in bio-oil.

Among them, a more extent study of the feasibility of generating *in situ* nascent hydrogen in bio-oil by means of the oxidation of Zn metal is performed. Furthermore, the effect of this hydrotreating on bio-oil properties is evaluated: firstly by the reduction of acidity by means of the consumption of bio-oil protons which is one of the challenges for the improvement of bio-oil properties and; secondly by the possible reduction of the oxygenated compounds to increase the bio-oil calorific power and its stability.

8.2. Hydrogenation processes: preliminary assessment

Results obtained from the preliminary assessment of the different hydrogenation processes are shown in this section, including molecular hydrogen and nascent hydrogen generated electrochemically and via metal oxidation.

First of all, it is assessed the feasibility of generate *in situ* nascent hydrogen in bio-oil by means of generating electrolytic hydrogen and via metal oxidation using bio-oil as acidic medium, which has not been tested before in literature.

For electrolytic nascent hydrogen generation, a platinum electrode is submerged into bio-oil which acts as a cathode. Another platinum electrode is submerged into a solution of KCl (3M) inside a syringe which behaves as anode. Both electrochemical cells are joined by a salt bridge (see section 3.3.3). When a potential of 31.6 V is applied between both electrodes, it is observed the appearance of bubbles in the anode of the electrochemical cell. They are the oxygen generated demonstrating that water electrolysis are achieved in this conditions. Hydrogen bubbles are not observed at the first moment due to the colours and viscosity of bio-oil although bio-oil foam is formed by hydrogen gas release during the first 24h of reaction time. Moreover, it is observed that after 6 h of reaction time, bio-oil is separated in two layers (organic and aqueous). Therefore, these observations indicates the production of electrolytic nascent hydrogen at the tested conditions.

Regarding to the production of nascent hydrogen via zinc oxidation using bio-oil as acidic medium, three vessels are prepared with 35 g of bio-oil in order to carry out the preliminary assessment of this system. In the first one, it is added 2.5 wt % of Al; in the second 2.5 wt % of Zn and; the last one without metal to use it as blank (see section 3.3.3.). After 44 days of reaction time, metal is separated from bio-oil and weighted. A weight reduction is observed indicating a consumption of the metal added to bio-oil probably due to its oxidation which might means the viability of this hydrogenation process.

Molecular hydrogen injection directly in bio-oil at ambient temperature and atmospheric pressure is carried out as it is described in section 3.3.3. is also carried out.

Once it is assumed that all hydrogenation processes are viable, possible bio-oil chemical composition changes are evaluated comparing raw and hydrogenated bio-oil compounds by means of a GC-MS analysis (see section 3.1.6) using 1,1,3,3-tetrahydropropane as internal standard. With this aim, the variation percentage between the area ratio relative to 1,1,3,3-tetrahydropropane of hydrogenated and raw bio-oil for each identified bio-oil compound is calculated for each hydrogenation process using Equation 8.1. Area ratio (AR) is defined as the area of the target compound relative to the area of the internal standard.

$$\%\ variance = \frac{(AR_{hydrogenated\ bio-oil}) - (AR_{raw\ bio-oil})}{(AR_{raw\ bio-oil})} \cdot 100 \qquad \text{Equation 8.1.}$$

Moreover, a t-test analysis to assess if the chemical composition change are statistical different or not is carried out. Results are shown in Table 8.1. For all the experiments, the same compounds are identified before and after the hydrogenation processes which means that there is not a noticeable formation of new compounds or they are produced in small amounts making them not detectable for GC-MS analysis. However, there is significant changes in bio-oil composition in all the considered processes as it can be observed in Table 8.1. Although these results are not decisive,

they permit to have a global idea of differences between these hydrogenation processes on bio-oil properties.

Regarding to hydrogen molecular injection experiment, 45 compounds are identified in bio-oil. Among them, 39 compounds reduce or raise their concentration in bio-oil after 5 days of reaction time. 75 compounds are identified in bio-oil hydrogenated by electrolytic hydrogen, 51 of them decrease their concentration and four increase their concentration after 6h of reaction time. Comparing both hydrogenation processes, it is observed that electrolytic hydrogen generates higher percentages of variance for half of comparable compounds. Thus, electrolytic hydrogen generated at ambient temperature and atmospheric pressure seems to have more effects on bio-oil composition.

Furthermore, it is evaluated the most effective metal to generate nascent hydrogen using bio-oil as acidic medium by means of the variation percentage of each compound using Zinc or aluminium as oxidation agent. Results show that after 44 days of reaction time, 55 compounds of the 75 identified ones reduce or raise their concentration in bio-oil when zinc metal is used. Whereas, only 77 compound undergo changes during the upgrading process using aluminium metal. Thus, bio-oil composition changes are observed after 44 days of reaction time. Therefore, these results indicate that some reactions are taking place between the metals and bio-oil at atmospheric pressure and ambient temperature, although further work is needed in order to understand the cause of this bio-oil composition changes. This composition changes might be produced by the hydrogenation of bio-oil with the produced nascent hydrogen resulting in the deoxygenation of some compounds. Also, they might be produced by a catalytic effect of the metal. Moreover, these results show that there are more bio-oil composition changes when zinc metal is used. Thus, a priori, zinc is a more efficient metal than aluminium for this process. At first, it is an unexpected results due to the reduction potential of aluminium is higher than the zinc one. However, the passivation

phenomenon of the aluminium, caused by the formation of aluminium oxide in the surface of the metal by the contact with the oxygen in the atmosphere, prevents the aluminium oxidation and consequently making aluminium less reactive than zinc. It important to highlight that zinc also undergo a passivation phenomenon, although it is not so strong.

Electrolytic hydrogen generation and nascent hydrogen generation via zinc oxidation obtained results are similar. With the obtained data, it is not possible to select which is the most effective method. However, producing nascent hydrogen via zinc oxidation is a much simpler process than electrolytic hydrogen generation to implement in an industrial process due to it only requires adding zinc pieces in a tank with a good agitation, instead of design an electrode system. Because of that, *in situ* generation of nascent hydrogen via Zn oxidation using bio-oil as acidic medium is selected to perform more extent study of nascent hydrogen production feasibility and the effect of this hydrotreating on bio-oil properties.

Table 8.1. Variation percentage of bio-oil composition between raw and treated bio-oil by hydrogenation processes. (m/z: mass to charge, RT: retention time, n. d.: no significant differences)

Compost	m/z	RT (min)	H_2	Electrolytic hydrogen	Nascent hydrogen (H·)	
					via Al oxidation	via Zn oxidation
Methyl acetate	43	9.27	-38	-25	n.d.	-25
Formic acid	46	9.22	-13	n.d.	n.d.	n.d.
1,3-cyclopentadiene	66	9.67	-18	-22	n.d.	-23
2-propen-1-ol	57	10.04	-14	-14	n.d.	n.d.
Hydroxyacetaldehyde	31	10.18	n.d.	n.d.	-13	-72
2,3-butanedione	43	10.90	-12	-12	n.d.	29
2-butanone	72	11.51	-24	-23	42	30
1,1-dimethoxy-ethane	59	22.93	-	-86	15	-70
Acetic acid	60	13.26	n.d.	n.d.	38	43
Methyl propionate	57	13.44	-	-29	n.d.	-24
2-butenal	70	14.03	n.d.	n.d.	n.d.	-39
2-propanone, 1-hydroxy	43	14.70	36	n.d.	n.d.	-30
2,2-dimethoxy-propane	73	15.55	-	-42	n.d.	n.d.
2-hexene-2-one	55	16.32	-	n.d.	n.d.	289
3-methyl-2-butanone	43	17.02	-	-	n.d.	-88
2,3-pentanedione	57	17.32	-	-16	-	-21
Propionic acid	74	19,00	-	n.d.	n.d.	n.d.
3-penten-2-one	69	21.28	-	-18	n.d.	n.d.
1-hydroxy-2-butanone	57	23.48	-	n.d.	-13	-35
Cyclopentanone	55	24.48	-	-16	n.d.	-16
2-butenoic acid	30	27,39	-	-18	-42	n.d.
2-cyclopenten-1-one	82	29.65	n.d.	n.d.	n.d.	-26
Furfural	95	30.05	-16	14	-68	-20
2(5H)furanone	55	36.06	n.d.	n.d.	n.d.	27
2,5-dimethoxy-tetrahydro-furan	101	36.53	24	-78	n.d.	-64
2-methyl-2-cyclopenten-1-one	67	37.41	-	-22	n.d.	40
1-(2-furanyl)-ethanone	95	38.01	-	-27	17	n.d.
3-methyl-2,5-furandione	68	38.41	-24	-26	13	n.d.
2,5 Hexanedione	99	38.70	-21	-15	n.d.	-44
5-methyl-2(5H)furanone	55	38.95	-	n.d.	n.d.	n.d.
2-hydroxy-1,2 cyclopenten-1-one	98	39.15	-28	-	n.d.	n.d.
1-(acetyloxy)-2-butanone	57	42.50	-	-21	n.d.	-88
3-methyl-2-cyclopenten-1-one	67	42.54	-	-23	n.d.	256
3-methyl-2(5H)-furanone	69	42.70	-	n.d.	n.d.	-21
Pentanoic acid	75	42.91	-	-88	n.d.	-18
3-methyl-dihydro-2,5-furandione	42	44.15	-	n.d.	n.d.	-37
4-oxo-pentanoic acid, methyl ester	43	44.48	-	n.d.	13	-22
Phenol	94	45.43	-	14	n.d.	n.d.
4-methyl-5H-furan-2-one	69	48.34	-25	n.d.	n.d.	-12
2-hydroxy-3-methyl-2-cyclopenten-1-one	112	49.03	-32	-17	n.d.	n.d.

.Table 8.1. (Continued) Variation percentage of bio-oil composition between raw and treated bio-oil by hydrogenation processes (m/z: mass to charge, RT: retention time, n. d.: no significant differences).

Compost	m/z	RT (min)	H_2	Electrolytic hydrogen	Nascent hydrogen (H·)	
					via Al oxidation	via Zn oxidation
2,3-dimethyl-2-cyclopenten-1-one	67	50.07	-19	-27	n.d.	35
2-methyl-phenol	107	52.03	-33	-28	n.d.	-12
Hydroxymethylcyclopropane	44	52.58	-	10	n.d.	n.d.
1-(2-furanyl)-2-hydroxy-ethanone	95	53.40	-	n.d.	n.d.	-13
4-methyl-phenol	107	53.66	-31	-27	n.d.	-23
Guaiacol	124	54.82	-25	-18	n.d.	-10
Maltol	126	56.07	-23	-15	n.d.	-46
3 ethyl-2-hydroxy-2-cyclopenten-1-one	126	57.01	-13	-19	-13	n.d.
2,4-dimethyl-phenol	107	59.72	-25	-35	n.d.	-13
2,3-dihydroxybenzaldehyde	138	60.80	-22	-20	n.d.	-14
4-ethyl-phenol	107	61.16	-	-34	n.d.	-84
2-methoxy-5-methyl-phenol	123	62.24	-21	-29	n.d.	-77
2-methoxy-4-methyl-phenol	123	63.32	-22	-30	n.d.	n.d.
3,4-anhydro-d-galactosan	71	64.03	-	n.d.	-40	n.d.
5-(hydroxymethyl)-2-Furancarboxaldehyde	126	64.01	-22	13	n.d.	-16
2,3-anydro-d-mannosan	71	65.54	-	-18	13	-16
2,4-dimethoxytoluene	109	66.57	-	-39	n.d.	58
2-ethyl-5-methy-phenol	121	66.98	-	-34	n.d.	-18
4-(2-propenyl)-phenol	134	67.46	-18	-31	n.d.	-14
3-(1-methylethyl)-2,4-pentanedione	85	68.14	-	n.d.	n.d.	-12
3-methyl-1,2-benezenediol	124	67.86	-21	-12	-	-
Hydroquinone	110	68.52	-	n.d.	-11	-11
1H-Inden-1-one, 2,3,-dihydro	104	69.63	-	-34	n.d.	n.d.
3,4-dihydroxyacetophenone	137	69.87	-	-24	n.d.	-29
4-ethyl-2-methoxy-phenol	137	69.78	-27	-31	n.d.	-14
4-methyl-1,2 benzenediol	124	69.99	-22	-15	n.d.	-15
1-(2,5-dihydrox-5-methylphenyl)-Ethanone	150	72.03	-18	-54	-11	-18
Eugenol	164	75.20	-22	-33	-12	-40
2-methoxy-4-propyl-phenol	137	76.07	-21	-37	n.d.	n.d.
4-ethyl-1,3 benzenediol	123	76.45	-22	-22	n.d.	-46
Vanillin	151	76.90	-17	-27	n.d.	-16
2-methoxy-4-(1-propenyl)-phenol (Z)	164	78.55	-20	-34	n.d.	-16
2-methoxy-4-propyl-phenol	137	80.80	-31	-15	n.d.	-14
2-methoxy-4-(1-propenyl)-phenol	164	81.25	-21	-61	n.d.	-13
Acetovanillin	151	82.79	-18	-26	-12	n.d.
D-allose	60	83.08	n.d.	n.d.	-11	n.d.
1-(4-hydroxy-3-methoxyphenyl)-2-propanone	137	85.30	-25	-21	n.d.	-

8.3. *In situ* generation of nascent hydrogen via Zn oxidation

In this section, it is showed the results obtained from the study of the feasibility to generate *in situ* nascent hydrogen via zinc metal at different experimental conditions is studied. 15 experiments are carried out with this aim using different initial weight of Zn, temperatures, stirring type and Zn metal size, as it is described in section 3.3.4. The reaction is followed by means of Zn^{2+} production during 22 days of reaction time since Zn^{2+} generated is stoichiometrically related to the nascent hydrogen produced. Furthermore, the pH changes are followed during the reaction time as an indication of the reduction of H^{+} to nascent hydrogen.

8.3.1. Zn^{2+} generation

Presence of Zn^{2+} is observed in all hydrogenated bio-oils under the different tested conditions, as it is observed in Figures 8.1, 8.2, 8.3 and 8.4. This fact demonstrates that Zn oxidation to Zn^{2+} takes place, what is more, it indicates that nascent hydrogen is produced during the process under any of the tested experimental conditions. Moreover, it is observed that Zn^{2+} concentration depends on the experimental conditions, because of that the influence of temperature, agitation, concentration of initial zinc metal and its size on the Zn^{2+} production, and consequently, nascent hydrogen generation is assessed.

The effect of the temperature can be observed in Figure 8.1. Comparing experiments carried out using 4.5 wt % of initial Zn metal of 2.5 x 8 mm and orbital stirring at 20ºC and 37ºC (Figure 8.1.c.), 60 % more mmol Zn^{2+} per gram of bio-oil are generated at 37 ºC and 6 days of reaction time than at 20 ºC and 22 days of reaction time. Therefore, a higher nascent hydrogen production at 37 ºC than at 20 ºC. Moreover, there is more reaction at 37 ºC than at 20 ºC at any of the initial weight of Zn probably due to bio-oil is less viscous at this temperature letting a better agitation, homogenization and metal-bio-oil contact.

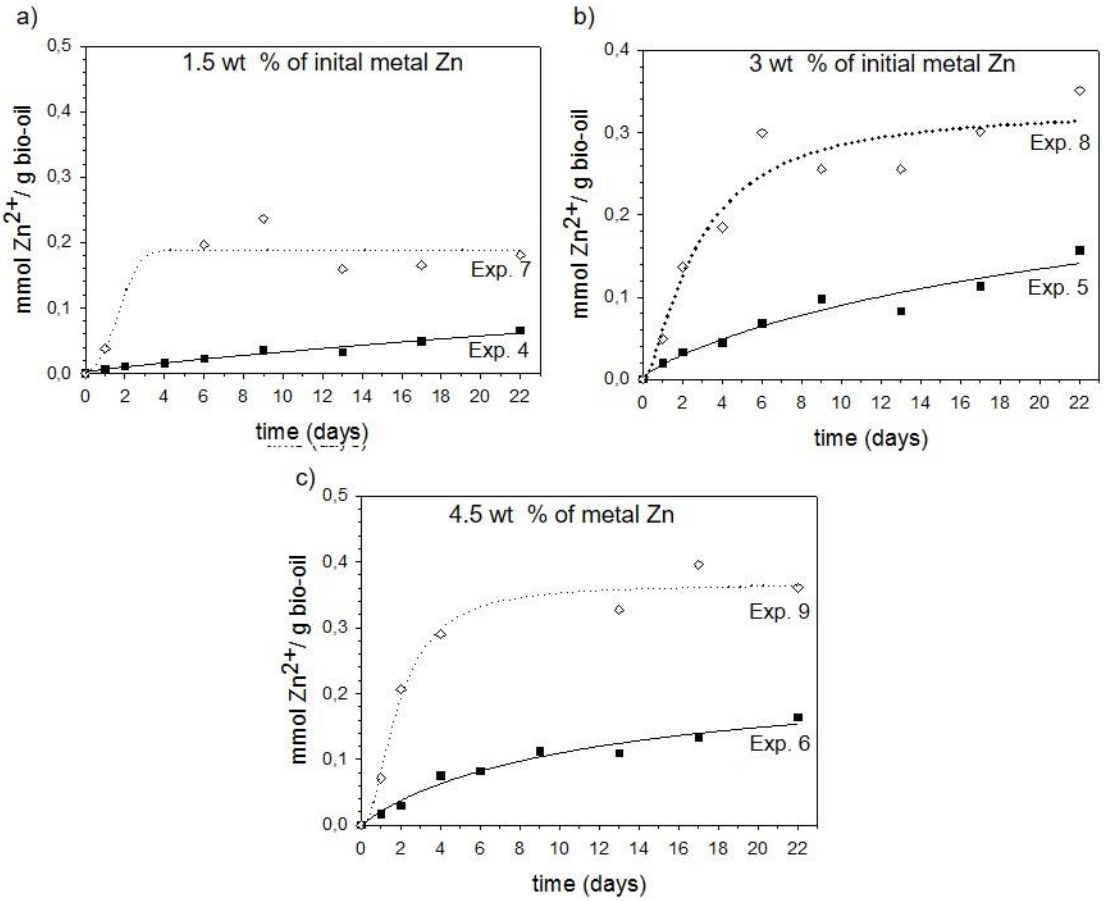

Figure 8.1. Influence of temperature on nasce0nt hydrogen production expressed as mmol Zn^{2+} per g bio-oil. Comparison of experiments carried out at 20 ºC (-■-) and 37 ºC (··◊··) using orbital stirring and zinc size of 2.5x 8 mm under different initial weights of Zn: 1,5 wt % (a), 3 wt % (b), 4,5 wt % (c).

For studying the agitation effect, firstly, experiments results obtained without stirring and with orbital stirring (Figure 8.2.a, Figure 8.2.b., Figure 8.2.c) are compared. Taking as example the experiments carried out at 20 ºC and 4.5 wt % of initial zinc metal of 2.5 x 8 mm (figure 8.2.c), experiment under orbital stirring achieves 30 % more mmol Zn^{2+} per g of bio-oil in comparison to non-stirred one, and consequently, more generation of nascent hydrogen. Secondly, experiments under orbital stirring and under rotational stirring, both carried out at 37 ºC and 4.5 wt % of initial zinc metal of 2.5 x 8 mm (figure 8.2.d) are compared. In this case, there is a higher reactivity of Zn to Zn^{2+} of a 30 % in experiment under rotational stirring in comparison to the orbital stirred one. This is because zinc metal is settled at the bottom of the vessel under orbital stirring,

provoking less bio-oil-metal contact in comparison to the rotating stirring where the zinc metal is continuously moving within the bio-oil. Thus, the better bio-oil-metal contact is, the higher is the nascent hydrogen produced. Moreover, the orbital stirring does not permit a good bio-oil homogenisation and, consequently, it is observed a fluctuating Zn^{2+} generation through the reaction time. To sum up, vertical rotational stirring achieves higher nascent hydrogen production, as well as a more homogenous process.

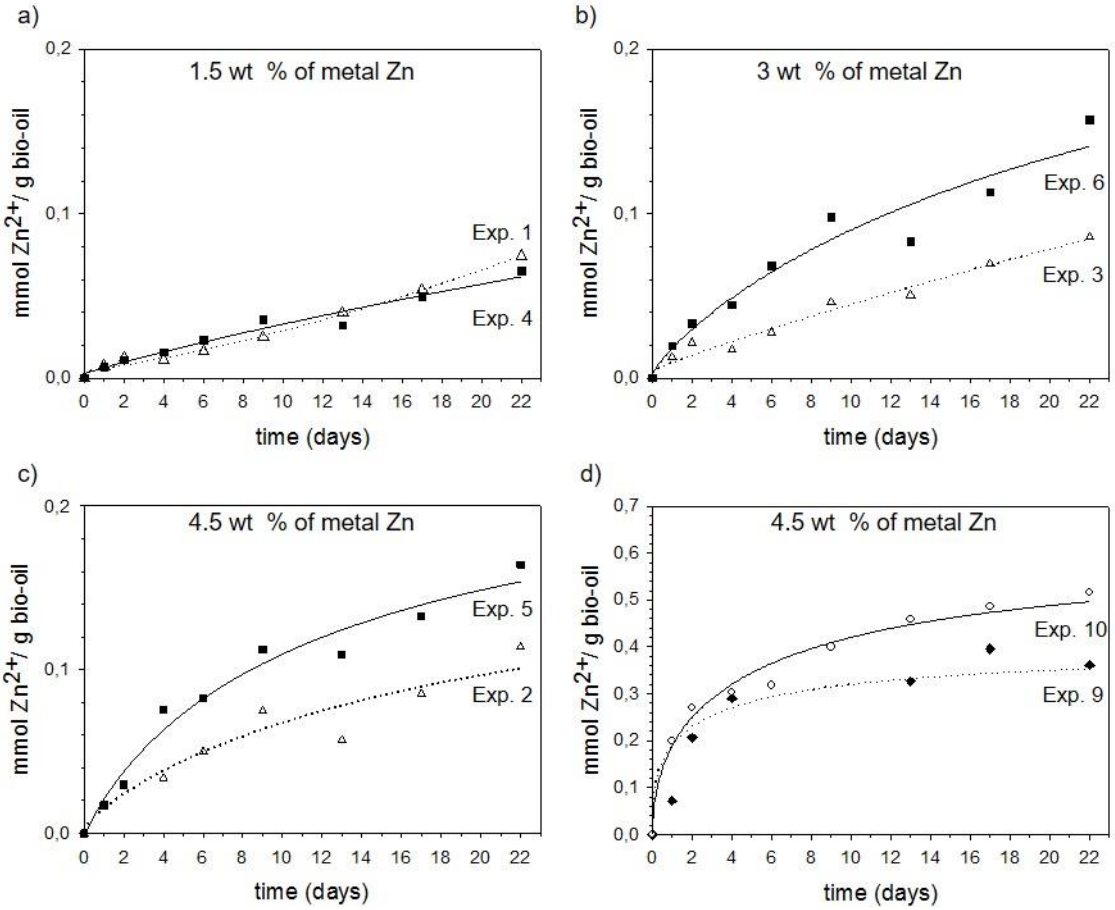

Figure 8.2. Influence of agitation on nascent hydrogen production expressed as mmol Zn^{2+} per g bio-oil. Comparison of non-stirring (··Δ··) and orbital stirring (-■-) at 20 ºC using zinc metal pieces of 2.5x 8 mm under different initial weights of initial zinc metal: 1.5 wt % (a), 3 wt % (b) and 4.5 wt %. And comparison between orbital stirring (··♦··) and rotational stirring (-o-) at 37 ºC using 4.5 wt % of initial metal zinc of 2.5x 8 mm (d).

The comparison between experiments performed at different zinc metal pieces size permits to study the effect of zinc pieces size on the reaction effectiveness (Figure

8.3.). Observing Figure 8.3.a, at the first 2 days of reaction time, there is not effect of the Zn size. However, after this time, there are more reaction when 2.5 x 8 mm Zn pieces are used. When it is compared experiments at 37 ºC and rotational stirring but with higher amount of initial Zn, it is not observed significant differences regarding to the Zn size effect. Thus, it can be concluded that there is not an influent effect of the metal pieces size due to both of them permit a good contact and homogenization.

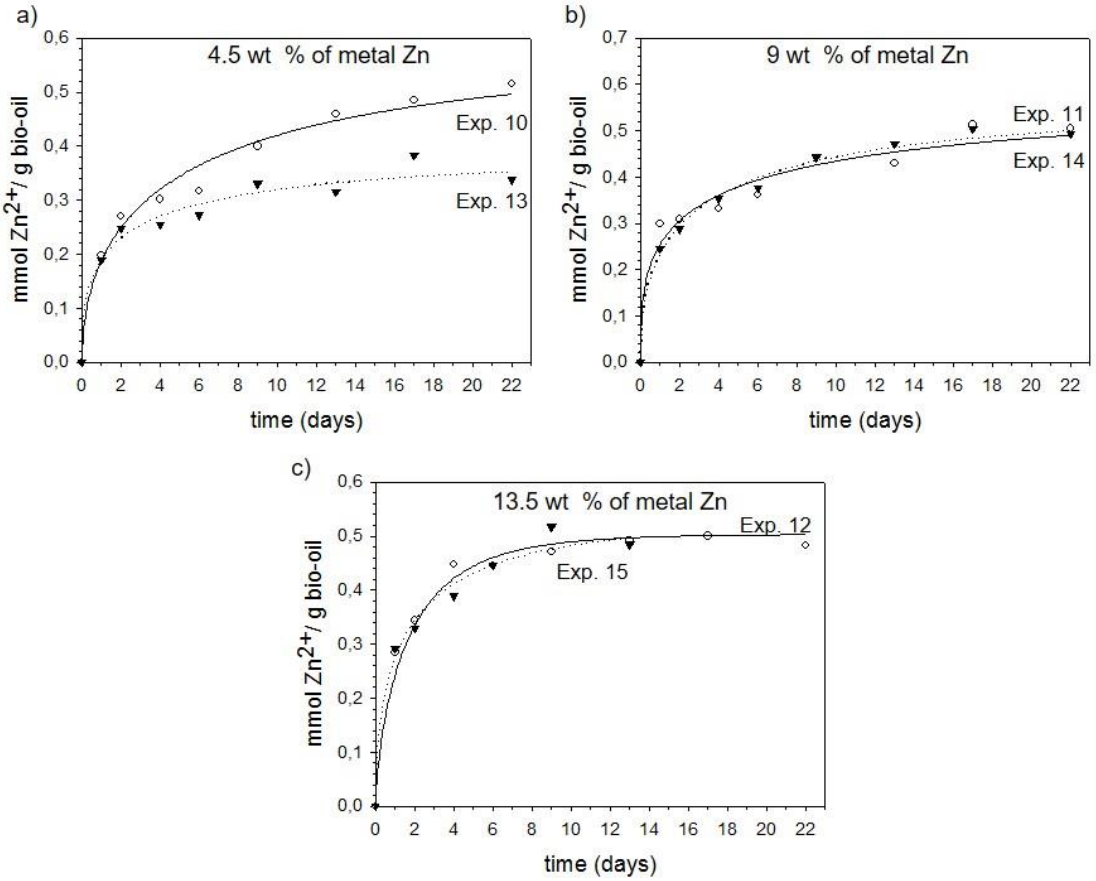

Figure 8.3. Influence of zinc metal pieces size on nascent hydrogen production expressed as mmol Zn^{2+} per g bio-oil. Comparison between using zinc metal pieces of 2.5x 8 mm (- -▼- -) and 2.5 x 80 mm (-o-) under 37 ºC, rotational stirring and different initial concentrations of zinc metal: 4.5 wt % (a), 9 wt % (b) and 13.5 wt %(c).

Finally, the effect of initial weight of zinc metal on nascent hydrogen generation is assessed. Firstly, the different initial weight of Zn are compared under 37 ºC, orbital stirring and 2.5 x 8 mm Zn pieces size (Figure 8.4 a.). Zinc ion (Zn^{2+}) production is 47 %

higher when it is used 3 wt % of initial zinc metal Zn and 153 % higher when it is used 4.5 wt % of initial zinc metal, both relative to experiments carried out using 1.5 wt % of initial zinc metal. Therefore, it can be stated that nascent hydrogen generated is increased with the initial weight of metal used. What is more, it also rises the initial velocity of reaction. Secondly, considering the experiments carried out under 37 ºC, vertical rotation shaker, 2.5 x 8 mm Zn pieces size, the generation of zinc is similar at 4.5, 9 and 13.5 wt % Zn (Figure 8.4.b), as well as similar initial velocities of reaction are achieved. Thus, weight percentages of Zn above 4.5 wt % permit a maximum nascent hydrogen production.

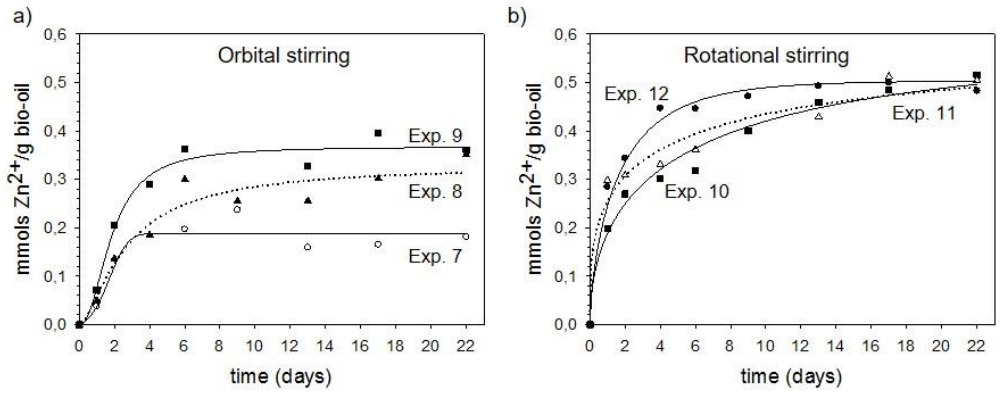

Figure 8.4. Influence of the initial amount of zinc metal on nascent hydrogen production expressed as mmol Zn^{2+} per g bio-oil. Comparison between using 1.5 wt % of initial zinc metal (-o-), 3 wt % of initial zinc metal (··▲··) 4.5 wt % of initial zinc metal (-■-), 9 wt % of initial zinc metal (··Δ··) and 13.5 wt % of initial zinc metal (-●-) under 37 ºC using zinc metal pieces of 2.5 x 8 mm and stirring types: orbital stirring (a) and rotational stirring (b)different initial concentrations of zinc metal: 4.5 wt % (a), 9 wt % (b) and 13.5 wt %(c).

To sum up, the parameter that has more influence on the nascent generation is the temperature due to it reduces bio-oil viscosity and permits a better agitation, homogenization and bio-oil metal-contact. Furthermore, a proper agitation is a crucial parameter to obtain a representative and homogenous process. A minimum of 4.5 wt % of Zn is necessary to achieve the maximum nascent hydrogen production at the tested conditions. And finally, the tested size of Zn does not have a significant influence,

although small pieces present higher reactivity since it enables higher metal-bio-oil contact.

8.3.2. pH changes

Moreover, it is observed that bio-oil pH increases at all the tested experimental conditions (Fig 8.5, 8.6, 8.7, 8.8). This pH increase is associated to H^+ reduction to H through the reaction time, reconfirming that the proposed reaction takes place at any tested conditions. What is more, this H^+ consumption reduces bio-oil acidity, which is one of the drawbacks of raw bio-oil due to the associated problems of its corrosiveness when it is applied in an engine. Moreover, it is observed that acidity reduction depends on the experimental conditions, because of that the influence of temperature, agitation, concentration of initial zinc metal and its size on the acidity reduction.

The initial weight of Zn and temperature are the most influential parameters on pH evolution, as well as for the production of Zn^{2+}. When the experiment is carried out at initial weights of Zn above 4.5 wt % (Figure 8.5.b), at 37 ºC and at any other condition the pH achieves a value of between 3.8 and 4. The reaction time needed to achieve that pH depends, basically, on the agitation (Figure 8.6.d.): 6 days when it is used orbital shaker and only 2 days with a vertical rotational shaker. At lower initial weight of Zn (below 4.5 wt %) and at 37 ºC (Figure 8.5.a), pH rises to lower values too, around 3.2. Finally, the achieved pH at 20 ºC are very low due to low reactivity of Zn at this temperature, as it is observed with Zn^{2+} production (Figure 8.7.). Taking into account the initial zinc metal pieces size, it does not have a notable influence (Figure 8.8.)

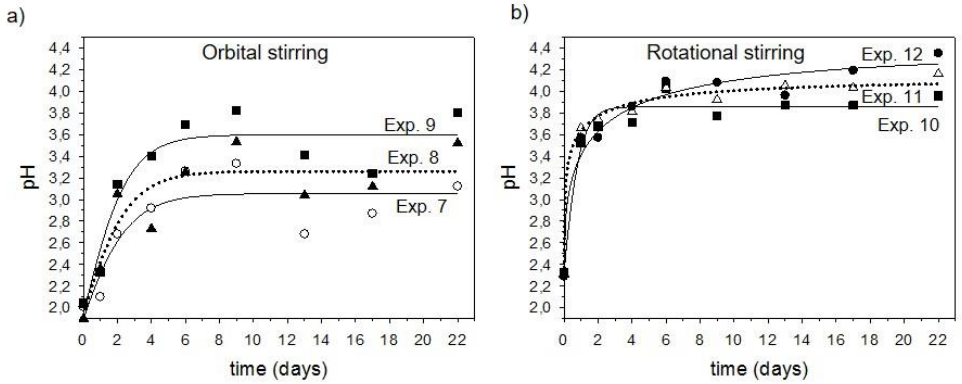

Figure 8.5. Influence of the initial amount of zinc metal on bio-oil acidity expressed as pH. Comparison of using 1.5 wt % of initial zinc metal (-o-), 3 wt % of initial zinc metal (··▲··) 4.5 wt % of initial zinc metal (-■-), 9 wt % of initial zinc metal (··Δ··) and 13.5 wt % of initial zinc metal (-●-) under 37 ºC using zinc metal pieces of 2.5 x 8 mm and stirring types: orbital stirring (a) and rotational stirring (b).

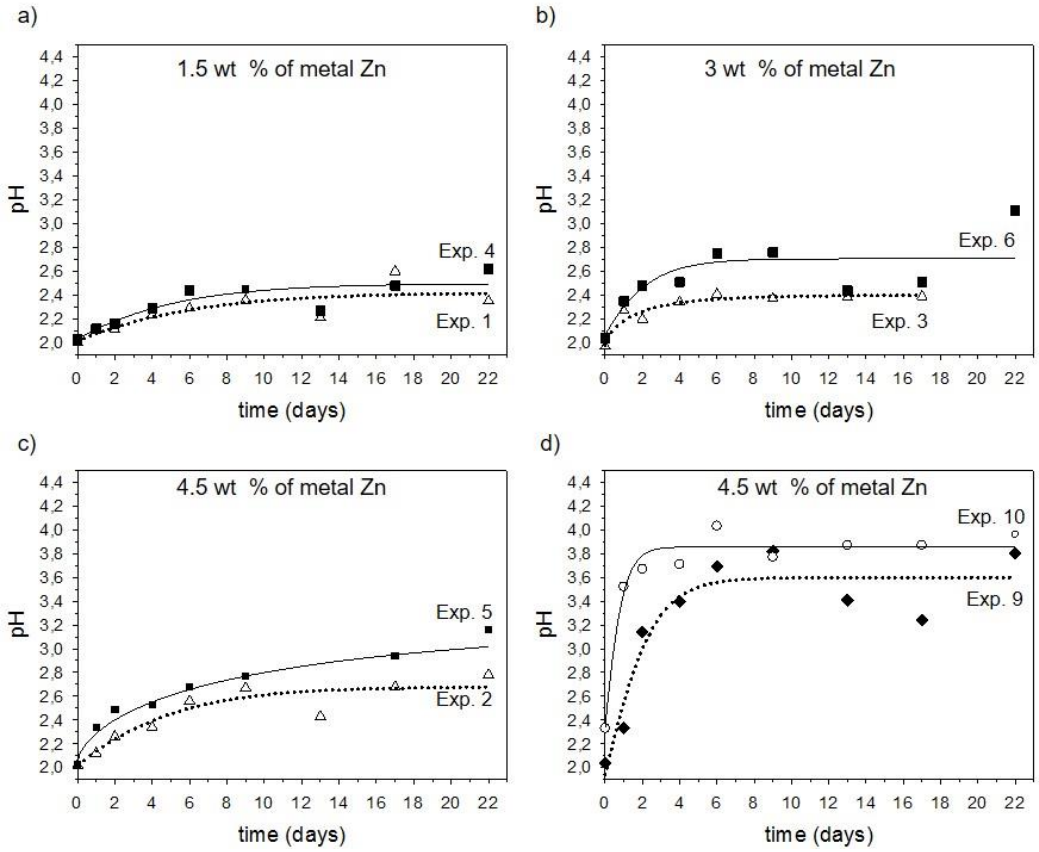

Figure 8.6. Influence of agitation on bio-oil acidity expressed as pH. Comparison of non-stirring (··Δ··) and orbital stirring (-■-) at 20 ºC using zinc metal pieces of 2.5x 8 mm with different initial weights of initial zinc metal: 1.5 wt % (a), 3 wt % (b) and 4.5 wt %. And comparison between orbital stirring (··♦··) and rotational stirring (-o-) at 37 ºC using 4.5 wt % of initial metal zinc of 2.5x 8 mm (d)

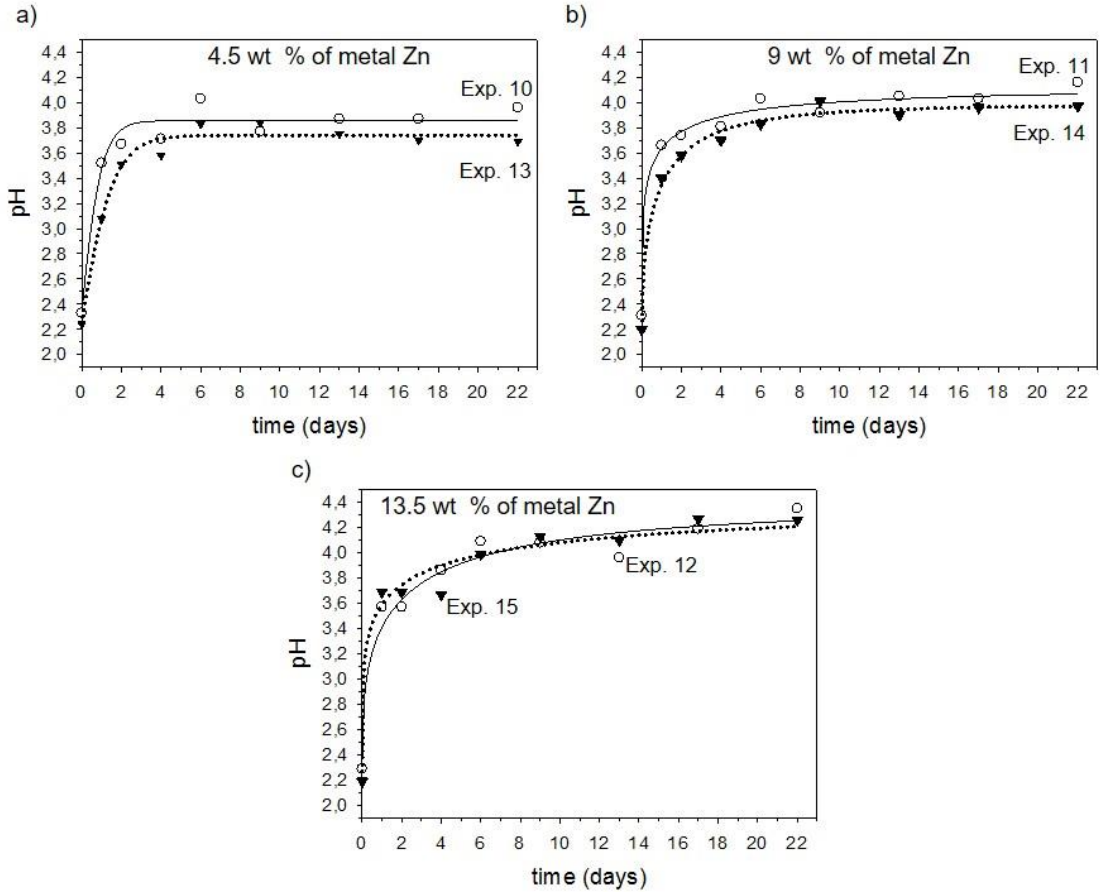

Figure 8.7. Influence of agitation on bio-oil acidity expressed as pH. Comparison of experiments carried out at 20 ºC (-■-) and 37 ºC (··◊··) using orbital stirring and zinc size of 2.5x 8 mm under different initial weights of Zn: 1,5 wt % (a), 3 wt % (b), 4,5 wt % (c).

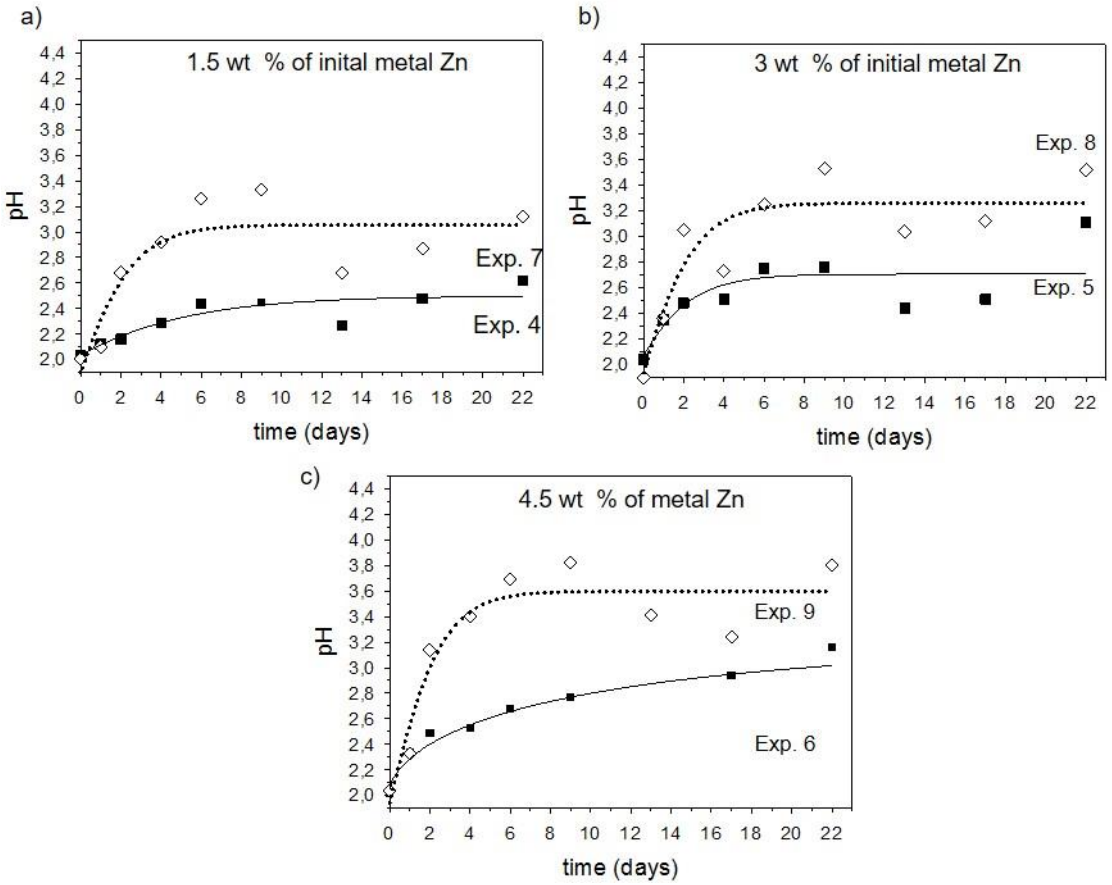

Figure 8.8. Influence of agitation on bio-oil acidity expressed as pH. Comparison of using zinc metal pieces of 2.5x 8 mm (- -▼- -) and 2.5 x 80 mm (-o-) under 37 ºC, rotational stirring and different initial concentrations of zinc metal: 4.5 wt % (a), 9 wt % (b) and 13.5 wt %(c).

8.3.3. DAN test

In this chapter, it is used Differential Acid Number (DAN) analytical method to assess bio-oil acidity changes since TAN analysis presents some problem to detect properly the final point of the titration (see section 2.1.9.). DAN is defined as the difference between the acid number of raw bio-oil ($AN_{raw\ bio\text{-}oil}$) calculated as the amount of potassium hydroxide (KOH) in mmol needed to achieve a set pH per gram of raw bio-oil and the acid number of treated bio-oil ($AN_{treated\ bio\text{-}oil}$). Thus, to define the Differential Acid Number (DAN) test is necessary to set a final point (pH). With this aim, it is performed the DAN test at different final points setted between 9 and 12, in order to

study the possible effect of the set final point on DAN values. In Figure 8.9., it is shown the result of AN $_{raw\ bio\text{-}oil}$ and AN $_{treated\ bio\text{-}oil}$, as well as the calculated DAN value at different final points (pH 9, 10, 11 and 12). pH values below 9 are not tested since it is necessary to select a high enough pH to ensure that most of acidic groups have been titrated.

Figure 8.9. Evaluation of the fixed final point for the DAN test: DAN (▼), AN raw bio-oil (●) and AN treated bio-oil (○).

As it can be observed in Figure 8.9., both $AN_{raw\ bio\text{-}oil}$ and $AN_{treated\ bio\text{-}oil}$ values increase when pH increases. This is an expected result due to the higher is the set pH, the higher is the number of titrated acidic groups. Moreover, this value does not become constant, implying that not all the acidic groups are titrated at pH 12.

Also, $AN_{raw\ bio\text{-}oil}$ value is higher than the $AN_{treated\ bio\text{-}oil}$ value, indicating that during the generation of nascent hydrogen, the number of acidic groups in bio-oil decreases. Therefore, there is a reduction of bio-oil acidity.

Finally, it is observed that DAN value is approximately constant at any of the tested set final points. Therefore, DAN value does not depend on the set pH. Because of that, it is selected pH 9 as fixed pH for all DAN measurement on this work.

8.3.4. Nascent hydrogen production under optimum tested condition.

After testing different experimental condition, it is selected 4.5 wt % of initial Zn of 2.5 x 8 mm at 37 ºC and vertical rotation stirring as the optimum tested conditions to perform a thorough and more accurate determination of nascent hydrogen production. The obtained results are shown in Figure 8.10.

Figure 8.10. DAN (-▽-), Zn^{2+} (··▲··) and pH (-o-) changes through 10 days of reaction time at 37 ºC, vertical rotation agitation, 4,5 wt % of initial Zn and 8 x 2.5 mm Zn size and pH (-●-)of the blank at the same conditions.

The obtained results are very similar to the obtained ones at the same experimental conditions (experiment 10 see Figure 8.2. and Figure 8.6.), which indicates a good reproducibility of the process.

At the first 24 hours of reaction time, there is a high and quick reaction, producing 0.22 mmol Zn^{2+}/g bio-oil which equates to 0.44 mmol/g of nascent hydrogen. After that time, the reaction continues but in a slow way. DAN values are between of 0.28 and 0.30 mmol KOH/g bio-oil after the first 24 h of reaction time. If it is considered that nascent hydrogen is produced from the reduction of H^+ of bio-oil, it was expected that DAN value

should be the double of Zn^{2+} generated because of the stoichiometry of the reaction. However, DAN value is 1.5 lower than the equivalent nascent hydrogen from Zn^{2+} generated. Thus, taking into account the stoichiometry, it is produced 1.5 times more Zn^{2+} than H^+ consumed. That might be explained if it is considered that: (1) zinc might be oxidised by some bio-oil organic compounds, not only by H^+ and (2) nascent hydrogen generated could be also oxidised to H^+ reacting with bio-oil organic compounds.

Regarding to pH, after 24 hours of reaction time, it remains constant between values of 3.6 and 3.8. For the blank (same conditions without Zn), pH value remains constant between 2.1 and 2.3 at any reaction time. Thus, it can be said, comparing this two values, that there is a reduction of bio-oil acidity of 1.5 units of pH, produced for the consumption of H^+ when they are reduced to nascent hydrogen.

Apart from the production of nascent hydrogen, it is observed the presence of part of the initial zinc metal in the vessel although the reaction stops or reduces its velocity. Furthermore, it is observed a bio-oil phase separation of the treated bio-oil after 24-48 hours of reaction time. These observations are further discussed below.

8.3.5. Influence of bio-oil acidity on nascent hydrogen generation

Despite the fact that at optimum tested conditions pH, DAN and Zn^{2+} generation are settled at 24-48 hours of reaction time, it is observed that there is presence of zinc metal in the vessel which means that not all the initial Zn is oxidised. This fact might be explained by the reduction of bio-oil acidity after 24-48 hours of reaction time. The obtained bio-oil with reduced acidity might become a non-enough acidic medium for Zn oxidation or to avoid the Zn surface passivation. To corroborate this hypothesis, an experiment carried out at optimum tested conditions for three days. After that time, concentrated acid is added to bio-oil in order to recover the raw bio-oil acidity and hold for 5 extra days (see section 3.3.4.). Moreover, a blank experiment is carried out under the same conditions without acid addition. Results are shown in Table 8.2.

Table 8.2. pH and Zn^{2+} (mmol Zn^{2+}/g bio-oil) changes at 0,3, 6 and 8 days of reaction time for acid addition experiment and the blank. (*) before/ after acid addition.

	pH				Zn^{2+} (mmol Zn^{2+}/g bio-oil)
Reaction time (days)	0	3	6	8	6
Blank experiment	2.2	3.7	-	-	0.32
Acid addition experiment	2.2	3.6 /2.1 (*)	3.2	3.7	0.43

It is important to notice that pH and Zn^{2+} obtained values in blank experiment are consistent with the obtained once with the same conditions (Figure 8.4.). Secondly, the fact that pH is recovered to values of 3.7 after acid addition might be attributed to a reactivation of the reaction due to there is proton consumption, and consequently, oxidation of Zn and generation of nascent hydrogen. What is more, it is observed that Zn^{2+} generation is 25 % higher after acid addition in comparison to the blank. Finally, it is observed that this reactivation is slower than the initial one because is needed more reaction time to achieve the same pH (from 3 to 5 days).

8.3.6. Phase separation influence on ion zinc distribution

After some reaction time (24-48 h), the samples are less homogeneous and it is observed a phase separation and solid particles at the bottom of the vessel when the sample rest for few minutes. These phenomena are described in bibliography with hydrogenation processes at high temperatures (250-350 ºC) and pressure (100-200 bar). Conventional bio-oil hydrogenation process, generally, results in the formation of two liquid phases after reaction, a yellowish water phase and a brown oil phase with a density higher than that of the water phase [54]. In addition, in hydrogenation processes, charring or coking of bio-oil occurs due to repolymerization reaction [59]. This undesirable reaction becomes more significant at low temperatures and when non-catalyst is used [60]. Other possibility for the solid precipitate, it is the formation of zinc acetate. During the process, Zn^{2+} is generated together with acetic acid present in bio-oil which might form zinc acetate. The salt presence might also assist the phase

separation due to it is known that salts might break the weak balance resulting in a phase separation [18,61]

Phase separation might present some advantages for this process. The presence of Zn^{2+} in the treated bio-oil is undesirable to use it as liquid fuel. Zn^{2+}, as an ion, has more affinity for the water phase which can be separated and treated separately while the oil phase might contain a higher calorific power due to the reduction of water content.

To separate the phases and determine the zinc distribution of each phase, it is run an experiment under optimum tested conditions and 7 days of reaction time (see section 3.3.4.). The obtained results are 3.89 wt % of Zn^{2+} in water phase and 1.23 wt % of Zn^{2+} in oil phase. Although most of Zn^{2+} is in the water phase, its presence in oil phase is not insignificant. Because of that, a liquid-liquid extraction of Zn^{2+} in the oil phase is carried out resulting in a 0.23 wt % of Zn^{2+} in the oil phase. That suppose 81 % of reduction of Zn^{2+} content in this oil phase obtaining an oil phase with low content of Zn^{2+} which might be combusted as a fuel.

8.3.7. Influence of nascent hydrogen generated on bio-oil properties

Apart from the reduction of bio-oil acidity, the possible bio-oil chemical changes produced by the nascent hydrogen generated by means of GC-MS, elemental composition and high heating value are addressed.

The chemical composition of raw bio-oil and treated bio-oil at different reaction time is analysed by means of a GC-MS analysis using 1,1,3,3-tetrahydroxypropane as internal standard (see section 3.1.6). To carry out the comparison between treated and raw bio-oil, it is calculated the percentage of variance between the area ratio relative to 1,1,3,3-tetrahydroxypropane for each compound at determined reaction time (t_x) and the area ratio relative to 1,1,3,3-tetrahydroxypropane for each compound in raw bio-

oil, following the Equation 8.1. Area ratio (AR) is defined as the area of the target compound relative to the area of the internal standard.

$$\%\ variance = \frac{(AR_{treated\ bio-oil})t_x - (AR_{raw\ bio-oil})}{(AR_{raw\ bio-oil})} \cdot 100 \qquad \text{Equation 8.1.}$$

Moreover, the chemical composition of treated bio-oil is compared to raw bio-oil composition by One Way Variance Analysis at all reaction times to assess if the chemical changes are significant different.

Table 8.3 shows the obtained results. A total of 129 compounds among the more than 200 detected are identified by a probability match > 800 by comparison with spectra from the NIST mass spectral library in raw bio-oil and treated bio-oil at any reaction time. Although the same compounds are identified in treated bio-oil, there is a variation on the area ratio of some compounds comparing treated and raw bio-oil.

Table 8.3. Bio-oil chemical compounds ordered by area ratio (AR) with it confidence interval (CI) and percentage of variance at each reaction time relative to initial time (m/z: quantifying mass-to-charge ratio).

Compost		Time (hours)								
		0	48		96		144		240	
	m/z	AR ± CI	AR ± CI	% var.	AR ± CI	% var.	AR ± CI	% var.	AR ± CI	% var.
1-hydroxy-2-propanone	43	21 ± 2	13 ± 3	-41	12 ± 2	-43	10 ± 1	-51	10 ± 4	-54
Hydroxyacetaldehyde	32	6.6 ± 0.7	4 ± 2	-45	4 ± 2	-39	2.1 ± 0.4	-69	2.0 ± 0.4	-69
D-allose	60	5.0 ± 0.9	6 ± 1	12	6.4 ± 0.9	28	6.6 ± 0.4	32	7.0 ± 0.4	40
Methyl acetate	43	3.0 ± 0.2	3.5 ± 0.2	16	4.5 ± 0.9	49	4.5 ± 0.9	46	4.8 ± 0.8	59
Acetic acid ethenyl ester	43	2.6 ± 0.9	1.6 ± 0.3	-39	1.9 ± 0.6	-26	1.5 ± 0.1	-43	1.1 ± 0.4	-58
Acetic acid	60	2.1 ± 0.2	2.6 ± 0.1	24	3.4 ± 0.5	59	3.4 ± 0.6	60	3.5 ± 0.3	64
1-(acetyloxy)-2-propanone	43	1.8 ± 0.2	1.5 ± 0.6	-19	1.6 ± 0.6	-13	1.5 ± 0.6	-17	1.9 ± 0.6	4
1.1-dimethoxy-ethane	59	1.07 ± 0.06	0.55 ± 0.02	-48	0.6 ± 0.1	-45	0.45 ± 0.09	-57	0.34 ± 0.02	-68
1.1-dimethoxy-hexane	75	0.90 ± 0.02	0.045 ± 0.003	-95	0.03 ± 0.01	-96	0.035 ± 0.002	-96	0.03 ± 0.01	-97
2(5H)furanone	55	0.75 ± 0.05	0.6 ± 0.2	-23	0.63 ± 0.07	-16	0.7 ± 0.1	-10	0.6 ± 0.1	-24
Formic acid	46	0.7 ± 0.2	1.6 ± 0.4	134	1.9 ± 0.2	179	2.6 ± 0.5	282	2.3 ± 0.4	237
2-2-ethoxy-1-methoxyethyl-furan	111	0.63 ± 0.06	0.082 ± 0.003	-87	0.06 ± 0.02	-91	0.04 ± 0.01	-93	0.03 ± 0.01	-95
1.2-benzenediol	110	0.59 ± 0.06	0.54 ± 0.05	-9	0.6 ± 0.1	7	0.73 ± 0.08	23	0.71 ± 0.01	19
1.1.1-trimethoxy-ethane	89	0.6 ± 0.2	0.16 ± 0.04	-74	0.15 ± 0.03	-75	0.06 ± 0.02	-90	0.07 ± 0.02	-88
Hydroxymethylcyclopropane	44	0.5 ± 0.1	0.8 ± 0.1	65	0.94 ± 0.05	101	1.09 ± 0.04	132	1.17 ± 0.09	150
2-methoxy-4-methyl-phenol	123	0.41 ± 0.03	0.39 ± 0.04	-5	0.45 ± 0.06	10	0.52 ± 0.05	26	0.52 ± 0.04	25
2-methoxy-phenol	124	0.33 ± 0.03	0.30 ± 0.03	-8	0.34 ± 0.04	4	0.38 ± 0.02	18	0.36 ± 0.06	12
2.5-dimethoxy-tetrahydro-furan	101	0.29 ± 0.02	0.09 ± 0.01	-70	0.09 ± 0.01	-69	0.07 ± 0.01	-75	0.055 ± 0.003	-81
3-butoxy-2-methyl-1-butene	71	0.28 ± 0.02	0.28 ± 0.05	2	0.31 ± 0.04	11	0.37 ± 0.05	33	0.37 ± 0.03	32
2.2-dimethoxy-ethanol	75	0.27 ± 0.04	0.04 ± 0.01	-84	0.036 ± 0.004	-87	0.03 ± 0.01	-89	0.03 ± 0.01	-89
1-hydroxy-2-butanone	57	0.26 ± 0.05	0.15 ± 0.03	-41	0.11 ± 0.01	-56	0.14 ± 0.03	-47	0.12 ± 0.05	-53
2-hydroxy-3-methyl-2-cyclopenten-1-one	112	0.24 ± 0.01	0.17 ± 0.02	-28	0.15 ± 0.03	-36	0.164 ± 0.005	-32	0.15 ± 0.02	-39
4-penten-2-one	43	0.23 ± 0.04	0.30 ± 0.09	31	0.4 ± 0.1	79	0.42 ± 0.08	80	0.48 ± 0.05	105
4-methyl-5H-furan-2-one	69	0.21 ± 0.03	0.187 ± 0.004	-11	0.20 ± 0.03	-2	0.22 ± 0.03	6	0.20 ± 0.04	-4
Acetaldehyde	44	0.21 ± 0.02	0.17 ± 0.02	-19	0.17 ± 0.03	-21	0.17 ± 0.03	-18	0.16 ± 0.05	-23

Table 8.3. (Continued) Bio-oil chemical compounds ordered by area ratio (AR) with its confidence interval (CI) and percentage of variance at each reaction time relative to initial time (m/z: quantifying mass-to-charge ratio).

Compost		Time (h)								
		0	48		96		144		240	
	m/z	AR ± IC	AR ± CI	% var.	AR ± CI	% var.	AR ± CI	% var.	AR ± CI	% var.
3-methyl-3-buten-2-one	41	0.20 ± 0.01	0.044 ± 0.003	-78	0.05 ± 0.01	-74	0.06 ± 0.01	-69	0.05 ± 0.02	-75
4-ethyl-2-methoxyphenol	137	0.19 ± 0.02	0.17 ± 0.04	-6	0.21 ± 0.03	13	0.25 ± 0.03	32	0.25 ± 0.02	32
Tetrahydrol-2-furanmethol	71	0.18 ± 0.02	0.06 ± 0.01	-68	0.06 ± 0.02	-66	0.06 ± 0.01	-65	0.056 ± 0.003	-69
4-hydroxy-3-methoxy-benzeneacetic acid	137	0.17 ± 0.04	0.19 ± 0.02	10	0.22 ± 0.06	26	0.25 ± 0.01	43	0.25 ± 0.02	47
Vanillin	151	0.17 ± 0.03	0.17 ± 0.02	2	0.20 ± 0.04	18	0.23 ± 0.02	38	0.22 ± 0.03	31
4-methyl-4-penten-2-one	43	0.16 ± 0.01	0.22 ± 0.04	37	0.26 ± 0.08	61	0.30 ± 0.03	84	0.31 ± 0.05	91
1.3-dioxan-5-ol	45	0.16 ± 0.01	0.16 ± 0.04	4	0.14 ± 0.02	-11	0.18 ± 0.03	13	0.17 ± 0.03	7
4-methyl-1.2 benzenediol	124	0.15 ± 0.02	0.13 ± 0.02	-12	0.16 ± 0.03	5	0.18 ± 0.03	20	0.17 ± 0.01	14
1.1-dimethoxy-propane	75	0.14 ± 0.01	0.051 ± 0.002	-64	0.05 ± 0.01	-63	0.048 ± 0.003	-67	0.038 ± 0.004	-73
2-cyclopenten-1-one	82	0.14 ± 0.01	0.127 ± 0.03	-9	0.14 ± 0.01	3	0.16 ± 0.01	14	0.13 ± 0.02	-5
Acetovanilline	151	0.14 ± 0.03	0.13 ± 0.02	-2	0.16 ± 0.02	18	0.19 ± 0.01	40	0.19 ± 0.01	40
2-propanol	45	0.14 ± 0.01	0.18 ± 0.04	35	0.22 ± 0.07	61	0.23 ± 0.05	73	0.24 ± 0.01	77
3-hydroxy-2-butanone	45	0.02	0.4 ± 0.01	166	0.3 ± 0.1	157	0.47 ± 0.04	251	0.5 ± 0.1	297
Furfural	95	0.13 ± 0.01	0.044 ± 0.004	-66	0.05 ± 0.01	-65	0.03 ± 0.01	-74	0.029 ± 0.001	-77
Butanoic acid	60	0.13 ± 0.01	0.13 ± 0.01	2	0.14 ± 0.03	11	0.14 ± 0.01	12	0.14 ± 0.04	6
Phenol	94	0.12 ± 0.01	0.11 ± 0.01	-11	0.118 ± 0.001	-4	0.14 ± 0.01	16	0.12 ± 0.02	0
1-(4-hydroxy-3-methoxyphenyl)-2-propanone	137	0.12 ± 0.02	0.11 ± 0.03	-7	0.14 ± 0.02	16	0.16 ± 0.01	36	0.17 ± 0.01	40
Propanoic acid	74	0.12 ± 0.02	0.13 ± 0.02	10	0.16 ± 0.01	34	0.17 ± 0.01	42	0.16 ± 0.03	36
4-methyl-phenol	107	0.11 ± 0.01	0.10 ± 0.01	-9	0.12 ± 0.01	3	0.14 ± 0.02	21	0.13 ± 0.01	13
2-methyl-2-cyclopenten-1-one	67	0.11 ± 0.01	0.11 ± 0.02	-3	0.14 ± 0.01	22	0.14 ± 0.02	21	0.13 ± 0.02	12
2-methoxy-4-(1-propenyl)-phenol	164	0.11 ± 0.02	0.10 ± 0.03	-8	0.12 ± 0.01	10	0.14 ± 0.01	24	0.13 ± 0.01	18
4-ethyl-1.3 benzenediol	123	0.11 ± 0.01	0.10 ± 0.02	-9	0.12 ± 0.03	9	0.14 ± 0.02	31	0.134 ± 0.004	27
2.3-dimethyl-butane	71	0.10 ± 0.01	0.08 ± 0.01	-12	0.10 ± 0.01	0	0.09 ± 0.01	-4	0.09 ± 0.01	-5
5-methyl-2(5H)furanone	55	0.09 ± 0.01	0.10 ± 0.02	2	0.10 ± 0.02	5	0.13 ± 0.03	34	0.12 ± 0.01	22
2.5-dihydro-furan	42	0.09 ± 0.03	0.06 ± 0.02	-39	0.06 ± 0.02	-38	n.d	-100	n.d	-100

Table 8.3. (Continued) Bio-oil chemical compounds ordered by area ratio (AR) with it confidence interval (CI) and percentage of variance at each reaction time relative to initial time. (m/z: quantifying mass-to-charge ratio).

Compost		Time (hours)								
		0	48		96		144		240	
	m/z	AR ± IC	AR ± IC	% var.	AR ± IC	% var.	AR ± IC	% var.	AR ± IC	% var.
3-methyl-2(5H)-furanone	69	0.09 ± 0.01	0.08 ± 0.03	-15	0.08 ± 0.01	-15	0.09 ± 0.01	-4	0.07 ± 0.02	-18
Eugenol	164	0.09 ± 0.01	0.085 ± 0.002	-2	0.10 ± 0.02	19	0.12 ± 0.01	43	0.12 ± 0.02	39
2.3-pentanedione	57	0.086 ± 0.005	0.07 ± 0.01	-23	0.07 ± 0.02	-15	0.07 ± 0.01	-18	0.08 ± 0.02	-7
4-hydroxy-2-pentanone	43	0.08 ± 0.02	0.10 ± 0.02	23	0.11 ± 0.02	37	0.12 ± 0.02	43	0.12 ± 0.01	41
2-methoxy-4-propyl-phenol	137	0.079 ± 0.002	0.08 ± 0.01	1	0.10 ± 0.02	21	0.11 ± 0.01	39	0.11 ± 0.01	36
2-hydroxy methyl propionate	45	0.08 ± 0.03	0.4 ± 0.1	394	0.4 ± 0.1	406	0.5 ± 0.2	603	0.9 ± 0.4	1014
2-propen-1-ol	57	0.074 ± 0.004	0.082 ± 0.002	10	0.11 ± 0.02	47	0.11 ± 0.03	48	0.112 ± 0.004	51
2-butanone	72	0.07 ± 0.01	0.23 ± 0.05	231	0.23 ± 0.08	235	0.24 ± 0.05	238	0.21 ± 0.07	201
3.4-hydroxy-3-methoxyphenyl-2-propenal	77	0.07 ± 0.01	0.02 ± 0.01	-71	0.02 ± 0.01	-73	0.02 ± 0.01	-73	0.01 ± 0.01	-81
Hexanoic acid	60	0.069 ± 0.003	0.02 ± 0.01	-70	0.02 ± 0.01	-69	0.026 ± 0.005	-62	0.02 ± 0.01	-75
2-hydroxy-1.2 cyclopenten-1-one	98	0.07 ± 0.01	0.06 ± 0.01	-10	0.072 ± 0.003	8	0.083 ± 0.001	25	0.079 ± 0.004	18
2.2-dimethoxy-propane	73	0.063 ± 0.003	0.01 ± 0.01	-90	0.009 ± 0.002	-86	0.009 ± 0.003	-86	0.006 ± 0.002	-91
3-methyl-1.2-benezenediol	124	0.063 ± 0.004	0.064 ± 0.002	1	0.08 ± 0.02	24	0.07 ± 0.02	18	0.07 ± 0.01	14
Hydroquinone	110	0.06 ± 0.01	0.06 ± 0.01	-7	0.07 ± 0.02	17	0.09 ± 0.02	42	0.086 ± 0.004	37
2-methyl-tetrahydro-2-furanol	71	0.06 ± 0.01	0.06 ± 0.01	-7	0.064 ± 0.005	7	0.078 ± 0.005	30	0.07 ± 0.01	16
Dihydro-3-methyl-2.5-furanone	42	0.06 ± 0.01	0.04 ± 0.02	-34	0.04 ± 0.01	-24	0.03 ± 0.01	-50	0.03 ± 0.01	-49
2-methoxy-vinyl-phenol	150	0.06 ± 0.03	0.15 ± 0.02	166	0.15 ± 0.01	163	0.16 ± 0.02	184	0.19 ± 0.03	222
methyl propionate	57	0.06 ± 0.01	0.06 ± 0.01	7	0.06 ± 0.01	17	0.09 ± 0.01	55	0.08 ± 0.01	49
2.3-dimethyl-2-cyclopenten-1-one	67	0.051 ± 0.005	0.06 ± 0.01	18	0.08 ± 0.02	51	0.08 ± 0.02	58	0.084 ± 0.005	64
Cyclopentanone	55	0.051 ± 0.001	0.047 ± 0.003	-8	0.05 ± 0.01	2	0.06 ± 0.01	16	0.05 ± 0.01	7
1-(acetyoxy)-2-butanone	57	0.05 ± 0.01	0.05 ± 0.02	-7	0.06 ± 0.01	23	0.07 ± 0.01	32	0.06 ± 0.02	20
2-methyl-phenol	107	0.049 ± 0.004	0.040 ± 0.004	-18	0.04 ± 0.01	-18	0.04 ± 0.01	-9	0.04 ± 0.01	-16
4-oxo-pentanoic acid	56	0.049 ± 0.001	0.04 ± 0.01	-9	0.05 ± 0.01	-4	0.05 ± 0.01	13	0.052 ± 0.001	8
3-methyl-2-cyclopenten-1-one	67	0.05 ± 0.01	0.04 ± 0.01	-7	0.05 ± 0.01	7	0.06 ± 0.01	32	0.06 ± 0.01	25
5-(hydroxymethyl)-2-furancarboxaldehyde	126	0.047 ± 0.001	0.046 ± 0.003	-3	0.05 ± 0.01	3	0.06 ± 0.01	19	0.05 ± 0.01	16

Table 8.3. (Continued). Bio-oil chemical compounds ordered by area ratio (AR) with it confidence interval (CI) and percentage of variance at each reaction time relative to initial time. (m/z: quantifying mass-to-charge ratio).

Compost		Time (hours)								
		0	48		96		144		240	
	m/z	AR ± CI	AR ± CI	% var.	AR ± CI	% var.	AR ± CI	% var.	AR ± CI	% var.
3-penten-2-one	69	0.04 ± 0.01	0.019 ± 0.003	-57	0.018 ± 0.002	-60	0.016 ± 0.003	-63	0.014 ± 0.005	-68
2.4-dimethyl-phenol	107	0.04 ± 0.01	0.045 ± 0.009	5	0.06 ± 0.01	34	0.06 ± 0.01	31	0.054 ± 0.003	26
2-(2-propenyl)-1.3-dioxolane	73	0.04 ± 0.01	0.038 ± 0.001	-9	0.04 ± 0.01	2	0.05 ± 0.01	23	0.052 ± 0.004	23
1-(2-furanyl)-2-hydroxy-ethanone	95	0.042 ± 0.004	0.05 ± 0.02	28	0.058 ± 0.002	39	0.06 ± 0.01	44	0.051 ± 0.003	23
3-methyl-4-hexene-2-one	69	0.042 ± 0.003	0.005 ± 0.010	-88	0.009 ± 0.002	-77	0.012 ± 0.003	-72	0.010 ± 0.004	-75
2-cyclopentene-1.4-dione	42	0.038 ± 0.003	0.04 ± 0.02	-8	0.043 ± 0.003	13	0.05 ± 0.02	20	0.047 ± 0.004	24
4-(3-hydroxy-1-propenyl)-2-methoxy-phenol	137	0.038 ± 0.004	0.02 ± 0.01	-48	0.017 ± 0.003	-55	0.03 ± 0.01	-25	0.01 ± 0.03	-84
3-methylene-dihydro-2.5-furandione	68	0.04 ± 0.01	0.05 ± 0.01	46	0.07 ± 0.02	73	0.07 ± 0.01	74	0.067 ± 0.004	79
2.3-pentanedione	57	0.03 ±0.01	0.020 ± 0.003	-41	0.02 ± 0.01	-31	0.020 ± 0.003	-42	0.020 ± 0.003	-41
2-propenoic acid	72	0.03 ± 0.01	0.01 ± 0.03	-63	0.020 ± 0.002	-38	0.03 ± 0.01	-16	0.03 ± 0.01	-8
Maltol	126	0.03 ± 0.01	0.019 ± 0.005	-41	0.019 ± 0.004	-41	0.019 ± 0.005	-39	0.021 ± 0.004	-35
4-ethyl-phenol	107	0.032 ± 0.003	0.021 ± 0.004	-34	0.021 ± 0.002	-34	0.03 ± 0.01	-21	0.02 ± 0.01	-30
1-(2-furanyl)-ethanone	95	0.030 ± 0.003	0.028 ± 0.005	-5	0.032 ± 0.003	9	0.039 ± 0.001	31	0.041 ± 0.004	39
1.2.6-trimethoxy-hexane	71	0.027 ± 0.003	0.032 ± 0.009	18	0.04 ± 0.01	47	0.05 ± 0.02	81	0.032 ± 0.004	17
1.3-cyclopentadiene	66	0.027 ± 0.002	0.027 ± 0.003	1	0.02 ± 0.01	-18	0.013 ± 0.005	-52	0.011 ± 0.004	-59
Tetrahydro-2-furanmethanol	71	0.023 ± 0.001	0.01 ± 0.01	-72	0.008 ± 0.002	-66	0.014 ± 0.002	-40	0.01 ± 0.01	-78
4-penten-2-ol	45	0.02 ± 0.01	0.013 ± 0.003	-42	0.012 ± 0.003	-44	0.011 ± 0.003	-52	0.007 ± 0.003	-69
3-methyl-2-butanone	41	0.021 ± 0.002	0.05 ± 0.01	133	0.04 ± 0.02	87	0.07 ± 0.02	223	0.08 ± 0.05	294
5-hexene-2-one	43	0.017 ± 0.002	0.015 ± 0.005	-11	0.02 ± 0.01	14	0.019 ± 0.004	14	0.022 ± 0.005	29
2-methoxy-6-methyl-phenol	126	0.02 ± 0.01	0.12 ± 0.01	621	0.18 ± 0.02	939	0.25 ± 0.03	1404	0.31 ± 0.09	1759
Nonanoic acid	60	0.017 ± 0.002	0.015 ± 0.004	-10	0.019 ± 0.002	13	0.02 ± 0.01	46	0.02 ± 0.01	25
3-ethyl-2-hydroxy-2-cyclopenten-1-one	126	0.015 ± 0.005	0.015 ± 0.005	5	0.014 ± 0.003	-2	0.02 ± 0.01	19	0.02 ± 0.01	20

Table 8.3. (Continued) Bio-oil chemical compounds ordered by area ratio (AR) with it confidence interval (CI) and percentage of variance at each reaction time relative to initial time. (m/z: quantifying mass-to-charge ratio).

Compost		Time (hours)								
		0	48		96		144		240	
	m/z	AR ± CI	AR ± CI	% var.	AR ± CI	% var.	AR ± CI	% var.	AR ± CI	% var.
3-methyl-2.5-furandione	68	0.014 ± 0.002	0.013 ± 0.004	-7	0.011 ± 0.001	-21	0.014 ± 0.004	2	0.012 ± 0.004	-15
2.6-dimethyl-1.4-benzenediol	138	0.012 ± 0.002	0.010 ± 0.002	-18	0.031 ± 0.008	163	0.05 ± 0.01	294	0.05 ± 0.02	314
3.4-dimethyl-2-cyclopenten-1-one	67	0.011 ± 0.004	0.01 ± 0.01	-40	0.010 ± 0.001	-7	0.0111 ± 0.0002	2	0.012 ± 0.001	11
2.3 dihydroxybenzaldehyde	138	0.011 ± 0.001	0.008 ± 0.003	-22	0.011 ± 0.003	3	0.012 ± 0.001	11	0.014 ± 0.004	31
2-methoxy-5-methyl-phenol	123	0.011 ± 0.001	0.006 ± 0.002	-41	0.006 ± 0.003	-46	0.006 ± 0.002	-39	0.005 ± 0.001	-51
4-ethyl-1.3-cyclopentanedione	126	0.009 ± 0.001	0.0086 ± 0.0003	-3	0.009 ± 0.003	6	0.012 ± 0.002	33	0.012 ± 0.002	35
vanillic acid methyl ester	151	0.008 ± 0.001	0.006 ± 0.002	-26	0.008 ± 0.001	-1	0.007 ± 0.003	-12	0.007 ± 0.003	-17
4-(2-propenyl)-phenol	134	0.008 ± 0.002	0.009 ± 0.001	22	0.009 ± 0.004	19	0.010 ± 0.002	31	0.011 ± 0.005	41
Ethyl acetate	70	0.007 ± 0.001	0.007 ± 0.002	-13	0.008 ± 0.002	6	0.009 ± 0.001	19	0.008 ± 0.002	9
2-furanaldehyde	95	0.007 ± 0.001	0.008 ±0.002	10	0.009 ± 0.001	24	0.010 ± 0.002	32	0.007 ± 0.002	0
3.4-dihydroxyacetophenone	137	0.007 ± 0.001	0.005 ± 0.002	-34	0.007 ± 0.001	-2	0.003 ± 0.006	-62	0.002 ± 0.004	-73
2.3.-dihydro-1H-Inden-1-one	104	0.0060 ± 0.0004	0.005 ± 0.002	-23	0.006 ± 0.001	6	0.007 ± 0.002	11	0.007 ± 0.001	17
2.4-dimethoxytoluene	109	0.0057 ± 0.0009	0.005 ± 0.001	-7	0.006 ± 0.001	1	0.007 ± 0.001	22	0.007 ± 0.001	23
3.5-dimethylanisole	136	0.005 ± 0.002	0.005 ± 0.001	4	0.005 ± 0.001	3	0.007 ± 0.001	40	0.007 ± 0.003	39
Butanoic acid ethenyl ester	71	0.004 ± 0.001	0.005 ± 0.001	9	0.005 ± 0.001	11	0.006 ± 0.001	45	0.005 ± 0.002	19
2-ethyl-5-methy-phenol	121	0.020 ± 0.004	0.001 ± 0.003	-97	0.001 ± 0.003	-93	n.d	-100	n.d	-100
2-butenoic acid	86	0.019 ± 0.002	0.017 ± 0.002	-6	0.020 ± 0.001	9	0.024 ± 0.003	29	0.03 ± 0.01	41
2H-pyran-2-one	68	0.017 ± 0.002	0.012 ± 0.007	-33	0.016 ± 0.002	-9	0.017 ± 0.002	1	0.018 ± 0.001	3

The percentage of variation of the area ratio of the most abundant bio-oil chemical compounds at each reaction time accordingly to the area ratio are plotted in Figure 8.11.

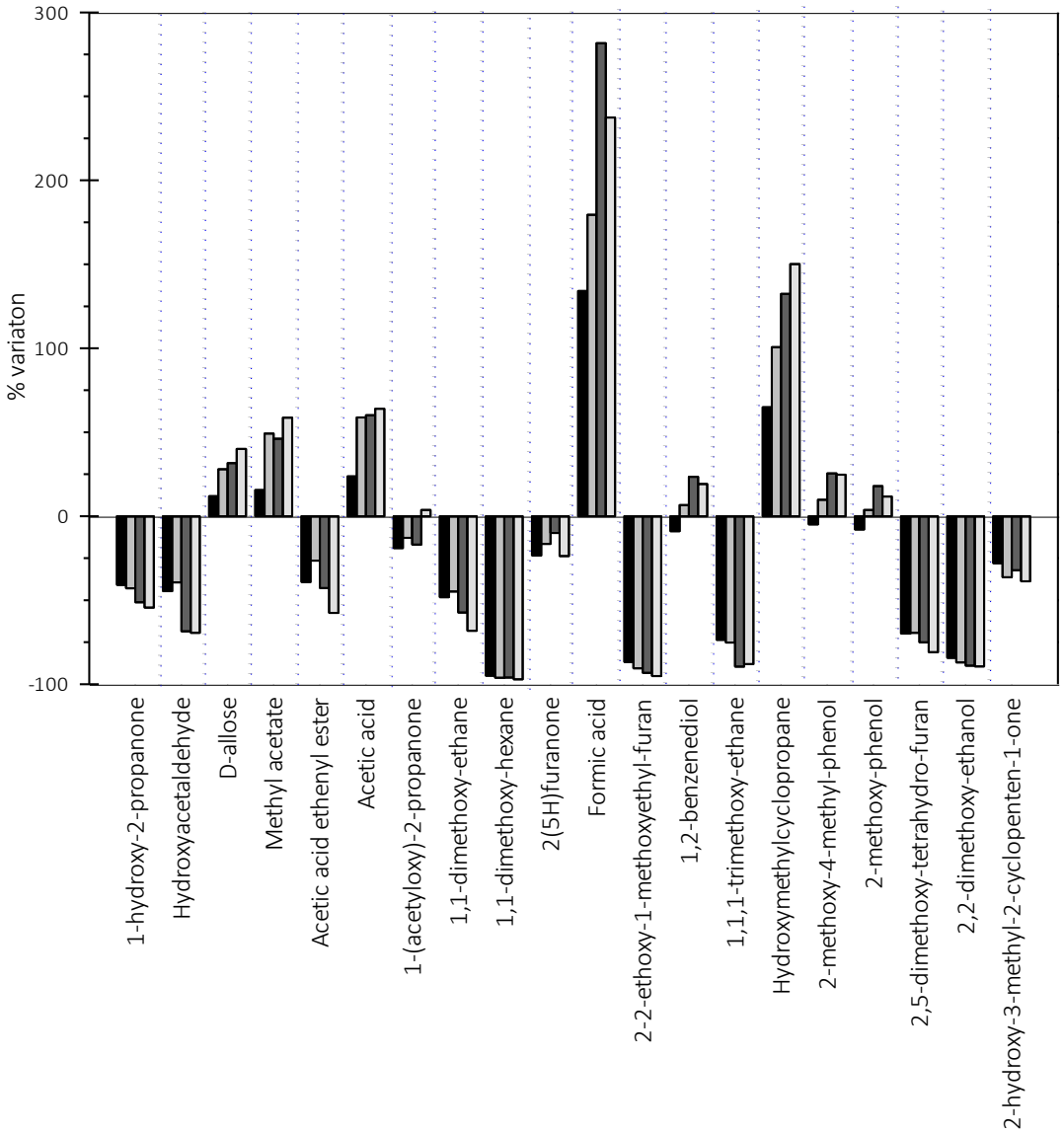

Figure 8.11. Twenty most abundant bio-oil chemical compounds accordingly to area ratio and their percentage of variance at each reaction time relative to initial time (48 h, 96h, 144 h, 240 h).

Fourteen out of the twenty most abundant compounds have a significant percentage of variation accordingly to ANOVA test. The six compounds that do not have significant percentage of variation are 1-(acetyloxy)-2-propanone, 2(5H)furanone, 1,2-benzenediol, 2-methoxy-4-methyl- phenol, 2-methoxy-phenol and 2-hydroxy-3-methyl-2-cyclopenten-1-one. Once more, it seems that the reaction stops at 2 days.

Some compounds, the carboxylic acids (acetic acid and formic acid) and levoglucosan increase their area ratio through the reaction time, while aldehydes and alcohols reduce their area ratio. Regarding to phenols, they do not suffer changes through the process. Finally, other chemical families, as ketones, furans and esters do not have a clear tendency, their behaviour depends on the specific compound. Thus, although the evidences of some changes in bio-oil composition, no specific pathway can be described to explain these changes due to the high diversity of compounds in the bio-oil and the span of potential reactions [7].

The rest of the identified compounds have smaller areas ratio. Due to the high complexity of bio-oil, there might be interferences between analytes or with the base line which might provoke an erroneous integration of peaks. Although this fact is minimised by the use of mass to charge, it might have a noticeable influence on small peaks provoking this random variability on peak areas between days. This fact might explain why significant differences are not observed between the treated and raw bio-oil for these bio-oil compounds. Percentage of variance of most of these compounds are random through the time, meaning, they do not show a clear tendency of chemical changes.

The results of High Heating Value and Elemental composition are shown in Table 8.5. Both high heating value and elemental composition do not show significant differences between treated bio-oil at 4 days of reaction time and untreated or raw bio-oil.

Table 8.4. Bio-oil properties of untreated and treated bio-oil.

Property	Untreated bio-oil	Treated bio-oil
High Heating value (HHV) (MJ / kg)	23.4 ± 1.8	21.6 ± 2.7
Elemental composition, dry basis (wt %)		
C	55	55
H	6.6	6.8
O	38.4	38.2

As it can be observed in the results showed in Figure 8.11., despite some chemical changes occur, they do not imply a noticeable change of bio-oil properties.

As it is said, the diminution of bio-oil acidity reduces or stops the nascent hydrogen production at the tested experimental conditions due to the medium is not acidic enough to enable Zn reduction. Because of that, the production of this really reactive reducer agent may not be enough to entail significant reduction of bio-oil organic compounds. In this way, it is necessary further work to improve the production of nascent hydrogen. Also, in order to improve the reduction of organic compounds, the use of catalysts may improve the transfer of nascent hydrogen to organic substrates, as well as, the reduction of coke formation [60,62].

8.4. Conclusions of Chapter 8: reduced cost bio-oil hydrogenation processes

In this chapter, different hydrogenation processes at ambient temperature and atmospheric pressure are considered to reduce the economic and environmental cost of the conventional hydrotreating process: molecular hydrogen injection and *in situ* nascent hydrogen production by means of water electrolysis and via metal oxidation using bio-oil as acidic medium

The feasibility of generate *in situ* nascent hydrogen in bio-oil both via bio-oil water electrolysis and via Zn oxidation using bio-oil as acidic medium at ambient temperature and atmospheric pressure is proved. A preliminary assessment indicates that hydrogenate bio-oil with nascent hydrogen produces more bio-oil composition changes than molecular hydrogen bio-oil hydrogenation at tested conditions. That fact might point out a high reactivity of nascent hydrogen in comparison to molecular hydrogen at this temperatures which might imply a further bio-oil oxygenated compounds reduction at reduced economic costs since it is produced at ambient temperature and atmospheric pressure.

Taking into account this remarks, an extent study of the feasibility of produce nascent hydrogen via zinc oxidation is performed at different operational conditions to optimize the nascent hydrogen generation. Among the tested conditions, high temperature and proper agitation increases the hydrogen nascent production due to this conditions permit to reduce bio-oil viscosity, a better homogenization and bio-oil metal-contact. Moreover, a minimum of 4.5 wt % of initial Zn of 2.5 x 8 mm is required to achieve the maximum nascent hydrogen production at the tested conditions. An increase of nascent hydrogen production suppose an increase of this reducing agent which might reduce bio-oil oxygenated compound, and consequently, improve bio-oil properties as fuel.

At the same time, the nascent hydrogen generation implies a consumption of H^+ of bio-oil, reducing its acidity to pH values around 4.0 at optimum conditions. However,

this reduction of bio-oil acidity becomes bio-oil into a non-enough acidic medium for Zn oxidation, reducing or stopping the reaction at 24-48 h of reaction time at the tested conditions which might be reactivated by reacidification of the medium.

Moreover, zinc metal oxidation to produce nascent hydrogen produce zinc ions, which might suppose a problem for the combustion of this treated bio-oil. Despite that fact, treated bio-oil phase separation permits concentrating Zn^{2+} in the water phase which might be separated and treated. Moreover, the obtained oil phase with reduced content of water might has a higher calorific value. Further reduction of Zn^{2+} content in the oil phase is achieved by liquid-liquid extraction of the ion with water, removing the 81 % of Zn^{2+} content in the oil phase.

Regarding to bio-oil composition chemical changes, nascent hydrogen reacts with bio-oil generating some chemical changes in the main bio-oil compounds (accordingly to area ratio). Nonetheless, they do not imply a noticeable change on bio-oil properties as high heating value and elemental composition.

After all, bio-oil hydrogenation process by nascent hydrogen does not result in a final product but provides a new route to hydrogenate bio-oil. An active storage of bio-oil generating *in situ* nascent hydrogen in a bio-oil storage tank at 37 ºC is an easy and cheap operational way to improve some of its properties. Moreover, bio-oil hydrogenation by nascent hydrogen holds a promising way for supplying molecular hydrogen in current hydrotreating and stabilization processes due its high reactivity in comparison to molecular hydrogen and the reduction of the associated risk for the handling, storage and use of molecular hydrogen. However, further optimization of the nascent hydrogen generation process is needed by, for example, the use of catalysts.

References of Part III

[1] Demirbas MF. Biorefineries for biofuel upgrading: A critical review. Appl Energy 2009;86:151–61.

[2] Czernik S, Bridgwater A V. Overview of Applications of Biomass Fast Pyrolysis Oil. Energy & Fuels 2004;18:590–8.

[3] Mohan D, Pittman C, Steele P. Pyrolysis of Wood/Biomass for Bio-oil: A Critical Review. Energy & Fuels 2006;20:848–89.

[4] Bridgwater AV, Peacocke GVC. Fast pyrolysis processes for biomass. Renew Sustain Energy Rev 2000;4:1–73.

[5] Gallezot P. Conversion of biomass to selected chemical products. Chem Soc Rev 2012;41:1538–58.

[6] Qi Z, Jie C, Tiejun W, Ying X. Review of biomass pyrolysis oil properties and upgrading research. Energy Convers Manag 2007;48:87–92.

[7] Mortensen PM, Grunwaldt J-D, Jensen P a., Knudsen KG, Jensen a. D. A review of catalytic upgrading of bio-oil to engine fuels. Appl Catal A Gen 2011;407:1–19.

[8] Bridgwater A V. Review of fast pyrolysis of biomass and product upgrading. Biomass and Bioenergy 2012;38:68–94.

[9] Huber GW, Iborra S, Corma A. Synthesis of transportation fuels from biomass: chemistry, catalysts, and engineering. Chem Rev 2006;106:4044–98.

[10] Corma A, Huber G, Sauvanaud L, Oconnor P. Processing biomass-derived oxygenates in the oil refinery: Catalytic cracking (FCC) reaction pathways and role of catalyst. J Catal 2007;247:307–27.

[11] Dickerson T, Soria J. Catalytic fast pyrolysis: A review. Energies 2013;6:514–38.

[12] Venderbosch RH, Ardiyanti AR, Wildschut J, Oasmaa A, Heeres HJ. Stabilization of biomass-derived pyrolysis oils. J Chem Technol Biotechnol 2010;85:674–86.

[13] Elliott DC. Historical Developments in Hydroprocessing Bio-oils. Energy & Fuels 2007;21:1792–815.

[14] Wildschut J, Melián-Cabrera I, Heeres HJ. Catalyst studies on the hydrotreatment of fast pyrolysis oil. Appl Catal B Environ 2010;99:298–306.

[15] Meier D. New Methods for chemical and physical characterization and round robin testing. Fast pyrolysis biomass a Handb. 2nd ed., Newbury: CPL Press; 1999.

[16] Garcia-perez M, Garcia-nunez JA, Lewis T, Kruger C, Kantor S. Methods for Producing Biochar and Advanced Bio-fuels in Washington State. Part 3: Literature Review of Technologies for Product Collection and Refining. Third Proj Report Dep

Biol Syst Eng Cent Sustain Agric Nat Resour Washingt State Univ Pullman, WA 2012:129.

[17] Ingram L, Mohan D, Bricka M, Steele P, Strobel D, Crocker D, et al. Pyrolysis of Wood and Bark in an Auger Reactor : Physical Properties and Chemical Analysis of the Produced Bio-oils. Energy & Fuels 2008:614–25.

[18] Song Q-H, Nie J-Q, Ren M-G, Guo Q-X. Effective Phase Separation of Biomass Pyrolysis Oils by Adding Aqueous Salt Solutions. Energy & Fuels 2009;23:3307–12.

[19] Pakdel H, Zhang H-G, Roy C. Production and characterization of carboxylic acids from wood, part II: High molecular weight fatty and resin acids. Bioresour Technol 1994;47:45–53.

[20] Fullana a, Contreras J, Striebich R, Sidhu S. Multidimensional GC/MS analysis of pyrolytic oils. J Anal Appl Pyrolysis 2005;74:315–26.

[21] Marsman JH, Wildschut J, Evers P, de Koning S, Heeres HJ. Identification and classification of components in flash pyrolysis oil and hydrodeoxygenated oils by two-dimensional gas chromatography and time-of-flight mass spectrometry. J Chromatogr A 2008;1188:17–25.

[22] Marsman JH, Wildschut J, Mahfud F, Heeres HJ. Identification of components in fast pyrolysis oil and upgraded products by comprehensive two-dimensional gas chromatography and flame ionisation detection. J Chromatogr A 2007;1150:21–7.

[23] Djokic MR, Dijkmans T, Yildiz G, Prins W, Van Geem KM. Quantitative analysis of crude and stabilized bio-oils by comprehensive two-dimensional gas-chromatography. J Chromatogr A 2012;1257:131–40.

[24] Christensen ED, Chupka GM, Luecke J, Smurthwaite T, Alleman TL, Iisa K, et al. Analysis of Oxygenated Compounds in Hydrotreated Biomass Fast Pyrolysis Oil Distillate Fractions. Energy & Fuels 2011;25:5462–71.

[25] Branca C, Giudicianni P, Blasi C Di. GC/MS Characterization of Liquids Generated from Low-Temperature Pyrolysis of Wood. Ind Eng Chem Res 2003;42:3190–202.

[26] Sfetsas T, Michailof C, Lappas A, Li Q, Kneale B. Qualitative and quantitative analysis of pyrolysis oil by gas chromatography with flame ionization detection and comprehensive two-dimensional gas chromatography with time-of-flight mass spectrometry. J Chromatogr A 2011;1218:3317–25.

[27] Aubin H, Roy C. Study on the corrosiveness of wood pyrolysis oils. Fuel Sci Technol Int 1990;8.

[28] Oasmaa A, Peacocke C. Properties and fuel use of biomass-derived fast pyrolysis liquids. A guide. 2010.

[29] Elliott DC. Water, alkali and char in flash pyrolysis oils. Biomass and Bioenergy 1994;7:179–85.

[30] Garcia-Perez M, Chaala A, Pakdel H, Kretschmer D, Roy C. Characterization of bio-oils in chemical families. Biomass and Bioenergy, vol. 31, 2007, p. 222–42.

[31] Oasmaa A, Leppämäki E, Koponen P, Levander J, Tapola E. Physical characterization of biomass-based pyrolysis liquids. Application of standard fuel oil analyses. Espoo, Tech Res Cent Finl 1997.

[32] Weitkamp J. Zeolites and catalysis. Solid State Ionics 2000;131:175–88.

[33] Corma A. State of the art and future challenges of zeolites as catalysts. J Catal 2003;216:298–312.

[34] Corma A. Catálisis con zeolitas: Desde el laboratorio a su aplicación industrial. Arbor 2011;187:83–102.

[35] Csicsery S. Shape-selective catalysis in zeolites. Zeolites 1984;4:202–13.

[36] Degnan TF. The implications of the fundamentals of shape selectivity for the development of catalysts for the petroleum and petrochemical industries. J Catal 2003;216:32–46.

[37] Eder F, Stockenhuber M, Lercher JA. Brønsted Acid Site and Pore Controlled Siting of Alkane Sorption in Acidic Molecular Sieves. J Phys Chem B 1997;5647:5414–9.

[38] Luckham P, Rossi S. The colloidal and rheological properties of bentonite suspensions. Adv Colloid Interface Sci 1999;82:43–92.

[39] Adjaye JD, Bakhshi NN. Production of hydrocarbons by catalytic upgrading of a fast pyrolysis bio-oil. Part II: Comparative catalyst performance and reaction pathways. Fuel Process Technol 1995;45:185–202.

[40] Vijayakumar B, Nagendrappa G, Jai Prakash BS. Acid Activated Indian Bentonite, an Efficient Catalyst for Esterification of Carboxylic Acids. Catal Letters 2008;128:183–9.

[41] Moraes DS, Angélica RS, Costa CEF, Rocha Filho GN, Zamian JR. Bentonite functionalized with propyl sulfonic acid groups used as catalyst in esterification reactions. Appl Clay Sci 2011;51:209–13.

[42] Banat FA, Al-Bashir B, Al-Asheh S, Hayajneh O. Adsorption of phenol by bentonite. Environ Pollut 2000;107:391–8.

[43] Lu Q, Zhu X, Li W, Zhang Y, Chen D. On-line catalytic upgrading of biomass fast pyrolysis products. Chinese Sci Bull 2009;54:1941–8.

[44] Oasmaa A, Elliott DC, Korhonen J. Acidity of Biomass Fast Pyrolysis Bio-oils. Energy & Fuels 2010;24:6548–54.

[45] Huang J, Long W, Agrawal PK, Jones CW. Effects of Acidity on the Conversion of the Model Bio-oil Ketone Cyclopentanone on H−Y Zeolites. J Phys Chem C 2009;113:16702–10.

[46] Guo X, Zheng Y, Zhang B, Chen J. Analysis of coke precursor on catalyst and study on regeneration of catalyst in upgrading of bio-oil. Biomass and Bioenergy 2009;33:1469–73.

[47] Gayubo AG, Valle B, Aguayo T, Bilbao J. Attenuation of Catalyst Deactivation by Cofeeding Methanol for Enhancing the Valorisation of Crude Bio-oil. Energy & Fuels 2009;23:4129–36.

[48] Adjaye JD, Bakhshi NN. Production of hydrocarbons by catalytic upgrading of a fast Part I: Conversion over various catalysts. Fuel Process Technol 1995;45:161–83.

[49] Song M, Zhong Z, Dai J. Different solid acid catalysts influence on properties and chemical composition change of upgrading bio-oil. J Anal Appl Pyrolysis 2010;89:166–70.

[50] Adjaye JD, Bakhshi NN. Catalytic conversion of a biomass-derived oil to fuels and chemicals I: Model compound studies and reaction pathways. Biomass and Bioenergy 1995;8:131–49.

[51] Murwanashyaka JN, Pakdel H, Roy C. Step-wise and one-step vacuum pyrolysis of birch-derived biomass to monitor the evolution of phenols. J Anal Appl Pyrolysis 2001;60:219–31.

[52] Huber GW, Iborra S, Corma A. Synthesis of transportation fuels from biomass: chemistry, catalysts and engineering. Chem Rev 2006;106:4044–98.

[53] Vitolo S, Seggiani M, Frediani P, Ambrosini G, Politi L. Catalytic upgrading of pyrolytic oils to fuel over different zeolites. Fuel 1999;78:1147–59.

[54] Wildschut J, Mahfud FH, Venderbosch RH, Heeres HJ. Hydrotreatment of Fast Pyrolysis Oil Using Heterogeneous Noble-Metal Catalysts. Ind Eng Chem Res 2009;48:10324–34.

[55] Laborda F, Bolea E, Baranguan MT, Castillo JR. Hydride generation in analytical chemistry and nascent hydrogen: When is it going to be over? Spectrochim Acta - Part B At Spectrosc 2002;57:797–802.

[56] Singhal R. Electronics Engineering. 9th editio. Krishna Parakashan Media; 2009.

[57] Jensen william B. Whatever happened to the Nascent State? Bull Hist Chem 1990:26–36.

[58] Pham VH, Pham HD, Dang TT, Hur SH, Kim EJ, Kong BS, et al. Chemical reduction of an aqueous suspension of graphene oxide by nascent hydrogen. J Mater Chem

2012;22:10530.

[59] Oasmaa A, Kuoppala E. Fast Pyrolysis of Forestry Residue. 3. Storage Stability of Liquid Fuel. Energy & Fuels 2003;17:1075–84.

[60] Venderbosch RH, Ardiyanti A, Wildschut J, Oasmaa A, Heeres HJ. Insights in the hydroprocessing of biomass derived pyrolysis oils. 2009.

[61] Chen H-W, Song Q-H, Liao B, Guo Q-X. Further Separation, Characterization, and Upgrading for Upper and Bottom Layers from Phase Separation of Biomass Pyrolysis Oils. Energy & Fuels 2011;25:4655–61.

[62] Johnstone R a. W, Wilby AH, Entwistle ID. Heterogeneous catalytic transfer hydrogenation and its relation to other methods for reduction of organic compounds. Chem Rev 1985;85:129–70.

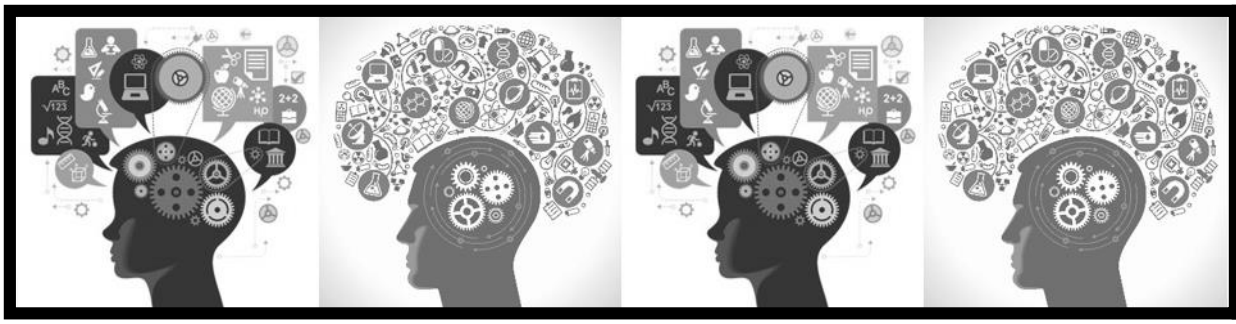

IV

CONCLUSION

9. Conclusions

This dissertation pretends to add value to agro-forestry biomass residues as enhanced biofuels by means of thermochemical biomass conversion processes, as well as to achieve upgraded liquid biofuels by novel upgrading processes at low energy consumption to move towards a more sustainable energy model.

The general conclusions of this thesis work are:

- Torrefaction process is demonstrated to be a technical and economic viable process to be implemented in a rural region to add value to agricultural biomass waste produced locally as torrefied pellets.
- Bio-oil reliable quantification method of bio-oil target organic compounds by means of a GC-MS analysis is achieved assessing the precision of the method and different internal standard calibration methods. The methods that use toluene and 1,1,3,3-tetrahydropropane as internal standards are the most appropriate for bio-oil chemical quantification.
- Bio-oil upgrading using bentonites and zeolites as catalysts at 60 ºC in order to reduce the energy cost of the conventional processes permits the reduction of bio-oil acidity, although the catalytic function and bio-oil properties enhancement is limited.
- The feasibility of generating *in situ* nascent hydrogen at ambient temperature and atmospheric pressure is proved both via electrolysis of water contained in bio-oil and via metal oxidation using bio-oil as acidic medium which might permit the reduction of energy costs of hydrotreating conventional processes.
- This research work, jointly to projects of this kind, is the first steps to move towards to a bioeconomy system, not only in the energetic field but also in production of chemical within the biorefinery scenario. This project combines an

environmental friendly project with the aim of boosting the local and circular economy.

The specific findings of this dissertation are addressed at the end of each results chapter, being the most relevant ones summarised in the following sections for each chapter.

Adding value of agricultural waste biomass as torrefied pellets

- A complete characterisation of potentially valuable agricultural waste biomass produced in a rural region is achieved to assess the operation conditions that might be treated in the torrefaction plants.
- Torrefied pellets produced in the pilot torrefaction plant have characteristics within the European law standards of pellets demonstrating they are marketable products.
- The assessment of torrefaction liquid potential uses, mainly as chemical platform to obtain bio-products and bio-chemicals is reached by means of its characterisation. Thus, a product which is considered, up to now, a residue might be converted into torrefaction process by-product increasing its efficiency and viability.
- The enhancement of calorific value on the torrefied biomass is between 6-15 % in comparison to raw biomass and torrefied pellet has a calorific value between 13-18 % higher than torrefied pellets. Therefore, torrefaction process can enhance the calorific value of the product up to 25-30 %.
- Intensive production of torrefaction pellets is a more economically viable scenario of implementing torrefaction technology than the moderate one. However, it is important to take into account that torrefaction process implementation at small scale favoured the management efficiency of the process and reduce their logistic costs from an economic and environmental point of view.

Bio-oil characterisation

- Bio-oil proper characterisation and the start-up of the required analytical methods permit the assessment of the upgrading processes developed in this thesis work, as well as the further knowledge of this product and its potential application as biofuel or chemical platform.
- Regarding to chemical characterisation analysis:
    - The precision assessment demonstrates a good instrumental and intraday precision, and an improvable interday precision. The use of internal standards to improve the method precision results in a not noticeable influence when toluene and 1,1,3,3-tetramethoxypropane as intern standards and a negative influence when 1-octanol is used.
    - A proper quantification analysis is achieved by means of any of the tested internal standard calibration methods (using toluene, 1,1,3,3-tetramethoxypropane and 1-octanol as internal standards) and without them. However, the obtained concentrations of each bio-oil compound are significantly different depending on the calibration method used.
    - Interday precision is improved when the calibration method is carried out using toluene and 1,1,3,3-tetramethoxypropane as internal standards.

Catalytic upgrading process

- The effect of both HZSM-5 and bentonite on bio-oil at 60 ºC is the reduction of bio-oil acidity, being HZSM-5 the most efficient (around 28 % on pH value).
- Acidity reduction is considered to be caused by the acid-base interaction or adsorption of bio-oil compounds into the catalyst causing an earlier deactivation of the catalyst limiting its catalytic function, and consequently, the bio-oil upgrading.
- HZSM-5 deactivation takes place in less than 15 min. HZSM-5 replacement throughout the upgrading process permits a further acidity reduction (around 25 %).

Bio-oil hydrogenation processes

- Zinc metal is more effective metal than aluminium to generate *in situ* nascent hydrogen via metal oxidation using bio-oil as acidic medium.
- Electrolysis of water contained in bio-oil and zinc oxidation using bio-oil as acidic medium are more effective processes to generate *in situ* nascent hydrogen than molecular hydrogen injection at ambient temperature and atmospheric pressure, being zinc oxidation procedure the simplest one.
- Bio-oil acidity is lessened simultaneously with nascent hydrogen production when it is produced via zinc oxidation. Temperature, proper agitation and initial zinc amount about 4.5 wt % are the key parameters to maximize nascent hydrogen production, and consequently, to increase the potential of reduce oxygenated bio-oil compounds and therefore to enhance bio-oil properties as biofuel.
- Bio-oil acidity diminution converts bio-oil into a non-enough acidic medium to oxidase zinc metal for hydrogen nascent production, which might be reactivated by reacidification of the medium.
- Nascent hydrogen produces some bio-oil chemical changes, although they do not imply noticeable changes on bio-oil properties as high calorific value and elemental composition.

- During the hydrotreating process, bio-oil phase separation is observed. The presence of zinc ions in bio-oil (produced during zinc oxidation reaction) can be eliminated in a 81 % with the water phase. Thus, the obtained organic phase with low water content and low zinc ion concentration might be a potential higher calorific value enhanced biofuel.
- Bio-oil hydrogenation by *in situ* nascent hydrogen is a promising route to perform an active, easy and cheap bio-oil storage to enhance some of its properties, although further optimization of the process is required.

10. Future perspectives

The research performed within this thesis work, as well as the obtained results, open up new research perspective on this research field. Some of them are listed in the following sections for each chapter.

Adding value of agricultural waste biomass as torrefied pellets

- Performing more pilot projects of adding value of agricultural waste biomass as torrefied pellets in other rural areas in order to promote and make public this technology and their products, as well as its benefits in the implementation zone. Thus, the implementation of this kind of technologies in a near future might be facilitated.
- To carry out a focus group with the stakeholders of the torrefaction plant implementation zone, as farmers, local government, torrefaction plant company and citizens). That might permit the assessment of their perceptions, opinions, beliefs and attitudes towards the implementation of torrefaction plant in their region.
- Carrying out a detailed study of the potential uses of torrefaction liquid and developing an extraction method of its value added products or the intermediate once for obtaining bio-chemical or bio-products, for example acetic acid, furfural or phenol. In this way, torrefaction liquid which currently is a residue might be converted into a by-product of the torrefaction process.
- To perform a complete energy and mass balance of the overall torrefaction process to assess in deep the torrefaction mass and energy distribution on the torrefaction products.
- Assessing the environmental impacts associated with the production of torrefied pellets such as Life Cycle Assessment, Risk Assessment, Economic Valuation and Multi-Attribute Approaches in order to consider all the stages of a product's life from raw material extraction through materials processing, manufacture,

distribution, use, repair and maintenance of the plant and disposal or recycling of the residues of the process.

Bio-oil characterisation

- Characterising bio-oil chemical composition by means of other analytic technics in order to obtain a more complete bio-oil chemical composition, as for example HPLC-MS to identify the non-volatile bio-oil compounds.

Bio-oil hydrogenation processes

- To study the use of catalyst in nascent hydrogen hydrogenation process via zinc oxidation in order to favour the reduction of bio-oil oxygenated compounds to achieve an upgraded bio-oil.
- To evaluate the use of zinc (or other metals) nanomaterial and nanomotors in order to increase the nascent hydrogen diffusion on bio-oil to boost the reduction of bio-oil oxygenated compounds to achieve an upgraded bio-oil.
- To further study the phase separation process that occurs during the nascent hydrogen hydrotreating process via zinc oxidation in order to: (1) characterise the organic and aqueous phase separately in order to assess their potential uses. A priori, aqueous phase as chemical platform for extraction of bio-chemical and bio-products and organic phase as enhanced liquid biofuel; (2) further eliminate the zinc ion from the bio-oil organic phase by means of liquid-liquid extraction to favour its use as biofuel.
- Further evaluating the hydrogenation process by means of electrolysis of water contained in bio-oil as a possible viable hydrogenation process to enhance bio-oil properties.

V

ANNEX

11. Publications and conferences

Publications

Artigues A, Puy N, Bartrol J, Fabregas E. Comparative Assessment of Internal Standards for Quantitative Analysis of Bio-oil Compounds by Gas Chromatography / Mass Spectrometry Using Statistical Criteria. Energy & Fuels 2014;28:3908–15

Martínez JD, Veses A, Mastral AM, Murillo R, Navarro M V., Puy N, Artigues A, Bartrolí J and García T. Co-pyrolysis of biomass with waste tyres: Upgrading of liquid bio-fuel. Fuel Process Technol 2014; 119:263–71.

Artigues A, Cañadas V, Puy N, Gasol CM, Alier S, Bartolí J. Torrefied pellets production from wood crop waste as valuable product in agricultural sector: techno-economical pilot test assessment. Biomass and Bioenergy. Under review.

Conferences

Artigues A, Puy N, Fábregas E, Bartrolí J. Second generation biofuel production y zeolite catalysis and added-value products assessment. Oral comunication. II Congreso Iberoamericano sobre Biorrefinerías. Jaen, 2013. Organized by Sociedad Iberoamericana para el Desarrollo de las Biorrefinerías (SIADEB) y la Universidad de Jaén.

Artigues A, Puy N, Fábregas E, Bartrolí J. Catalytic pyrolysis oil upgrading using bentonite and zeolist as catalysts. Poster. European Biomass Conference and Exhibition. Milano (Italy), 2012. Organized by ETA-Florence Renewable Energies.

Veses A, Artigues A, Puy N, Martínez JD, García T, Murillo R, López JM. Production and characterization of biofuels by co-pyrolysis of biomass and waste tyres. Poster. European Biomass Conference and Exhibition. Milano (Italy), 2012. Organized by ETA-Florence Renewable Energies.

Artigues A, Puy N, Fábregas E, Bartrolí J. Bio-oil characterization to develop an upgrading process to obtain a second-generation biofuel and added-value products. Poster. 9th Green Chemistry Conference. Alcalá de Henares (Madrid), 2011. Organized by IUTC y Universidad de Alcalá.

Artigues A, Puy N, Fábregas E, Bartrolí J. Bio-oil upgrading using nanomaterials (CNTs). Step 1 - Characterisation of biomass-based pyrolysis product. Poster. 19th European Biomass Conference and Exhibition. Berlin (Germany), 2011. Organized by ETA-Florence Renewable Energies.

Puy N, Artigues A, Murillo R, García T, Bartrolí J. Shifting towards renewable sources: biomass pyrolysis as a strategy to produce energy and raw materials. Oral Communication. Congreso Internacional Pico del Petróleo: ¿Realidad o Ficción? Barbastro (Huesca), 2011. Organized by UNED-Barbastro.